

Abstract

Title of Document: MODELING THE PH DEPENDENT OPTICAL
PROPERTIES OF AQUATIC, TERRESTRIAL
AND MICROBIAL HUMIC SUBSTANCES

Lynne Page Heighton,
Doctor of Philosophy, 2013

Directed By: Alice C. Mignerey
Department of Chemistry and Biochemistry

Humic substances (HS) and chromophoric dissolved organic matter (CDOM) are ubiquitous, widely impacting environmental processes, yet despite decades of study the link between structure and the unique optical properties evident in HS/CDOM remains elusive. Model compounds derived from a solely microbial source, as well as terrestrial sources from both aquatic environments and soil systems, exhibit many of the same optical properties despite their disparate methods of generation and sources. All show a pH dependent absorbance, exhibit increasing absorbance as wavelength decreases and a loss of absorbance upon borohydride reduction.

The link between colored humic substances is their ability to form electronic interactions that extend long wavelength absorbance. The underlying processes by which charge transfer bands or electronic interactions in HS/CDOM are generated are investigated by optical and potentiometric titrations of untreated and borohydride reduced material. Borohydride reduction targets carbonyl functional groups such as aromatic ketones and quinones. The reduction of these groups affects the optical

properties by reducing long wavelength absorbance and causing a blue shift in the fluorescence emission spectra.

A direct comparison of divergent sources of fulvic and humic acids including an aquatic fulvic acid, Suwannee River Fulvic Acid (SRFA) and a microbial source of fulvic acid, Pony Lake Fulvic Acid (PLFA), the soil derived humic acids, Elliott (EHA) and Leonardite Humic Acids (LHA), an aquatic humic acid Suwannee River Humic Acid (SRHA) as well as Lignin Alkali Carboxylate (LAC) highlights differences between sources of humic material as exemplified by borohydride induced optical changes such as absorbance intensity in the UV and visible range, difference (ΔA), fractional difference, spectral slope (S), fluorescence excitation-emission matrix spectra (EEMS), and differential emission spectra (ΔF) as well as quantum yield.

Traditional Raman spectroscopy, although capable of providing relevant chemical functional group information, cannot be applied to untreated CDOM because of high fluorescence background. Surface enhanced Raman scattering (SERS) provides the capability of overcoming the fluorescence background, thus providing useful Raman spectral data. SERS spectra of model compounds and CDOM were collected using roughened silver electrodes. Functional groups were identified from selected borohydride reduced CDOM SERS spectra.

MODELING THE PH DEPENDENT OPTICAL PROPERTIES OF AQUATIC,
TERRESTRIAL AND MICROBIAL HUMIC SUBSTANCES

By

Lynne Page Heighton

Dissertation submitted to the Faculty of the Graduate School of the
University of Maryland, College Park, in partial fulfillment
of the requirements for the degree of
Doctor of Philosophy
2013

Advisory Committee:
Professor, Chair Alice C. Mignerey
Professor Catherine C. Fenselau
Professor Alba Torrents
Professor Amy S. Mullin
Dr. Walter F. Schmidt

© Copyright by
Lynne Page Heighton
2013

Dedication

For My Family, Kevin, James and Henry

Acknowledgements

I would like to thank Professor Neil V. Blough for the financial support of my project as well as for providing me with access to laboratory space at the University of Maryland. I would especially like to acknowledge my friend and mentor Dr. Walter Schmidt for providing me with laboratory space and access to equipment at the USDA. Walter has helped me realize the value of doing work that you really love. I have made some wonderful friends in graduate school including Cassie Taylor, Dr. Kathy Goodson, Dr. Lenard Demoranville, and Dr. Mara Dougherty, Andrea Andrew, Yi Zhang, Kelli Sikorski, Dr. Min Jia and Dr. Qhing Zhu. I want to thank them for many all the help and advice that they have given me. I want to thank Dr. Marguerite Tonjes for teaching me the value of persistence in learning new things. I also want to acknowledge the Dr. Clifford Rice from the Agricultural Research Service, who has generously allowed me to use his lab like it was my own resulting in some great papers. My sincerest thanks to my advisor Dr. Alice Mignerey; she has always been in my corner. Finally, thanks to the Department of Chemistry staff who magically know how to get things done and have keys to everything.

Table of Contents

Dedication.....	ii
Acknowledgements.....	iii
List of Figures.....	ix
List of Tables.....	xvi
Dissertation Overview.....	xvii
Chapter 1 Background.....	1
Chapter 1 Overview.....	1
1.1 Objectives.....	1
1.2 What are Humic Substances (HS), Dissolved Organic Matter (DOM) and Chromophoric Dissolved Organic Matter (CDOM)?.....	3
1.2.1 Operational Definitions.....	6
1.2.2 The Importance of CDOM in Aquatic Environments.....	6
1.2.3 The Optical Properties of CDOM in Aquatic and Marine Ecosystems.....	9
Chapter 2 Sample Descriptions and Locations.....	12
Chapter 2 Overview.....	12
2.1 Model Humic Substances.....	12
2.1.1 Soil Humic Acids.....	14
2.1.2 Freshwater Aquatic Humic Substances.....	15
2.1.3 Microbial Humic Substance.....	16
2.2 Recalcitrant Material in DOM.....	17
2.2.1 The Composition of Lignin.....	21
2.2.2 The Link between Lignin and Humic Acids.....	24

2.2.3 Chemical Components of Pony Lake Fulvic Acid.....	25
Chapter 3 Models.....	29
Chapter 3 Overview.....	29
3.1 Electronic Interaction or Charge Transfer Model.....	29
3.1.1 Terrestrial CDOM and HS in Relation to Electronic Interaction Model.....	31
3.1.2 Extending the Electronic Interaction Model to Microbial Sources of CDOM.....	34
3.2 NICA-Donnan model.....	39
Chapter 4 The Chemical Probe Sodium Borohydride.....	41
Chapter 4 Overview.....	41
Chapter 5 Sodium Borohydride Reduction of Terrestrial Humic Acids and Microbial Fulvic Acid	
.....	48
Chapter 5 Overview.....	48
5.1 Introduction.....	49
5.2 Materials and Method.....	51
5.2.1. Materials.....	51
5.2.3 Optical Measurements.....	52
5.2.4 Preparation of Humic and Fulvic Acids.....	53
5.2.5 Borohydride Reduction.....	54
5.3 Results and Discussion.....	56
5.3.1 Borohydride Reduction.....	56
5.3.2 Optical Properties of Borohydride Reduced Humic Substances (SRFA, SRHA), Lignin Alkali Carboxylate (LAC) and Natural Humic Substances from the Mid-Atlantic Shelf and Delaware Bay.....	59

5.3.3 Untreated and Borohydride Reduced Spectral Slope Values.....	75
5.3.4 Untreated and Borohydride Reduced Fluorescence Spectra.....	79
5.3.5 Fluorescence Quantum Yield (Φ).....	90
5.3.6 Cyanoborohydride Reduction of Selected Samples.....	93
5.3.7 Molar Absorptivity of Phenone Compounds.....	96
5.4 Conclusions.....	102
Chapter 6 Optical Titrations of Aquatic, Terrestrial and Microbial Humic Substances.....	106
Chapter 6 Overview.....	106
6.1 Introduction.....	106
6.2. Materials and Methods.....	109
6.2.1 Materials.....	109
6.2.2 Apparatus.....	109
6.2.3 Optical Titration Measurements.....	110
6.3. Results and Discussion.....	112
6.3.1 Concentration of the Borohydride Reduced Humic and Fulvic Acids.....	113
6.3.2 Titration of Untreated and Borohydride Reduced Humic and Fulvic Acids Differences in Ionic Strength.....	118
6.3.3 First Derivative Plots of Titrations of Humic Substances.....	123
6.3.4 Parameterized Spectral Slope (S) Values as a Function of pH.....	129
6.3.5 Optical Titration Spectra and Difference Plots.....	142
6.4 Conclusions.....	155
Chapter 7 Raman Spectroscopy of Lignin Phenols, Quinones and Suwannee River Humic and Fulvic Acids.....	157

Chapter 7 Overview	157
7.1 Introduction.....	157
7.2 Materials and Methods.....	159
7.2.1. Materials	159
7.2.2. Apparatus	160
7.2.3 Preparation of Silver Electrodes	161
7.2.4 Preparation of Silver Plate	161
7.3 Results and Discussion	162
7.3.1 Oxidation-Reduction Cycle.....	162
7.3.2 Calibration of the silver electrodes and plate.....	164
7.3.2.1 SERS Spectra of Pyridine	164
7.3.2.2 SERS Spectra of Crystal Violet	167
7.3.3 SERS Spectra of Terrestrially Sourced Monomer Compounds.....	169
7.3.3.1 Quinones	169
7.3.3.2 Lignin Phenols	171
7.3.4 SERS spectra of Suwannee River humic acids.....	173
7.4 Conclusions and Future Work	177
Appendix 1 NICA-Donnan Model.....	182
Appendix 2 Supplementary Information for Chapter 6: Optical Titrations of Aquatic, Terrestrial and Microbial Humic Substances	192
Appendix 3 Raman Theory.....	217
A.3.1 Raman Spectral Theory.....	217
A.3.2 Surface Enhanced Raman Scattering (SERS).....	219

Bibliography 221

List of Figures

1.1	The operational definition of Humic and Fulvic Acids, and their link to humic substance (HS) and colored dissolved organic matter (CDOM).....	4
1.2	Chromophoric dissolved organic matter (CDOM) is a continuum in the environment that can be used to trace the global carbon cycle.....	5
1.3	Universal optical properties of CDOM.....	11
2.1	Origin of terrestrial humic acids.	15
2.2	The Suwannee River watershed.....	16
2.3	Theoretical van Krevlin plot.....	18
2.4	The structure of Lignols.....	22
2.5	Compounds used to study CDOM.....	24
2.6	Allantion.....	27
3.1	Electronic Interaction Model.....	30
3.2	Electronic Interaction Model, Donors, and Acceptors	32
3.3	Ubiquinone.....	35
3.4	Menaquinone.....	36
3.5	1, 10-phenathroline.....	37
3.6	Heterocyclic charge transfer donors and acceptors.....	38
4.1	Borohydride reduction of carbonyl functional groups.....	42
4.2	Generation of a phenoxy radical, hydrogen ion and a solvated electron by photo-dissociation.....	43
5.1	Concentration dependence of the borohydride reduction of LHA.....	58

5.2	Absorbance, difference and fractional difference of the reduction and reoxidation of aquatic CDOM and humic acids materials.....	62
5.3	Absorbance, difference and fractional difference spectra of the reduction and reoxidation of soil derived humic acids.....	64
5.4	Absorbance, difference, fractional difference spectra of the reduction and reoxidation of microbial humic acid.....	71
5.5	Time dependence of the borohydride reduction and reoxidation of Suwannee River fulvic acid and Pony Lake fulvic acid	72
5.6	Time dependence of the borohydride reduction and reoxidation of humic and fulvic acids	73
5.7	Difference and fractional difference spectra of fulvic acids	74
5.8	Parameterized absorbance of Elliott (EHA), Leonardite (LHA) and Suwannee River humic acid (SRHA).....	77
5.9	Parameterized absorbance of Suwannee River fulvic acid (SRFA), Pony Lake fulvic acid (PLFA) and Lignin Alkali Carboxylate (LAC).....	78
5.10	The fluorescence optical properties of untreated and borohydride reduced humic and fulvic acids	81
5.11	Fluorescence properties of Elliott humic acid and Leonardite humic acid prior to and following reduction with sodium borohydride.....	85
5.12	Fluorescence optical properties of Pony Lake fulvic acid following reduction with sodium borohydride.....	86
5.13	pH dependence of the fluorescence emission properties of borohydride reduced humic and fulvic acids.....	88

5.14	pH dependence of the fluorescence emission properties of borohydride reduced CDOM samples.....	89
5.15	Wavelength dependence of emission maxima and fluorescence quantum yields samples before and after sodium borohydride reduction.....	92
5.16	Time dependence of the reaction of LHA, SRFA, Duraquinone (DQ) and Methyl-p-benzoquinone (MBQ) with cyanoborohydride (CB). Time dependence of the reduction of MBQ with sodium borohydride (BH).....	95
5.17	Structures of benzophenone (BP) (a) and 2-acetonaphthone (2-AN) (b).....	97
5.18	Absorbance spectra of untreated benzophenone (BP) in (50:50) MeOH:water showing π to π^* to n to π^* absorbance and molar extinction coefficients.....	98
5.19	Absorbance of the borohydride reduction of benzophenone.....	99
5.20	Absorbance spectra of untreated 2-acetonaphthone.....	100
5.21	Absorbance of the borohydride reduction of 2-acetonaphthone	101
6.1	Standard curves correlating the absorbance with concentration of untreated and borohydride reduced fulvic acids	116
6.2	Standard curves correlating the absorbance with the concentration of untreated and borohydride reduced humic acids.....	117
6.3	Titrations and first derivative plots of selected fulvic acids.....	124
6.4	Titrations and first derivative plots selected humic acids	125
6.5	Spectral slope (S) as a function of pH. Untreated and borohydride reduced, carbon normalized.....	130
6.6	Parameterized, carbon normalized untreated and borohydride reduced Elliott humic acid (EHA) absorbance as a function of pH.....	132

6.7	Parameterized, carbon normalized untreated and borohydride reduced Leonardite humic acid (LHA) absorbance as a function of pH.....	133
6.8	Parameterized, carbon normalized untreated and borohydride reduced Suwannee River humic acid (SRHA) absorbance as a function of pH.....	134
6.9	Parameterized carbon normalized untreated and borohydride reduced Suwannee River fulvic acid (SRFA) absorbance as a function of pH.....	135
6.10	Parameterized, carbon normalized untreated and borohydride reduced Pony Lake fulvic acid (PLFA) absorbance as a function of pH.....	136
6.11	Parameterized, carbon normalized untreated and borohydride reduced Lignin Alkali Carboxylate (LAC) absorbance as a function of pH.....	137
6.12	Absorbance spectra of the optical titration and difference plots of carbon normalized Suwannee River fulvic acid (SRFA) untreated and borohydride reduced	143
6.13	Absorbance spectra of the optical titration and difference plots of carbon normalized Pony Lake fulvic acid (PLFA) untreated and borohydride reduced.....	144
6.14	Absorbance spectra of the optical titration and difference plots of carbon normalized Suwannee River humic acid (SRHA) untreated and borohydride reduced.....	145
6.15	Absorbance spectra of the optical titration and difference plots of carbon normalized Elliott humic acid (EHA) untreated and borohydride reduced.....	146
6.16	Absorbance spectra of the optical titration and difference plots of carbon normalized Leonardite humic acid (LHA) untreated and borohydride reduced.....	147
6.17	Absorbance spectra of the optical titration and difference plots of carbon normalized Lignin Alkali Carboxylate (LAC) untreated and borohydride reduced.....	151

6.18	Visible range absorbance spectra of the optical titration and difference plots of carbon normalized Suwannee River fulvic acid untreated and borohydride reduced.....	153
6.19	Visible range absorbance spectra of the optical titration and difference plots of carbon normalized Pony Lake fulvic acid untreated and borohydride reduced.....	154
7.1	Oxidative Reduction cycle from the potentiostat presented as current (A) as a function of potential (V) shows the development of nanostructures.....	163
7.2	SERS spectra of pyridine on silver plate.....	165
7.3	Crystal Violet SERS spectra on silver roughed electrode.....	168
7.4	SERS spectra of selected untreated quinones.....	170
7.5	SERS spectra of selected untreated lignin phenols.....	172
7.6	SERS spectra of borohydride reduced SRFA and p-methyl benzoquinone.....	174
7.7	SERS spectra of borohydride reduced SRHA from 750 – 1200 cm^{-1}	175
7.8	SERS spectra of borohydride reduced SRHA from 1200 – 1800 cm^{-1}	176
A1.1	NICA-Donnan Model example.....	182
A2.1	Absorbance and difference spectra of untreated and borohydride reduced Suwannee River humic Acid (SRHA) at 0.01 mole L^{-1} ionic strength.....	195
A2.2	Absorbance and difference spectra of untreated and borohydride reduced (lower panels) Suwannee River humic Acid (SRHA) at 0.10 mole L^{-1} ionic strength.....	196
A2.3	Absorbance and difference spectra of untreated and borohydride reduced Suwannee River humic Acid at 1.00 mole L^{-1} ionic strength.....	197
A2.4	Absorbance and difference spectra of untreated and borohydride reduced Suwannee River fulvic acid at 0.10 mole L^{-1} ionic strength.....	198

A2.5	Absorbance and difference spectra of untreated and borohydride reduced Suwannee River fulvic Acid 1.00 mole L ⁻¹ ionic strength.....	199
A2.6	Absorbance and difference spectra of untreated and borohydride reduced Elliott humic acid at 0.01 mole L ⁻¹ ionic strength.....	200
A2.7	Absorbance and difference spectra of untreated and borohydride reduced Elliott humic acid at 0.10 mole L ⁻¹ ionic strength.....	201
A2.8	Absorbance and difference spectra of untreated and borohydride reduced Elliott humic acid at 1.00 mole L ⁻¹ ionic strength.....	202
A2.9	Absorbance and difference spectra of untreated and borohydride reduced Leonardite humic acid at 0.01 mole L ⁻¹ ionic strength.....	203
A2.10	Absorbance and difference spectra of untreated and borohydride reduced Leonardite humic acid at 0.10 mole L ⁻¹ ionic strength.....	204
A2.11	Absorbance and difference spectra of untreated and borohydride reduced Leonardite humic acid at 1.00 mole L ⁻¹ ionic strength.....	205
A2.12	Absorbance and difference (ΔA) spectra of untreated and borohydride reduced Pony Lake fulvic acid at 0.10 mole L ⁻¹ ionic strength.....	206
A2.13	Absorbance and difference spectra of untreated and borohydride reduced Pony Lake fulvic acid at 1.00 mole L ⁻¹ ionic strength.....	207
A2.14	Absorbance and difference spectra of untreated and borohydride reduced Lignin Alkali Carboxylate at 0.01 mole L ⁻¹ ionic strength.....	208
A2.15	Absorbance and difference spectra of untreated and borohydride reduced Lignin Alkali Carboxylate at 0.10 mole L ⁻¹ ionic strength.....	209

A2.16	Absorbance and difference spectra of untreated and borohydride reduced Lignin Alkali Carboxylate at 1.00 mole L ⁻¹ ionic strength.....	210
A2.17	Absorbance as a function of SRHA untreated and borohydride reduced at ionic strengths 0.01 mole L ⁻¹ , 0.10 mole L ⁻¹ and 1.00 mole L ⁻¹	211
A2.18	Absorbance as a function of SRFA untreated and borohydride reduced at ionic strengths 0.01 mole L ⁻¹ , 0.10 mole L ⁻¹ and 1.00 mole L ⁻¹	212
A2.19	Absorbance as a function of EHA untreated and borohydride reduced at ionic strengths 0.01 mole L ⁻¹ , 0.10 mole L ⁻¹ and 1.00 mole L ⁻¹	213
A2.20	Absorbance as a function of LHA untreated and borohydride reduced at ionic strengths 0.01 mole L ⁻¹ , 0.10 mole L ⁻¹ and 1.00 mole L ⁻¹	214
A2.21	Absorbance as a function of PLFA untreated and borohydride reduced at ionic strengths 0.01 mole L ⁻¹ , 0.10 mole L ⁻¹ and 1.00 mole L ⁻¹	215
A2.22	Absorbance as a function of LAC untreated and borohydride reduced at ionic strengths 0.01 mole L ⁻¹ , 0.10 mole L ⁻¹ and 1.00 mole L ⁻¹	216
A3.1	Raman Scattering Energy Levels, including Rayleigh radiation and Stokes/Anti-Stokes scattering radiation that produce Raman scattering.....	218

List of Tables

2.1	Sample descriptions and abbreviations.....	14
5.1	Sodium borohydride needed to achieve uniform reduction of Leonardite humic acid at pH 10.4 and pH 7.6 as measured by decrease absorbance	57
5.2	Specific absorbance (S) values of humic and fulvic acids.....	63
5.3	Reoxidation induced pH changes for Suwannee River fulvic acid (SRFA), Suwannee River humic acid (SRHA), Leonardite humic acid (LHA), Elliott humic acid (EHA), and Pony Lake fulvic acid (PLFA).....	66
5.4	Percent change of spectral slope coefficients (S) for untreated and borohydride reduced humic and fulvic acid samples.....	76
6.1	Summary of the ϵ for untreated and borohydride reduced humic and fulvic acid samples and change in ϵ (% loss) at absorbance 350 nm OD and pH 7.6.....	115
6.2	Titrations of untreated and borohydride reduced humic substances, at three ionic strengths (0.01, 0.10 and 1.00 mole L ⁻¹ NaCl).....	122
6.3	pH dependence of spectral slope values associated with UV concentration range optical titrations and borohydride reductions at pH 7.6.	131
7.1	Experimental, historical and theoretical symmetry of pyridine from SERS spectra.....	166
A2.1	Summary of high concentration visible absorbance range (350-800 nm) figures presented in Appendix 1.....	194

Dissertation Overview

Humic substances (HS) and chromophoric dissolved organic matter (CDOM) are related and dynamic parts of the global carbon cycle. The unique optical properties of CDOM/HS are integral to their environmental behavior. CDOM/HS have been studied for decades but limited understanding of how their optical properties are generated remains elusive. The complexity of their environmental interactions in combination with limited understanding of the structural underpinnings make the chemical and physical behavior of CDOM/HS relevant to a broad range of scientific fields including microbial science, soil science, the study of the fate and transport of metals and anthropological chemicals, and the behavior of other nutrient cycles. In this study, the optical properties were chemically probed using a reductant that specifically targeted carbonyl groups. The optical and potentiometric behavior of the selected model CDOM compounds representing specific ecosystems (soil, fresh water aquatic and marine) were compared before and after reduction in order to ascertain their similarities and differences. Several spectroscopic techniques were used to measure the chemical reductant and pH induced changes to the optical properties including UV-Vis, fluorescence and Raman spectroscopy with the goal of identifying the chemical species involved in generating the unique optical properties universally found in CDOM.

This dissertation is divided into 8 chapters and 3 appendixes. Chapter 1 details the objectives of the study, the interrelations between dissolved organic matter (DOM), chromophoric dissolved organic matter (CDOM), and humic substances (HS) and their optical properties. Chapter 2 provides sample descriptions and locations. Chapter 3 presents two established models that provide justification for the experiments conducted in the subsequent chapters. The first model presented is the electronic interaction model which seeks to explain the

unique optical properties associated with all CDOM/HS. The second model presented is a combination of the non-ideal competitive absorption model (NICA) and the Donnan gel model. Chapter 4 presents the mechanism and rationale for using the chemical reductant sodium borohydride. Chapter 5 presents experimental results of the optical properties of untreated samples and changes that occur to the optical properties upon treatment with the chemical probe sodium borohydride as well as interpretation of the results in the context of existing models. Chapter 6 details the experimental results of optical titrations and interpretation of the experimental results in the context of relevant models. Chapter 7 is a limited study of surface enhanced Raman spectra of model compounds. Chapter 8 provides conclusions and insight into future work. Appendix 1 provides the mathematical background information for the NICA-Donnan model presented in Chapters 3 and 5. Appendix 2 is a compilation of spectra that is supplemental information to Chapter 6. Appendix 3 details the background theory of Raman and surface enhanced Raman spectroscopy in support of the experiments presented in Chapter 7.

Chapter 1 Background

Chapter 1 Overview

The importance of dissolved organic matter (DOM), humic substances (HS) and chromophoric dissolved organic matter (CDOM) to environmental processes make understanding of DOM/HS/CDOM fate and function in the environment critical to (1) understanding the global carbon cycle, (2) the fate of many anthropological chemicals (3) their interaction and impact on other nutrient cycles and (4) their ability to regulate metals and anthropogenic chemicals in the environment. The objectives of this study are presented in Sec. 1.1. Humic substances (HS), dissolved organic matter (DOM) and chromophoric dissolved organic matter (CDOM) are described in Sec. 1.2. Finally, the pH dependence and unique optical properties associated with all HS/CDOM samples are presented in Sec. 1.3.

1.1 Objectives

Many studies have shown a positive correlation of lignin phenols and DOM/CDOM in marine environments making the link between terrestrial inputs of plant material in the marine environment but the processes that give rise to the optical properties remains elusive. Studies seeking to elucidate and possibly decouple the complex relationship between CDOM generated in-situ in the marine environment from contributions from terrestrial sources, including this work, are needed in order apportion the global carbon mass balance. The study of humic substances from different sources may elucidate the underlying structure that gives rise to the common physical and chemical properties that exist between HS and CDOM and ultimately

enhance knowledge of global dissolved organic matter and dissolved organic carbon (DOM/DOC) fate and transport. Further, the ability to model differences in the optical and potentiometric properties of HS from sources of different origins may provide insights about the commonality or lack thereof of processes (biological, chemical, physical) that generate the optical properties universally associated with CDOM. The objectives of this study are to:

1. Investigate the optical differences between HS standards or reference material of different origins including the terrestrial and microbial sources and compare them to well studied aquatic model compounds Suwannee River humic and fulvic acids.
2. Utilize the chemical reductant sodium borohydride to selectively reduce carbonyl groups within the selected HS and follow the changes in optical properties, kinetics of the changes, response to oxygen and change in pH.
3. Measure the concentration dependence of borohydride reduction of terrestrial humic substance using the International Humic Substance Society (IHSS) standard Leonardite humic acid (LHS).
4. Optically titrate selected HS model compounds pre- and post-reduction with sodium borohydride.
5. Collect surface enhanced Raman (SERS) of untreated lignin phenols, quinones and borohydride reduced Suwannee River humic acids.
6. Interpret the experimental results in the context of the electronic interaction and NICA-Donnan models.

1.2 What are Humic Substances (HS), Dissolved Organic Matter (DOM) and Chromophoric Dissolved Organic Matter (CDOM)?

Humic Substances (HS) are ubiquitous in the environment, found in soil, fresh water aquatic and marine environmental systems. HS are decomposition products of plants and animals, as well as microbial exudates combining to varying degrees depending on the source material and how it is acted upon environmentally. They are a large and critical part of the global carbon cycle, impacting the fate and transport of other nutrient cycles, metals and anthropogenic chemicals. The ubiquitous nature and complexity of HS has led to the development of operationally defined sub-fractions that allow for continuity of definition and discussion in the scientific community. Two important sub-fractions are Dissolved Organic Matter (DOM), which is the filtrate of 0.2 μm solutions of HS, and Chromophoric Dissolved Organic Matter (CDOM), which is the fraction of DOM that can absorb light. This distinction is presented in Fig. 1.1. Both of the sub-fractions have been used to trace the fate and transport of the global carbon cycle (Hernes and Benner (2003)).

What is chromophoric dissolved organic matter (CDOM)?
 The link to dissolved organic matter (DOM)
 and humic substances (HS)

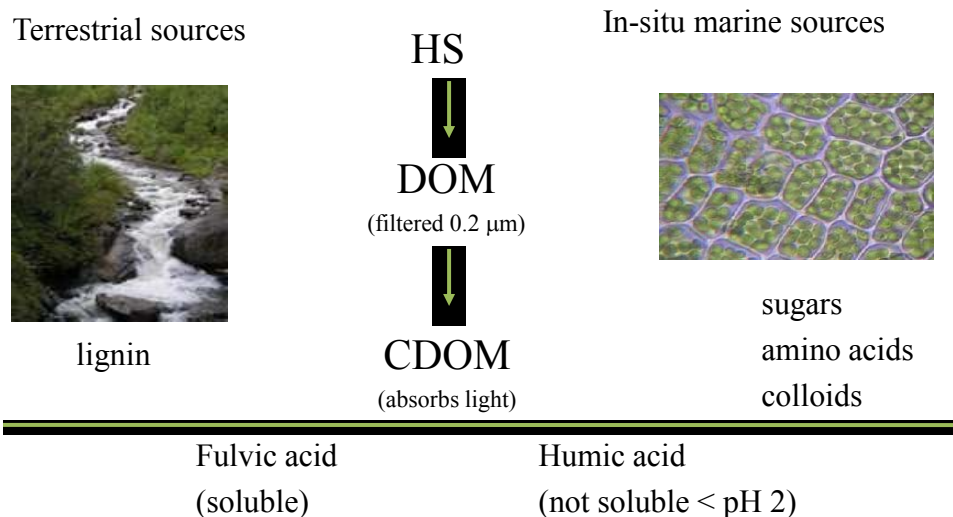


Figure 1.1 The operational definition of humic and fulvic acids, and their link to humic substance (HS) and colored dissolved organic matter (CDOM).

Two sources of CDOM have been identified based on their environmental persistence and resultant fingerprint. One source is microbially based and the other has a terrestrial origin. The microbially based source is comprised of decomposition products of complex sugars, amino acid groups and colloids possibly combining to form condensation products or decomposing and forming condensation products. The second source of CDOM is terrestrial in origin, stemming from lignin, which provides structural integrity to terrestrial plants (Fig. 1.1). These two sources of CDOM have been used to model the fate and transport of HS and are combined or isolated from each other depending of sinks and sources in the environment, as illustrated in Fig. 1.2.

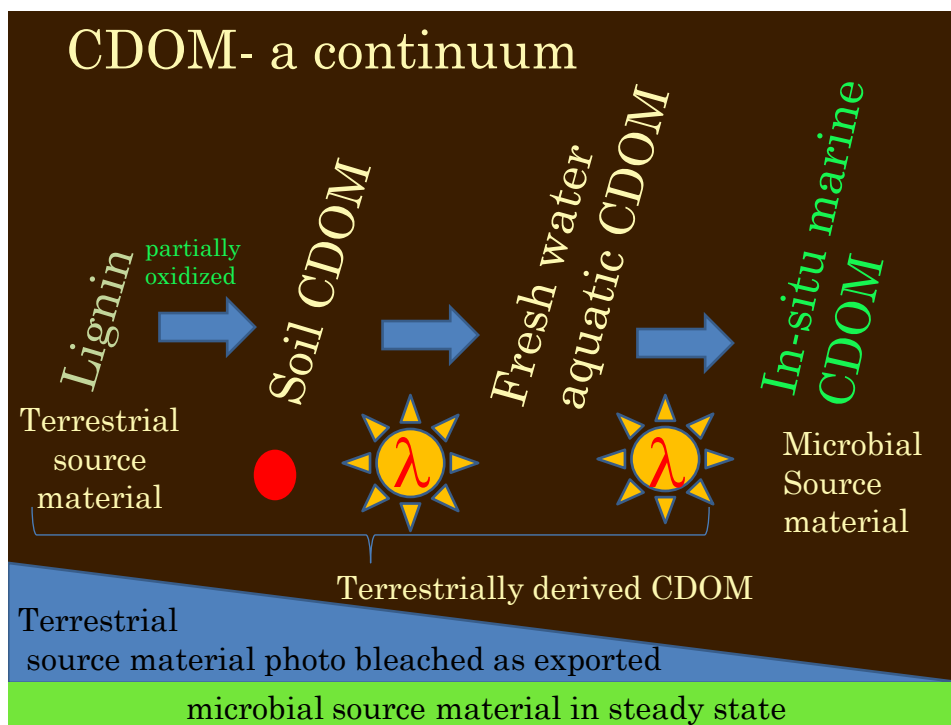


Figure 1.2 Chromophoric dissolved organic matter (CDOM) in the environment.

DOM is acknowledged as one of the largest pools of reduced carbon on the Earth's surface, but little is known about its chemical constituents or mechanism of formation (Jørgensen, Stedmon, Kragh, Stiig Markager, Middelboe and Søndergaard (2011)). If DOM is described on the basis of dissolved organic carbon (DOC), then estimates of the CDOM pool range from as little as 20 % to as much as 70 % of the total DOC/DOM (Lanne and Koole (1982)), ((Jørgensen, Stedmon, Kragh, Stiig Markager, Middelboe and Søndergaard (2011)). This wide range of reported values of the fraction of CDOM in DOC/DOM reflects a real deficit in understanding of the fate and transport of DOM and all of its sub-fractions in the environment.

1.2.1 Operational Definitions

Organic matter, exported from terrestrial environments and generated in aquatic and marine environments, has been studied for decades (Coble (2007)), (Hayes (1989)). Historically user defined fractions were employed to describe specific components of analytical interest. The continuum of processes that occur as organic and inorganic matter is exported from terrestrial environments, co-mingled with aquatic and marine sources of organic and inorganic matter, and transformed is complex and ultimately leads to ambiguity in the form, fate and even time scale of interactions (Coble (2007)), (Hayes (1989)), (Moran, Sheldon and Zepp (2000)), (Nelson and Guarda (1995)), (Hernes and Benner (2003)), (Del Vecchio and Blough (2004)). This complexity has led to a need to simplify the focus of experiments in order to generate relevant and manageable scientific data. Precise, artificial operational definitions have been developed in order to avoid ambiguity (Fig. 1.1 and Sec. 1.1).

1.2.2 The Importance of CDOM in Aquatic Environments.

CDOM is a not completely understood component in the global carbon cycle, frequently used to trace DOM and impacting environmentally and or economically relevant fields at fundamental levels (Jørgensen, Stedmon, Kragh, Markager, Middelboe and Søndergaard (2011)), (Hansell, Carlson, Repeta and Schlitzer (2009)). CDOM absorbs ultraviolet (UV-A and UV-B) and visible light (Blough and Zepp (1995)), (Moran, Sheldon and Zepp (2000)), (Blough and Del Vecchio (2002)), (Del Vecchio and Blough (2002)), (Vodacek, Blough, DeGrandpre, Peltzer and Nelson (1997)). It regulates the penetration depth of solar radiation in aquatic systems and as such plays a central role in the protection of aquatic organisms from potentially harmful UV radiation (Whitehead, de Mora, Demers, Gosselin, Monfort and Mostajir (2000)), (Blough and

Del Vecchio (2002)), (Blough and Zepp (1995)). In coastal waters with riverine inputs the ability of CDOM to absorb solar radiation in the visible region at blue wavelengths causes direct competition with phytoplankton, thus limiting primary production directly (Vodacek, Hoge, Swift, Yungel, Peltzer and Blough (1995)), (Vodacek, Blough, DeGrandpre, Peltzer and Nelson (1997)), (Blough and Del Vecchio (2002)). CDOM sunlight absorption causes formation of photochemical intermediates and products including reactive oxygen species (ROS) (Voelker and Sedlak (1995)), (Voelker, Morel and Sulzberger (1997)), (Kieber and Blough (1990)), (Vaughan and Blough (1998)), (Southworth and Voelker (2003)), (Blough and Del Vecchio (2002)).

The photochemical reactions produced by solar radiation working on CDOM substrate have extensive consequences, including the destruction of CDOM, which can alter the aquatic light field causing increases in primary production near shore and possibly loss of primary production off-shore due to increased solar penetration, changes in metal ion speciation due to direct photochemistry (Barbeau, Rue, Bruland and Butler (2001)), or reactions with reactive oxygen species (ROS) (Zafiriou, Voelker and Sedlak (1998)). Additionally, photo-oxidative degradation of organic matter by production of ROS increases the biologically available low molecular weight organic compounds, releasing nutrients such as nitrogen, sulfur and iron (Rose and Waite (2006)), (Rose and Waite (2003)), (Moore and Blough (2002)), (Dahl, Saltzman and Bruyn (2003)), (Moran and Zepp (1997)), (Goldstone, Pullin, Bertilsson and Voelker (2002)). Finally, the production of atmospherically important trace gases such as CO₂, CO and COS (as well as the fate of dimethyl sulfide) is tied to photochemical reactions operating on CDOM as a substrate (Johannessen and Miller (2001)), (Xie, Liu, Fu, Wang, Liu and Wei (2004)), (Jones and Amador (1993)), (Toole, Slezak, Kiene, Kieber and Siegel (2006)) and (Galí and Simó (2010)).

An increase in the use of satellite ocean color measurements to determine biomass production and seawater constituents, such as chlorophyll, also necessitates a better understanding of the CDOM contribution to the total absorption spectra (Blough and Del Vecchio (2002)).

In marine environments, two main pools of CDOM have been postulated recently by (Jørgensen, Stedmon, Kragh, Markager, Middelboe and Søndergaard (2011)). The first is microbial in origin stemming from fluorescent amino acids tryptophan and tyrosine. This pool is found in direct association with biota at the sea surface layer (0-200 m). The concentration of amino-acid-like CDOM decreases with ocean depth. It is thought to be labile to moderately labile, available to varying degrees as a microbial substrate, parts of it immediately utilized by biota and the remainder utilized when other available substrates are depleted. The second pool is described as humic-like, stemming from terrestrial DOM. Although the humic acid fraction of CDOM attributed from terrestrial sources has been used to trace riverine inputs into the ocean and to trace ocean water mass patterns, an unknown contribution in quantity and structure appears to be marine in origin. DOM generated in-situ in marine environments is by far the largest contributor to DOM in the ocean. Riverine inputs to the Pacific Ocean are currently estimated to be $\leq 1\%$ of total DOM and $\leq 3\%$ in the Atlantic Ocean (Hernes and Benner (2003)). These numbers are likely to rise in response to global surface temperature increases and subsequent export of Arctic terrestrial DOM as snow cover is reduced, introducing sunlight absorbing biomass (Amon, Rinehart, Duan, Louchouart, Prokushkin, Guggenberger, Bauch, Stedmon, Raymond, Holmes, McClelland, Peterson, Walker and Zhulidov (2012)), (Letscher, Hansell and Kadko (2011)), (Stedmon, Amon, Rinehart and Walker (2011)).

The carbon export from river sources is enough to support the carbon load in the oceans, but the direct link from terrestrial sources has an estimated lifetime of up to 100 years, with the

exception of black carbon which has a much longer lifetime, on the scale of 1000's of years. The main process that depletes terrestrial inputs of DOM/CDOM in the marine environment is known to be photo oxidative degradation in sunlit waters and microbial degradation in dark water (Goldstone, Del Vecchio, Blough and Voelker (2004)), (Hernes and Benner (2002)), (Hernes and Benner (2003)). Given that the recalcitrant CDOM from terrestrial sources are such a small percent of the overall carbon budget, it has a huge impact on the biogeochemistry of the ocean.

1.2.3 The Optical Properties of CDOM in Aquatic and Marine Ecosystems

Optical studies of CDOM, with the exclusion of CDOM linked to amino acids, have shown no distinct absorption bands but instead show a continuum of absorption and fluorescence (Bricaud, Morel and Prieur (1981)), (Green and Blough (1994)), (Hayes (1989)). The absorption spectra decrease with increasing wavelength and can be described by an exponential curve as in Eq. 1.1 and Fig. 1.3,

$$a(\lambda) = a(\lambda_0) \exp^{-S(\lambda - \lambda_0)}, \quad (1.1)$$

where $a(\lambda)$ and $a(\lambda_0)$ are the absorption coefficients at wavelength λ and the reference wavelength, respectively. S is the spectral slope coefficient. The spectral slope coefficient has been observed to change in relation to the geographical position of the sampling site, increasing as the sampling site moves from fresh waters and coastal waters to the open ocean (Hayes (1989)), (Hernes and Benner (2003)), (Del Vecchio and Blough (2004)), (Moran, Sheldon and Zepp (2000)), (Vodacek, Blough, DeGrandpre, Peltzer and Nelson (1997)), (Whitehead, de Mora, Demers, Gosselin, Monfort and Mostajir (2000)). The increase denotes less visible light absorbance as CDOM moves from the inland and coastal environments to the open ocean. The

physical changes that occur during this transit have not been thoroughly investigated and are not completely understood. Positive correlation has been found between reduction of molecular weight of CDOM and increases in the value of S (Benner and Kaiser (2010)), (Obernosterer and Benner (2004)), (Chin, Aiken and O'Loughlin (1994)).

The excitation emission (EEMS) fluorescence spectra of untreated CDOM samples exhibit a red shift in peak emission maxima as the excitation wavelength is increased. This is shown in Fig 1.3. Upon chemical or photochemical reduction and concurrent with the increased value of S and the decrease in molecular weight, a blue shift in the emission spectra is observed for off-shore, irradiated water (Hayes (1989)), (Obernosterer and Benner (2004)), (Chin, Aiken and O'Loughlin (1994)), (Lou and Xie (2006)), (Yacobi, Alberts, Takacs and McElvaine (2003)) and borohydride reduced CDOM (Ma, Del Vecchio, Golanoski, Boyle and Blough (2010)).

The quantum yield is the ratio of photons fluorescing in response to the photons absorbed and has a pattern that combines the absorbance and fluorescence spectra as seen in Fig 1.3. The quantum yield increases from low wavelength to a maximum that corresponds to the fluorescence emission maxima and then decreases at long wavelengths.

Optical Properties of PLFA

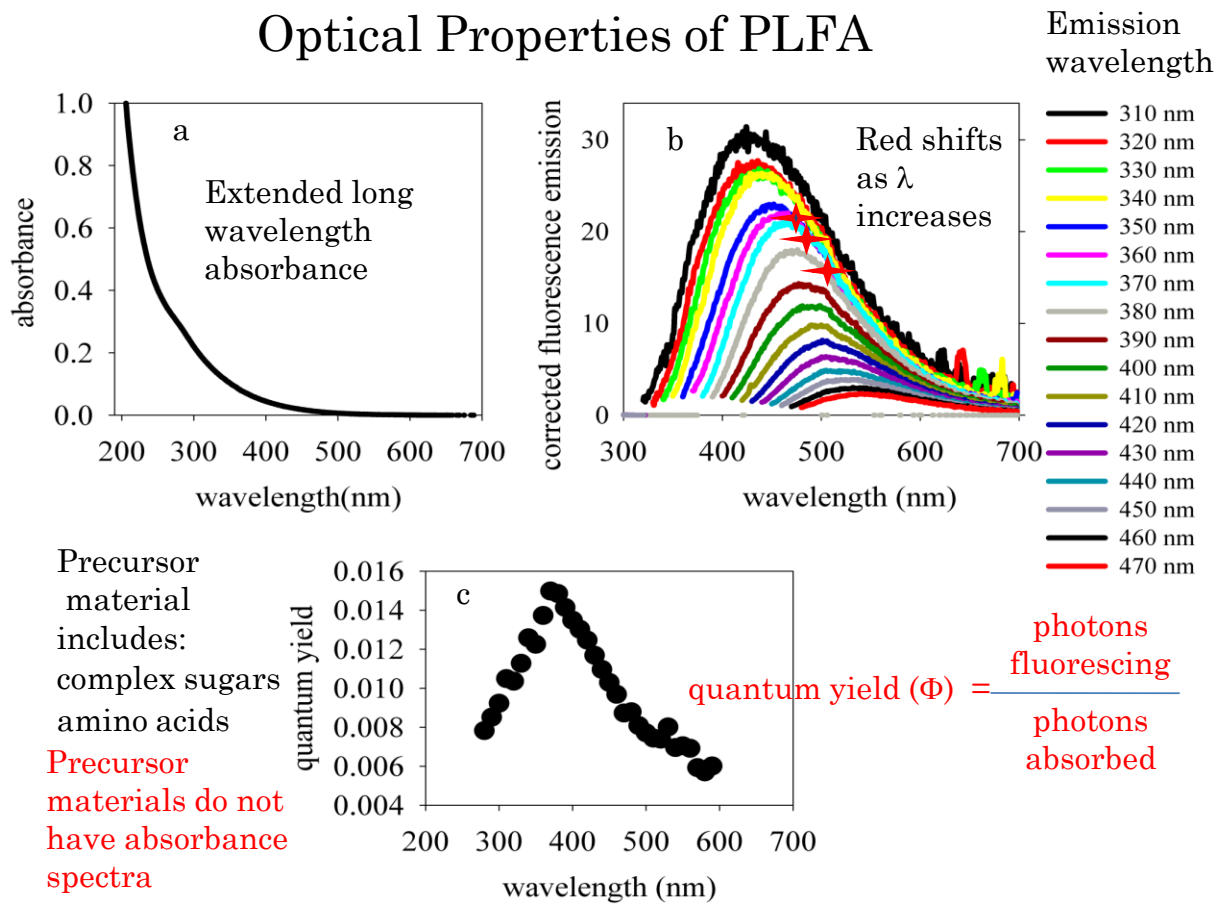


Figure 1.3 Universal optical properties of CDOM. Absorbance (panel a), fluorescence (panel b) and quantum yield (panel c)

Chapter 2 Sample Descriptions and Locations

Chapter 2 Overview

This chapter provides a description of the model compounds used in the study and the sources of those model compounds. It is divided into three sections. The first section (Sec. 2.1) describes the model humic substances (HS) and is divided into three subsections. Sec. 2.1.1 details soil humic substances. Sec. 2.1.2 details freshwater aquatic humic substance. Sec. 2.1.3 details microbial humic substances. The second section (Sec. 2.2) is a survey of recalcitrant material in dissolved organic matter (DOM). It is divided into two sections, the composition of lignin (Sec 2.2.1) and the link between lignin and humic acids (Sec 2.2.2). The third section of Chapter 2 covers the chemical components of Pony Lake fulvic acid (PLFA) (Sec. 2.2.3).

2.1 Model Humic Substances

The International Humic Substances Society (IHSS) since the late 1970's has provided standards and reference materials so that scientists working on humic substances can standardize their experiments to better compare results. In the following series of experiments several standards and a reference material from IHSS as well as a commercial lignin standard will be used. The aim is multifold. First, a comparison of the optical properties from different source materials will be made. The second series of experiments will investigate changes in the optical properties due to chemical reduction alone or in combination with potentiometric titration. The inclusion of HS generated from different origins serves to highlight chemical and optical differences or similarities among HS and CDOM.

The standards from IHSS and their catalog numbers:

1. Suwannee River Fulvic Acid (SRFA) (2S101F)
2. Suwannee River Humic Acid (SRHA) (2S101H)
3. Leonardite Humic Acid (LHS) (1S104H)
4. Elliot Humic Acid (EHS) (1S102H)
5. Pony Lake Fulvic Acid (PLFA)* (1R109F)
6. Alkali Carboxylated Lignin (LAC)[&]

*Reference material, which means it has not been fully accepted as a standard, [&] from Fisher Scientific.

The samples used in this study, a description of each sample and their abbreviation are presented in Table 2.1.

Table 2.1 Sample descriptions and abbreviations of the materials used in this study

Sample name	Description	Abbreviation
Elliott Humic Acid	Central plains IO, USA Soil type Mollisol sub order: Aquic Arguidoll- poorly drained prairie soil	EHA
Leonardite Humic Acid	Lignite Coal precursor fossilized plant material SD, USA	LHA
Suwannee River Humic Acid	Suwannee River, GA USA Drains the Okeefenokee swamp a cypress wetland	SRHA
Suwannee River Fulvic Acid	Suwannee River, GA Drains the Okeefenokee swamp a cypress wetland	SRFA
Pony Lake Fulvic Acid	Hypereutrophic pond, Antarctica	PLFA
Delaware Bay - colored dissolved organic matter	Delaware Bay, DE Drains Delaware River into the Atlantic Ocean	DB-CDOM
Mid-Atlantic Bight Shelf-colored dissolved organic matter	Atlantic Ocean, open water	MAB-CDOM
Lignin Alkali Carboxylate	Commercial Form of Lignin	LAC

2.1.1 Soil Humic Acids

Leonardite Humic material is derived from oxidized lignite. It is obtained from the central plains and is mined commercially. Lignite is derived from peat that has been buried. The increased pressure associated with burial over time leads to increased compaction and decreased levels of oxygen (IHSS). Elliott Humic material is obtained from the O and A horizons of a mid-western prairie grassland soil. It contains more oxygen than does Leonardite humic acid. The origins of these two samples represent terrestrially generated material, as depicted in Fig. 2.1.

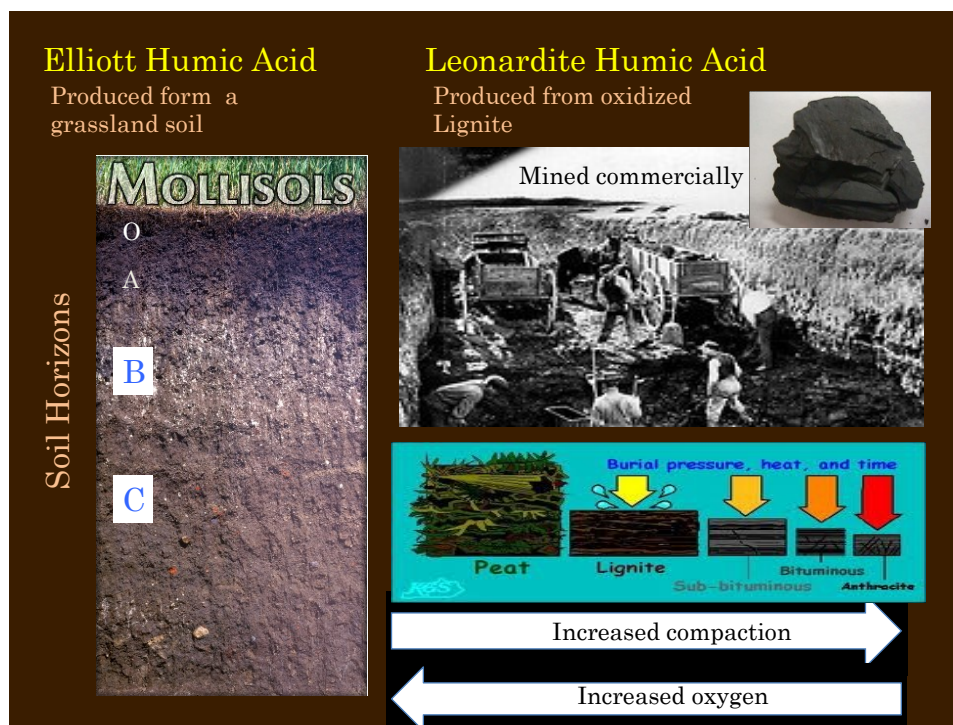


Figure 2.1 Origin of terrestrial humic acids used in this study

2.1.2 Freshwater Aquatic Humic Substances

Standards from Suwannee River (SRFA) and (SRHA) are obtained from the Suwannee River watershed, shown in Fig. 2.2. These two standards represent fulvic and humic acid from a fresh water aquatic source. The dissolved organic carbon (DOC) in the watershed is between 25-75 mg L⁻¹ and the pH of the river is 4. It is derived from decomposing plants.



Figure 2.2 The Suwannee River Watershed, which is the site of the source material for the standards SRFA and SRHA

2.1.3 Microbial Humic Substance

Pony Lake Fulvic Acid (PLFA) is obtained from a saline, hypereutrophic lake in Cape Royds, Costal Ross Sea, Antarctica. This lake lacks plant or soil derived DOM. It is a reference compound for microbially derived CDOM. Although fulvic acids have higher nitrogen levels than do humic acids, PLFA has higher than usual nitrogen levels among fulvic acids. The conjecture supported by solid state NMR findings is that the lake may be receiving extra nitrogen from penguin guano (Fimmen, Cory, Chin, Trouts and McKnight (2007)). Despite the possible addition of non-microbial inputs PLFA meets the requirements of IHSS reference material and will be used as such in these experiments (Brown, McKnight, Chin, Roberts and Uhle (2004)), (McKnight, Andrews, Spaulding and Aiken (1994)), (Chin, Aiken and O'Loughlin (1994)). Recall that the IHSS standards and reference materials are operationally defined fractions of DOM and may have been physically altered during the extraction process; as such they may not provide a completely representative model compound for natural DOM or CDOM.

2.2 Recalcitrant Material in DOM

In addition to lignin, other chemical classes of recalcitrant material of terrestrial origin found in DOM are black carbon, long chain fatty acids, and sugars (polysaccharides), postulated to be from microbial cell walls, as seen in Fig. 2.3 (Hwang and Druffel (2003)), (Hernes and Benner (2003)), (Hedges, Keil and Benner (1997)), (Hedges, Mayorga, Tsamakis, McClain, Aufdenkampe, Quay, Richey, Benner, Opsahl and Black (2000)), (Aluwihare, Repeta and Chen (1997)), (Leenheer, Wershaw and Reddy(1995)).

Recalcitrant components in terrestrial HA:

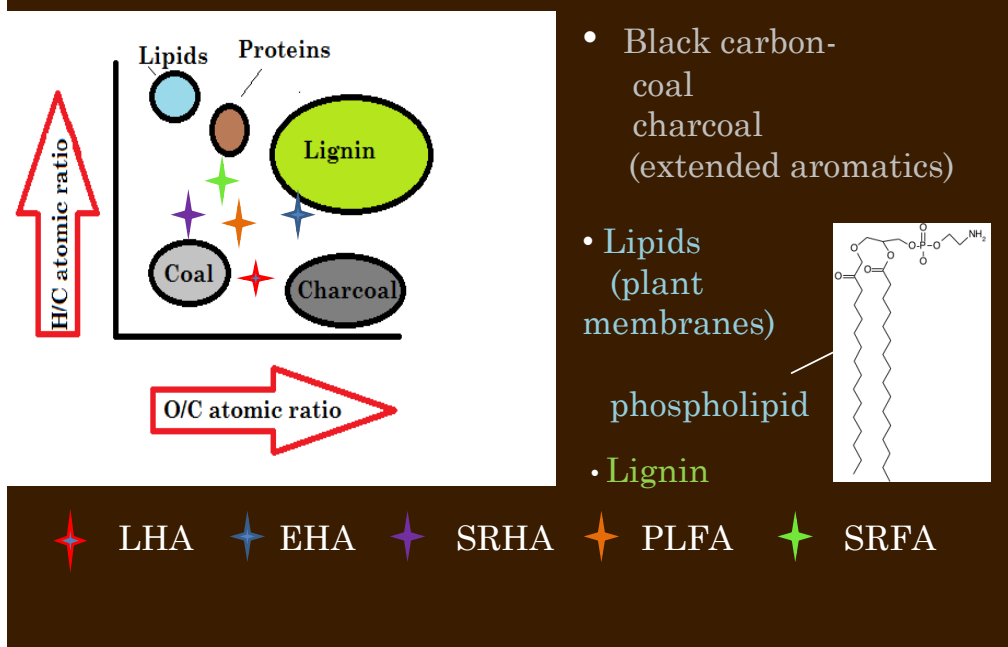


Figure 2.3 Theoretical van Krevelin plot of the possible precursor components incorporated in terrestrially derived humic acid and a projection of where selected CDOM samples might fall on the plot of hydrogen/carbon atomic ratio versus oxygen/carbon atomic ratio, including Leonardite humic acid (LHA), Elliott humic acid (EHA), Suwannee River humic (SRHA), Suwannee River fulvic acid (SRFA), and Pony Lake fulvic acid (PLFA).

Although long chain fatty acids and neutral sugars have been identified, they do not absorb or fluoresce independently and do not include chemical moieties that can participate in charge transfer or electronic interactions. However, this does not preclude further chemical reactions, including a Millard reaction or other condensation pathways that would be able to generate a colored product. Advances in analytical abilities in the 1990's revealed that organic nitrogen in soil and seawater is found as an amide, while ocean sediments and condensation products or melanoidins are aromatic compounds, making condensation reactions unlikely as the

primary pathway of DOM formation in the environment (Hedges, Mayorga, Tsamakis, McClain, Aufdenkampe, Quay, Richey, Benner, Opsahl and Black (2000)).

Black carbon is generated by charring of plant material and is commonly found in terrestrial HS (Mao and Schmidt-Rohr (2004)), (Krull, Baldock and Skjemstad (2003)), (Baldock and Skjemstad (2000)), (Mahieu, Randall and Powlson (1999)), (Haumaier and Zech (1995)). It consists of extended aromatic systems with a high C:H ratio. Black carbon has also been found in ocean sediments and is postulated to be transferred into the ocean via aeolian inputs before descending to the sediment layer as particle organic matter (POM). It does not appear to interact with the microbial food web (Dittmar (2008)), (Hernes and Benner (2002)).

Soil humic and fulvic acids are derived from the same material as aquatic humic and fulvic acids but the differences in environmental processes that each type (soil or aquatic) is subjected to may dictate their physical properties in several ways, such as black carbon concentration, nucleic acid distributions, levels of molecular oxygen, as well as ability to accept electrons (EAC).

Black carbon is defined as extended conjugated carbon ring systems. It is found ubiquitously in the environment. Dissolved black carbon ring systems as measured by high-performance liquid chromatography and diode array detection indicate that the extent of the conjugated system and the number rings in the conjugated system decreases in marine waters as a function of distance from the coast. Samples taken in the Gulf of Mexico 80 km offshore identified 0.9 % of the DOC in a conjugated structure, corresponding to 7- six-member rings in a conjugated arrangement as determined by mass spectral analysis following nitric acid oxidation (Dittmar (2008)). Algae samples analyzed in the same study had negligible amounts of black carbon, less than 0.02% of the total DOC. Near shore samples in the Gulf of Mexico exhibited

2.6 % conjugation of the total DOC and higher extent of conjugation (Dittmar (2008)). NMR studies of conjugated carbon systems in Pony Lake fulvic acid identified an average maximum amount of conjugation to be 7 6-member rings (Mao, Cory, McKnight and Schmidt-Rohr (2007)). Higher black carbon concentrations are found in soil humic acids such as Elliott and Leonardite humic acids than in aquatic, lignin derived humic/fulvic acids according to NMR studies. Black carbon is found in marine sediments but the primary input of black carbon to ocean sediments is thought to be aeolian with additional secondary input from exported fresh water humic and fulvic acids reflecting the loss of black carbon as a function of off-shore distance (Hernes and Benner (2002)). Aeolian inputs of black carbon are not incorporated into exported humic/fulvic acids as they are observed to be depleted in off-shore samples.

Amino acids are found in all sources of humic substances with the exception of Leonardite humic acid. The lack of amino acids in Leonardite humic materials is likely linked to fossilization and subsequent loss of biological processes.

Aeschbacher, in electrochemical reductions of model HS demonstrated a hierarchy of electron accepting capacities (EAC) in humic and fulvic acids (Aeschbacher, Sander and Schwarzenbach (2010)). The highest EAC's were found in terrestrial humic acids. Higher EAC supports the presence of higher oxidation level moieties in soil derived HS. Soil derived HS may be more closely related to plant source material than aquatic HS and, as such, may be more heterogeneous in the functional groups represented in its structure. In work done by (Thorn, Younger and Cox (2010)) loss of functional groups in Nordic aquatic fulvic acid and Suwannee River acids exposed to UV irradiation showed a preferential loss during all irradiation of ketones, aromatic, and O-alkyl carbons. Alkyl carbon was recalcitrant to UV irradiation. Soil derived humic substances are not subjected to UV radiation to the extent that aquatic HS are.

Further, Leonardite humic acid is derived from naturally oxidized lignite, which by definition is fossilized plant material (Allard (2006)). Leonardite humic acid has proportionally on a mass basis less oxygen than Elliott humic acid. Elliott humic acid is derived from a Mollisol order soil in the sub-order Aquic Arguidoll. Aquic arguidoll is a poorly drained prairie soil found in Iowa, USA (Brady and Weil (2002)).

Long chain fatty acids and polysaccharides are postulated to be from degraded bacterial cell wall material. They are frequently described in relation to the microbial food web as moderately labile, entering the microbial food web only after more accessible substrates have been depleted (Aluwihare, Repeta and Chen (1997)). The magnitude and mode of incorporation or interaction of long chain fatty acids and polysaccharide into the macrostructure of DOM are not as well known as that of lignin phenol. Functional groups that have been identified by nuclear magnetic resonance (NMR) and other techniques, such as electro-spray ionization mass spectroscopy and pyrolysis confirm the presence of functional groups derived from long chain fatty acids and polysaccharides (Nocentini, Certini, Knicker, Francioso and Rumpel (2010)), (Fang, Chua, Klaus Schmidt-Rohr and Thompson (2010)), (Mao and Schmidt-Rohr (2006)), (Haumaier and Zech (1995)).

2.2.1 The Composition of Lignin

The current knowledge of the composition of lignin, the polymeric precursor of humic substances and ultimately terrestrial and aquatic CDOM, provides the justification for the selection of CDOM model compounds (Obernosterer and Benner (2004)), (Chen, Bissett, Coble, Conmy, Gardner, Moran, Wang, Wells, Whelan and Zepp (2004)), (Yacobi, Alberts, Takacs and McElvaine (2003)), (Lou and Xie (2006)), (Del Vecchio and Blough (2002)), (Benner,

Louchouart and Amon (2005)), (Opsahl and Benner (1997)). The polymeric structural organization of lignin and the identity of lignin monomers from many soft and hard woods are known (Vermerris and Nicholson (2006)). Lignin from sources used by the paper and wood product manufacturing industries has been well studied for many decades. The polymeric structural organization of lignin from many terrestrial plants not used commercially is less well known, but the basic monomer compositional units are undebated and identified as the lignols: p-coumaryl alcohol, coniferyl alcohol and sinapyl alcohol, as presented in Fig. 2.4 (Glasser (2000)).

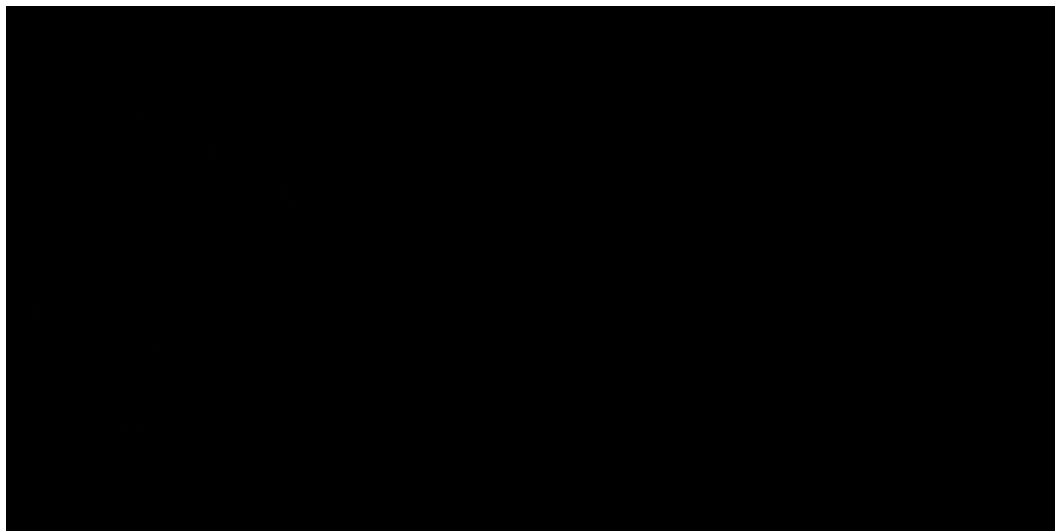
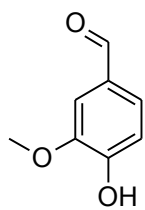


Figure 2.4 Structures of sinapyl, coniferyl and p-coumaryl alcohols

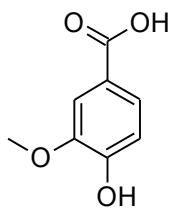
The parameters that are widely accepted as important for lignin analysis inform the analysis of CDOM, namely: (a) identity of the basic repeating units; (b) chemistry of the repeating bonds; (c) molecular size/weight considerations; (d) inter/intra molecular bonds (Glasser (2000)). Enzymatic and chemical degradation of the lignin macromolecule has been

used to predict basic monomer units of CDOM. Presence of specific phenols and methoxy-phenols in chemical oxidation reactions of CDOM infers terrestrial origin. In experiments done in the early 2000's Hernes and Benner linked digenesis of lignin phenol to photo-oxidative degradation. They also found microbial decomposition occurred, but to a much lower extent, and that microbial action did not affect the acid to aldehyde ratio of lignin phenols. The work of Hernes and Benner lead directly to the use of lignin phenols as tracers of riverine input of terrestrial DOM input into the ocean, as well as their use as a tracer of ocean water mass movements (Hernes and Benner (2002)).

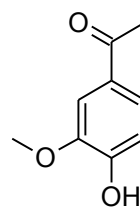
The compounds in Fig. 2.5 are routinely used to study CDOM. The ratio of acid to aldehyde ratio indicates the state of digenesis and the source of the original plant material (Kögel-Knabner (2002)), (Hernes and Benner (2002)). It easily follows that further oxidative reactions can easily produce quinones and hydroquinones within the structural framework of the CDOM polymer.



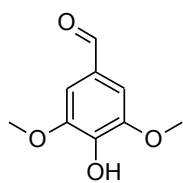
vanillin



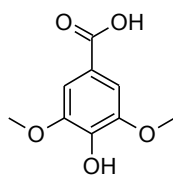
vanillic acid



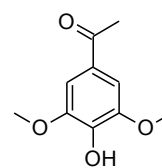
acetovanillone



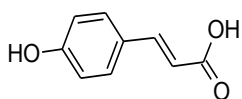
syringaldehyde



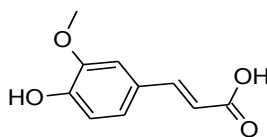
syringic acid



acetosyringone



para-coumaric acid



ferulic acid

Figure 2.5 Compounds used to study the terrestrial origin of CDOM

2.2.2 The Link between Lignin and Humic Acids

Terrestrial humic and fulvic acids extracted from soil or water environmental systems are derived from lignin phenols (Kögel-Knabner (2002)), (Hernes and Benner (2002)). The kinetics of photobleaching of CDOM by solar radiation in natural waters provides insight into the loss of recalcitrant terrestrial organic matter in the ocean and in freshwater systems. The

photobleaching process for terrestrial derived CDOM is attributed to the continuing oxidative destruction of the chromophores associated with DOM or CDOM (Lou and Xie (2006)), (Hernes and Benner (2003)), (Goldstone, Pullin, Bertilsson and Voelker (2002)), (Wetzel (2001)), (Moran, Sheldon and Zepp (2000)). The loss of a chromophore can occur by direct or indirect photochemical reactions. Direct photochemical reactions may lead to the cleavage of the CDOM into smaller fragments, thus destroying the chromophore. A reasonable understanding of the rates and mechanisms of photobleaching has yet to be obtained (Lou and Xie (2006)), (Hernes and Benner (2003)), (Yacobi, Alberts, Takacs and McElvaine (2003)), (Goldstone, Pullin, Bertilsson and Voelker (2002)), (Moran, Sheldon and Zepp (2000)).

2.2.3 Chemical Components of Pony Lake Fulvic Acid

Pony Lake Fulvic Acid (PLFA) is a HS derived solely from microbial sources. All fulvic acids exhibit increasing absorbance as wavelength decreases (McKnight, Andrews, Spaulding and Aiken (1994)). Fulvic acids derived solely from microbial sources have a yellow color but have been found to absorb less light than fulvic acids from terrestrial sources (McKnight Andrews, Spaulding and Aiken (1994)). Pony Lake fulvic acid has a lower percentage dissolved organic carbon (DOC) (13-22%) than does fulvic acids from temperate lakes with terrestrial input (30-60%) (Brown, McKnight, Chin, Roberts and Uhle (2004)), (McKnight, Andrews, Spaulding and Aiken (1994)), (Thurman, 1985). Elemental analysis of International Humic Substance Society (IHSS) standards and reference materials, conducted by Huffman Laboratories in Wheat Ridge, Colorado, clearly shows that PLFA is much richer in nitrogen, sulfur and phosphorus than any of the other humic substances (Brown, McKnight, Chin, Roberts

and Uhle (2004)). Functional group analysis conducted by (Mao, Cory, McKnight and Schmidt-Rohr (2007)) using a variety of nuclear magnetic spectroscopy techniques confirms that PLFA does not contain chemical functional moieties such as aromatic methoxy groups (-OCH₃) associated with the presences of higher plants and terrestrial sources of humic acids. The chemical constituents (C, H, and O) are the same as those found in terrestrial sources of humic acids but the connectivity differs and nitrogen is incorporated at a much higher level than is found in other fulvic acids.

In NMR analysis, comparing the precursor algae thought to be the major source of PLFA to PLFA itself significant changes were found to exist between the algae and the resultant fulvic acid. The NMR findings identified a large fraction of quaternary carbon bonded to nitrogen, a 8% increase in aromatic non-protonated carbon, but no large domains of polysaccharides or aromatic regions, as well as an increase in keto groups, ethyl groups (CH₂) and carboxylic (COOH) groups. Branched alkyl structures appear to be 25-50 % of the carbon in PLFA. Peptides were implicated by the presence and NMR shift of CH and CN groups (Mao, Cory, McKnight and Schmidt-Rohr (2007)). Components associated with sugar rings (OCH, O-CH-O and OCH₂) were identified by spectral editing (Mao, Cory, McKnight and Schmidt-Rohr (2007)). As previously stated, PLFA is enriched in nitrogen when compared to other fulvic acids and the increase has been in part attributed to penguin guano decomposition products, specifically a five-member ring metabolite of purine (Fang, Mao, Cory, McKnight and Schmidt-Rohr (2011)). The structure consistent with the chemical shifts was found to be allantoin, as presented in Fig. 2.6.

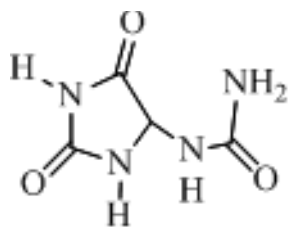


Figure 2.6 Allantoin

Although PLFA is structurally different than other humic acids, it nevertheless behaves optically and electrochemically in a manner consistent with aquatic humic acids from terrestrial sources (Fimmen, Cory, Chin, Trouts and McKnight (2007)), (Brown, McKnight, Chin, Roberts and Uhle (2004)), (McKnight, Boyer, Westerhoff, Doran, Kulbe and Andersen (2001)), (McKnight Andrews, Spaulding and Aiken (1994)). Absorbance extends past 350 nm, decreasing with increasing wavelength indicating the presence of charge transfer complexes (Fig 1.3). Clearly, charge transfer bands cannot be generated in the same manner as attributed to terrestrial sources of humic acids via the partial oxidation of lignin phenols but moieties capable of forming charge transfer structures are present and are potentially capable of producing extended absorbance in the visible range (> 350 nm).

Pony Lake fulvic acid exhibits fluorescence emission that is a wide distribution centered between 350 and 360 nm, depending on the excitation wavelength. The fluorescence emission characteristics indicate that PLFA fluorescence is not directly or solely linked to the three amino acids capable of producing fluorescence, but instead is a product of decomposition products that may have a chemically or photolytically degraded amino acid source.

In a recent global scale oceanic survey seven distinct fractions of fluorescence were identified by Excitation Emission Matrix Spectroscopy (EEMS) and analyzed with multivariate

data analysis technique Parallel Factor (PARAFAC) (Jørgensen, Stedmon, Kragh, Stiig Markager, Middelboe and Søndergaard (2011)). Two of the fluorescence fractions were linked directly to terrestrial humic material. Four of the identified fluorescence fractions were attributed to the amino acids tryptophan, tyrosine or possibly phenylalanine directly or linked to protein(s). The final fluorescence fraction could not be related directly to amino acids or terrestrial humic material (Jørgensen, Stedmon, Kragh, Stiig Markager, Middelboe and Søndergaard (2011)). Fluorescence emission spectra of microbial and terrestrial fulvic acids indicate microbially linked sources of fulvic acids have fluorescence fractions with shorter wavelength maxima (< 400 nm) than terrestrial sources of fulvic acids, with wavelength maxima between 350-360 nm that red shift as excitation wavelengths lengthen (Jørgensen, Stedmon, Kragh, Markager, Middelboe and Søndergaard (2011)). Microbially linked fluorescence fractions have emission spectra with a sharp emission profile when compared to fluorescence fractions linked to terrestrial sources.

Chapter 3 Models

Chapter 3 Overview

This chapter is divided into two sections. Section 3.1 presents the electronic interaction or charge transfer model, which is the basis for the chemical probe experiments completed in Chapter 4, the optical titrations completed in Chapter 5 and the Raman spectroscopy investigations completed in Chapter 6. Section 3.2 presents the non-ideal competitive absorption model in combination with the Donnan gel model (NICA-Donnan), which is the model basis for the optical titrations completed in Chapter 6.

3.1 Electronic Interaction or Charge Transfer Model

Two possible models have been proposed to explain the optical properties of CDOM and HS; the superposition model and the charge transfer model. The superposition model explains the optical phenomena as the sum of independently acting chromophores that are electronically isolated. The electronic interaction model depicted in Fig 3.1 proposes electronic interactions from related chromophores in physical proximity to each other creating new, lower energy optical transitions or charge transfer bands (Blough and Del Vecchio (2002)). In Fig. 3.1, the absorbance spectra of quinones (red line) and phenols (green line) generated by the partial oxidation of lignin phenols as detailed in Sec. 2.2.2 interact electronically to form charge transfer bands (blue line) that extend the absorption spectra to wavelengths that are not present in the absorption spectra of either quinones or phenolic groups individually (Ma, Del Vecchio, Golanoski, Boyle and Blough (2010)).

Electronic Interaction Model

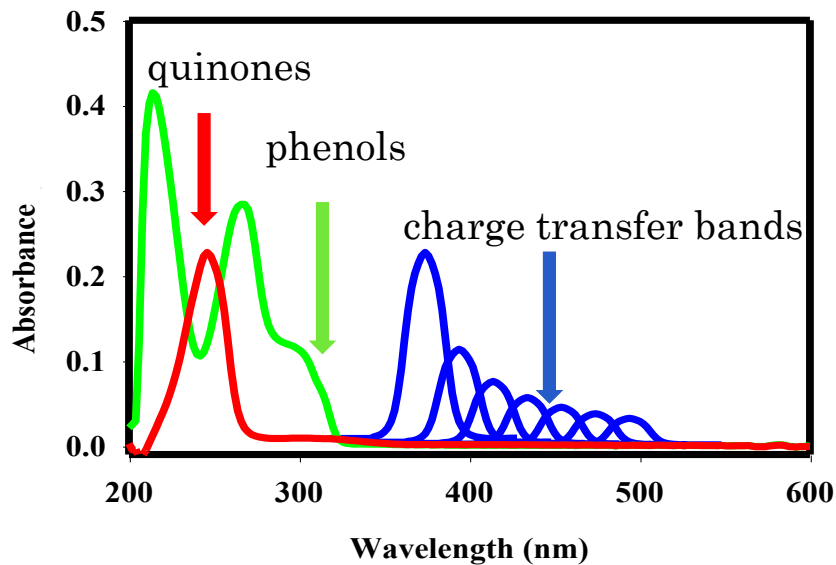


Figure 3.1 Quinones (red line) and phenols (green line) potentially interact electronically to form charge transfer bands (blue lines) (Blough Group)

3.1.1 Terrestrial CDOM and HS in Relation to Electronic Interaction Model

Recent studies provide evidence that the optical properties of CDOM cannot be described by a simple superposition of absorptions and emissions (Ma, Del Vecchio, Golanoski, Boyle and Blough (2010)), (Boyle, Guerriero, Thiallet, Del Vecchio and Blough (2009)), (Lou and Xie (2006)), (Del Vecchio and Blough (2004)). Instead electronic couplings between ground state donors (polyhydroxylated aromatics) and electron acceptors, possibly aromatic ketones, aldehydes or quinones such as those found in partially oxidized lignin, can account for the long wavelength absorption tail characteristic of CDOM and HS (> 350 nm). Figure 3.2 shows possible interactions between donor groups (D) and acceptor groups (A) in the electronic interaction model using a model humic substance. Charge transfer interactions or excited state electron transfer interactions are proposed to be occurring between phenol, hydroxyl or methoxy donors and carbonyl-containing acceptors.

Lignin polymer chains can support a greater number and variety of donor-acceptor interactions leading to a broad cohort of transition energies that lengthen the absorption emission tail of lignin derived materials such as HS and CDOM into the visible region. As in the case of lignin, CDOM and HS are photolytically degraded; the concurrent loss of molecular weight would physically disrupt optically active charge transfer bands leading to the loss of the long wavelength absorption tail. Other naturally occurring compounds also able to support charge transfer interactions are polyphenols, tannins and melanin, all of which have terrestrial plant based origins.

Electronic Interaction Model

terrestrial humic acids

Electronic interaction between donors (hydroxy-/methoxy-aromatics) and acceptors (quinones, aromatic ketones) within CDOM structure producing new optical transitions.

Long range interaction - excited state electron transfer

Short range interaction - charge transfer

D = donors (phenols, hydroxy or methoxy)

A = acceptors (carbonyl-containing moieties such as quinones, aromatic ketones)

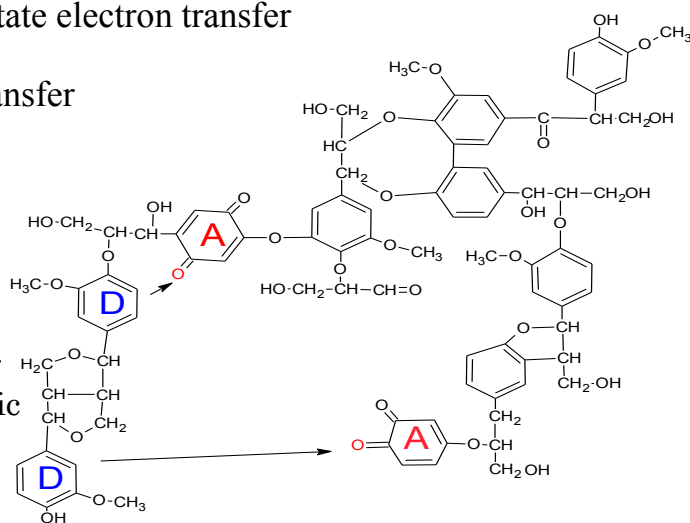


Figure 3.2 shows possible interactions within a model humic acid compound between donor (D) groups and acceptor (A) groups

As previously stated in Chapter 2.2.2; terrestrial derived CDOM has been positively linked with lignin phenol content (Del Vecchio and Blough (2002)), (Benner, Louchouart and Amon (2005)), (Opsahl and Benner (1998)), (Opsahl and Benner (1997)). Lignin is composed of polyhydroxylated aromatics and phenols that individually do not absorb light in the visible region (Vermerris and Nicholson (2006)). Oxidized aromatics can be generated when lignin is environmentally altered by oxidation, fostering charge transfer from polyhydroxylated aromatics and phenols to the oxidized aromatics. Charge transfer bands have been generated in laboratory scale experiments using CDOM, HS, hydroquinone-quinone solutions (Del Vecchio and Blough (2004)) and lignin (Xing, McGill, Dudas, Maham and Hepler (1994)).

The electronic interaction model postulates that lignin, a structurally rigid polymer generated by terrestrial plants, degrades due to natural processes such as microbial decomposition and photochemical reactions, becoming the structural precursor of HS/CDOM. During degradation the basic conformational units of lignin, the lignols, sinapyl, coniferyl and p-coumaryl alcohol are partially oxidized producing phenols, hydroxy and methoxy phenols (Fig. 2.4). The eight compounds (vanillin, vanillic acid, acetovanillone, syringaldehyde, syringic acid, acetosyrinone, p-coumaric acid and ferulic acid) the structures of which are highlighted in Fig. 2.5, represent partially oxidized lignols and have been successfully used to track terrestrial CDOM in the environment (Hernes and Benner (2002)). Quinones and other aromatic ketones are easily produced by further redox reactions and comprise a substantial portion of partially oxidized lignin.

Charge transfer bands or electronic interactions can be generated by physical association/proximity between donor and acceptor groups (Tossell (2009)). It follows that partially oxidized lignin would be able to generate charge transfer bands or electronic

interactions within its structure with donors proposed to be phenols with poly-methoxylated or hydroxylated groups and acceptors, a combination of aromatic ketones (aldehydes) and quinones. The charge transfer model as it pertains to HS and CDOM was proposed by (Del Vecchio and Blough (2004)) to explain the long tail absorbance universally observed in operationally defined HS fractions humic and fulvic acids, and CDOM.

In electronic interaction model formerly, the charge transfer model, initially absorbed radiation ($h\nu$) generating an excited state returns to ground state or losses energy via sequentially lower energy charge transfer bands. Each transfer band has a sequentially lower energy excited state donor-acceptor complex. These transfer bands extend into visible wavelengths (Fig 3.1). The extended absorbance tail cannot be accounted for by the absorbance of individual functional groups alone (Ma, Del Vecchio, Golanoski, Boyle and Blough (2010)), (Del Vecchio and Blough (2004)). It is widely accepted as a viable explanation for the long wavelength optical properties of CDOM and HS.

3.1.2 Extending the Electronic Interaction Model to Microbial Sources of CDOM

Model compounds representing the underlying structure of microbial sources of CDOM/HS have not been identified as they have been in lignin or terrestrially derived CDOM/HS. Speculatively, it may be possible to infer model compounds based on known precursor material of microbial sources of CDOM.

Quinones are present in microbial cellular structure ubiquitously, at concentrations that have historically provided biomarkers for microbial populations in wastewater treatment plants (Hiraishi, Ueda and Ishihara (1998)), (Hiraishi, Masamune and Kitamura (1989)), (Liu, Linning,

Nakamura, Mino, Matsuo and Forney (2000)). Because quinones are used as biomarkers they may be more recalcitrant than other cell wall components and are potentially acting as acceptors in the electronic interaction model. Ubiquinone 10, shown in Fig. 3.3, has been found at high concentrations (moles mg^{-1} dried cells) (Hiraishi, Ueda and Ishihara (1998)). Its half reaction is reported to have a pKa of 10.7 for the reaction $\text{QH}^- + \text{H}^+ \leftrightarrow \text{QH}_2$ and a pKa of 12.5 for the $\text{Q}_2^- + \text{H}^+ \leftrightarrow \text{QH}$ half reaction (Zhu and Gunner (2005)). Napthaquinones with multiple isoprene side chains were also identified by Hiraishi (Hiraishi, Ueda and Ishihara (1998)).

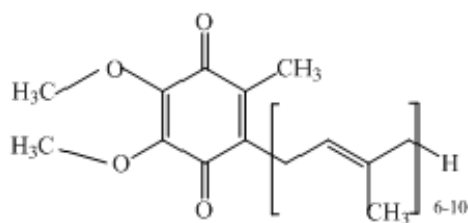


Figure 3.3 Ubiquinone ₆₋₁₀

Ubiquinone, a quinone with two methoxy groups and an extended conjugation has pKa's substantially higher than un-substituted quinones and as HS are a heterogeneous combination of moieties, species with higher pKa values should be expected. Ubiquinone and its nitrogen containing analogue menaquinone, presented in Fig. 3.4, have been shown experimentally to produce charge transfer complexes (CT) with an ionic form of the amino acid thiolate in the presence of a positive counter ion (Inaba, Takahashi, Ito and Hayashi (2006)).

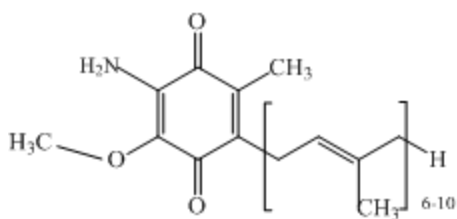


Figure 3.4 Menaquinone ₆₋₁₀

The resultant CT absorbance bands were found at 500 nm for the ubiquinone complex and at 550 nm for the menaquinone complex. In computational studies presented by Inaba, Takahashi, Ito, Hayashi 2006, CT bands were generated theoretically, using multiconfigurational quasidegenerate perturbation theory (Nakanoa (1993)). Computational results showed two nearly degenerate and low-lying CT excited states characterized by the excitations from each of two lone pairs of thiolate to a π^* orbital of benzoquinone. Excitation energies of the CT states were calculated to be 510 and 487 nm. This is consistent with Inaba's experimental results. Ubiquinone is unlikely to be explicitly present in PLFA at a high enough concentration to produce CT bands defacto; methoxy groups were not identified at high concentrations in NMR spectra of PLFA, but it is a likely model compound for the further study of microbial sources of CDOM (Mao, Cory, McKnight and Schmidt-Rohr (2007)). Menaquinone is structurally identical to ubiquinone except for the replacement of an aromatic methoxy (-OCH₃) group with an aromatic amine (-RNH₂) group (Hiraishi, Ueda and Ishihara (1998)). Identification of naphthaquinone with long side chain constituents (isoprene repeating units), and menaquinone in activated sludge generated from bacterial sources clearly indicate quinone species are not immediately labile and may persist for some time in environmental samples. Further, the presence of menaquinone- and naphthaquinone- like moieties in PLFA is consistent with NMR

spectra of PLFA (Fang, Mao, Cory, McKnight and Schmidt-Rohr (2011)), (Mao, Cory, McKnight and Schmidt-Rohr (2007)), (Hiraishi, Ueda and Ishihara (1998)).

Charge transfer bands have been experimentally produced between heterocyclic compounds and amino acids with aromatic side chains such as tyrosine and tryptophan (Yamauchi and Odani, 1985). Both tyrosine and tryptophan are highly absorbent between 200 and 300 nm with molar extinction coefficients at wavelength maxima of $1,440 \text{ M}^{-1}\text{cm}^{-1}$ (274 nm) and $5,050 \text{ M}^{-1}\text{cm}^{-1}$ (280 nm), respectively. In experiments investigating the regulation of aromatic ring stacking, charge transfer bands were found to form between 1, 10-phenanthroline and protonated tryptophan, as well as protonated tyrosine in aqueous solutions. The structure of 1, 10-phenanthroline is presented in Fig. 3.5. Wavelength maxima for each associated pair were found to be 360 and 370 nm with molar extinction coefficients (ϵ) of $640 \text{ M}^{-1}\text{cm}^{-1}$ and $820 \text{ M}^{-1}\text{cm}^{-1}$, respectively (Yamauchi and Odani (1985)).

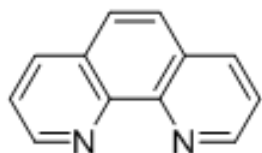


Figure 3.5 1, 10-phenanthroline

Amino acids have been found to be moderately recalcitrant, existing environmentally on a time scale of months to a couple of years. In contrast, lignin decomposition products are highly recalcitrant, existing environmentally on the scale of decades (Hernes and Benner (2003)). As terrestrial material is exported from soil environments through aquatic systems and out to the

open ocean, amino acids are likely continually cycling leading to a steady state concentration of sugars and amino acids linked to biological activity.

Decomposition products of amino acids, peptidoglycans, and other biological molecules may produce additional heterocyclic molecules such as shown in Fig. 3.6. All three of these examples of heterocyclic moieties carbazole, N-vinyl carbazole and phenothiazine are known to participate as donors in intra molecular charge transfer complexes as donors when copolymerized with acceptors such as quinoline (Jenekhe, Lu and Alam (2001)). The chemical species presented in Fig. 3.6 exemplify model compounds that are potentially identifiable within the macrostructure of PLFA in the same way that lignin phenols provide model compounds for the investigation of terrestrially derived humic substances.

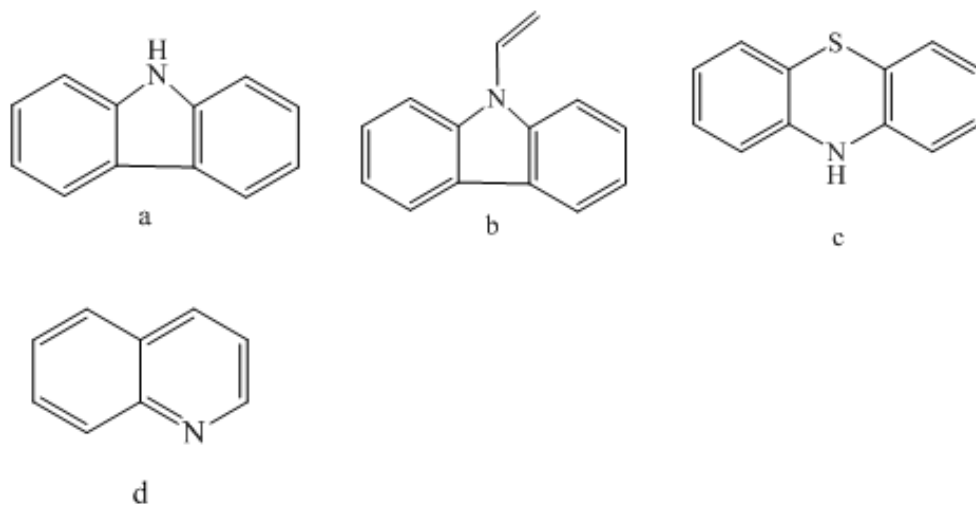


Figure 3.6 Heterocyclic moieties capable of generating charge transfer complexes as donors include (a) carbazole, (b) N-vinyl carbazole, and (c) sulfur containing molecules such as phenothiazine. An example of heterocyclic acceptors is (d) quinoline.

Charge transfer bands are potentially forming between secondary amine heterocyclic donors and tertiary amines, heterocyclic moieties, quinones or cyclic ketone acceptors. Amino acid/decomposition products of amino acid and/or peptidoglycan decomposition products can potentially form secondary and tertiary amines, as well as other heterocyclic moieties (sulfur containing) supplying both donor and acceptor groups in a charge transfer complex.

3.2 NICA-Donnan model

Some limited work has been done toward using optical titrations in an effort to model proton binding in humic substances, but that work was limited in the scope of materials used. The aim of that work was to use the pH dependent optical properties to address some of the deficits in more well known models, such as the non-ideal competitive adsorption model (NICA) combined with the Donnan model which extends the NICA model to include electrostatic interactions. The NICA-Donnan model requires significant amounts of material and is time consuming to complete.

The use of the NICA-Donnan model requires a large amount of material to complete for two reasons. The first is the high concentration of material need to generate sufficient data points on the titration curve to engender confidence in the experimental result. The second reason for the large amount of material need is the multiple trials at different electrolyte concentrations are needed to generate the master curve, which serves to separate the intrinsic chemical affinity (affinity in this case means no variance with (1) pH, in the presence of (2) other absorbing ions or (3) ionic strengths) between the HS and the absorbing species (cation or proton) from the electrostatic affinity for proton or metal binding to HS. The derivation of the NICA-Donnan Model is presented in Appendix 1.

Researchers interested in investigating natural materials such as CDOM from marine systems utilizing potentiometric models have difficulty obtaining material in sufficient quantities to complete titrations need for the NICA-Donnan model. If an optical titration could be used in place of NICA-Donnan model the amount of sample needed would be greatly reduced. A problem with this approach is that in many environmental systems the link between CDOM and DOM are not clearly elucidated despite the fact that CDOM is frequently used as a tracer of DOM. Questions remain as to the quantity of the contribution to the CDOM pool from in-situ marine DOM sources, the kinetics of the mixing between in-situ marine DOM, the timing and seasonal dynamics of any potential mixing. Further, it is highly unlikely that the contribution from in-situ marine processes is consistent seasonally or geographically. One can conclude that using optical titrations, which would only reflect the CDOM pool, to model the potentiometric titration of the DOM pool, would underestimate the acidic sites and is premature without a better understanding of the dynamics of the system. Potentiometric titrations can provide insight and background for optical titrations.

A second and possibly more interesting reason to study the optical titrations of humic substances is the unique insights that can be provided about the redox state of the system and its potential as a redox buffer in soil and wetland ecosystems (Maurer, Christl and Kretzschmar (2010)), (Aeschbacher, Sander and Schwarzenbach (2010)).

Chapter 4 The Chemical Probe Sodium Borohydride

Chapter 4 Overview

This chapter has one section that describes the basic mechanism of the reduction of carbonyl groups by sodium borohydride. More detailed procedures about how borohydride reduction was applied to each set of experiments are provided in the materials and methods sections (Sec. 5.2, 6.2, and 7.2) of the chapters that detail the experiments executed in this study.

Sodium borohydride (NaBH_4) selectively reduces carbonyl groups by a hydride transfer mechanism presented in Fig. 4.1 (Cleyden, Greeves, Warren and Wothers (2001)). The carbon atom of the carbonyl group acts as an electrophile and hydrogen with two electrons is transferred to the carbonyl carbon reducing the carbonyl to an alkoxide (RO^-) or phenoxide intermediate. In aqueous solution hydrogen is then abstracted from water effectively raising the pH of an aqueous solution and converting the alkoxide or phenoxide intermediate to an alcohol. The H^- does not act as a nucleophile because its 1s orbital is too small, the sigma B-H is the highest occupied molecular orbital (HOMO) and transfers two electrons to the π^* of the carbonyl lowest unoccupied molecular orbital (LUMO) (Cleyden, Greeves, Warren and Wothers (2001)).

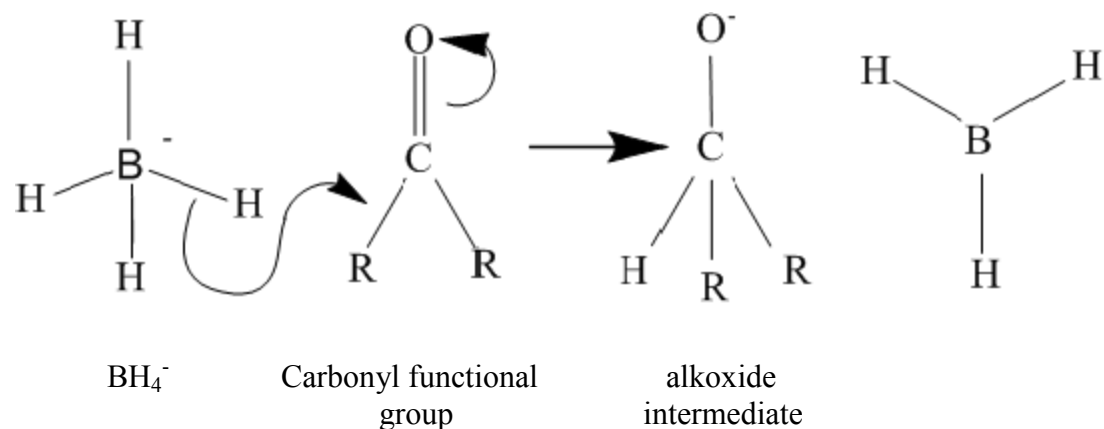


Figure 4.1 Borohydride reduction of a carbonyl group to an alkoxide intermediate

Quinones are known to be generated from phenols by photo-dissociation reactions of a phenol to a phenoxy radical, hydrogen ion and a solvated electron as presented in Fig. 4.2. In the presence of molecular oxygen the solvated electron can induce formation of hydroxy (HO^\bullet) and hydroperoxy (HOO^\bullet) radicals which act upon the phenoxy radical to produce quinones (Shkrob, Depew and Wan (1992)).

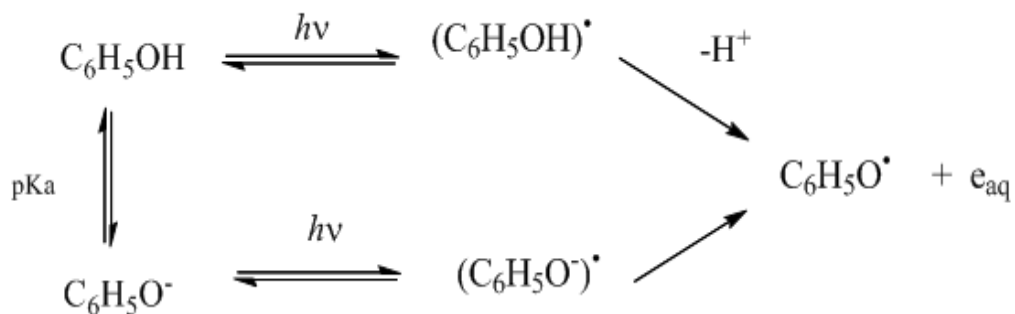


Figure 4.2 Generation of a phenoxy radical, hydrogen ion and a solvated electron by photo-dissociation

Sodium borohydride (NaBH_4) can chemically reduce carbonyl groups of aliphatic and aromatic ketones, quinones, and aldehydes. The reaction yields secondary alcohols and hydroxyquinones/phenols respectively. The reduction products of quinones are not stable at standard temperature, pressure (oxygen concentration) and therefore must be protected from aerobic conditions. This method of reduction when applied to humic substances (HS) and chromophoric dissolved organic matter (CDOM) has been successfully used to generate primary and secondary alcohols with a concurrent loss of aromatic and aliphatic ketones as identified by fourier transform infrared (FTIR) and proton nuclear magnetic resonance ($^1\text{H-NMR}$) spectroscopy (Tinnacher and Honeyman (2007)).

The ability of borohydride to selectively reduced molecular oxygen containing moieties within the HS/CDOM provides an effective probe that can be used to illuminate the relationship between oxidation state of a HS/CDOM, its structural underpinning and the resultant influence on the optical properties. Further, having such a probe allows for differentiation of continuum of HS/CDOM; including material exported from terrestrial environments, through open waterways

to the open ocean; those stored in terrestrial ecosystems, and finally HS/CDOM generated solely from microbial sources.

By directly comparing the optical properties of borohydride reduced and unreduced microbially generated HS to lignin derived HS/CDOM this study seeks to elucidate the similarities and differences between microbial and terrestrial sources of HS/CDOM in an effort to partition contributions from each source to overall optical absorption/emission spectra. The charge transfer model seeks to link the optical properties of HS/CDOM to underlying structural characteristics through examination of the redox state generated differences or similarities among HS/CDOM from various sources (terrestrial, aquatic, marine/microbial). Direct comparison of humic substances from a variety of sources is a relevant test of the ruggedness of the charge transfer or electronic interaction model. This is especially true of HS/CDOM generated from solely microbial sources that may lie outside of the preview of the charge transfer model in that they do not derive from terrestrially sourced lignin. Model HS from solely microbial sources have higher concentrations of molecular nitrogen and sulfur than found in HS/CDOM derived from lignin (Brown, McKnight, Chin, Roberts and Uhle (2004)), (McKnight, Andrews, Spaulding and Aiken (1994)) yet they have optical properties that are superficially consistent with terrestrial HS/CDOM perhaps indicating (1) an alternative mode of generating charge transfer bands, or (2) a different mechanism altogether. Additionally the source (aquatic/terrestrial) and degree of humification potentially affect the optical properties of humic material. Comparison of terrestrial humic material from soil sources when compared to aquatic sources may provide insight about the fate and transport of humic material in the environment.

That the optical properties of humic substances have a pH dependence is well known (Ma, Del Vecchio, Golanoski, Boyle and Blough (2010)) but the underlying structural

components that contribute to pH based changes are dependent upon are less well known but speculated to be a bimodal distribution of carboxylic moieties at acidic pH and phenolic moieties at basic pH participating in charge transfer reactions. This is an oversimplification in that neither site is composed entirely of carboxylic groups or phenolic groups but instead encompasses a distribution of acidic pKa groups centered at pK 3 and a distribution of basic pKa groups with a range of pK 8-10 (Christensen, Tipping, Kinniburgh, and Christensen (1998)). The bimodal distribution of humic substances (HS) such as Suwannee River fulvic acid (SRFA), Suwannee River humic acid (SRHA) and Leonardite humic acid (LHA) and Elliott humic acid (EHA), as well as other model and natural compounds have been modeled using the NICA-Donnan model as detailed in Chapter 3 and Appendix 1. Optical titrations of untreated and borohydride reduced model compounds are presented in Chapter 6.

Borohydride reduction is carried out above pH 7.0, in order to minimize loss of borohydride through competition with water (Gardiner and Collat (1965)). At alkaline pH the carboxylic distribution is deprotonated and does not contribute to the pH dependent optical properties in a dynamic way. The phenolic group distribution is speculated to include aromatic ketones (aldehydes), quinones, and phenols. The pKa of phenol in water is 9.98 (Gross and Seybold (2001)), pKa = 10.0 (Lind, Shen, Eriksen and Merenyi, (1990)). Cathchol is slightly lower with a pKa of 9.5 (Gross and Seybold (2001)). Addition of a methoxy, methyl or amino substituent increases the pKa of the phenolic group to between 10.0 and 10.3 (Gross and Seybold, 2001), (Lind, Shen, Eriksen and Merenyi, (1990)). A quinone upon a one electron reduction forms a semi-quinone that is reversible in aerobic systems. A two electron reduction yields a reversible hydroquinone (Aeschbacher, Vergari, Schwarzenbach and Sander (2011)), (Guin, Das and Mandal (2011)), (Aeschbacher, Sander and Schwarzenbach (2010)). These

three oxidation states have associated pH dependence because the loss of each electron corresponds to the gain of a proton in a coupled reaction depicted in Fig. 4.2.

Aeschbacher et al., 2011, in studies of proton and electron transfer equilibria ($\text{pH} \leq 6$, unreduced HS) showed that HS exhibited a broad range of reduction potentials (+0.15 to -0.3 V at pH 7.0) (Aeschbacher, Vergari, Schwarzenbach and Sander (2011)). These reduction potentials were consistent with the reduction potentials of model quinones from the same study. In separate experiments Electron Accepting Capacities (EAC) were measured by mediated electrochemical reduction for eight humic acids and five fulvic acids. Aeschbacher found that humic acids had higher EAC than fulvic acids and terrestrial humic acids had higher EAC than aquatic humic acids (Aeschbacher, Sander and Schwarzenbach (2010)).

Chemical borohydride reduction of the aquatic humic and fulvic standards, Suwannee River humic acid (SRHA) and Suwannee River fulvic acid (SRFA) resulted in as much as a 70 % reduction of differential absorbance and loss of the long wavelength absorbance tail (> 350 nm), a concurrent blue shift and 2-3 fold increase in the intensity in emission spectra (Ma, Del Vecchio, Golanoski, Boyle and Blough (2010)). The loss of absorbance and rise in fluorescence produces a substantial increase in quantum yield in SRFA/HA. Additionally, the parameterized spectral slope coefficient (S) will be quantified for untreated and borohydride reduced sources of humic and fulvic acids. Spectral slope has historically been used to describe the absorbance of profile of HS/CDOM. As coastal CDOM is exported to marine environments the spectral slope parameter has been observed to increase (Hayes (1989)), (Hernes and Benner (2003)), (Del Vecchio and Blough (2004)), (Moran, Sheldon and Zepp (2000)), (Vodacek, Blough, DeGrandpre, Peltzer and Nelson (1997)), (Whitehead, de Mora, Demers, Gosselin, Monfort and Mostajir (2000)). Based on this historical data it can be expected that spectral slope coefficients

(S) of terrestrially sourced HA/FA, should have a lower S value than that of fresh water aquatic HA/FA and further that marine sources of FA should have a higher spectral slope than aquatic FA. If marine CDOM is closely related to microbial sources of fulvic acids, then the S coefficient of PLFA should reflect this and its spectral slope (S) will be greater than the other source of fulvic acid in this study SRFA as well as the other sources of humic acids. It should also be expected that borohydride reduction of all humic and fulvic acid samples should generate an increase in spectral slope when compared to untreated samples because of unquenched donors and acceptors within the charge transfer system now able to contribute directly to the absorbance spectra in the UV region.

Chapter 5 Sodium Borohydride Reduction of Terrestrial Humic Acids and Microbial Fulvic Acid

Chapter 5 Overview

The electronic interaction model or charge transfer model seeks to explain the unique optical properties of terrestrial sources of CDOM/HS by investigating the chemical moieties that participate in generating the long wavelength absorption that is characteristic of CDOM/HS. In Chapter 5, the chemical underpinnings of CDOM/HS are investigated using a chemical reductant, sodium borohydride. The chemical probe sodium borohydride is used to eliminate carbonyl groups within the structure of CDOM/HS with the idea that loss of the carbonyl groups would affect the optical and potentiometric properties of the examined samples and standards. Further, the electronic interaction model was extended to include sources of microbial CDOM/HS that differ in source material and thus have potentially different donors and acceptors participating in generating the extended long wavelength absorption that is characteristic of CDOM/HS. Section 5.2 describes materials and methods used in this chapter including materials (Sec. 5.2.1), apparatus (Sec. 5.2.2), optical measurements (Sec. 5.2.3), preparation of the CDOM/HS (Sec. 5.2.4) and borohydride reduction procedures. Section 5.3 details the results and discussion of the series of experiments. This work includes optimization of sodium borohydride concentration (Sec. 5.3.1), the changes that occur to the absorbance properties, pH and absorbance recovery of CDOM/HS used in the study due to borohydride reduction in an aerobic atmosphere and reoxidation post-borohydride reduction (Sec. 5.3.2), untreated and borohydride reduced fluorescence spectra (Sec. 5.3.4), quantum yield of CDOM/HS pre- and

post-borohydride reduction (Sec. 5.3.5). Also included in Sec. 5.3 are the results and discussion of an unsuccessful cyanoborohydride reduction of selected samples (Sec. 5.3.6) and in Sec. 5.3.7 are molar absorptivity coefficients of two phenone compounds benzophenone and 2-acetonaphthone pre- and post-borohydride reduction. Section 5.4 summarizes the conclusions that can be generated from the experimental results from this chapter.

5.1 Introduction

The optical properties of charge transfer bands generated between amino acids or heterocyclic aromatic species and quinones could be expected to differ from lignin generated charge transfer bands in several ways:

1. Historically, marine sources of CDOM have higher spectral slope (S) coefficients than do near shore CDOM samples. If marine sources of CDOM are closely related to or contain a high proportion of bacterial source FA than untreated PLFA should have a high spectral slope when compared to aquatic FA, namely SRFA.
2. The spectral slope coefficient (S) of borohydride reduced material such as SRFA, a source of terrestrial humic acid, would potentially differ from the spectral slope of borohydride reduced PLFA, a microbial source of humic acid, due to the difference in the donor moieties in charge transfer bands. If the short wavelength absorbance of PLFA (210-350 nm) can be attributed to largely amino acids/peptidoglycan decomposition products producing heterocyclic amines with additional but proportionally less quinone and aromatic ketone groups, then the spectral slope should be steeper than the spectral slope of SRFA, a terrestrial source of FA. Carboxylic acids from amino acids or other sources are not reduced by borohydride. Amines (secondary or tertiary) are not reducible

by simple borohydride reduction. The only nitrogen containing compounds easily reducible by borohydride are imides, which may be present as they are used in biological systems to produce amino acids from keto acids in an enzymatically driven system (Cleyden, Greeves, Warren and Wothers (2001)). SRFA when compared to PLFA would not be enriched with nitrogen but would contain a substantially different group of reducible ketones potentially lacking in PLFA. Loss in absorbance due to borohydride reduction in terrestrial sources represents higher relative percent carbonyl moieties than that of PLFA and the spectral slope, between 290-820 nm should reflect that difference.

3. Borohydride reduction of PLFA may yield less overall (190-800 nm) absorbance loss when compared to SRFA. Suwannee River FA potentially has more types and a higher concentration of reducible moieties due to the presence of decomposition products from lignin phenols making SRFA able to form more diverse and larger numbers of charge transfer bands.
4. Absorbance of PLFA reduced with borohydride and reoxidized would be expected to recover to a greater extent than SRFA upon reoxidation if quinones are enriched when compared to aromatic ketones. Aromatic ketones are present in PLFA, but when compared to SRFA and the diverse suite of aromatic ketone acceptors generated by lignin phenols in terrestrial sources of HA/FA, the proportion of aromatic ketones in PLFA, is expected to be lower. Quinones may be enriched when compared to aromatic ketones as quinones are ubiquitous in microbial systems.

Extending borohydride reduction methodology, specifically the reduction-reoxidation impact on the absorbance and emission properties of standard HS material provides insight into similarities or differences that may exist between various sources (soil, aquatic and microbial) of

HS. Elucidation of the structural underpinnings that give rise to the observed optical properties found in all humic materials is critical to understanding the fate and transport of this important component of the global carbon cycle.

5.2 Materials and Method

5.2.1. Materials

Leonardite Humic Acid Standard (LHA) 1S104H-S, Elliot Humic Acid Standard (EHA) 1S102H, Suwannee River Humic Acid (SRHA), Suwannee River Fulvic Acid and Pony Lake Fulvic Acid (PLFA) were obtained from the International Humic Substance Society. Chromophoric Dissolved Organic Matter (CDOM) samples were prepared according to the procedure in previous publication (Boyle, Guerriero, Thiallet, Vecchio and Blough (2009)). Twenty-L water samples were filtered with 0.2-mm Gellman filters, acidified to pH 2 and pumped through a C-18 extraction column from United Chemical Technologies, Inc. at a flow rate of 50 mL min⁻¹. The extracted material was eluted from the C-18 cartridges with high purity methanol and evaporated to dryness using a rotary evaporator at 30-35 °C. The dried material was reconstituted in 1-2 mL of Milli-Q water. The pH was adjusted with sodium hydroxide to pH 7 and refrigerated until analysis.

Aromatic ketones, including 2-acetonaphthone (99% purity) (2AN) and benzophenone (purum) (> 99%) (BP), were obtained from Flucka AG; 2, 5-dimethyl-p-benzoquinone and duroquinone were acquired from Acros; methyl benzoquinone was obtained from Sigma-Aldrich. Methyl benzoquinone was further purified by sublimation. Benzophenone and 2-Acetonaphthone were purified by re-crystallization. Sodium cyanoborohydride (95%) (NaBH₃CN) and sodium borohydride (NaBH₄) were obtained from Sigma-Aldrich. Water was

purified to 18 Ω using an Academic Milli Q water system equipped with a carbon filter. Quinine sulfate dihydrate and potassium hydrogen phthalate were reagent grade from Fisher Scientific.

5.2.2 Apparatus

A Shimadzu UVPC 2401 spectrophotometer was used to acquire UV-visible absorption spectra. Fluorescence measurements were made with an Aminco-Bowman AB-2 luminescence spectrophotometer. A 4-cm aperture was used for excitation and emission. These instruments are located in the Blough Laboratory at the University of Maryland.

5.2.3 Optical Measurements

All experiments were conducted using 1-cm quartz cuvettes with Milli-Q water adjusted to the appropriate pH with 0.10 mole L^{-1} hydrochloric acid (HCl) or 0.10 mole L^{-1} sodium hydroxide (NaOH). Molar extinction coefficients were determined using a mixture of 50:50 methanol and water. Absorption spectra were recorded from 190 to 820 nm against pH adjusted Milli-Q water. Difference spectra (ΔA) were calculated by subtracting an absorbance spectra at time t ($A(t)$) from the original spectra ($A(0)$). Fractional difference spectra were generated by dividing an absorbance spectra at time t ($A(t)$) by the original spectra $A(0)$. Fluorescence emission spectra were collected from 280-600 nm excitation range. In order avoid inner filter effects, fluorescence measurements were kept between 0.05 and 0.1 optical density (OD). Differential emission spectra (ΔF) were calculated by subtracting the original spectra $F(0)$ by subsequently borohydride reduced spectra at time $F(t)$ where t was 24 hours. Quinine sulfate was used to standardize the fluorescence quantum yield measurements according to the method

developed by the U.S. Department of Commerce, National Bureau of Standards publication 260-64 Standard Reference Materials: A Fluorescence Standard Reference Material: Quinine Sulfate Dihydrate (Velapodi and Mielenz (1980)). Fluorescence measurements were made initially at pH 7.6, reduced pH 10 and reduced reoxidized pH 7.6.

Specific absorbance (a^*) was calculated according to equation 5.1.

$$a^*(350 \text{ nm}) = 2.303 a(\lambda)/(b * c), \quad (5.1)$$

where $a^*(350 \text{ nm})$ is specific absorbance at 350 nm (henceforth referred to as a^*), $a(\lambda)$ = absorbance at a given wavelength, $b = 0.01$ is the absorbance path length in meters (1-cm cell), C is the total organic carbon in mg carbon L^{-1} . Total organic carbon was determined by high temperature oxidation using a Shimadzu 500A TOC analyzer calibrated using potassium hydrogen phthalate (KHP) at 680 $^{\circ}C$. The spectral slope parameter (S) was obtained by non-linear least squares fitting of the spectra over the range of 290-820 nm to expression (5.2)

$$a(\lambda) = a^*(\lambda_0) \exp^{-S(\lambda-\lambda_0)}, \quad (5.2)$$

where $a^*(\lambda_0)$ is the specific absorption coefficient at the reference wavelength of 350 nm.

Lignin Alkali Carboxylate (LAC) was normalized to the concentration of SRFA.

5.2.4 Preparation of Humic and Fulvic Acids

Humic Acids (HA) were dissolved in a minimum amount of sodium hydroxide, diluted to the desired concentration and pH adjusted using Milli-Q water and 0.1 mole L^{-1} hydrochloric acid (HCl) or 10 mmole L^{-1} , pH 7.6 phosphate buffer. Reductions with borohydride and cyanoborohydride were selectively conducted with both pH adjusted water or phosphate buffer. Initial reaction concentrations were chosen in order to generate absorbance spectrum at or below

1 absorbance unit (A.U.) in spectral ranges between 190 and 400 nm and 400 to 820 nm allowing for investigation of the UV and visible ranges of the spectrophotometer. The pH of each HA standard was adjusted from an average of 12 to the desired initial reduction pH of 10 or pH 7.6 and filtered with a 0.2 μm Nalgene nylon syringe filter (catalog number 195-2520) prior to final dilution. Fulvic acids (FA) were dissolved in pH adjusted Milli-Q water for the borohydride and cyanoborohydride reductions. The pH was adjusted to the desired pH prior to dilution if needed. Fulvic acids were not filtered.

5.2.5 Borohydride Reduction

Leonardite HA (50 mg L^{-1}) was reduced at pH 10.3 with 2 mg sodium borohydride and at pH 7.6 with 2, 5, and 10 mg of sodium borohydride. LHA (100 mg L^{-1}) was reduced with 4 mg sodium borohydride at pH 7.6. Each standard was purged with UHP nitrogen (N_2) fitted with either a Restek oxygen scrubber (catalog number 20601) or a SGE Analytical Sciences oxygen trap (catalog number 103486) for 30 minutes prior to the addition of the reductant and purged continually with ultra high purity N_2 throughout the time course of the reduction. All reductions of HA/FA were carried out for at least 24 hours and selected reductions were extended to 48 or 72 hours. The samples were reoxidized for 24 hours. Samples were protected from ambient light during reduction and reoxidation. Selected spectra were titrated to the original A(0) pH because addition of borohydride consistently increased the pH of the solution. The pH and absorbance spectrum of each reduction was measured at reoxidation time points of 10 minutes, 30 minutes, 1 hour, and 24 hours.

Molar extinction coefficients were calculated for the aromatic ketones benzophenone (BP) and 2-acetonaphthone (2-AN) in 50/50 solution of methanol and water. 2-Acetonaphthone 99%, ($C_{10}H_7COOCH_3$) with a molecular weight of $170.21 \text{ g mole}^{-1}$ and benzophenone >99% ($C_{13}H_{10}O$) with a molecular weight of $182.22 \text{ g mole}^{-1}$ were further purified by recrystallization. Super saturated solutions of BP and 2-AN was prepared separately in 20 mL of Mallinckrodt Chrom AR HPLC grade methanol. The solution was heated to 45°C . A minimal amount of water was added to the supersaturated solution and it was transferred to an ice bath. Crystals were collected after the supernatant was decanted. The recrystallized BP and 2-AN were dried for 24 hours in a desiccator. Recrystallized and dried BP was used to prepare two series of dilutions in order to illuminate the π to π^* ($5 - 102 \mu\text{mole L}^{-1}$) and n to π^* ($50.4 - 3.43 \text{ mmole L}^{-1}$) transitions. Re-crystallized and dried 2-AN was used to prepare a series of dilutions from $528.7 \mu\text{mole L}^{-1}$ to $12.5 \mu\text{mole L}^{-1}$ in 50:50 methanol:water (MeOH:water). The background corrected absorbance spectra were plotted as a function of wavelength and the π to π^* and n to π^* transitions for unreduced material was determined.

A concentration that did not exceed 1 A.U. in the spectral range of interest was chosen for the borohydride reduction of the aromatic ketones BP and 2-AN. 2-AN ($400 \mu\text{M}$) was reduced with 0.3 mg of sodium borohydride at an initial pH of 8.0 in a mixture of 50:50 methanol and water against a blank of 50:50 methanol and water. The solution was purged for 30 minutes with UHP nitrogen and purged throughout the reaction. BP (3 mmole L^{-1}) was reduced in the same manner as 2-AN.

5.3 Results and Discussion

5.3.1 Borohydride Reduction

The results presented in Table 5.1 and Fig. 5.1, show that the reduction of 50 mg L⁻¹ LHA with 2, 5, and 10 mg of sodium borohydride over a 24 hour period at a initial pH of 7.6 yields consistent absorbance loss if the ratio of material to borohydride was in 10 fold excess or less (5 and 10 mg borohydride). Fractional difference $A(T)/A(0)$ at 560 nm and an initial pH of 7.6 was 0.61 and 0.58 for the reduction of 50 mg L⁻¹ LHA with 5 and 10 mg of borohydride, respectively. The 25 fold excess (2 mg borohydride) yields less magnitude of reduction over the same time period. The fractional difference at 560 nm for a borohydride reduction of 50 mg L⁻¹ material and 2 mg borohydride was 0.78. A second experiment using a 25 fold excess (100 mg of LHA and 4 mg borohydride) exhibits a fractional difference loss at 560 nm of 0.47. The 25 fold excess of material to borohydride mass, when doubled in concentration, should yield a proportional loss of absorbance. The 50 and 100 mg L⁻¹ LHA reduced with 2 and 4 mg of borohydride are about 20 % different in the degree of maximum (560 nm) fractional difference absorbance loss indicating complete reduction cannot be achieved at this ratio. Additionally, a reduction of LHA (50 mg L⁻¹) with 2 mg borohydride at an initial pH of 10.5 had fractional absorbance loss of 0.64. This value is consistent with lower ratios of LHA and borohydride implicating the competition for borohydride between carbonyl target groups and the aqueous solvent. All subsequent reductions were completed using a 10 fold excess of humic substance.

Table 5.1 Sodium borohydride reduction of Leonardite Humic acid (LHA) at pH 10.4 and pH 7.6 as measured by decrease absorbance (290-820 nm)

Humic Acid (concentration mg L ⁻¹)	Borohydride concentration (mg)	pH	Fractional Difference loss A(T)/A(0) at 560 nm
Leonardite (50 mg L ⁻¹)	2 mg	10.4	0.64
Leonardite (50 mg L ⁻¹)	2 mg	7.6	0.78
Leonardite (50 mg L ⁻¹)	5 mg	7.6	0.61
Leonardite (50 mg L ⁻¹)	10 mg	7.6	0.58
Leonardite (100mg L ⁻¹)	4 mg	7.6	0.47

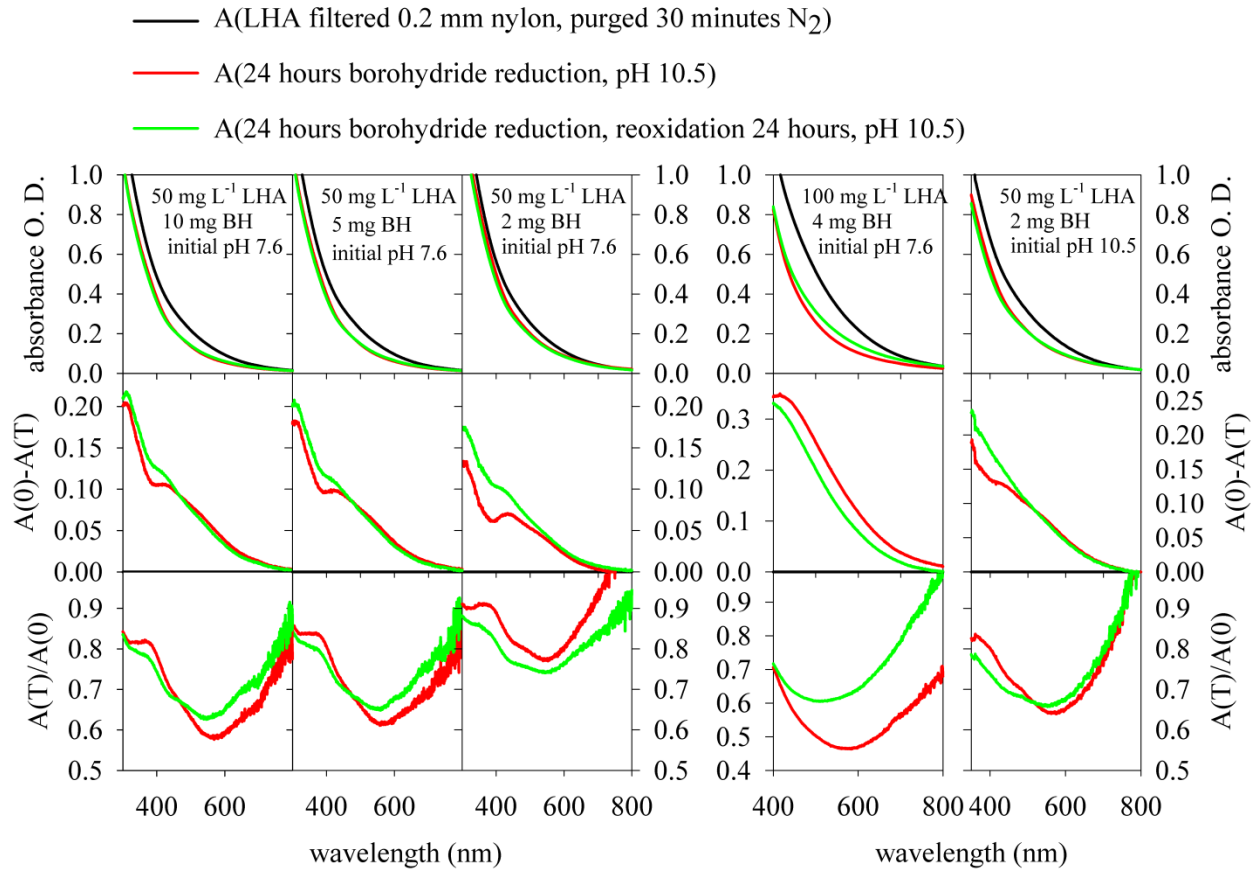


Figure 5.1 Concentration dependence of borohydride (BH) reduction of Leonardite humic acid (LHA)

Additionally, longer periods of time up to 72 hours of anaerobic reduction were used on selected HS samples to assess if the reduction was completed in 24 hours (not presented). The 5 mg borohydride treatment was used over a 24 hour time period to examine the optical behavior of the other standards as no further reduction was observed for extended reduction times.

5.3.2 Optical Properties of Borohydride Reduced Humic Substances (SRFA, SRHA), Lignin Alkali Carboxylate (LAC) and Natural Humic Substances from the Mid-Atlantic Shelf and Delaware Bay

Within the electronic interaction model concept it can be expected that as acceptor moieties are reduced, long wavelength (> 350 nm) will be lost due to lack of acceptor groups in charge transfer complexes, fluorescence emission will increase and emission maxima will blue shift because donor moieties within the electronic interaction model, likely methoxy- and hydroxyl- phenols are no longer being quenched by borohydride reduced acceptor moieties. Concurrent, with the loss of long wavelength absorbance tail and an increase in fluorescence emission will be an increase in fluorescence quantum yield (Ma, Del Vecchio, Golanoski, Boyle and Blough (2010)). Ma, 2010 found consistency between theory and experimental results supporting the electronic interaction model but questions remain about what proportion of donor moieties can be attributed to quinones and/or aromatic ketones. Quinones reduced to hydroquinones are expected to, upon exposure to oxygen, reoxidize as they are not stable unless protected from oxygen. (Ma, Del Vecchio, Golanoski, Boyle and Blough (2010)) did not observe extensive levels of long wavelength absorbance recovery, red shift of fluorescence maxima, or reduction of fluorescence emission when borohydride reduced samples were exposed

to air regardless of the length of air exposure. The lack of oxygen derived recovery could be attributed to several factors, (1) only a small percentage of the acceptor moieties are quinones with the majority being aromatic ketones such as phenones or some other as yet unidentified species, (2) secondary reactions could be preventing the cycling between hydroquinone and quinone, or (3) physical disruption of the fulvic or humic acid could prevent realignment of molecular level connections needed to establish charge transfer interactions. In this study, the pH, absorption and fluorescence emission trends as the system converts from an anaerobic system to an aerobic system is elucidated in greater detail and for a broader spectrum of model humic substances.

Results presented in Fig. 5.2 as well as previous results (Ma, Del Vecchio, Golanoski, Boyle and Blough (2010)) have shown that the aquatic humic substances SRHA and SRFA, extracts from the mid-Atlantic bight (Delaware Bay and Mid Atlantic Shelf) and lignin alkali carboxylate (LAC) show an irreversible loss of absorbance across the visible and ultraviolet wavelengths and a 2 to 3 fold blue shift emission increase. Borohydride reduction causes an increase in pH to an average of 10.5 due to abstraction of an aqueous proton by the reduced carbonyl and the temperature and pH dependent decomposition of sodium borohydride in water (Gardiner and Collat (1965)). Additional absorbance loss was observed when the borohydride derived pH increase was titrated from an average high of pH 10.5 back to pH 7.6 corresponding to the initial reduction conditions (Fig. 5.2). The natural sample from the Mid-Atlantic Shelf did not exhibit the same degree of response to post-oxidation changes in pH as did the other aquatic samples (SRFA, SRHA, Delaware Bay and LAC). This may stem from the lack of colored material in the off-shore samples when compared to the aquatic samples and the sample from the Delaware Bay. As the Mid-Atlantic Shelf sample is extensively photo bleached, it may not have

the concentration or variety of titratable moieties expected from HS generated from material closer to source material. Specific absorbance (a^*) was calculated for SRFA, SRHA and LAC as 7.49, 3.38 and 6.32 ($\text{L (mg org. C)}^{-1} \text{ m}^{-1}$) respectively using organic carbon data supplied by Kelli Sikorski (formerly Golanoski) (Golanoski, Fang, Del Vecchio and Blough (2012)). Specific absorbance (a^*) for borohydride reduced SRFA and SRHA are 1.88 and 4.55 ($\text{L (mg org. C)}^{-1} \text{ m}^{-1}$) respectively. Specific absorbance was not calculated for the MAB samples. Specific absorbance (a^*) values are presented in Table 5.2.

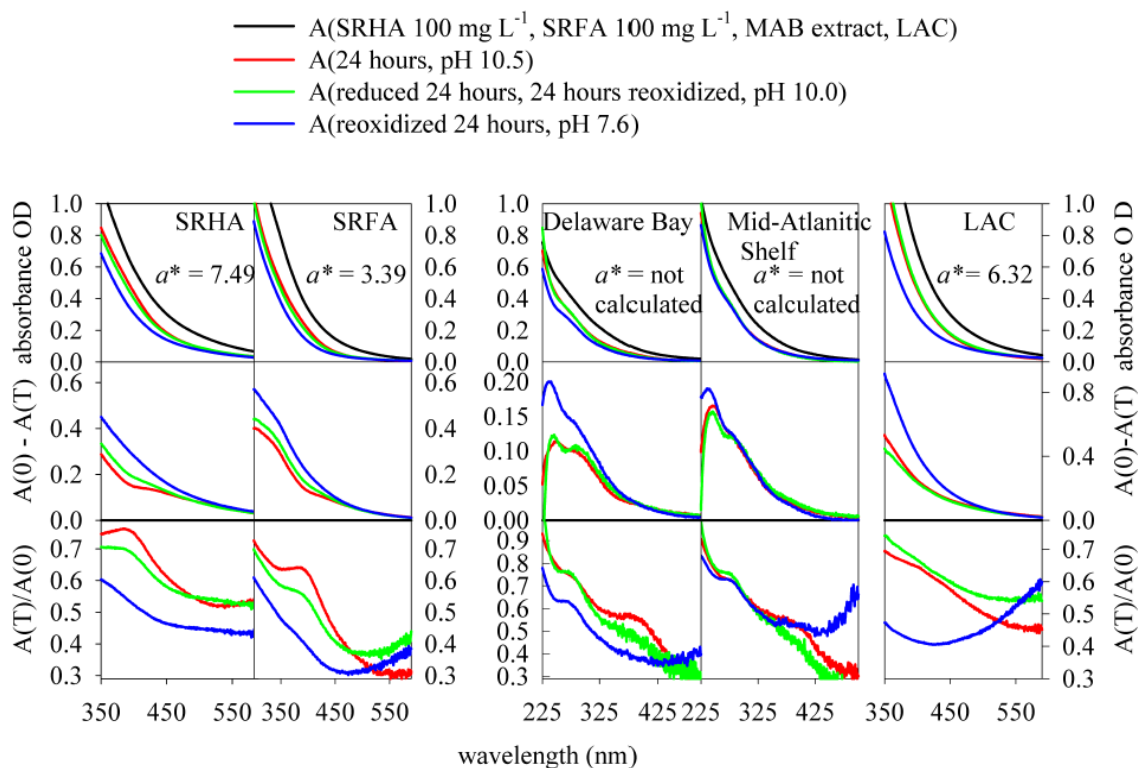


Figure 5.2 Absorbance, absorbance difference $A(0)-A(T)$ and fractional difference $A(T)/A(0)$ of the reduction and reoxidation of 100 mg L^{-1} Suwannee River humic acid (SRHA), 100 mg L^{-1} Suwannee River fulvic acid (SRFA), CDOM from the Delaware Bay, CDOM from the mid-Atlantic Bight and Lignin Alkali Carboxylate (LAC) with 5 mg sodium borohydride at an initial pH of 7.6. a^* is for untreated samples ($\text{L}(\text{mg org. C})^{-1}\text{m}^{-1}$).

Borohydride reduction of soil derived terrestrial material (Elliott and Leonardite Humic Acids) over a period of 24 hours decreases in absorbance across all wavelengths, but a maximum reduction is seen between 300 and 600 nm as presented in Fig. 5.3. The difference and fractional difference maximum loss is 50 % for both Elliott and Leonardite HS. This is a similar percentage loss as that found in SRHA but about 20 % less than the maximum fractional and differential fraction loss of SRFA (Figs. 5.2 and 5.3). Specific absorbance for untreated EHA and LHA were found to be $a^* = 8.87$ and $a^* = 20.38$ (L (mg org. C)⁻¹ m⁻¹) respectively (organic carbon data supplied by Kelli Sikorski). Specific absorbance for borohydride reduced EHA and LHA were found to be $a^* = 5.50$ and $a^* = 12.68$ (L (mg org. C)⁻¹ m⁻¹) respectively. Specific absorbance values are presented in Table 5.2.

Table 5.2 specific absorbance values for untreated and borohydride reduced humic and fulvic acids. a^* values were calculated at 350 nm and pH 7.6.

Sample identification	Specific absorption (a^*) (L (mg org. C) ⁻¹ m ⁻¹) ^{&}	
	untreated	borohydride reduced
Elliott humic acid (EHA)	8.87	5.50
Leonardite humic acid (LHA)	20.38	12.68
Suwannee River humic acid (SRHA)	7.49	4.55
Suwannee River fulvic acid (SRFA)	3.39	1.88
Pony Lake fulvic acid (PLFA)	1.37	1.17
Lignin Alkali Carboxylate (LAC)	6.32	—

[&] Organic carbon data provided by K. Sikorski.

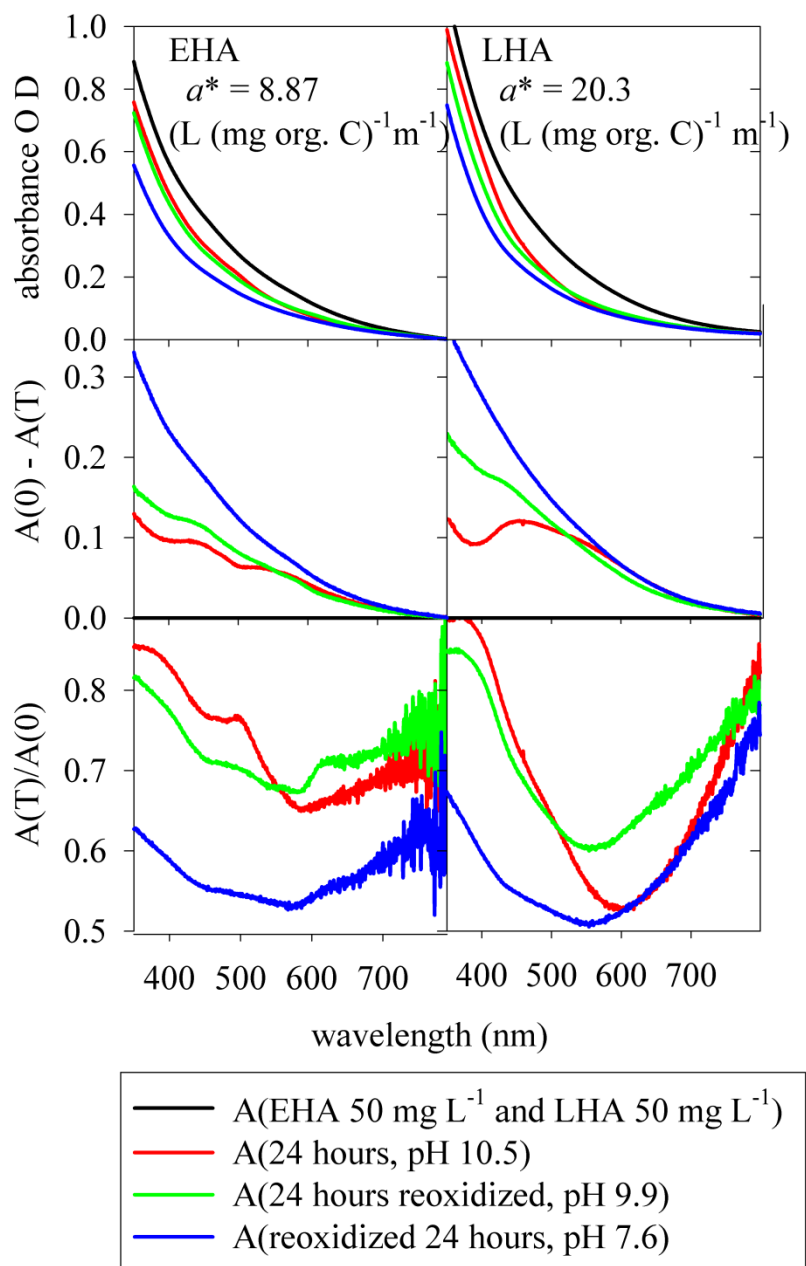


Figure 5.3 Absorbance, absorbance difference $A(0)-A(T)$ and fractional difference $A(T)/A(0)$ spectra of the reduction and reoxidation of 50 mg L^{-1} Elliott humic Acid (EHA) and 50 mg L^{-1} Leonardite humic acid (LHA) with 5 mg sodium borohydride at an initial pH of 7.6. a^* are for untreated samples.

As seen in Fig. 5.4 and Table 5.2 untreated and borohydride reduced Pony Lake fulvic acid (PLFA) have lower specific absorbance ($a^* = 1.34$ and $1.17 \text{ (L (mg org. C)}^{-1} \text{ m}^{-1})$) respectively - organic carbon data supplied by K. Sikorski) than all other untreated humic materials analyzed. Absorbance, difference and fractional difference spectra of PLFA (Fig. 5.4) show that borohydride reduction of 500 mg L^{-1} PLFA produces as much as 90 % loss in absorbance with maxima between 400-500 nm. Absorbance at wavelengths longer than 500 nm is very close to zero. Long wave length absorbance of PLFA is linearly related to concentration (data in Chapter 6, Fig. 3.1). The absorbance of PLFA at long wavelengths is very low, making the use of high concentration (500 mg L^{-1}) necessary in order to elucidate absorbance trends in this region (Fig 5.4). The absorbance increases sharply at wavelengths shorter than 350 nm. In order to capture absorbance trends across wavelength 230-800 nm and remain in the linear range of the spectrophotometer, reductions were carried out independently at two concentrations 50 mg L^{-1} from wavelength (230-350 nm) and at 500 mg L^{-1} (350-800 nm) (Fig. 5.4). A comparison of the time dependence measurements for PLFA and SRFA at low concentration is presented in Fig. 5.5 in order to highlight the time dependence differences in absorbance of the two fulvic acid samples. As seen in Fig. 5.6, at long wavelengths (350-800) the time dependence of borohydride reduction of all humic and fulvic acids behave in a similar manner. The majority of the borohydride induced reduction occurs within the first 2 hours of borohydride reduction initiation and continues at a lower rate for the 24 hour reduction period. Reoxidation over a period of 24 hours causes a smaller, continuing loss of absorbance at wavelengths 350 to 600 nm (Fig. 5.6). The 24 hour reoxidation period shows an absorbance loss that is concurrent with a reduction in pH as presented in Table 5.3.

Table 5.3 Reoxidation induced pH changes for Suwannee River fulvic acid (SRFA), Suwannee River humic acid (SRHA), Leonardite humic acid (LHA), Elliott humic acid (EHA), Pony Lake fulvic acid (PLFA).

sample	pH post 24 hour reduction	pH post 24 hour reoxidation	average $\mu\text{mole H}^+ \text{g}^{-1}_{\text{HA/FA}}$
SRFA 100 mg L ⁻¹	10.5	10.0	0.029 ± 0.012
SRFA 71 mg L ⁻¹	10.7	10.2	
SRHA 100 mg L ⁻¹	10.3	10.1	0.098 ± 0.009
SRHA 100 mg L ⁻¹	10.0	9.8	
LHA 50 mg L ⁻¹	10.3	9.5	0.145 ± 0.120
LHA 50 mg L ⁻¹	10.8	10.1	
EHA 50 mg L ⁻¹	10.5	9.9	0.075 ± 0.012
EHA 50 mg L ⁻¹	10.6	10	
PLFA 500 mg L ⁻¹	11.2	9.5	0.026 ± 0.017
PLFA 50 mg L ⁻¹	10.7	10.2	

Humic and fulvic acids exhibit absorbance that is pH dependent. High pH corresponds to high absorbance. Reduction in pH results in lower absorbance, indicating further borohydride induced loss of absorbance due solely to reoxidation unlikely. Reduced quinones are vulnerable to reoxidation, generating protons in an amount equivalent to the concentration of the quinone moieties in the humic/fulvic acid sample. Further there is strong evidence, as presented previously, that quinones are present in all humic and fulvic acids including PLFA (Chapter 3). Borohydride reduction generates an increase in pH from 7.6 to a pH range of 10.3 to 11.2 (Table 5.3). This range of pH coincides with a distribution of pK_as associated with phenols and amines, as well as possibly other unidentified species. The pK_a of phenol in water is 9.98 (Gross and Seybold (2001)), pK_a = 10.0 (Lind, Shen, Eriksen and Merenyi, (1990)). Cathchol is slightly lower with a pK_a of 9.5 (Gross and Seybold (2001)). Addition of a methoxy, methyl or amino

substituent increases the pKa of the phenolic group to between 10.0 and 10.3 (Gross and Seybold, 2001), (Lind, Shen, Eriksen and Merenyi, (1990)).

Terrestrial humic/fulvic acids derived, from lignin phenols may be reprotonated during reoxidation resulting in the observed drop in absorbance. Pony Lake fulvic acid at long wavelengths exhibits a loss in absorbance that is likely pH driven but cannot be attributed to phenolic moieties. Reprotonation of amine groups may lead to the change in absorbance seen in PLFA spectra from Figs. 5.4 and 5.5, making the mechanism of absorbance loss consistent but the identity of the titratable group different.

The pH drop associated with reoxidation was converted to $\mu\text{moles H}^+ \text{g}^{-1}_{\text{HA/FA}}$ and is tabulated in Table 5.3. The concentration of protons per gram of HA/FA was found to be significantly lower than the concentration of electrons per gram of HA/FA as measured by mediated electrochemical reduction found by (Aeschbacher, Sander and Schwarzenbach (2010)). Aeschbacher, found that reoxidation was not efficient with only 50% of the direct electrochemical reduction transferred to excess O_2 in LHS samples in 1 minute (Aeschbacher, Sander and Schwarzenbach (2010)). An additional 38% was transferred over the course of 24 hours and described as recalcitrant. No additional reoxidation was observed over the course of five days.

Aeschbacher, attributed the recalcitrant fraction of LHS to quinones and found the concentration of electrons associated with quinones to be $200 \mu\text{mol e}^- \text{g}^{-1}_{\text{LHA}}$. The concentration of protons $\text{g}^{-1}_{\text{HA/FA}}$ generated in 24 hours by reoxidation in this study is not of the magnitude of the concentration of e^- observed by (Aeschbacher, Sander and Schwarzenbach (2010)). The trends in HA/FA delineated in the Aeschbacher study are in part consistent with our results. Humic acids from soil terrestrial sources produced higher concentrations of protons per gram of

HA than did aquatic sources of HA from high concentration to low LHA>EHA>>SRHA. The fulvic acids SRFA and PLFA were not significantly different from each other and they were not significantly different from SRHA (Table 5.3). This may be a function of relatively high error associated with low concentration needed to remain within the linear range of the UV-Vis spectrophotometer. The drop in pH associated with reoxidation is qualitatively consistent with reoxidation of quinones in humic/fulvic acids, but given the inefficiency of quinone reoxidation shown by Aeschbacher, cannot be used to quantify their presence in humic substances (Aeschbacher, Sander and Schwarzenbach (2010)).

Examination of wavelength time dependent absorbance changes due to borohydride reduction are seen in Figs 5.5 and 5.6. Difference and fractional difference spectra (230 and 400 nm) of SRFA (35 mg L⁻¹) and PLFA (50 mg L⁻¹) each showing a pH dependent change in absorbance is displayed in Fig. 5.7. Suwannee River fulvic acid (SRFA) (35 mg L⁻¹) exhibits loss in absorbance over the entire UV-Vis spectrum upon borohydride reduction. This is consistent with previous published results concluding that no gain in absorbance is achieved via the expected complete or partial reoxidation of quinones. The lack of any observable recovery in may be due to a low concentration of quinones and their relatively small impact on the optical properties of terrestrially derived humic material. Clearly, evidence exists that quinones are present in terrestrial HS (soil and aquatic).

Experiments conducted by (Aeschbacher, Sander and Schwarzenbach (2010)) on electron accepting capacity (EAC) implicate quinones as an electron buffer. Quinones may play an important part in redox chemistry of HA but may be less important contributor to the optical properties. Pony Lake fulvic acid (PLFA) (50 mg L⁻¹) (Fig. 5.7) does not exhibit a continuum of absorbance loss across all wavelengths. Recovery can be seen at short wavelengths (< 350 nm)

but not at long wavelengths (400-800 nm). Difference $A(0)-A(T)$ and fractional difference spectra $A(T)/A(0)$ of PLFA (50 mg L^{-1}) show a continuous loss in absorbance with increasing wavelength due to reduction with borohydride in anaerobic conditions. The transition to an aerobic environment produces short wave length recovery that is not seen at wavelengths longer than 350 nm (Fig. 5.7).

Time dependent absorbance plots show recovery of PLFA over the 24 hour reoxidation period with a concurrent decrease in pH from 10.5 to 9.5 (Fig. 5.5). The pH of SRFA also decreases in pH from pH 10.7 to pH 10.2 but the reduction in pH associated with SRFA has an associated decrease in absorbance that is not evidence in PLFA. Changes in pH are likely driven by the partial reoxidation of quinones as they are reoxidized in a 1 to 1 e^- loss to proton gain relationship. Reduction of quinones may interfere with physical connectivity such as disruption of stacking between black-carbon conjugated systems or heterocyclic compounds. Quinones may be partially reoxidized but the physical connectivity that results in charge transfer bands may not be reestablished. Reoxidized quinones no longer participating in charge transfer complexes may be expected to exhibit increased absorbance at wavelengths between 230 and 300 nm as they are no longer being used as electron acceptors.

PLFA at high concentration (500 mg L^{-1}) was used to examine long wavelength absorbance trends (400 nm to 800 nm), while PLFA at low concentration (50 mg L^{-1}) was used to examine short wavelength trends ($< 350 \text{ nm}$) (Fig. 5.4). The absorbance recovery associated solely with PLFA may indicate that quinones play a more important role in microbially derived fulvic acids than they do in other fulvic and humic substances. It is unclear whether the recovery is a phenomenon of solely the availability of moieties able to form charge transfer bands in PLFA. A lack of heterogeneity of sites or low concentration of sites able to form charge transfer

bands or some combination of the two may support observable short wavelength recovery in PLFA. Terrestrially, sourced humic and fulvic acids may be using quinones to form charge transfer bands, but it is likely based on the lack of dynamic change to the absorbance spectra in response to reoxidation, post-borohydride reduction, that any effect provided by regeneration of quinone derived charge transfer bands may be masked by other types of moieties able to regenerate at higher concentration and/or in a more robust manner.

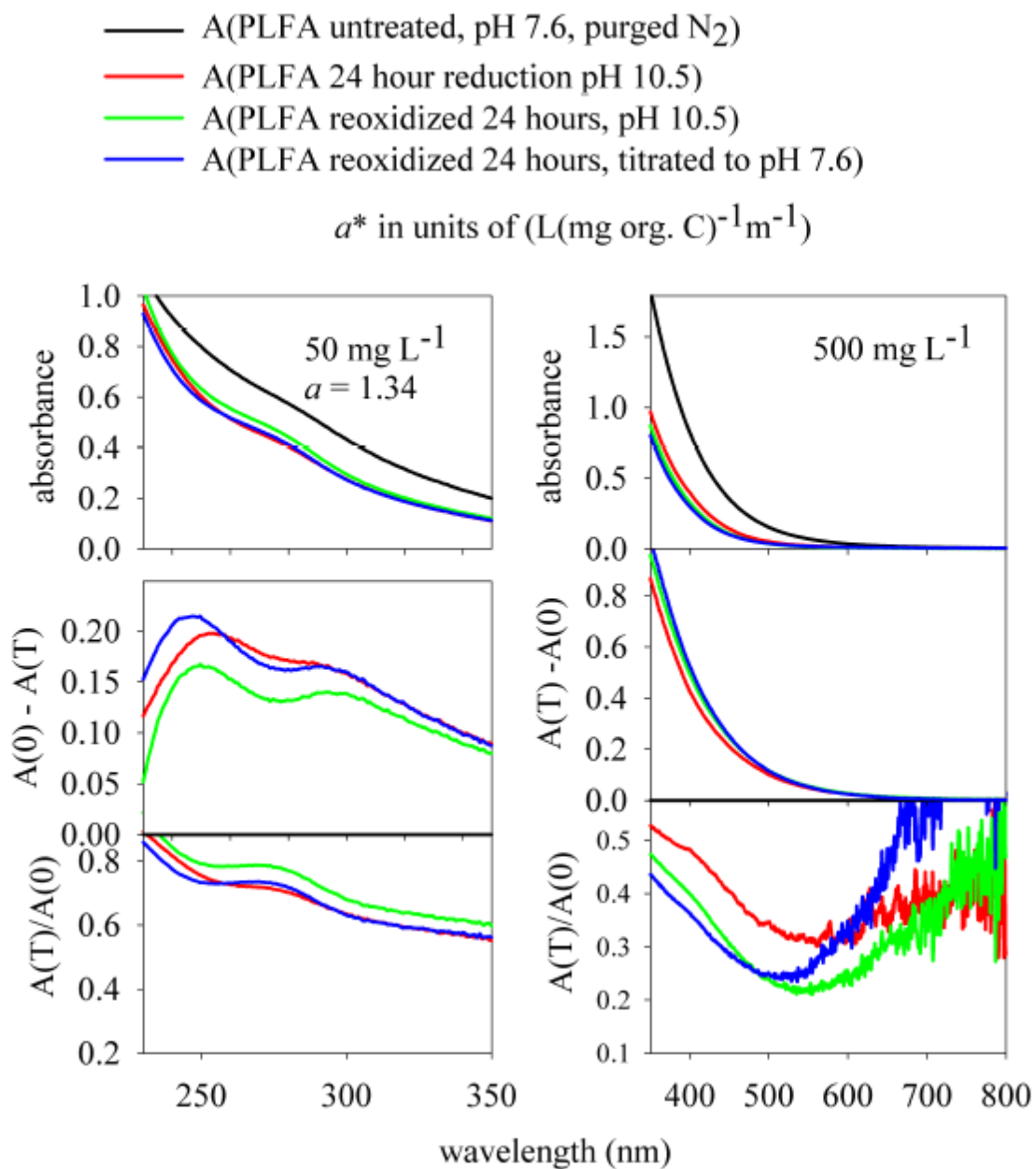


Figure 5.4 Absorbance, absorbance difference $A(0) - A(T)$, fractional difference $A(T)/A(0)$ of Pony lake fulvic acid (PLFA) at concentrations of 50 and 500 mg L⁻¹ reduced with 5 and 25 mg L⁻¹ sodium borohydride for 24 hours, reoxidized for 24 hours and titrated back to the initial pH condition of 7.6. a^* is for the untreated sample.

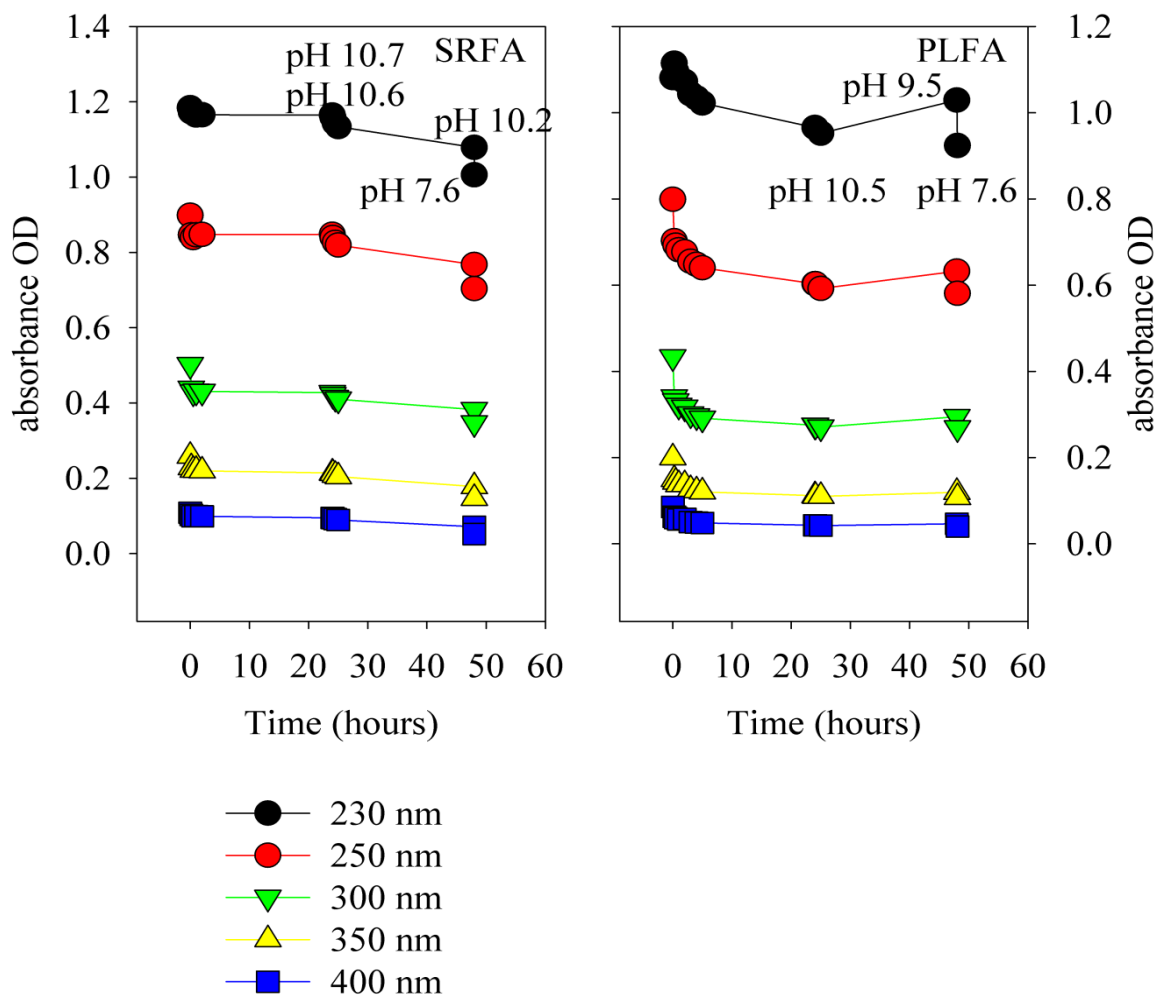


Figure 5.5 Time dependence of the absorbance for the borohydride reduction and reoxidation of Suwannee River fulvic acid (SRFA) (35 mg L^{-1}) and Pony Lake fulvic acid (PLFA) (50 mg L^{-1}) from 230 – 400 nm

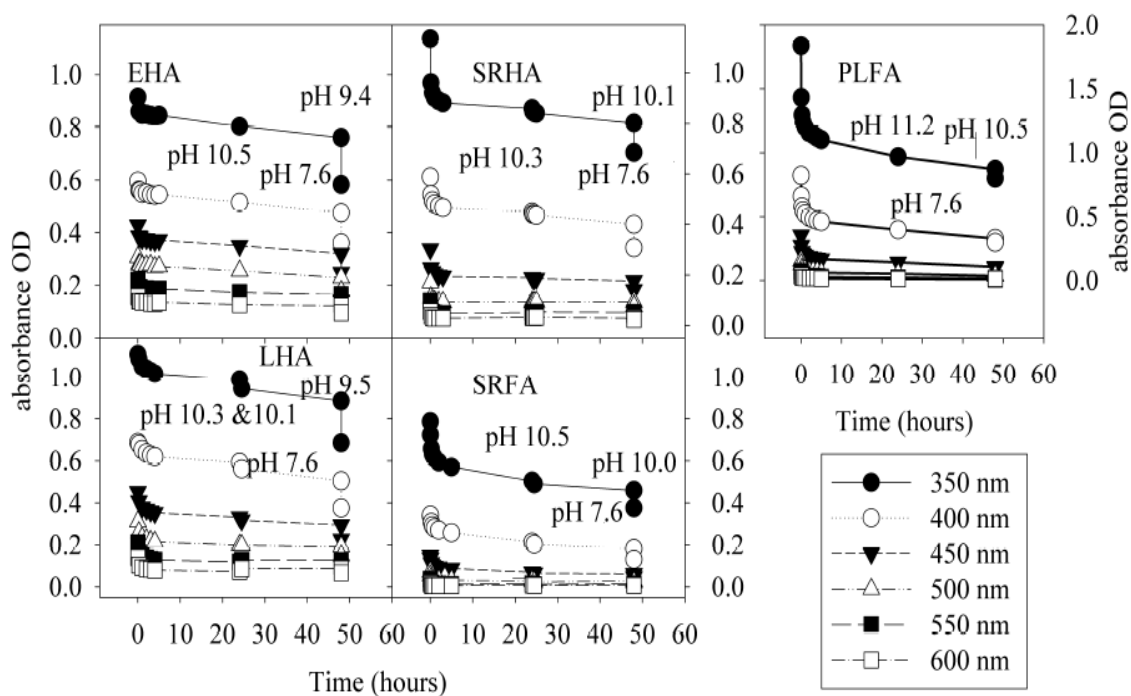


Figure 5.6 Time dependence of the absorbance for the borohydride reduction and reoxidation of Elliott humic acid (EHA), Leonardite humic acid (LHA), Suwannee River humic acid (SRHA), Suwannee River fulvic acid (SRFA) and Pony Lake fulvic acid at concentrations of 50 mg L^{-1} (EHA and LHA), 100 mg L^{-1} (SRHA and SRFA) and 500 mg L^{-1} (PLFA). All samples were reduced with sodium borohydride for 24 hours, reoxidized for 24 hours and titrated to pH 7.6.

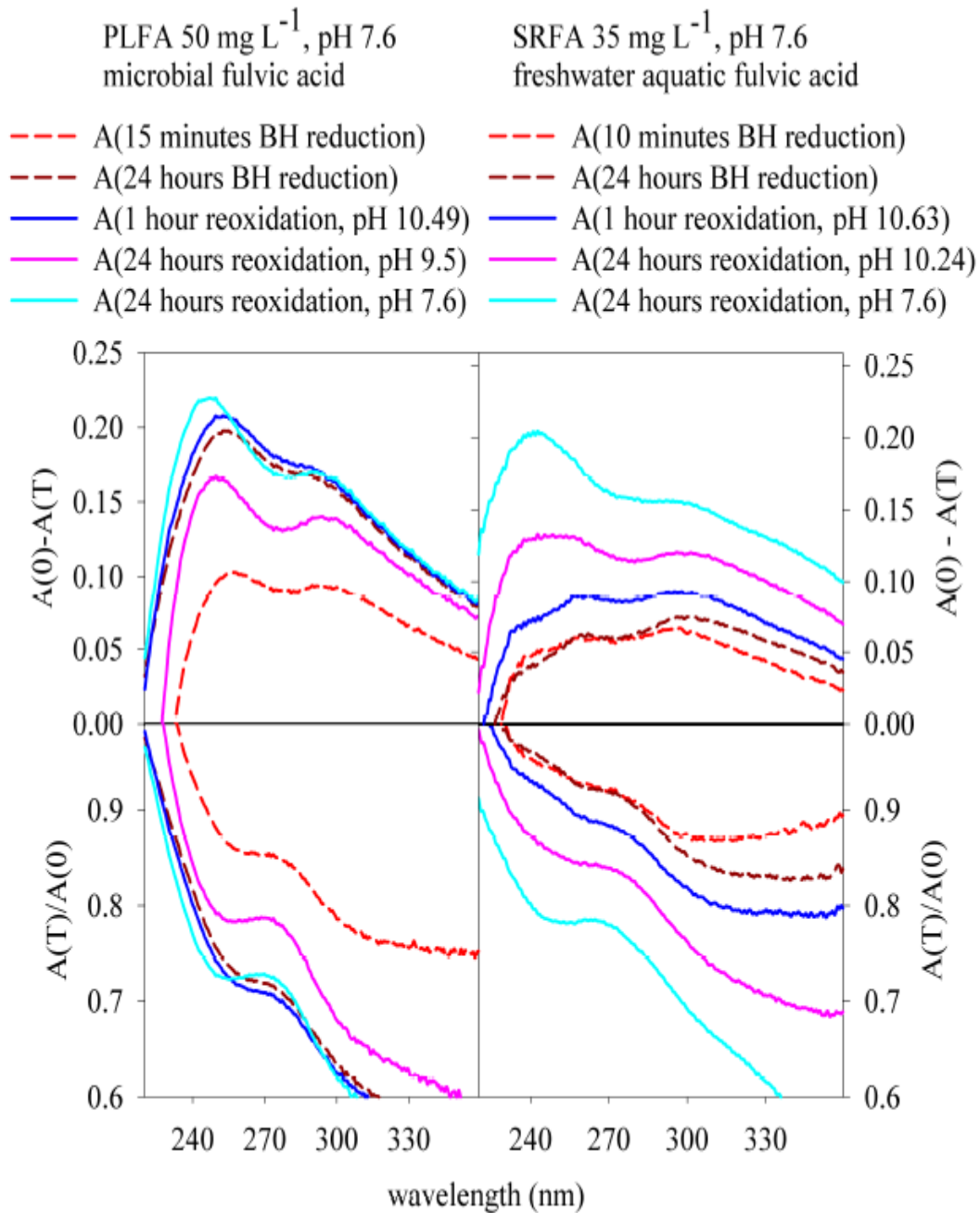


Figure 5.7 Absorbance difference $A(0)-A(T)$ and fractional difference $A(T)/A(0)$ of Pony Lake fulvic acid (PLFA) (50 mg L^{-1}) and Suwannee River fulvic acid (SRFA) (35 mg L^{-1}) reduced with 5 mg sodium borohydride (BH) for 24 hours, reoxidized for 24 hours and titrated to the initial pH 7.6 highlights differences in reduction and reoxidation behavior in fulvic acids from different sources.

5.3.3 Untreated and Borohydride Reduced Spectral Slope Values

Parameterized spectral slope data $a(\lambda) = a^*(\lambda_0) \exp^{-S(\lambda-\lambda_0)}$ (Eq. 5.2), with a wavelength interval of 290-820 nm, show that in all cases borohydride reduced materials have higher spectral slope values than do matched untreated materials as presented in Figs. 5.8, 5.9 and Table 5.4. The modeled a^* values, $(a^*(350 \text{ nm}) = 2.303 a(\lambda)/(b * c))$ (Eq. 5.1) are concentration dependent increasing as the sample concentration increases. The initial a^* values were calculated using pH 7.6 and 350 nm absorbance point and absorbance spectra carbon normalized prior to parameterization (Table 5.2 and Eq. 5.1). Untreated spectral slope coefficients ranked from high to low are:

$$\text{LAC} > \text{PLFA} > \text{SRFA} > \text{SRHA} > \text{LHA} > \text{EHA}$$

Borohydride reduction did not affect the order of S values with the exception of PLFA which had an S coefficient of 0.0194 ± 0.0006 . This value was on the same scale as LAC, $S = 0.0193 \pm 0.0008$. The borohydride reduced S coefficients of the aquatic materials SRHA and SRFA were 0.0149 ± 0.0004 and 0.0184 ± 0.0004 respectively. The borohydride reduced S coefficient of EHA was 0.0083 ± 0.0001 . Notably, the LHA S coefficient was 0.0108 ± 0.0005 . The percent change in spectral slope coefficient values provides insight into the underpinnings of the charge transfer mechanism (Table 5.4). The universal increase in spectral slope points to disruption of charge transfer bands and the loss of quenching of acceptor and /or donor moieties in the structural framework of the materials tested. The fulvic acids exhibit the highest percent change with 27 and 30 % for SRFA and PLFA respectively. The humic acids have about a 10 % difference between untreated and borohydride reduced spectral slope coefficient values. Notably, LHA has a 22 % difference which may reflect higher levels of black carbon or other chemical classes unaffected by borohydride reduction. In studies by Allard, it was determined

that lignite humic acids such as LHA are further in the humification process than other soil derived humic acids (Allard and Derenne, 2007), (Allard, 2006). LHA was found to have derived from plants with very little microbial input as measured by bound lipid fraction (Allard, 2006). The difference in untreated and borohydride reduced LAC S coefficient value changed by 15%. This is unlike either humic or fulvic acids tested.

Table 5.4 Percent change of spectral slope coefficients (S) for untreated and borohydride reduced samples Suwannee River humic (SRHA), Suwannee River fulvic acid, (SRFA), Elliott humic acid (EHA), Leonardite humic acid (LHA), Pony Lake fulvic acid (PLFA) and Lignin Alkali Carboxylate (LAC). Samples were not cleaned with Sephadex G-10. All data presented have correlation coefficients (r^2) > 0.99.

sample identification	untreated $S_{(290-820 \text{ nm})}$	borohydride reduced $S_{(290-820 \text{ nm})}$	% change
SRHA	0.0126 ± 0.0005	0.0149 ± 0.0004	9
SRFA	0.0144 ± 0.0004	0.0184 ± 0.0004	27
EHA	0.0075 ± 0.0003	0.0083 ± 0.0001	10
LHA	0.0088 ± 0.0002	0.0108 ± 0.0005	22
PLFA	0.0149 ± 0.0002	0.0194 ± 0.0006	30
LAC	0.0168 ± 0.0001	0.0193 ± 0.0008	15

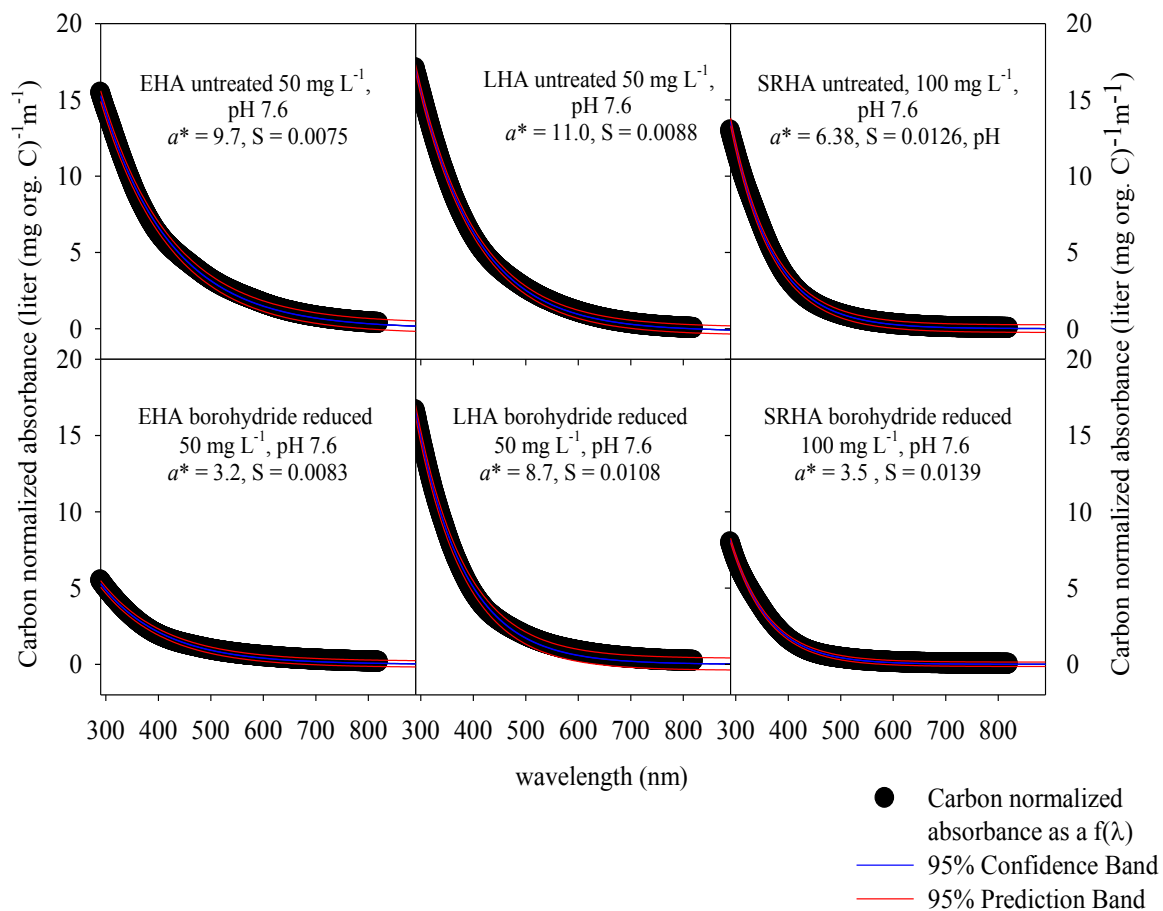


Figure 5.8 Parametrized HA absorbance of Elliot (EHA), Leonaridite (LHA) and Suwannee River humic acid (SRHA). Spectral slope values (S) are based on the exponential equation: $a(\lambda) = a(\lambda_0) \exp^{-S(\lambda-\lambda_0)}$ where $a(\lambda)$ and $a(\lambda_0)$ are the absorption coefficients at wavelength λ and reference wavelength λ_0 . λ_0 is 350 nm. Initial $a(\lambda) = 2.303 a(350 \text{ nm}) * \text{pathlength (m)}^{-1} * \text{concentration of organic carbon (mg)}$.

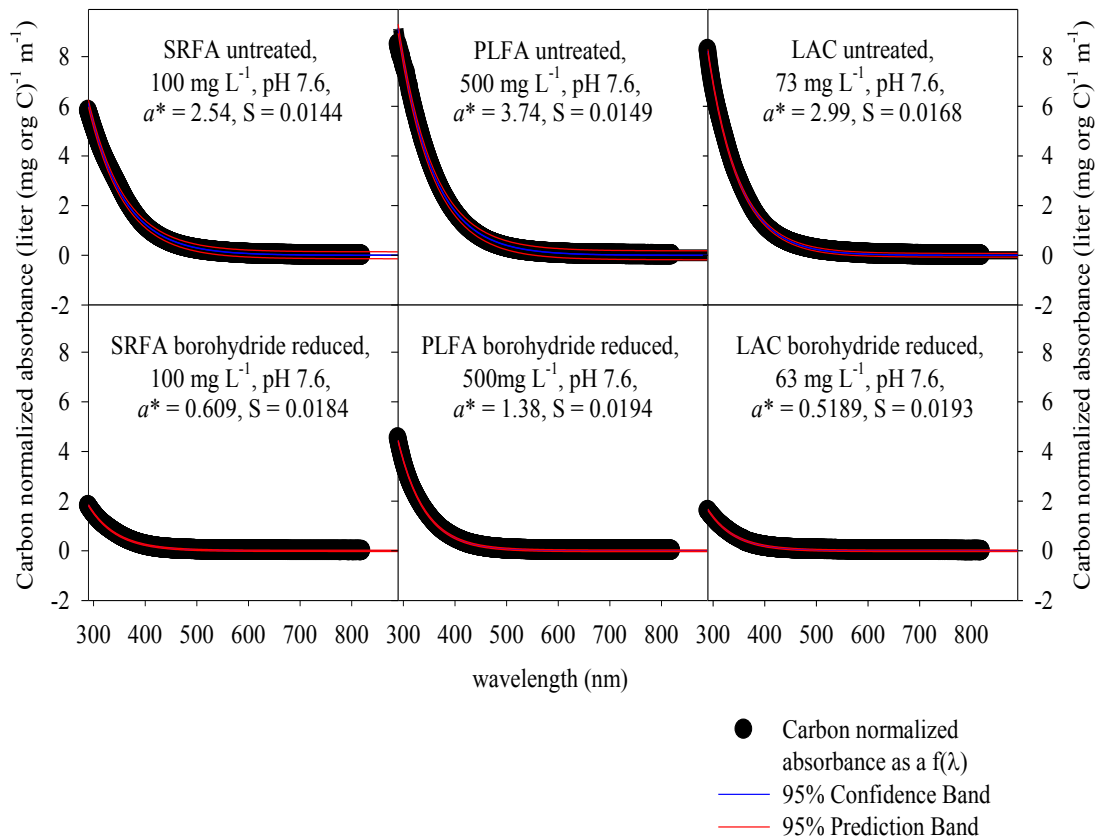


Figure 5.9 Paramaterized absorbance of Suwannee River (SRFA) and Pony Lake (PLFA) acids and Lignite Alkali Carboxylate (LAC). Spectral slope values (S) are based on exponential equation: $a(\lambda) = a(\lambda_0) \exp^{-S(\lambda-\lambda_0)}$ where $a(\lambda)$ and $a(\lambda_0)$ are the absorption coefficient at wavelength λ and reference λ_0 . λ_0 is 350 nm. Initial $a(\lambda) = 2.303 a(350 \text{ nm}) * \text{pathlength} (\text{m}^{-1}) * \text{concentration of organic carbon} (\text{mg})$.

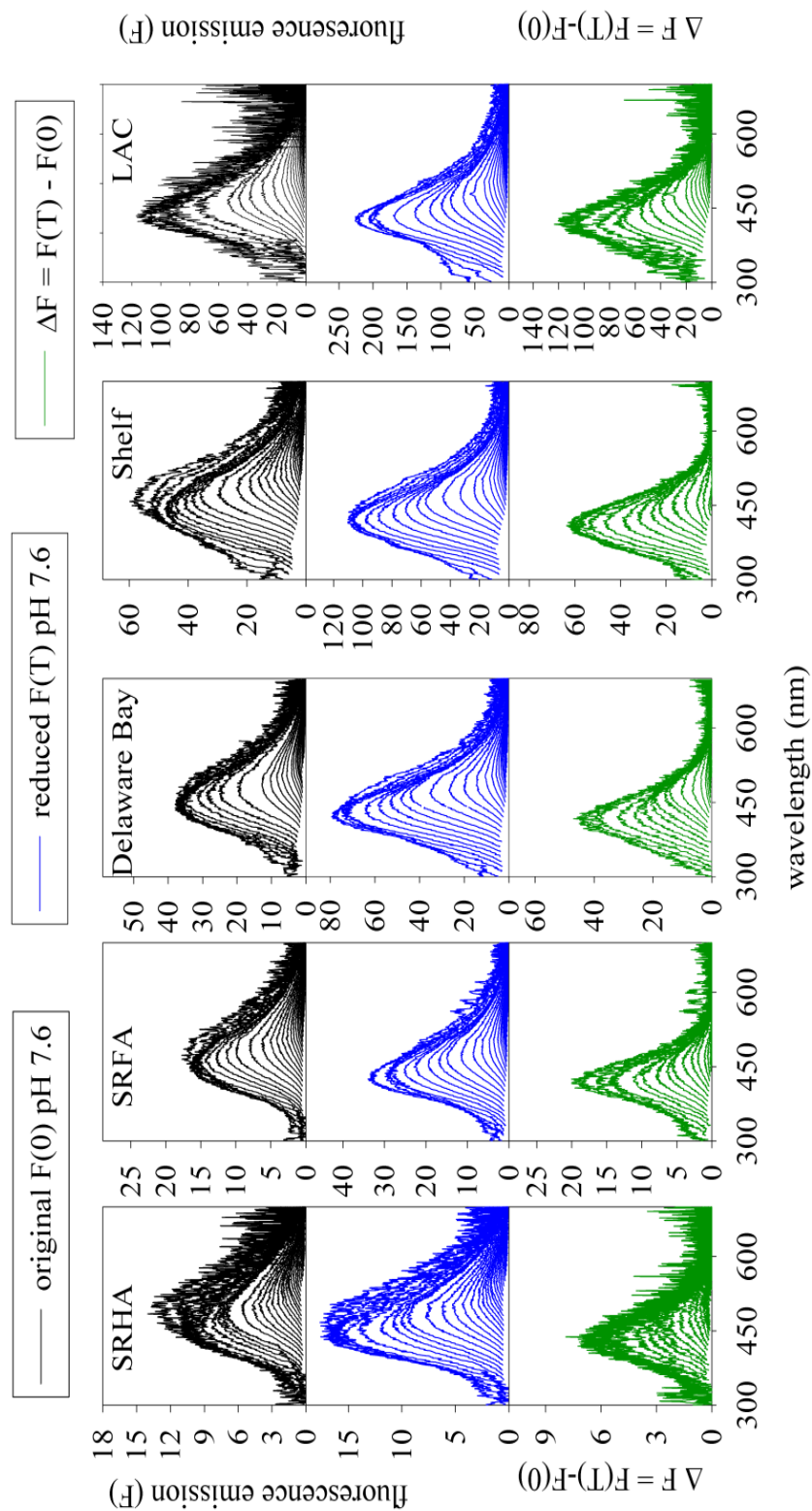
5.3.4 Untreated and Borohydride Reduced Fluorescence Spectra

The fluorescence measurements presented in Figs. 5.10, 5.11 and 5.12 include Suwannee River fulvic and humic acids, CDOM from Delaware Bay and the mid-Atlantic shelf as well as Lignin Alkali Carboxylate (LAC) (Fig. 5.10). Figure 5.11 includes soil humic acids, Elliott (EHA) and Leonardite (LHA) humic acid. Figure 5.12 presents the microbial fulvic acid, Pony Lake fulvic acid (PLFA). The untreated fluorescence excitation-emission matrix spectra (EEMS) $F(0)$ are in the top series of panels with excitation wavelengths progressing at 10 nm intervals from 280 to 600 nm and the fluorescence emission spectra collected at 10 nm longer wavelengths than the corresponding excitation wavelengths (290 to 610 nm) (black lines). The middle series of fluorescence excitation-emission spectra $F(T)$ (blue lines in Fig 5.10, black lines in Figs 5.11 and 5.12) are collected in an analogous manner as the initial $F(0)$ (EEMS), but they have been borohydride reduced for 24 hours, reoxidized for 24 hours and titrated back to the initial pH condition of 7.6. The bottom series of EEMS are the difference between $F(T)$ and $F(0)$ (green lines in Fig. 5.10 and black lines in Figs 5.11 and 5.12). A colored figure showing the excitation emission pattern of EEMS is presented in Chapter 1, Fig. 1.3.

The spectra were conducted using optically thin dilutions as determined by absorbance spectra between 0.05 and 0.1 optical density (OD) regardless of the initial concentration used for the reduction. Reduction caused irreversible changes in the emission spectra. All reduced spectra were seen to blue shift and increase in intensity when compared to the untreated emission spectra. The untreated (pH 7.6) and borohydride reduced (pH 7.6) emission spectra of SRFA, SRHA, LAC and the CDOM samples from the mid-Atlantic Bight self and Delaware Bay increase smoothly from long wavelength excitation to short wavelength excitation with the exception of very short wavelength (280-290 nm), which are noisier and shifted to the red (Fig.

5.10). The gain in fluorescence is quantified by $\Delta F = F(T) - F(0)$ with $F(T)$ representing 24 hours of reduction, 24 hours of reoxidation and titration back to the pH of 7.6. SRHA exhibits the smallest gain in fluorescence with an increase of 7 corrected fluorescence units, SRFA has an increase of 20, Delaware Bay increases by about 45, Atlantic shelf CDOM increases by approximately 62 and LAC increases by 120 corrected fluorescence units (Fig. 5.10).

Figure 5.10 Excitation-emission matrix spectra (EEMS) of Suwannee River humic acid (SRHA), Suwannee River fulvic acid (SRFA), CDOM from the Delaware Bay, CDOM from the mid-Atlantic shelf and Lignin Alkali Carboxylate (LAC) prior to F(0) (black lines) and following F(T) (blue lines) reduction with sodium borohydride at pH 7.6. ΔF (green lines) is the difference between the reduced emission spectra and the untreated emission spectra. Emission spectra were collected from 200 to 600 nm at 10 nm intervals. Each corresponding excitation wavelength is 10 nm less than the emission wavelength.



Excitation-emission matrix spectra (EEMS) of untreated terrestrial humic substances Elliott (EHA) and Leonardite (LHA) humic acids (Fig. 5.11, top spectra) differ from other HS instead of increasing intensity and blue shifted peak maxima previously seen in untreated aquatic HS and CDOM (Fig. 5.10, top spectra). The fluorescence emission maximum increases to 575 nm from excitation wavelength 600-440 nm. Emission decreases to 550 nm between excitation wavelengths 450-400 nm remaining at fluorescence emission 550 nm from excitation wavelengths 400-280 nm. Leonardite HS fluorescence emission increases smoothly to 500 nm from excitation wavelengths 600-420 nm. The fluorescence emission remains at 500 nm from excitation 420-280 nm (Fig. 5.11).

Following borohydride reduction the EEMS of (Fig. 5.11, middle spectra) EHA and LHA double in intensity and the emission maxima shifts to shorter wavelengths (blue shift) by approximately 100 nm. The EEMS of untreated terrestrial material (EHA and LHA) exhibit high fluorescence emission intensity at long wavelengths (red edge) relative to aquatic samples (Fig. 5.10). EEMS of aquatic samples at the red edge (long wavelength) recede to the baseline while the terrestrial samples show significant emission under the same optical conditions. Further, upon reduction the blue shift is on the scale of hundreds of nanometers for soil samples (EHA and LHA) as opposed to tens of nanometers found in aquatic samples (SRHA, SRFA and CDOM). Finally, aquatic samples appear to have smooth almost monotonic emission spectra as the excitation spectra increases in energy, with the exception of the previously noted short wavelengths (280-300 nm). No sub-features appear in the aquatic samples. This is not the case in the terrestrial samples where a secondary feature can be seen at low excitation wave lengths (Fig. 5.11).

It has already been noted in the introductory material in Chapter 2 that Leonardite humic acid (LHA) is operationally generated from lignite material and as such should be high in black carbon or black carbon-like materials. Elliott humic acid (EHA) is derived from prairie soil and is also expected to contain black carbon stemming from natural fires, but it is intuitive to think that LHA would have a higher concentration of black carbon or condensed carbon than does EHA, (Fang, Chua, Schmidt-Rohr and Thompson (2010)), (Mao, Fang, Schmidt-Rohr, Carmo, Hundal and Thompson (2007)), (Allard (2006)), (Krull, Baldock and Skjemstad (2003)). Skjemstad, Reicosky, Wilts and McGowan (2002) estimated that 10-30 % of recalcitrant material in terrestrial humic substances is black carbon or extended aromatic systems, possibly in a stacked configuration. Mao, Fang, Schmidt-Rohr, Carmo, Hundal and Thompson (2007) determined by solid state nuclear magnetic resonance that 64 % of soil HA from two Iowa soils is non-protonated aromatic carbon or part of a fused ring system. The high fluorescence at long wavelength emission is attributable to black carbon in a stacked conformation. Black carbon, composed of carbon and hydrogen in a stacked arrangement, should be unaffected by borohydride reduction as it does not contain large amounts of molecular oxygen. Comparing the difference ΔF plots of Elliot and Leonardite from Fig. 5.11 it is clear that LHA has higher levels of long wavelength emission than does EHA, which is consistent with what would be expected based on the sources of the sample material (Allard and Derenne (2007)), (Allard (2006)).

The fluorescence emission spectra of Pony Lake fulvic acid (PLFA) doubles in intensity at wavelengths below 500 nm and does not change appreciably at wavelengths longer than 520 nm when reduced with sodium borohydride. The emission spectra of both the untreated and borohydride treated PLFA blue shifts uniformly with decreasing excitation wavelength with the exception of the shortest excitation wavelengths from 280-300 nm. Reduction causes a 50-nm

blue shift in wavelength maxima of borohydride treated PLFA when compared untreated PLFA. An examination of the ΔF of PLFA shows a gain in fluorescence emission at 300 nm that is not observed in other HA/FA standards (SRHA, SRFA, EHA, LHA, LAC, CDOM from the Delaware Bay) but can be seen in the mid-Atlantic shelf CDOM sample (Figs. 5.10 and 5.12).

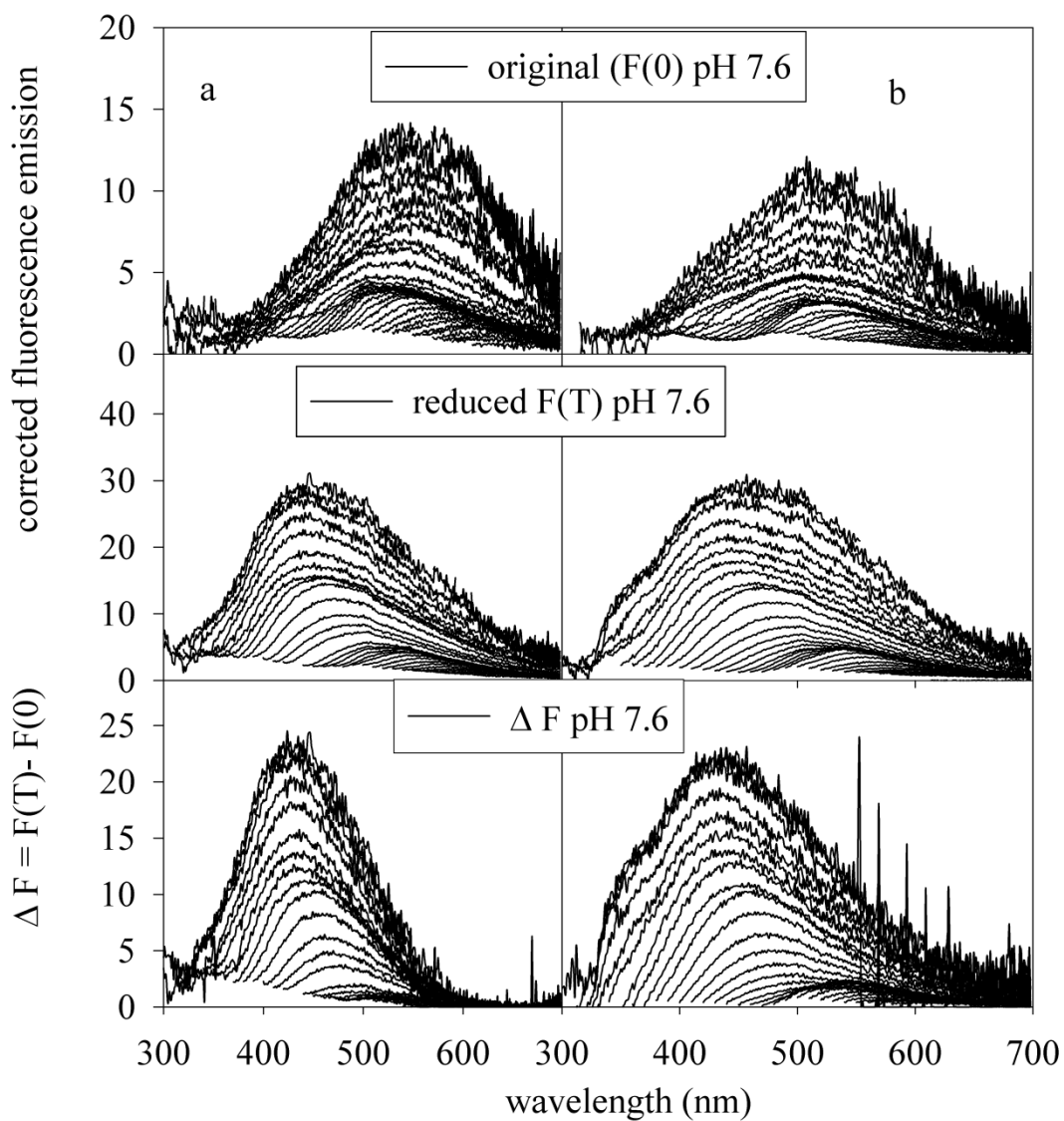


Figure 5.11 Excitation-emission matrix spectra (EEMS) of Elliott humic acid (EHA) (panel a) and Leonardite humic acid (LHA) (panel b) prior to (top panel) and following (middle panels) the reduction with sodium borohydride at pH 7.6. ΔF (bottom panels) represents the difference before and after reduction. Emission spectra were collected from 200 to 600 nm at 10 nm intervals. Each corresponding excitation wavelength is 10 nm less than the emission wavelength.

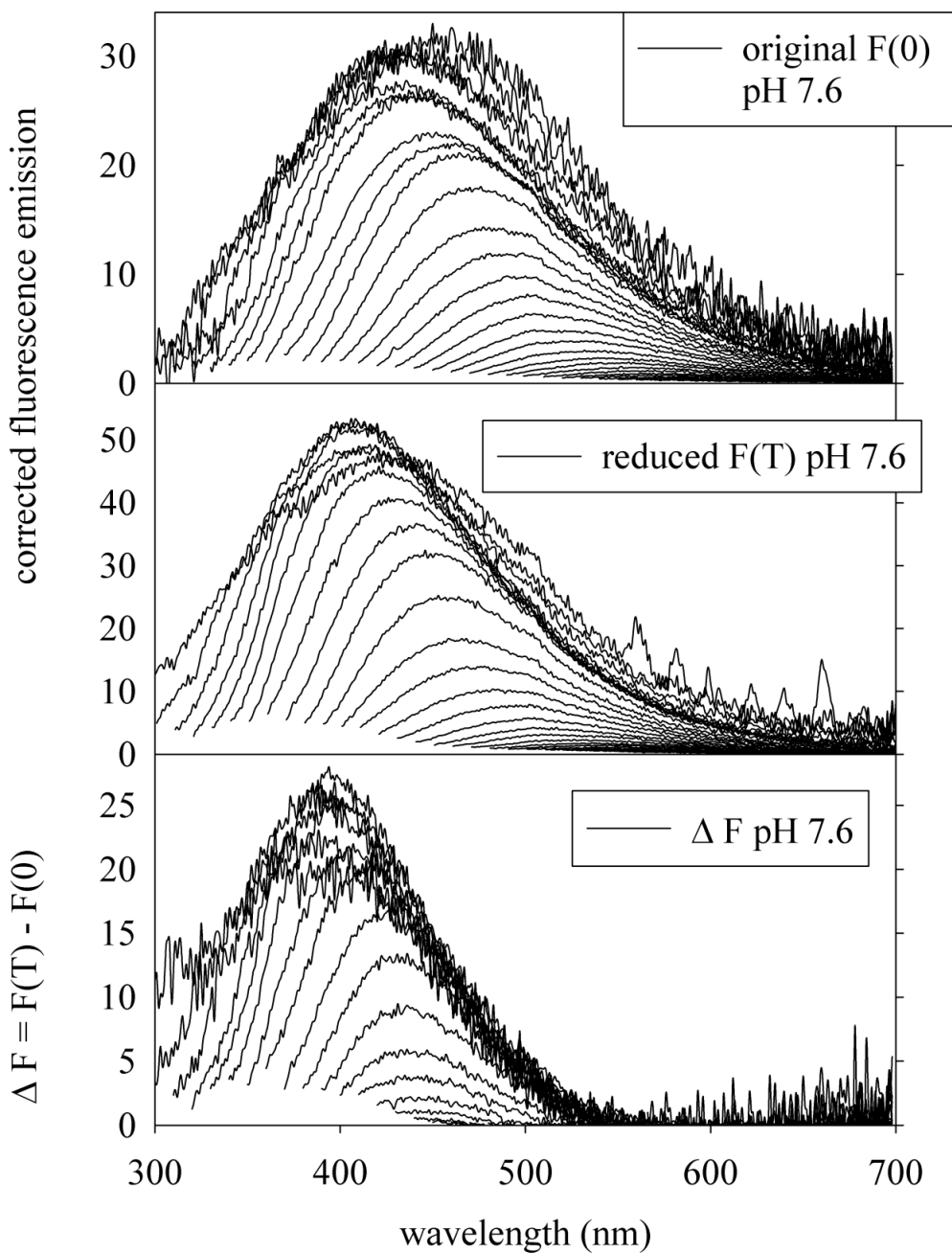


Figure 5.12 Excitation-emission matrix spectra (EEMS) of Pony Lake fulvic acid (PLFA). Untreated PLFA at pH 7.6 (upper panel), following sodium borohydride reduction and titrated back to the initial pH of 7.6 (middle panel) and the difference (ΔF) between untreated and borohydride reduced PLFA at pH 7.6 (bottom panel). Emission spectra were collected from 200 to 600 nm at 10 nm intervals. Each corresponding excitation wavelength is 10 nm less than the emission wavelength.

Comparisons of borohydride reduced EEMS at pH 10.5 (black lines) with borohydride reduced, reoxidized and titrated to pH 7.6 EEMS (white lines) are presented in Figs. 5.13 and 5.14 at intervals of 20 nm from 280 to 600 nm. Fig. 5.13 includes EHA, LHA, SRFA, PLFA, SRHA and PLFA. Fig. 5.14 includes CDOM samples from the mid-Atlantic shelf and the Delaware Bay. Emission spectral intervals were increased from 10 nm to 20 nm in order to simplify the figures. All previously presented spectra are based on 10 nm intervals. Leonardite HA, CDOM from the Delaware Bay and CDOM from the Atlantic Shelf exhibit no substantial change in either wavelength maxima or fluorescence emission intensity with exception of a small loss of emission on the red edge of the emission profiles (Fig. 5.14). Elliot HA, SRFA, SRHA and PLFA all show significant changes in intensity at the wavelength maxima and lost emission intensity on the red edge of the emission profiles. Suwannee River HA and SRFA lose 1/3 of the fluorescence emission intensity between 310 and 400 nm (Fig. 5.13). Elliott HA and PLFA lose 1/4 of their fluorescence emission intensity between 310 and 400 nm (Fig. 5.13). Lignin alkali carboxylate (LAC) has uniformly decreasing emission with a loss of 1/5 of its emission intensity (Fig. 5.13).

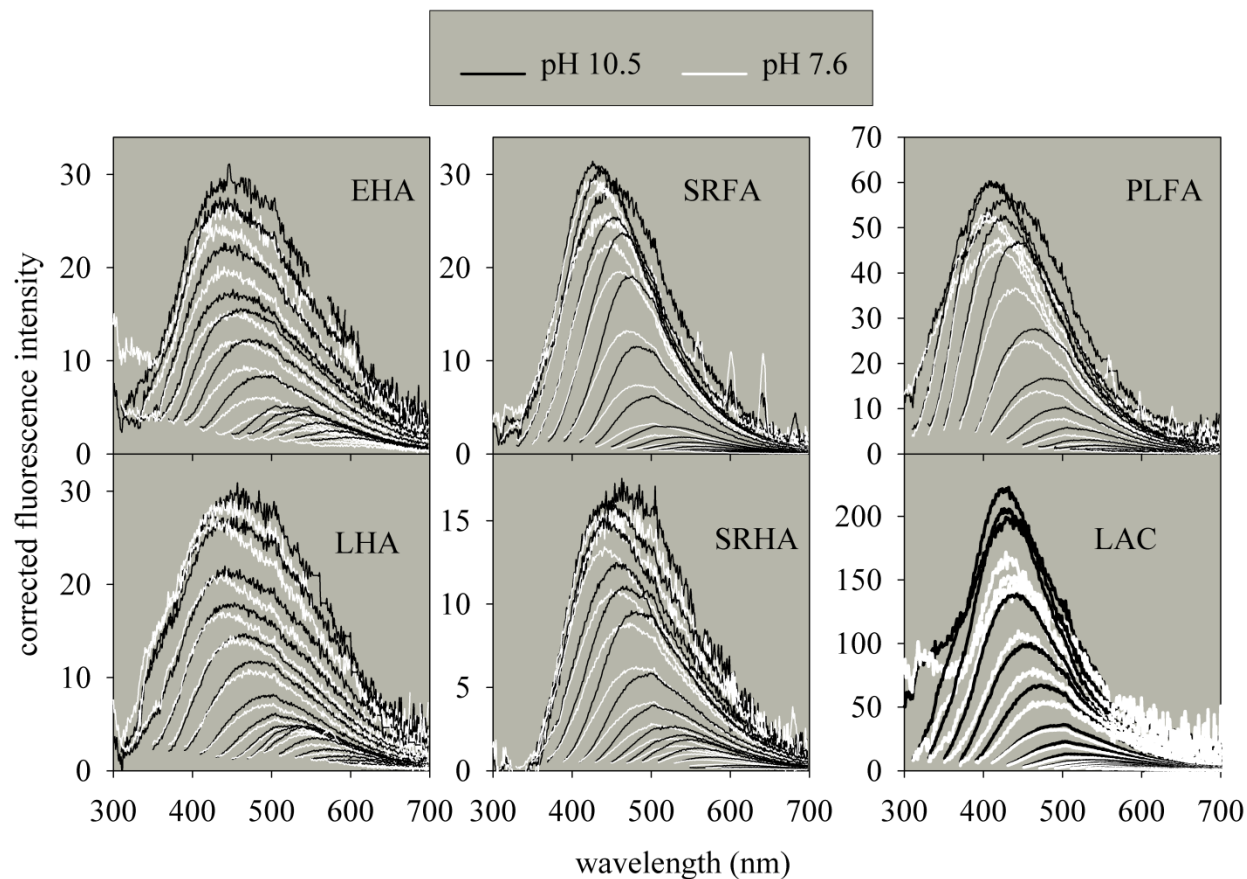


Figure 5.13 pH dependence of the excitation-emission matrix spectra (EEMS) of borohydride reduction at pH 10.5 (black lines) and reduced, reoxidized and titrated to pH 7.6 (white lines) of Elliott humic acid (EHA), Leonardite humic acid (LHA), Suwannee River humic acid (SRHA), Suwannee River fulvic acid (SRFA), Pony Lake fulvic acid (PLFA), and Lignin Alkali Carboxylate (LAC). Emission spectra were collected from 200 to 600 nm at 20 nm intervals. Each corresponding excitation wavelength is 10 nm less than the emission wavelength.

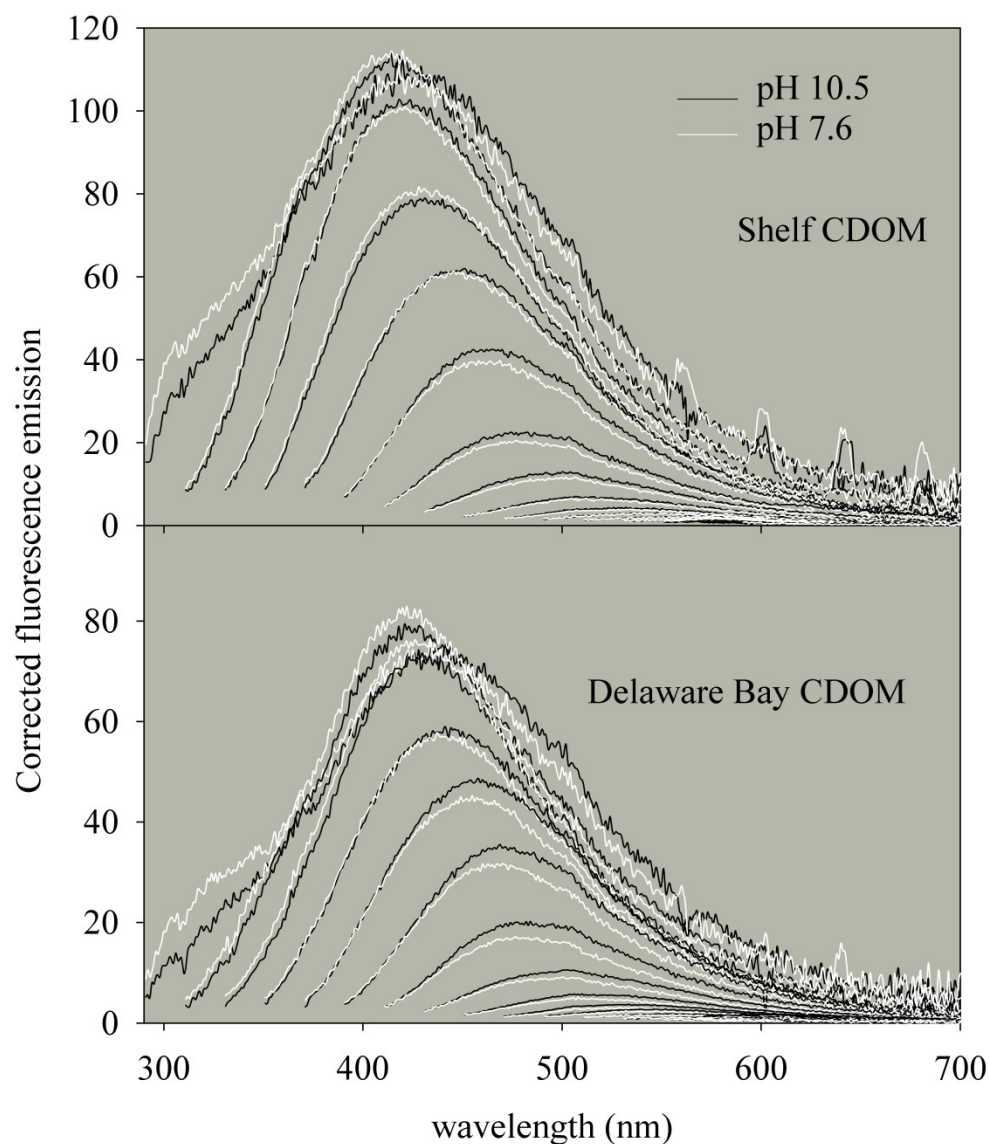


Figure 5.14 Excitation-emission matrix spectra (EEMS) of Delaware Bay CDOM and Mid-Atlantic Bight shelf CDOM borohydride reduced at pH 10.5 (black lines) and borohydride reduced, reoxidized and titrated to pH 7.6 (white lines). Emission spectra were collected from 200 to 600 nm at 20 nm intervals. Each corresponding excitation wavelength is 10 nm less than the emission wavelength.

5.3.5 Fluorescence Quantum Yield (Φ)

Quantum yield (Φ) is the ratio of photons fluorescing to the number photons absorbed (Chapter 1, Fig. 1.3). The quantum yields and wavelength maxima of SRHA, SRFA, CDOM from Delaware Bay, CDOM from mid-Atlantic shelf, LAC, PLFA, LHA and EHA are presented in Figure 5.15. The quantum yields and wavelength maxima reflect differences between soil and aquatic HS derived from lignin phenol. Two points are evident (1) soil humic substances (LHA) and (EHA) have contributions to their fluorescence emission spectra that are not represented in aquatic materials (SRFA) and (SRHA) (Figs. 5.10 and 5.11). Borohydride reduction eliminates the long wavelength fluorescence contributor in EHA and halves it in the LHA samples. This loss in long wavelength fluorescence may be an indication of disruption of stacking of black carbon. The inability to regenerate post-borohydride reduction physical proximity (stacking) required for the extended conjugation would concurrently lead to a reduction fluorescence emission at long wavelengths. (2) Untreated soil humic substances exhibit a plateau in fluorescence wavelength maxima that is not seen in other humic substances or observed post borohydride reduction as seen in Fig. 5.15. Speculatively, the soil wavelength maxima trend and the large fluorescence blue shift produced by borohydride reduction may be reflective of the lack of photochemical exposure and/or the relative physical stability afforded by the soil matrix, which may allow some moieties labile to photochemical alteration to be preserved in soil environments. It has been suggested that soil humic material is capable of forming micelles that can provide protection to labile moieties (Sutton and Sposito (2005)). Formation of micelles is unlikely due to the Beer Lambert behavior seen in all of the HS in this study and presented in Chapter 6. Other forms of protection such as encapsulation or association with cations or clays are known to provide protection from enzymatic attack (Heighton, Schmidt and Siefert (2008)),

(Hedges, Mayorga, Tsamakis, McClain, Aufdenkampe, Quay, Richey, Benner, Opsahl and Black (2000)). Borohydride reduction of soil HA (EHA and LHA) potentially captures additional types and a higher concentrations of reducible species than is seen in aquatic sources of lignin derived HA/FA (SRHA and SRFA).

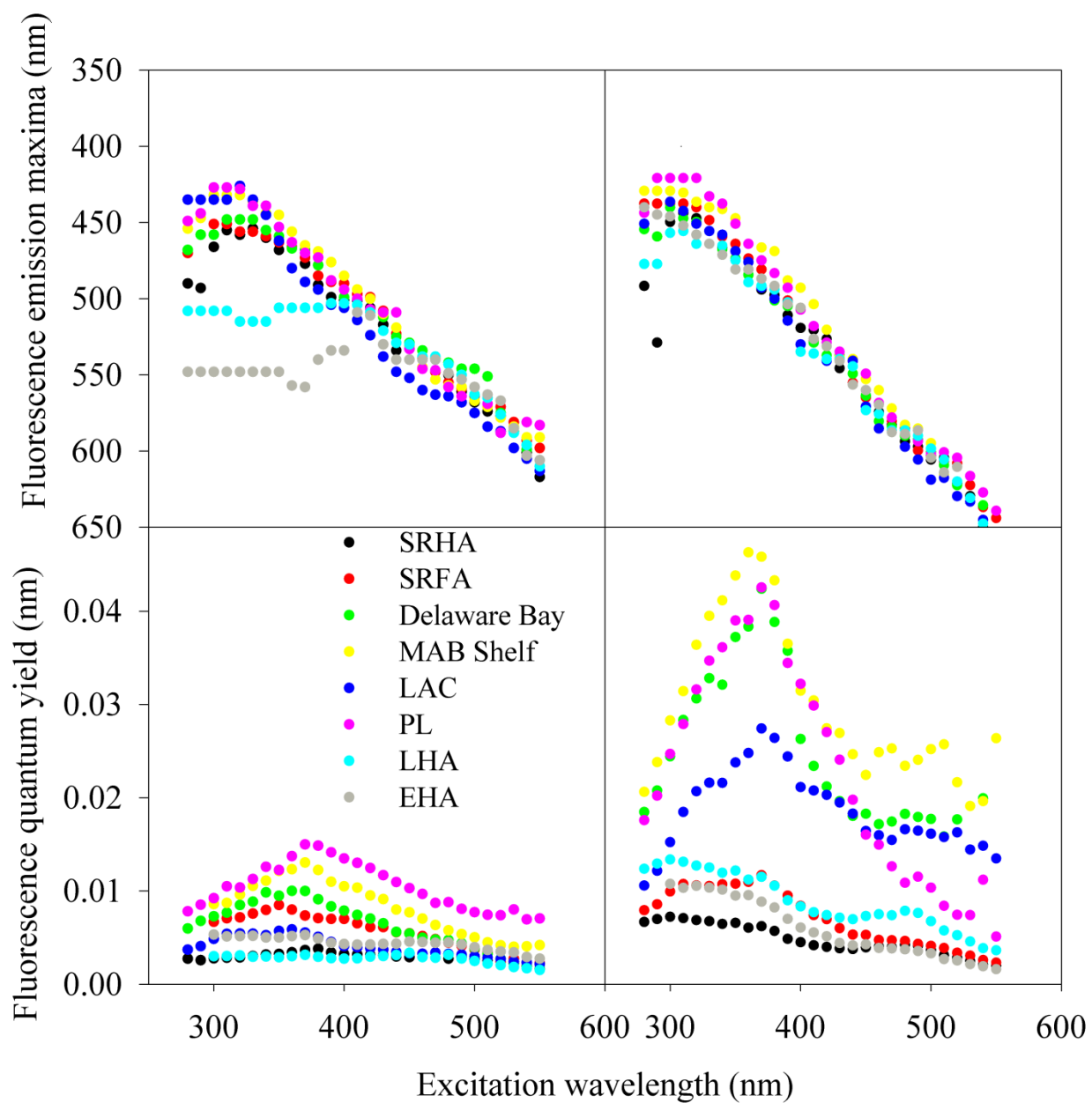


Figure 5.15 Wavelength dependence of emission maxima (top panels) and fluorescence quantum yields (bottom panels) for samples before (right panels) and after (left panels) 4 hours of sodium borohydride reduction.

5.3.6 Cyanoborohydride Reduction of Selected Samples

Cyanoborohydride (CNBH_3^-) is a chemical reducing agent that can preferentially target amine groups in the presence of aldehydes and ketones (Lane (1974)). In protonated solutions (water), in the presence of cyanoborohydride, an iminium ion ($\text{C}=\text{N}^+$) forms from an amine (primary or secondary) and a carbonyl group. The iminium ion is reduced at a much faster rate than carbonyl groups ($\text{C}=\text{O}$) at pH values from 3-8 (Lane (1974)). The formation of iminium ions in the presence of cyanoborohydride proceeds at neutral pH, but reduction of carbonyl groups is negligible between pH 7 and 8. Cyanoborohydride can effectively reduce carbonyls in acidic pH (pH 3-4) but cyanide is a potential by-product making the reaction in acidic conditions hazardous without appropriate laboratory controls. In this series of experiments, a terrestrial humic acid (LHA), an aquatic fulvic acid (SRFA) and two quinones were treated with cyanoborohydride at pH 7.6 - 7.7 in order to assess the usefulness of cyanoborohydride as a chemical probe at neutral pH. Duroquinone was selected because it is saturated with four methyl-groups in contrast with p-methyl benzoquinone that has one methyl group.

In Fig. 5.16 it is clear that Leonardite humic acid (LHA) and Suwannee river fulvic acid (SRFA) showed no time dependent decrease in absorbance at neutral pH when treated with sodium cyanoborohydride (NaCNBH_3). The kinetics of the reduction of duroquinone with cyanoborohydride (< 0.2 mg) exhibited an initial increase in absorbance across all wavelengths and then decreased in absorbance back to the original $A(0)$. Terrestrial HS, LHA (100 mg L^{-1}) showed no time dependent change in absorbance at an initial pH of 7.6 and cyanoborohydride concentration of 8 mg. SRFA (100 mg L^{-1}) at an initial pH of 7.7 when reacted with 40 mg of cyanoborohydride initially increased absorbance at 400 nm but then returned to the original $A(0)$ in a similar manner as duroquinone (DQ) (Fig. 5.16). There was minor reduction at long

wavelengths but not on the scale of borohydride reduction of SRFA. Methyl-p-benzoquinone (MBQ) ($1620 \mu \text{ mole L}^{-1}$) is quickly reduced by borohydride (Fig. 5.16). The absorbance spectra of MBQ ($1620 \mu \text{ mole L}^{-1}$) in the presence of $< 0.2 \text{ mg}$ cyanoborohydride is slightly reduced at the absorbance maxima of MBQ, a new absorbance peak appears at 289 nm (not presented). The spectral change suggests formation of a complex between the MBQ and cyanoborohydride or the formation of dimers (Lau, Dufresne, Belanger, Pietre and Scheigetz (1986)).

Lane (1974), reports in Synthesis, at pH 6-8 in the presence of cyanoborohydride and amines the reductive animation of aldehydes and ketones. At pHs between 7 and 8 cyanoborohydride can selectively reduce imines (Lau, Dufresne, Belanger, Pietre and Scheigetz (1986)), (Lane, 1974). Although, chemical reduction of HS and model compounds at neutral pH (pH 7-8) was ineffective extending reduction using cyanoborohydride as a chemical probe to lower pH values may yield better results. Further experiments, at acidic pH, with appropriate laboratory controls for the removal of hazardous by-products (HCN), may provide a useful chemical probe able to differentiate between carbonyl and amine groups in HS/CDOM. Use of cyanoborohydride as a chemical probe of Pony Lake fulvic acid (PLFA) may be particularly interesting because PLFA is enriched with nitrogen when compared to other fulvic/humic acids.

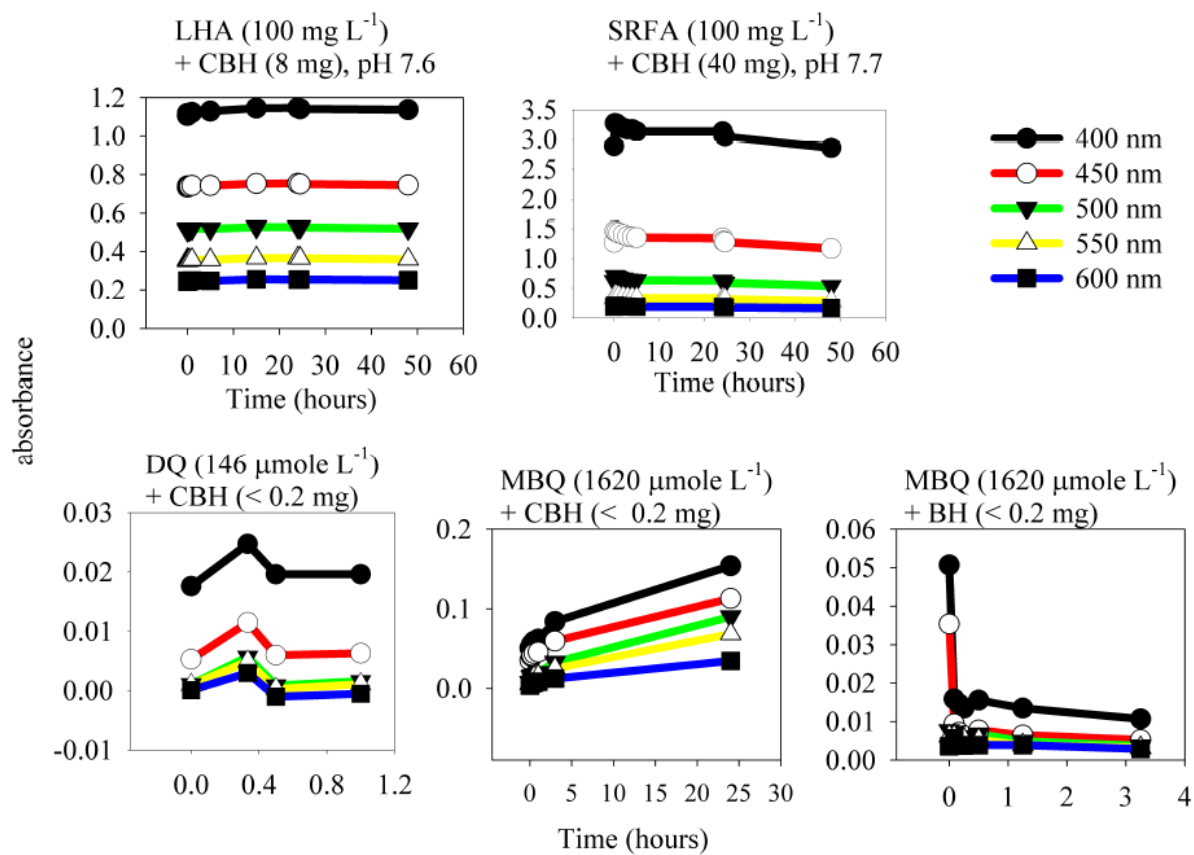


Figure 5.16 Time dependence of the reaction of Leonardite humic acid (LHA), Suwannee River fulvic acid (SRFA), duroquinone (DQ) and methyl-p-benzoquinone (MBQ) with cyanoborohydride (CBH). Time dependence of the reaction of methyl-p-benzoquinone (MBQ) with borohydride.

5.3.7 Molar Absorptivity of Phenone Compounds

Identification of model compounds that have chemical characteristics capable of generating charge transfer bands is integral to understanding the dynamics of how the long wavelength absorbance is generated by charge transfer bands in HS/CDOM. Aromatic ketones have been identified in terrestrial sources of humic acids (EHA, LHA, SRHA, and SRFA) and are capable of participating in the formation of charge transfer bands (Ma, Del Vecchio, Golanoski, Boyle and Blough (2010)). Molar extinction coefficients (ϵ) are an intrinsic measurement of how strongly a chemical species can absorb light at a specific wavelength. Chemical moieties that absorb strongly in the UV range through pi to pi* or n to pi* transitions but have no absorbance at wavelengths longer than 350 nm are compounds that may provide insight into how charge transfer bands work in the context of the electronic interaction model.

Two aromatic ketones, benzophenone and 2-acetonaphthone were investigated and their molecular structures are presented in Fig. 5.17. Molar absorptivity of benzophenone (BP) and 2-acetonaphthone (2-AN) were estimated from carefully prepared solutions. The pi to pi* transition for BP was determined spectrophotometrically as 256.5 nm with a molar extinction coefficient (ϵ) of 14550 L mol⁻¹ cm⁻¹ presented in Fig. 5.18. The n to π^* transition was determined to be 325.5 nm ($\epsilon = 293$ L mol⁻¹ cm⁻¹) (Fig. 5.18). The π to π^* transition for 2-AN was determined to be at 284 nm ($\epsilon = 11832$ L mol⁻¹ cm⁻¹) and the n to π^* was determined to be 340.5 nm ($\epsilon = 2323$ L mol⁻¹ cm⁻¹) presented in Fig. 5.20. Borohydride reduction reduced the n to p* of both BP and 2-AN absorption band to baseline in 10 and 15 minutes, respectively, as seen in Figs. 5.19 and 5.21. The π to π^* bands exhibited reduced emission and in the case of 2-AN blue shifted by 10

nm from 284 to 273 nm (Fig. 5.21). Benzophenone π to π^* wavelength do not change upon reduction (Fig. 5.19).

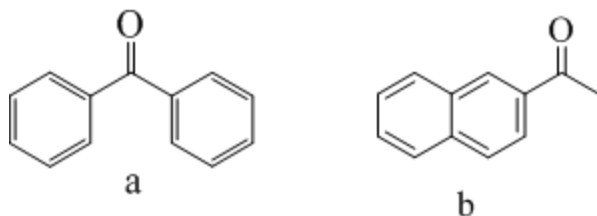


Figure 5.17 Structures of benzophenone (BP) (a) and, 2-acetonaphthone (2-AN) (b).

The presence of phenones in precursor material (algae and bacteria) of PLFA is unlikely because they are known to disrupt the membrane integrity and in such a capacity represent an antibiotic class. This is not to imply that they cannot be present as decomposition products of the entire suite of humic and fulvic acids.

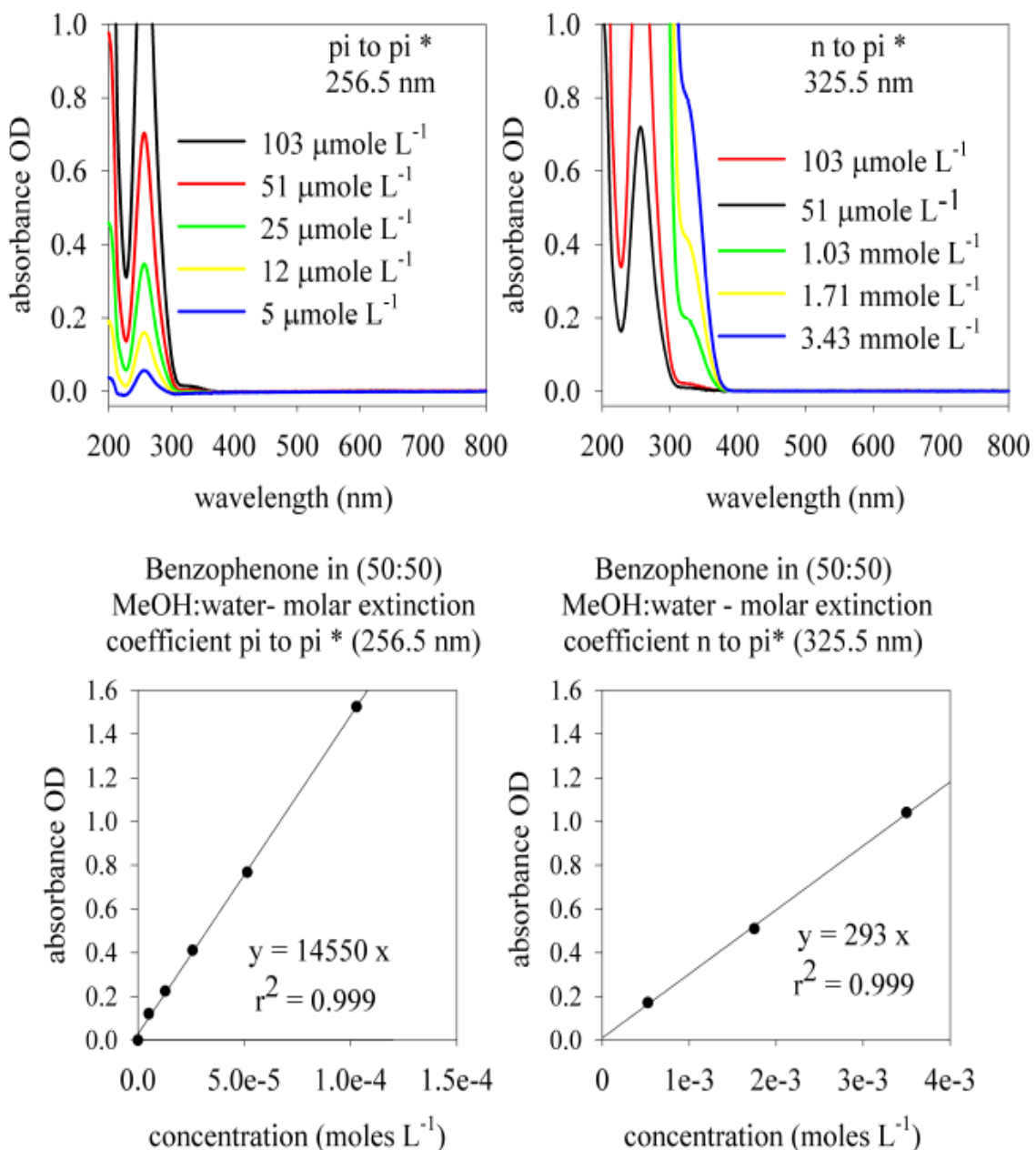


Figure 5.18 Absorbance spectra of untreated benzophenone (BP) in (50:50) MeOH:water showing π to π^* and n to π^* absorbance and molar extinction coefficients (ϵ).

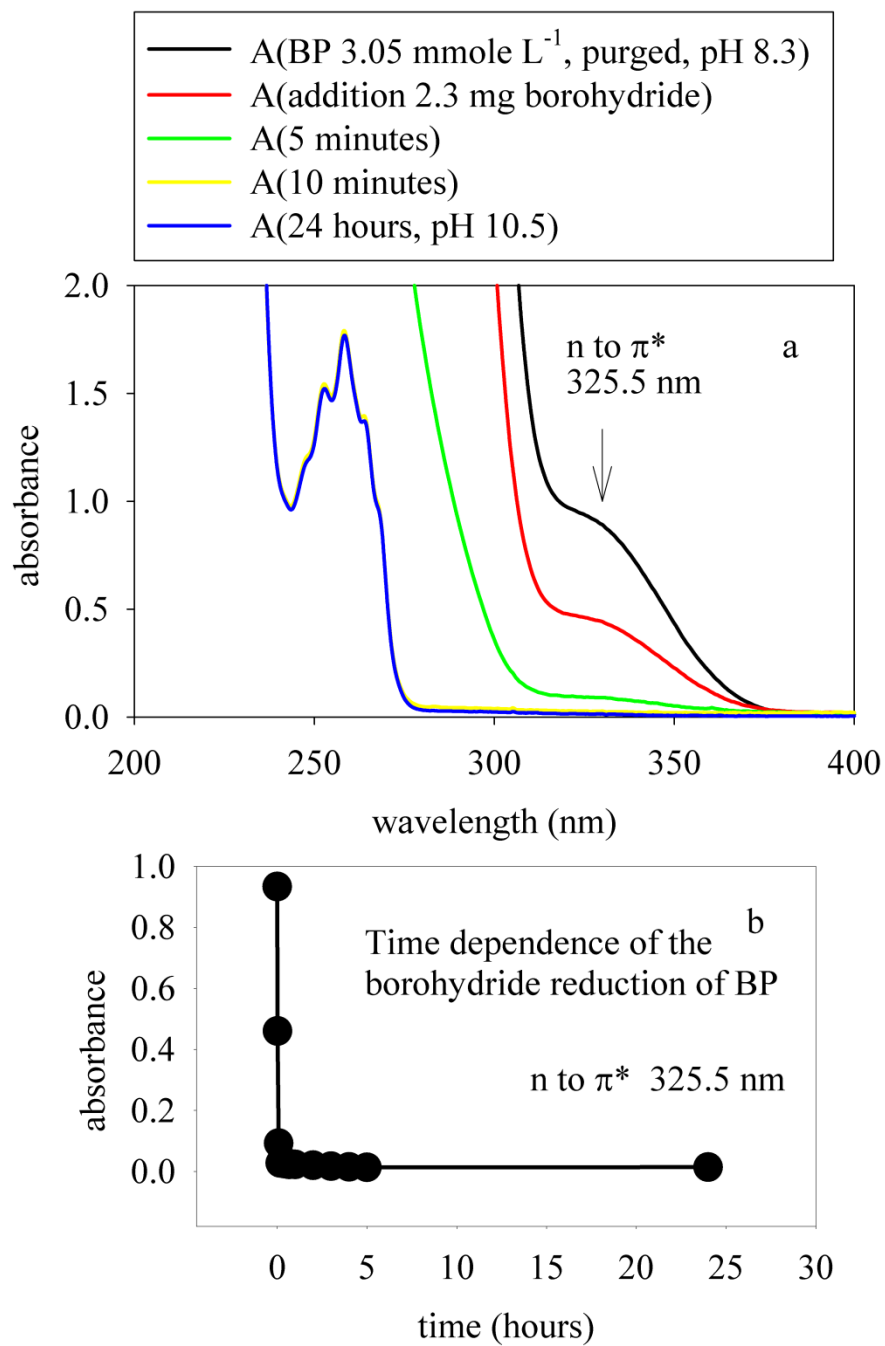
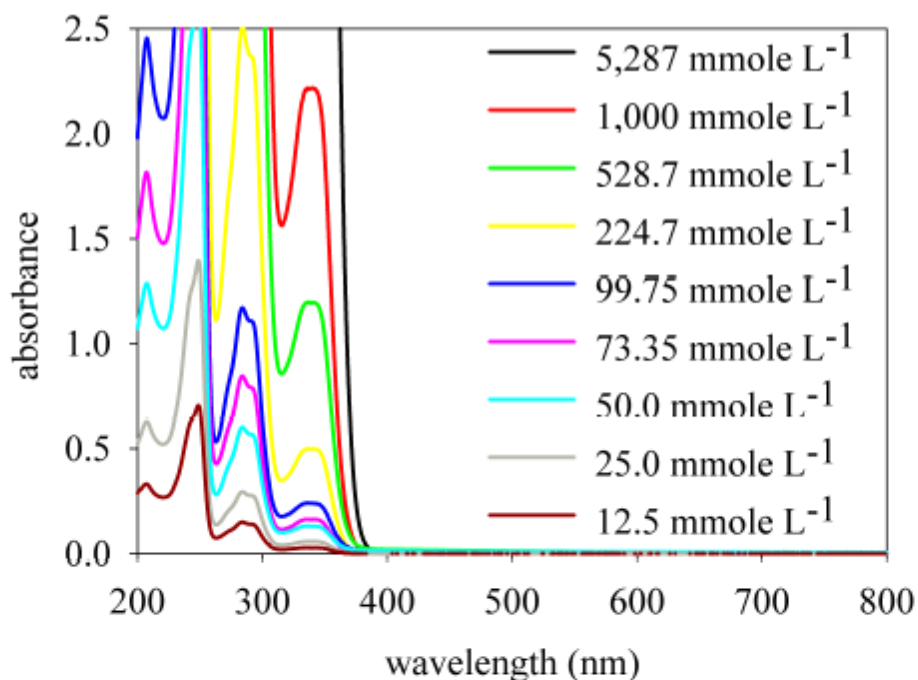
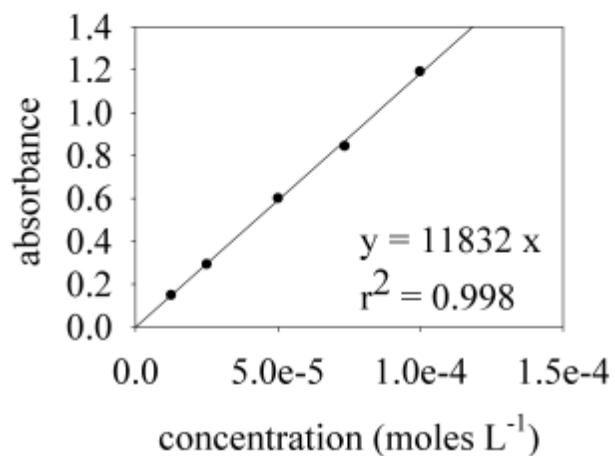


Figure 5.19 Absorbance of the borohydride reduction of benzophenone (BP) (3.05 mmole L⁻¹) over a 24 hour period (panel a). Kinetics of the reduction of the n to π^* optical transition (325.5 nm) (panel b).



2-Acetonaphthone in (50:50)
MeOH:water molar extinction
coefficient π to π^* (284 nm)



2-Acetonaphthone in (50:50)
MeOH:water molar extinction
coefficient n to π^* (340.5 nm)

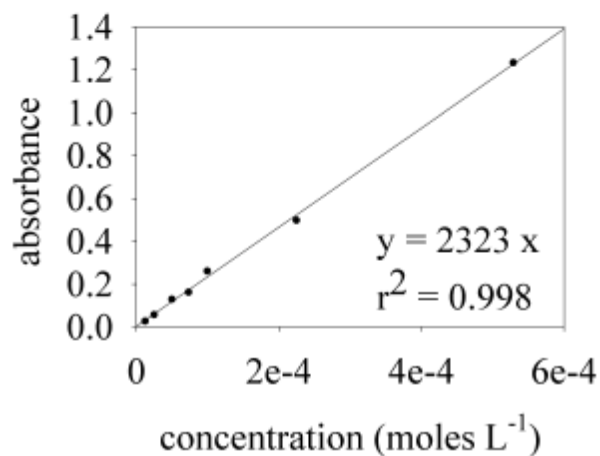


Figure 5.20 Absorbance spectra of untreated 2-acetonaphthone (2-AN) in (50:50) MeOH:water including the molar extinction coefficients for π to π^* and n to π^* .

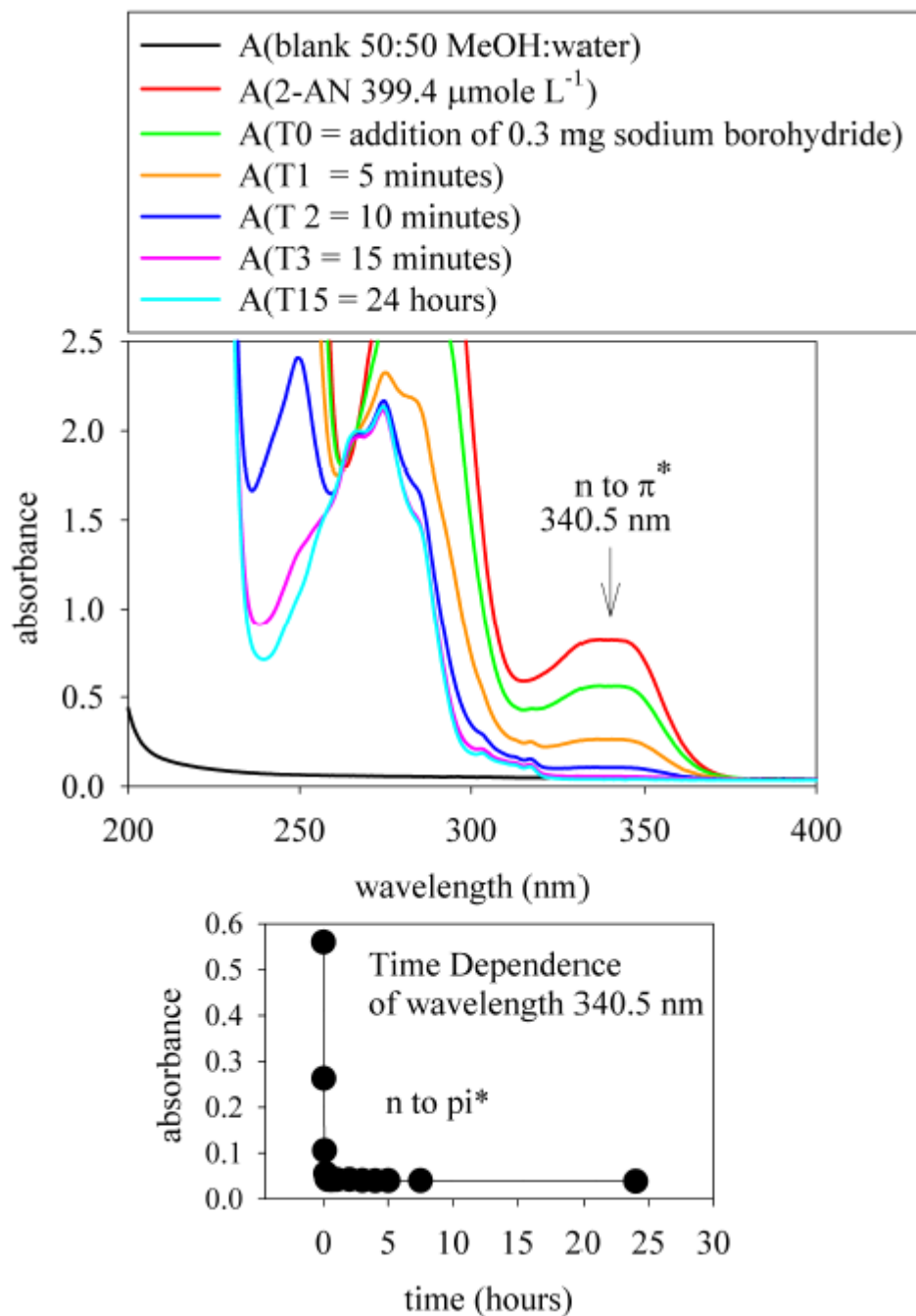


Figure 5.21 Absorbance of the borohydride reduction of 2-acetophenone (2-AN) ($344.5 \text{ mmole L}^{-1}$) over a 24 hour period (panel a). Kinetics of the reduction of n to π^* optical transition (340.5 nm) (panel b).

5.4 Conclusions

The mechanism generating long wavelength optical absorption bands, electronic interactions, is likely consistent between microbial sources of fulvic acid and terrestrial humic/fulvic substances generated from lignin phenol, but the constituents that act as the donor within the electronic interaction complexes differ based on the availability of source material. Microbial sources (PLFA) do not contain phenolic groups by definition but instead may employ decomposition products, such as heterocyclic moieties and secondary amines as donors and tertiary amines, quinones, aromatic ketones or other unidentified moieties as acceptors. Borohydride reduction of PLFA and the other humic/fulvic acids studied partially or completely remove acceptor moieties (quinones, aromatic ketones) from the charge transfer complex resulting in decreased absorbance, an increased spectral slope (S) coefficient and increased fluorescence emission intensity.

The relative amount of quinone moieties participating in electronic interactions of PLFA appears to be higher than found in the other fulvic and humic acids and can be seen in the recovery of absorbance in the UV range of the absorbance and difference spectra. Fractional difference plots of the borohydride reduction of PLFA show as much as a 90 % loss in absorbance while SRFA, the other fulvic acid in the study, loses 50 % of its absorbance. Borohydride reduction targets a specific chemical moiety namely carbonyl groups and, because of the specificity of the chemical reduction combined with the overwhelming loss of long wavelength (> 350 nm) absorbance in PLFA (90 %) compared to SRFA (50 %) over the same interval, it could be concluded that PLFA has much less heterogeneity in the structural components that are taking part in the generation of long wavelength absorbance. The loss of carbonyl population is either directly responsible for loss of absorbance or indirectly by

physically disruption of electronic interactions. Suwannee River humic acid (SRHA) may contain a more heterogeneous suite of chemical moieties able to participate in the generation of long wavelength absorbance, some of which are not reducible by sodium borohydride, or it may have inherent physical protection that hinders reduction by physical means, resulting in the protection of electronic interactions by stacking of cyclic hydrocarbons, association with metals or some other organic protectant.

Borohydride reduction may cause physical alterations in the macro structure preventing reassembly of optical components not directly affected by the reduction. This is exemplified by the loss of long wavelength fluorescence emission in the black carbon containing HS (LHA and EHA) and by the short wavelength absorbance recovery (< 350 nm) with no concurrent long wavelength recovery observed in PLFA. The quinone derived recovery of reoxidized HS, as measured by reoxidation driven pH changes, is small, much lower than the expected concentration observed by electrochemical means. This indicates that quinones although an important redox buffer, may not play a substantial role as a charge transfer acceptor and therefore do not play a large role in the optics of terrestrially sourced material (EHA, LHA, SRFA, SRHA) generated from lignin phenols.

Soil and aquatic sources of HA/FA should fit into a hierarchy of diagenesis. Soil derived humic acids spectral slope values (S) are low compared to untreated aquatic samples. Spectral slope parameterizes an exponential curve and as S increases the short wavelength part of the curve becomes steeper, while concurrently the long wavelength or visible region decreases substantially, indicating that borohydride reduction is disrupting charge transfer bands or electronic interactions that generate the characteristic long wavelength absorbance tail. Donors and or acceptor chemical moieties within the charge transfer model are no longer being

quenched, resulting in an increase in short wavelength absorbance and an increase in the spectral slope. The long wavelength tail does not regenerate when reoxidized implicating possible irreversible changes to the macrostructure. The fluorescence emission spectra of EHA and LHA differ from all of the other samples examined in that they have an underlying chromophore that is eliminated in the case of EHA or halved in the case of LHA upon borohydride reduction. It is possible that the underlying structural component is stacked conjugated carbon or black carbon that is physically disrupted during reduction.

The soil humic acids (LHA and EHA) have the lowest spectral slope values, followed by higher (S) for SRFA, SRHA and finally the largest (S) values were associated with PLFA and LAC. The relatively low spectral slope values of the soil derived humic acids could stem from the presence of chemical species that do not participate in the charge transfer mechanism but do contribute to the overall absorbance spectra. The soil humic acids EHA and LHA have a higher percentage of black carbon or conjugated cyclic carbon than is present in aquatic humic substances. The carbon content of LHA is potentially high when compared to EHA because LHA is derived from lignite, a precursor of coal.

Although, LHA potentially has significant amounts of black carbon, it is likely that titratable quinones shown to be associated with the surface structure of black carbon are not represented as fully as would be in the Mollisol derived EHA because EHA contains more oxygen than does LHA. This is consistent with the ability of each humic acid to mediate electrons. The higher amount of oxygen present in EHA could point to a larger array and overall number of oxygenated species able to participate in electronic interactions leading to an enhanced ability as an electron buffer, but a lower untreated spectral slope value than is observed for LHA which would potentially have a higher content of black carbon but less

oxygen. The fluorescence behavior of EHA and LHA support tangentially the premise that quinones are an important oxidation reduction buffer but not an important part of the optical properties of terrestrially derived humic and fulvic acids.

Further, as soil derived humic acids are exported to aquatic environments, labile components are lost, as reflected in spectral slope (S) values describing a more gradual curve associated with the low spectral slope (S) values associated with untreated EHA and LHA. The aquatic humic acid sample has a higher or less gradual spectral slope value consistent with the loss of labile material from the macro structure.

Surprisingly, the spectral slopes of SRFA and PLFA were very similar for both the reduced and untreated samples at pH 7.6. Further examination of these humic substances at low and high pH will be presented in Chapter 6 in order elucidate the underlying differences between the two fulvic acids. The untreated commercial source of lignin (LAC) has a high spectral slope value that increases upon borohydride reduction. It has very high fluorescence emission when borohydride reduced. LAC is the standard that is the closest to source material and as such has a heterogeneity of chemical moieties and a large population reflected in the borohydride induced high spectral slope value, fluorescence emission and quantum yield. The two marine CDOM samples represent the other end member of the lignin phenol digenesis. The recalcitrant backbone remains able to form electronic interactions that yield limited extended absorbance.

Chapter 6 Optical Titrations of Aquatic, Terrestrial and Microbial Humic Substances

Chapter 6 Overview

Many of the chemical species involved in generating the extended long wavelength absorbance associated with CDOM/HS have titratable protons that result in pH dependent absorbance spectra. The pH dependence of untreated and borohydride reduced CDOM/HS is investigated in this chapter. In Section 6.1 background information about the non-ideal competitive binding model (NICA) in combination with the Donnan model, is provided. More extensive material, including derivation of the model is provided in Chapter 3 and Appendix 1. Section 6.2 details the materials and methods used in this chapter, including materials (Sec.6.2.1), apparatus (Sec. 6.2.2) and methods of optical titration measurements (Sec. 6.2.3). Section 6.3 provides the results of the study and a discussion of the results in the context of the electronic interaction model, including the selection of the concentration of the reduced samples to be titrated (Sec. 6.3.1), the titrations of pre- and post- borohydride reduced HS samples (Sec 6.3.2), pH dependent spectral slope values (Sec. 6.3.4), and optical titration spectra and difference plots (Sec. 6.3.5). Section 6.4 focuses on conclusions that can be generated from experiments carried out in Chapter 6.

6.1 Introduction

The NICA-Donnan model has been used to successfully examine competitive binding of protons and metals in humic substances. It is described more fully in Chapter 3 and Appendix 1. (Koopal, Saito, Pinheiro and Riemsdijk (2005)), (Koopal, van Riemsdijk and Kinniburgh

(2001)), (Benedetti, Milne, Kinniburgh, Van Riemsdijk and Koopal (1995)), (De Wit, van Riemsdijk and Koopal (1993a)), (De Wit, van Riemsdijk and Koopal (1993b)). Generation of the terms, used to examine binding of protons and metals to HS/CDOM, requires a substantial amount of material (g Kg^{-1}). Multiple titrations at different ionic strengths are needed to generate the terms. The sample size, required to generate the NICA-Donnan model terms, limits its use to materials that can be gathered in large quantities (Appendix 1). Investigations of many colored dissolved organic samples (CDOM) using the NICA-Donnan model, becomes difficult or prohibitively expensive because of limited access to enough sample and/or cost of obtaining the sample. Optical titrations can supplement existing NICA-Donnan derived binding terms that are characteristic of individual HS, but accomplish this using smaller amount of HS/CDOM material.

The optical properties (absorbance) of humic and fulvic acids are known to have a positively increasing pH dependence, as pH increases absorbance increases concurrently (Maurer, Christl and Kretzschmar (2010)). In order to quantify the pH dependence of the optical properties of humic and fulvic acids used in this study (EHA, LHA, SRHA, SRFA, PLFA and LAC), they were titrated using strong acid or base at ionic strengths of 0.01, 0.10 and 1.00 mole L^{-1} sodium chloride (NaCl). Titrations were completed from pH 3.00 to pH 11.00, covering the bimodal pH distribution described by the NICA-Donnan model (Koopal, Saito, Pinheiro and Riemsdijk (2005)), (Kinniburgh, Milne, Benedetti, Pinheiro, Filius, Koopal and Van Riemsdijk (1996)), (Benedetti, Van Riemsdijk and Koopal (1996)), (Benedetti, Milne, Kinniburgh, Van Riemsdijk and Koopal (1995)), (De Wit, van Riemsdijk and Koopal (1993a)), (De Wit, van Riemsdijk and Koopal (1993b)). Additionally samples were reduced for 24 hours with sodium

borohydride in an anaerobic environment, reoxidized for 24 hours, and passed over a Sephadex G-10 column to remove residual borate and facilitate the titration of reduced samples.

Two NICA-Donnan identified titratable groups are at pH 4-5 representing carboxylic acids and, at pH 8-10 representing phenol like moieties (Milne, Kinniburgh and Tipping (2001)). Experimental titration curves of the HA/FA in this study and their first derivative plots are expected to match NICA-Donnan described titration curves. The diversity of samples used in may elucidate differences or similarities between sources of HA/FA. Reduction induced changes to either pH distribution group (centered at pH 4 or centered at pH 8) will provide insight into the identity of dominate chemical species present in the HA/FA. This is especially useful for differentiation of the two fulvic acids. Pony Lake fulvic acid (PLFA) is from a microbial source while Suwannee River fulvic acid derives from a terrestrial source (lignin). The ability to partition these two sources of fulvic acid is environmentally relevant, enabling more detailed fate and transport measurements of HS/CDOM in aquatic environments.

Optical titrations require lower amounts of humic material due to constraints of the UV-Vis spectrophotometer which inherently increases noise levels, but provides detailed spectral data that adds to current knowledge of organic carbon in the environment. Difference spectra (ΔA), has been used to examine the protonation behavior of several fulvic acids (Dryer, Korshin and Fabbicino (2008)). This method will be extended to humic acids (SRHA, LHA, and EHA), the microbial sample PLFA and Lignin alkali carboxylate (LAC) in order to elucidate differences and similarities in each of samples included in this study.

6.2. Materials and Methods

6.2.1 Materials

Leonardite Humic Acid Standard (LHA) 1S104H-S, Elliot Humic Acid Standard (EHA) 1S102H, Suwannee River Humic Acid (SRHA), Suwannee River Fulvic Acid and Pony Lake Fulvic Acid (PLFA) were obtained from the International Humic Substance Society. Sodium borohydride (NaBH_4) was obtained from Sigma-Aldrich. Water was purified to 18Ω using an Academic Milli-Q water system equipped with a carbon filter. Soil humic acids were filtered with a Nalgene 0.2- μm , 25-mm Nylon disposable syringe filter (catalog no. 195-2520) from Thermo Scientific. Sephadex G-10 was purchased from Sigma-Aldrich. Ultra high purity nitrogen was acquired from Airgas and equipped with an oxygen scrubber purchased from SGE analytical services. Sodium hydroxide and hydrochloric acid were obtained from Ricca Chemical Company. Sodium chloride (99.999%) was obtained from Sigma Aldrich.

6.2.2 Apparatus

A Shimadzu UVPC 2401 spectrophotometer was used to acquire UV-visible absorption spectra. All pH measurements were conducted using an Orion pH meter calibrated at pH 4.00, 7.00 and 10.00 daily. Calibrations were considered acceptable when the correlation coefficient was greater than 0.98. The instruments are located at the University of Maryland, Chemistry and Biochemistry Department in the laboratory of Neil V. Blough.

6.2.3 Optical Titration Measurements

Absorption spectra were recorded from 190 to 820 nm against pH adjusted Milli-Q water. Humic acid samples were borohydride reduced in a manner consistent with the method described in Chapter 5 and then passed over a Sephadex G-10 column until the pH of the sample was found to be between pH 7.0 and pH 7.6 in order to remove residual borate and facilitate background free titrations. The concentration of the column effluent was determined using a calibration curve of previously reduced samples at pH 7.6 and 350 nm. The absorptivity (ϵ) ($\text{L mg}^{-1}\text{cm}^{-1}$) of the absorbance as a function of concentration was derived according to Beer-Lambert Law detailed in equation 6.1,

$$A = \epsilon lc, \quad (6.1)$$

where A is the absorbance, l is the path length of the cell (cm) and c is the concentration of the sample (mg L^{-1}).

In order to investigate the effect of ionic strength on the optical properties of HS, ionic strengths of 0.01, 0.10 and 1.00 mole L^{-1} NaCl were added prior to titration of untreated and borohydride reduced samples at concentrations that were optimized for the visible region of the spectrum (1 A.U. at 350 nm). A second set of titrations was completed at concentrations appropriate for the investigation of the UV region of the spectra. These titrations were completed using ionic strength of 0.01 mole L^{-1} NaCl. The absorptivity (ϵ) was calculated for each of the untreated and borohydride reduced samples and used to determine the concentration of Sephadex cleaned samples.

Reduced samples were diluted to a concentration that was within the optical range of the spectrophotometer in the UV (200-300 nm) region. Untreated humic and fulvic acid samples were matched to absorbance of their corresponding borohydride reduced and Sephadex cleaned

samples. Titrations from pH 3.0 to 11.0 were completed using 0.250 mole L⁻¹ sodium hydroxide. Titrations from pH 11.0 to pH 3.0 were completed using 0.250 mole L⁻¹ hydrochloric acid. Titrants were delivered in 5 µL increments (1.25 µmole aliquots). The titrations in the UV range of absorbance had an ionic strength of 0.01 mole L⁻¹ provided by the addition of sodium chloride. Titrations of humic and fulvic acids, as well as lignin alkali carboxylate (LAC), at ionic strengths of 0.01, 0.10 and 1.00 mole L⁻¹ (as NaCl) were conducted at concentrations that maximized absorbance in the visible range from 350 nm to 800 nm. Untreated Suwannee River humic and fulvic acids (SRHA and SRFA) were titrated using a concentration of 100 mg L⁻¹, the untreated soil humic acids, LHA and EHA were titrated using a concentration of 50 mg L⁻¹ and the untreated PLFA was titrated using a concentration of 500 mg L⁻¹. LAC was prepared using a Sephadex column and matched optically to SRFA. The SRFA molar extinction coefficient (ϵ) was used to determine the concentration of the LAC samples.

Borohydride reduced and Sephadex cleaned humic and fulvic acids were titrated at the maximum concentration recovered from the Sephadex column. Borohydride reduced and Sephadex cleaned humic and fulvic samples were titrated at the following concentrations SRFA was titrated using 759 mg L⁻¹, SRHA was titrated using 200 mg L⁻¹, EHA was titrated using 48 mg L⁻¹, LHA was titrated using 75 mg L⁻¹, and PLFA was titrated using 260 mg L⁻¹. The concentration of acid in µmole per mg material was calculated from the titration of each sample from pH 3.0 to pH 11.0. All titrations were carried out using an initial volume of 3 mL. Each reduced, cleaned and titrated sample was carbon normalized. First derivative plots were generated for each of the visible range titrations in order to highlight titration inflection points. Difference plots were generated by subtracting all spectra x over the range of pH 3-11, $A(\text{pH } x)$ by the absorbance spectra corresponding to the lowest measured pH, $A(\text{pH } 3.0)$.

A second set of titrations was completed at concentrations appropriate for the investigation of the UV region of the spectra. These titrations were completed using ionic strength of 0.01 mole L⁻¹ NaCl only. Difference plots were generated for the UV titrations. The concentrations for the untreated and borohydride reduced and Sephadex cleaned UV range samples, respectively were: SRHA 20 and 19 mg L⁻¹, SRFA 26 and 28 mg L⁻¹, PLFA 75 and 30 mg L⁻¹, EHA 10 and 48 mg L⁻¹, LHA 13 and 11 mg L⁻¹.

Other parameters were modeled including spectral slope (S) and the wavelength dependence of the specific absorbance coefficient (*a*^{*}) at low (pH 3.0), high (pH 11.0) and neutral pH (pH 6.0-7.6) at an initial wavelength 350 nm, as exemplified in equation 6.2,

$$a(\lambda) = a^*(\lambda_0) \exp^{-S(\lambda-\lambda_0)}, \quad (6.2)$$

The initial calculated *a*^{*} value was determined using equation 6.3. The spectral slope and (*a*^{*}) were determined using a non-linear least square method.

$$a^*(350 \text{ nm}) [\text{liter (mg organic carbon)}^{-1} \text{ m}^{-1}] = a(\lambda)/b * c, \quad (6.3)$$

where b is the path length (m) and c is mg of organic carbon.

6.3. Results and Discussion

Titrations of aquatic, microbial and terrestrial samples examined several parameters, 1. How much acid is required to titrate from pH 3.0 to pH 11.0 on a mass basis? 2. How does borohydride reduction of the concentration matched samples affect the amount of acid needed to titrate over the same pH range? 3. Do changes to the ionic strength affect the titration volume, the inflection points associated with the first derivative plots or the structural integrity of the titrated material? 4. How does pH change spectral slope values? 5. What differences can be observed between sources of material based on pH dependent difference plots. Fundamental to

these questions is the accurate determination of the concentration of each sample. Concentrations of samples post-Sephadex cleaning were determined by calibration curves constructed from non-Sephadex cleaned samples.

6.3.1 Concentration of the Borohydride Reduced Humic and Fulvic Acids

Molar absorptivity (ϵ) values were calculated for untreated and borohydride reduced Suwannee River humic (SRHA) and Suwannee River fulvic (SRFA) acids, Elliott humic acid (EHA), Leonardite humic acid (LHA), Pony Lake fulvic acid (PLFA) and Lignin Alkali Carboxylate (LAC). Table 6.1 provides a summary of absorptivity values (ϵ), the correlation coefficient (r^2) associated with each value and, the % loss of each absorptivity values (ϵ) due to borohydride reduction. The absorbance as a function of concentration and corresponding equation of the line are presented in Fig. 6.1 and 6.2. Figure 6.1 contains the untreated (upper panels) and borohydride reduced (lower panels) fulvic acids, Suwannee River fulvic acid (SRFA) (left panels) and Pony Lake fulvic acid (PLFA) (right panels). Figure 6.2 contains the untreated (upper panels) and borohydride reduced (lower panels) humic acids, Suwannee River humic acid (SRHA) (left panels), Elliott humic acid (EHA) (center panels) and Leonardite humic acid (right panels). Each standard curve was replicated a minimum of 3 times.

The absorbance of untreated and borohydride reduced fulvic and humic acids are linearly correlated with concentration at pH 7.6 and 350 nm absorbance. The absorptivity was consistently higher for the humic acids than for the fulvic acids studied. Untreated humic/fulvic acids ranked from greatest to least absorptivity are:

$$\text{EHA} > \text{LHA} > \text{SRHA} > \text{SRFA} > \text{PLFA}$$

A variable decrease in absorptivity was observed in both fulvic and humic acids subjected to borohydride reduction for 24 hours and reoxidized for 24 hours at pH 7.6 and at 350 nm

absorbance. The absorptivity of borohydride reduced SRFA and PLFA decreased by 55 % and 39 % respectively when compared to untreated samples. The absorptivity (ϵ) of SRHA, EHA and LHA decreased by 29 %, 48 % and 29 % respectively when compared to untreated samples (Figs. 6.1, 6.2 and Table 6.1).

Upon borohydride reduction humic acids remained higher in absorptivity than fulvic acids, but LHA had higher borohydride reduced absorptivity than did EHA resulting in reduced LHA having a higher absorptivity than EHA for the borohydride reduced samples. The borohydride reduced humic/fulvic acids ranked from greatest to least molar absorptivity are:

LHA>EHA>SRHA>SRFA>PLFA

LHA is derived from lignite the precursor to coal; it has higher levels of conjugated ring systems or black carbon. Black carbon may not be participating in formation of charge transfer bands but contributes to the overall absorbance spectra (Allard (2006)).

Table 6.1 Summary of the absorptivity for untreated and borohydride reduced humic and fulvic acid samples and change in absorptivity (% loss) at absorbance 350 nm and pH 7.6. All samples were borohydride reduced for 24 hours and reoxidized for 24 hours.

Sample Identification	absorptivity (L mg ⁻¹ cm ⁻¹) untreated pH 7.6, 350 nm, (r ²)		absorptivity (L mg ⁻¹ cm ⁻¹) borohydride reduced for 24 hours, reoxidized for 24 hours, pH 7.6, 350 nm absorbance, (r ²)		Loss of slope due to borohydride treatment (%)
SRFA	0.00786	(0.999)	0.00352	(0.999)	55
PLFA	0.00356	(0.999)	0.00220	(0.999)	38
SRHA	0.0114	(0.999)	0.00805	(0.999)	29
EHA	0.0205	(0.999)	0.0107	(0.999)	48
LHA	0.0194	(0.994)	0.0137	(0.999)	29

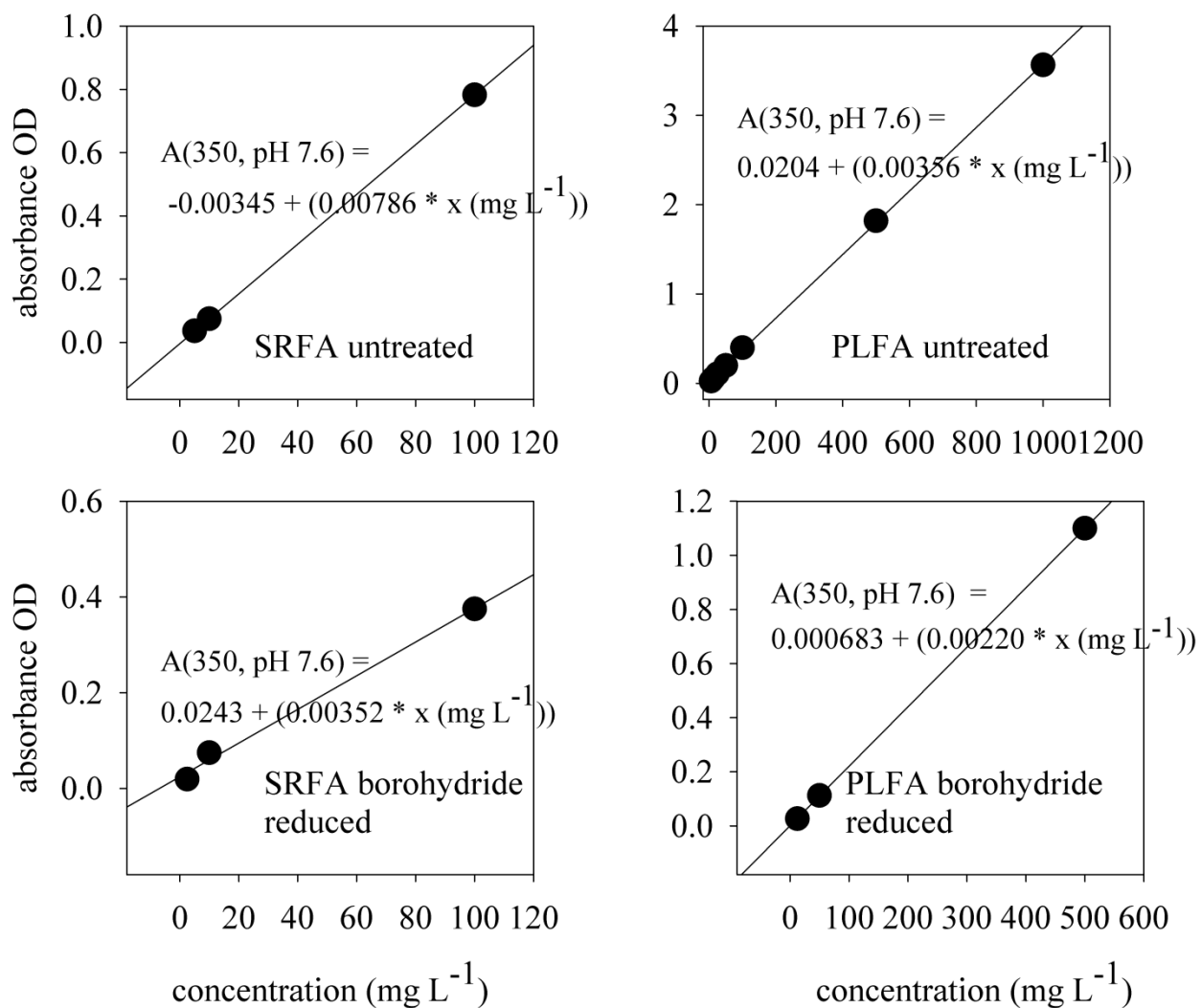


Figure 6.1 Standard curves correlating the absorbance with the concentration of the fulvic acids Pony Lake fulvic acid (PLFA) and Suwannee River fulvic acid (SRFA), untreated and borohydride reduced for 24 hours, reoxidized for 24 hours and titrated to pH 7.6. All absorbance measurements were made at 350 nm.

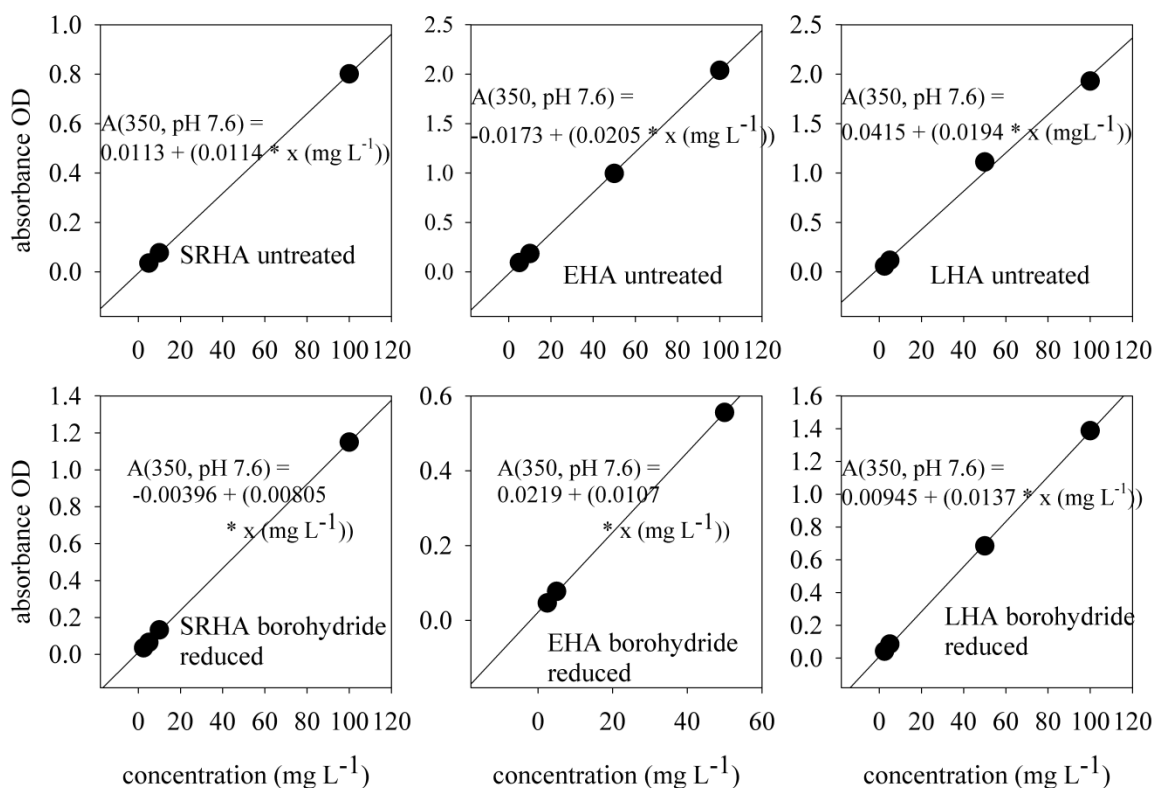


Figure 6.2 Standard curves correlating the absorbance with the concentration of the humic acids, Suwannee River humic acid (SRHA), Elliott humic acid (EHA) and Leonardite humic acid (LHA), untreated and borohydride reduced for 24 hours, reoxidized for 24 hours and titrated to pH 7.6. All absorbance measurements were made at 350 nm.

6.3.2 Titration of Untreated and Borohydride Reduced Humic and Fulvic Acids Differences in Ionic Strength

Untreated and borohydride reduced Suwannee River humic (SRHA) and Suwannee River fulvic (SRFA) acids, Elliott humic acid (EHA), Leonardite humic acid (LHA), Pony Lake fulvic acid (PLFA) and Lignin Alkali Carboxylate (LAC) were titrated at ionic strengths of 0.01, 0.10 and 1.00 mole L⁻¹. The quantity of acid needed ($\mu\text{mole mg}^{-1}$) to titrate from pH 3-11 for each ionic strength, and treatment is presented in Table 6.2.

All of the samples examined differed in the amount of acid needed to titrate from pH 3.0 to pH 11.0 on a μmole of acid per mg sample basis. Untreated samples at 0.01 mole L⁻¹ ionic strength ranked from greatest amount of acid to least amount of acid are: EHA (83 $\mu\text{moles mg}^{-1}$), SRHA (75 $\mu\text{moles mg}^{-1}$), LHA, (58 $\mu\text{moles mg}^{-1}$), SRFA (41 $\mu\text{moles mg}^{-1}$) and PLFA (15 $\mu\text{moles mg}^{-1}$) (Table 6.2). Untreated humic acid samples require more acid to titrate than do fulvic acids. Borohydride reduced samples at 0.01 mole L⁻¹ ionic strength ranked from greatest amount of acid to least amount of acid are: EHA (95 $\mu\text{moles mg}^{-1}$), LHA (55 $\mu\text{moles mg}^{-1}$), PLFA (25 $\mu\text{moles mg}^{-1}$), SRHA (22 $\mu\text{moles mg}^{-1}$) and SRFA (8 $\mu\text{moles mg}^{-1}$).

The trend observed for untreated samples differs from the trend observed upon borohydride reduction in several ways, but primarily reduction highlights differences in source material. Separating the examined materials into source groupings, such as soil derived humic acids (EHA and LHA), aquatic humic and fulvic acids (SRHA and SRFA), and microbially derived fulvic acids (PLFA) highlights these differences. Starting with soil humic acids, both untreated and borohydride reduced soil humic acids EHA and LHA require the greatest amount of acid to titrate over the pH range of 3-11. The EHA 0.01 mole L⁻¹ ionic strength acid requirement is slightly higher for the matched reduced sample at the same ionic strength

compared to the untreated sample while the reduced LHA sample, requires slightly less acid to titrate over the same range. The % difference between untreated and reduced soil humic acids at ionic strengths 0.01 and 0.10 mole L⁻¹ does not change by more than ± 20 %.

In contrast, the aquatic humic and fulvic acids at 0.01 mole L⁻¹ ionic strength decrease by 69 % for SRHA and 79 % for SRFA when comparing untreated to borohydride reduced samples. The microbial source of fulvic acid at an ionic strength of 0.01 mole L⁻¹ upon borohydride reduction exhibited a 72 % increase in acid requirement to titrate over the same range as the untreated sample.

The soil humic acids (EHA and LHA) require different amounts of acid to titrate on a mg basis but are internally consistent in that a comparison of untreated and reduced samples does not drastically change the acidity requirement to complete the titration over the selected range. A comparison between untreated and borohydride reduced soil humic acids showed LHA and EHA behave similarly to each other, but differ from the other sources of HS. EHA on a mg basis required close to double the amount of acid to titrated between pH 3.0 and pH 11.0 than did LHA. This may reflect the % carbon found in each sample. EHA has roughly double the % carbon when compared to LHA, 0.4760 % C and 0.2501 % C respectively, on a mass basis (Golanoski, Fang, Del Vecchio and Blough (2012)).

PLFA does not behave like any of the other samples in the study, highlighting its difference in form if not function. Unlike any other sample in the study it requires substantially more acid to titrate the reduced sample than it does the untreated sample. Pony Lake FA may have titratable moieties that do not participate in the extended optical absorbance tail produced by the charge transfer system. This would explain the limited change in absorbance upon

borohydride reduction of PLFA when compared to the more considerable loss in borohydride induced absorbance observed in SRFA (Figs. 5.2 and 5.4).

A more detailed examination of ionic strength shows variability in behavior between sources of material and titration behavior. Changes in ionic strength positively increase the amount of acid required to titrate from pH 3.0 to pH 11.0 between sample sources (aquatic, terrestrial, or microbial) but are consistent within samples sources (Table 6.2), with the exception of the 1.00 mole L⁻¹ ionic strength which required more acid to titrate when compared to lower ionic strength concentrations of 0.01 mole L⁻¹ and 0.10 mole L⁻¹. Notable exceptions were SRHA untreated series, which required the same amount of acid to titrate as the 0.10 mole L⁻¹ treatment as the 1.00 mole L⁻¹ treatment and, the LHA borohydride reduced and untreated samples. LHA borohydride reduced required less acid to titrate than the same concentration untreated samples but the difference between untreated and borohydride reduced titration concentrations was less than the difference other series of untreated and borohydride reduced samples. LHA untreated at an ionic strength of 1.0 mole L⁻¹ NaCl salted out and could not be titrated at the concentration used.

The borohydride reduced PLFA samples show a positive correlation, between increasing ionic strength and $\mu\text{moles of acid mg}^{-1}$ sample required to complete the titration. The untreated PLFA did not exhibit such a correlation but the 1.0 mole L⁻¹ ionic strength trial of untreated PLFA required more acid to titrate than did the lower concentration ionic strength treatment.

Untreated soil HA (EHA and LHA) exhibit little difference between borohydride reduced and untreated samples at all ionic strength excluding LHA at 1.0 mole L⁻¹ ionic strength. Low concentration changes in ionic strength, do not appear to impact the optical titrations at wavelengths greater than 350 nm as shown in Table 6.2 and Figs. 6.3 and 6.4. Based on ionic

strength data, the 0.01 mole L⁻¹ NaCl ionic strength was used to complete the titrations done in the UV spectral range. Figures 6.3 and 6.4 are presented in 6.3.3 First Derivative Plots of Titrations of Humic Substances.

Table 6.2 Titrations ($\mu\text{mole acid mg}^{-1}$ of sample) of untreated and borohydride reduced humic substances, at ionic strengths (0.01, 0.10, and 1.00 mole L^{-1} NaCl). Samples include Suwannee River humic acid (SRHA), Suwannee River fulvic acid (SRFA), Pony Lake fulvic acid (PLFA), Elliott humic acid (EHA) and Leonardite humic acid (LHA). – salted out of solution.

Sample	Treatment	Ionic strength (mole L^{-1})	$\mu\text{moles acid mg}^{-1}$ humic substance
SRHA	untreated	0.01	75.00
SRHA	untreated	0.10	87.50
SRHA	untreated	1.00	87.50
SRFA	untreated	0.01	41.67
SRFA	untreated	0.10	45.83
SRFA	untreated	1.00	62.50
PLFA	untreated	0.01	15.00
PLFA	untreated	0.10	15.00
PLFA	untreated	1.00	17.50
EHA	untreated	0.01	83.33
EHA	untreated	0.10	100.00
EHA	untreated	1.00	108.33
LHA	untreated	0.01	58.33
LHA	untreated	0.10	66.67
LHA	untreated	1.00	—
SRHA	borohydride reduced	0.01	22.93
SRHA	borohydride reduced	0.10	25.01
SRHA	borohydride reduced	1.00	31.37
SRFA	borohydride reduced	0.01	8.77
SRFA	borohydride reduced	0.10	8.77
SRFA	borohydride reduced	1.00	9.32
EHA	borohydride reduced	0.01	95.49
EHA	borohydride reduced	0.10	104.17
EHA	borohydride reduced	1.00	138.89
LHA	borohydride reduced	0.01	55.56
LHA	borohydride reduced	0.10	55.56
LHA	borohydride reduced	1.00	50.00
PLFA	borohydride reduced	0.01	25.81
PLFA	borohydride reduced	0.10	27.65
PLFA	borohydride reduced	1.00	35.03

6.3.3 First Derivative Plots of Titrations of Humic Substances

Titration curves of untreated and borohydride reduced Suwannee River humic (SRHA) and fulvic (SRFA) acids, Elliott humic acid (EHA), Leonardite (LHA), Pony Lake fulvic acid (PLFA) and Lignin Alkali Carboxylate (LAC) are presented with their respective first derivative plots ($\Delta y/\Delta x$) in two adjacent panels in Figs. 6.3 and 6.4. Fulvic acids (SRFA and PLFA) and lignin alkali carboxylate (LAC) are grouped in Fig. 6.3. The aquatic humic acid SRHA and the soil humic acids (EHA and LHA) are grouped in Fig. 6.4. Titrations were completed from pH 3 to pH 11 using 5- μL increments at ionic strengths 0.01 (blue lines), 0.10 (green lines) and 1.00 (black lines) mole L^{-1} . Each 5- μL increment is represented as a point on the appropriate titration curves. The first derivative of each ionic strength titration curve is represented by red, yellow and pink lines for 1.00, 0.10 and 0.01 mole L^{-1} ionic strength treatment.

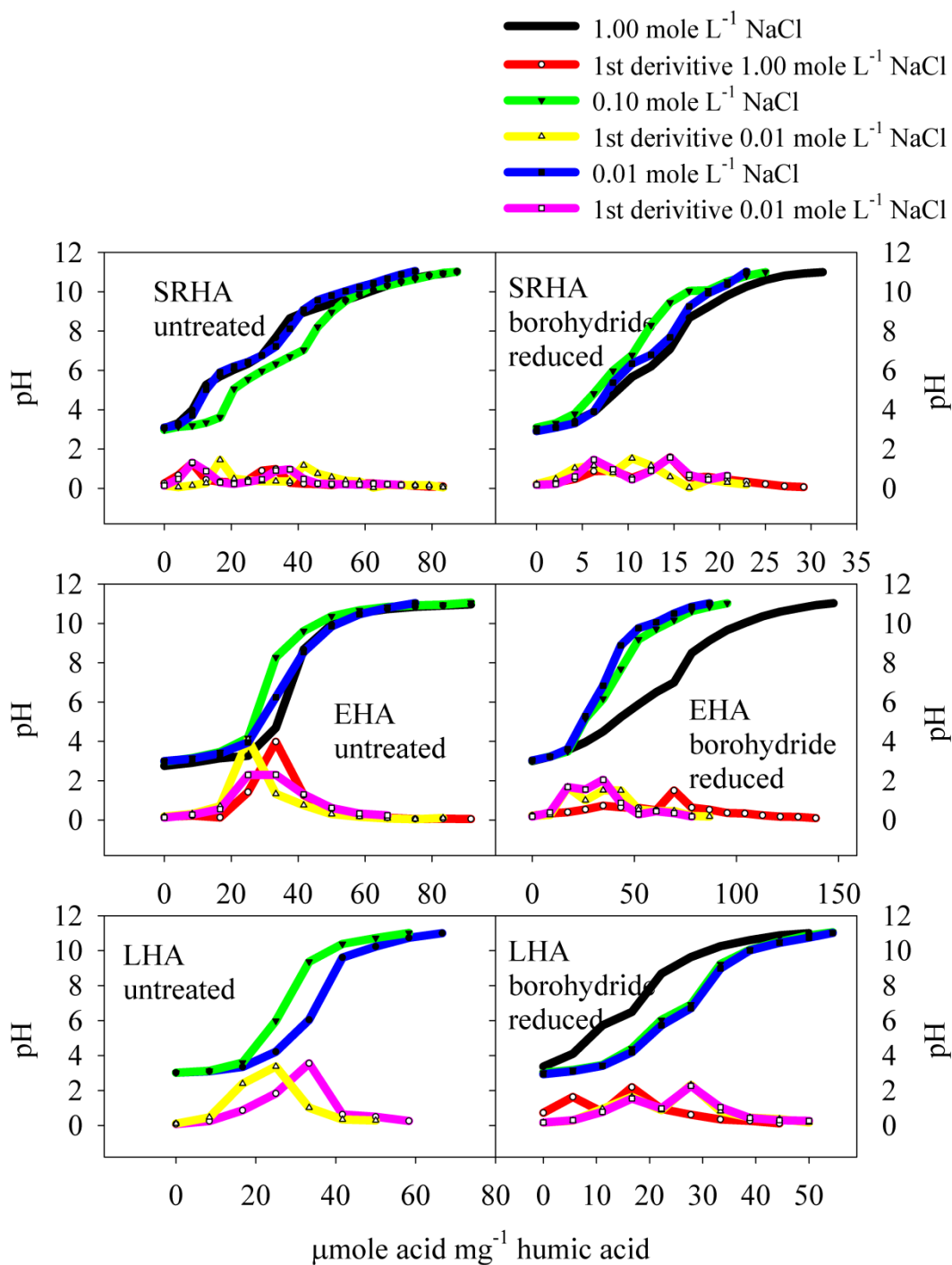


Figure 6.4 Titrations and first derivative plots (pH vs. $\mu\text{mole acid mg}^{-1}$ material) of Suwannee River humic acid (SRHA) (upper panels), Elliott humic acid (EHA) (middle panels), and Leonardite humic acid (LHA) (bottom panels). Untreated samples (left panels). Borohydride reduced samples (right panels).

First derivative plots of the titration profiles (pH as function $\mu\text{moles of acid mg}^{-1}$ of humic or fulvic acid) highlight differences between sources of HS (soil, aquatic and microbial), as well as how untreated samples are effected by borohydride reduction and changes in ionic strength. The LAC sample was standardized to SRFA using a Sephadex G-10 column and the concentration was determined using the SRFA molar extinction coefficient (Fig. 6.1). Samples were titrated at concentrations that were in the visible range of absorbance detection ($> 350 \text{ nm}$).

The NICA-Donnan model indicates the presence of two titratable groups in humic substances (Koopal, van Riemsdijk and Kinniburgh (2001), (Milne, Kinniburgh and Tipping (2001)). This is consistent with our findings using optical titrations. Two inflection points centered at pH 4 and pH 8 were observable for both untreated samples of SRFA and SRHA (Figs. 6.3 and 6.4). The inflection point at pH 4 is less pronounced for untreated SRFA than it is for untreated SRHA. The titration curve of borohydride reduced SRHA retained two inflection points centered at pH 4 and pH 8. It required less acid or the amount was unchanged to achieve the half-point at pH 4 and more acid to achieve the half-point at pH 8 when compared to the same concentration of unreduced SRHA (Figs. 6.3 and 6.4)

The soil humic acids (EHA and LHA) required less acid to titrate from pH 3.0 to pH 11.0 than did the aquatic humic acid SRHA. Instead of two distinct inflection points as found with untreated aquatic humic acid SRHA, untreated soil humic acids (EHA and LHA) have broad, indistinct inflection points starting between pH 3 and pH 4 and end, between pH 8 to pH 10. The lack of distinct inflection points may be indicative of the preferential physical and chemical protection supplied to soil humic substances by their environment. Soil humic substances especially those not at soil surfaces are protected from photobleaching and form complexes that

can provide protection from enzymatic attack (Heighton, Schmidt and Siefert (2008)), (Allard (2006)), (Brady and Weil (2002)), (Glasser (2000)). As soil humic acids are exported to aquatic environments, photobleaching increases, causing structural changes to humic and fulvic acids directly and disrupting complexation partnerships that can leave the humic/fulvic acid vulnerable to enzymatic attack (Christensen, Tipping, Kinniburgh, and Christensen (1998)). Borohydride reduced EHA forms two inflection points that are less distinct than the aquatic humic acid. The emergent soil inflection points are centered at pH 4 and pH 8 but, as with other terrestrially derived HS, require less acid to titrate to pH 4 and pH 8.

Untreated LAC at ionic strengths 0.01 and 0.10 mole L⁻¹ NaCl exhibit one inflection point centered at pH 8. Upon reduction the inflection point remained at pH 8 but, required less acid to titrate to pH 8.0. The 1.00 mole L⁻¹ ionic strength treatment of untreated and borohydride reduced LAC was not consistent with the other ionic strength treatments implicating ionic strength derived physical changes. The untreated 1.00 mole L⁻¹ NaCl sample has a less distinct inflection point at a lower pH. The borohydride reduced 1.00 mole L⁻¹ ionic strength LAC exhibits two inflection points at pH 6 and pH 8. It (LAC) requires substantially less acid to complete the titration than did the untreated sample (Fig. 6.3).

Untreated PLFA has an inflection point centered between pH 8 and pH 9. It has a much less pronounced inflection point centered at pH 4. Upon reduction two clear inflection points emerge centered at pH 4 and pH 7. The borohydride reduced PLFA samples required less acid to reach each inflection point and less over all acid to titrate from pH 3 to pH 11. The aquatic terrestrial samples (SRFA and SRHA) and microbial sample (PLFA) exhibit two distinct titratable groups. The untreated soil samples have a single broad peak that upon borohydride reduction separates into two titratable distributions. The LAC sample has one titratable group

evident at the lower ionic strengths centered at pH 8.00. Two titratable groups become evident at the high ionic strength (1.00 mole L⁻¹ NaCl) borohydride reduced sample.

Based on the first derivative plots the 0.01 and 0.10 mole L⁻¹ ionic strengths do not appear to have a large affect either of the fulvic acids (SRFA and PLFA) or Elliott (EHA) and Suwannee River humic acid (SRHA). The untreated Leonardite humic acid (LHA) titration could not be completed due to precipitation at low pH. The borohydride reduced 1.00 mole L⁻¹ ionic strength LHA treatment required less acid to titration than did the lower ionic strength titrations. The borohydride reduced high (1.00 mole L⁻¹) ionic strength LHA sample did not precipitate out of solution at low pH. LAC, both untreated and borohydride reduced first derivative plots at 1.00 mole L⁻¹ ionic strength were clearly different from the lower ionic strength titrations and first derivative plots, although neither exhibited visible evidence of precipitation.

The notable difference in the titration behavior of the fulvic acids in the study, SRFA and PLFA delineates how operational definitions used to describe humic substances may not be appropriate. The aquatic material SRFA and SRHA although requiring different amounts of acid to titrate behave in a consistent manner when compared to the behavior of other reduced and titrated samples.

6.3.4 Parameterized Spectral Slope (S) Values as a Function of pH

The pH dependence of the spectral slope (S) values $a(\lambda) = a^*(\lambda_0) \exp^{-S(\lambda-\lambda_0)}$ (Eq. 6.2), for untreated and borohydride reduced, Suwannee River humic (SRHA) and Suwannee River fulvic (SRFA) acids, Elliott humic acid (EHA), Leonardite humic acid (LHA), Pony Lake fulvic acid (PLFA) and Lignin Alkali Carboxylate (LAC) were modeled using equation 6.2. A summary of the pH dependent spectral slope (S) trends is presented in Fig. 6.5 for SRHA, SRFA, PLFA, EHA, and LHA. Table 6.3 tabulates spectral slope (S) values, and correlation coefficients (r^2) for the parameterization of (S), at acidic, neutral, and basic pH points of SRHA, SRFA, PLFA, EHA, and LHA. Included in Table 6.3 are titration points at pH 7.6. The pH 7.6 titration point compares humic or fulvic acids that have been Sephadex cleaned (Chapter 6) with the corresponding titration point of samples not cleaned with a Sephadex column (Chapter 5). Figures 6.6 through 6.11 show the carbon normalized parameterized spectral slope (S) values (black dots) as a function of wavelength from 290 to 820 nm, the 95% confidence band (blue lines), and the 95 % prediction band (red lines) for EHA, LHA, SRHA, SRFA, PLFA and LAC respectively. The left panels of these figures are the untreated samples at acidic pH (top panel), neutral pH (middle panel) and basic pH (bottom panel). The right panels are the corresponding borohydride reduced samples.

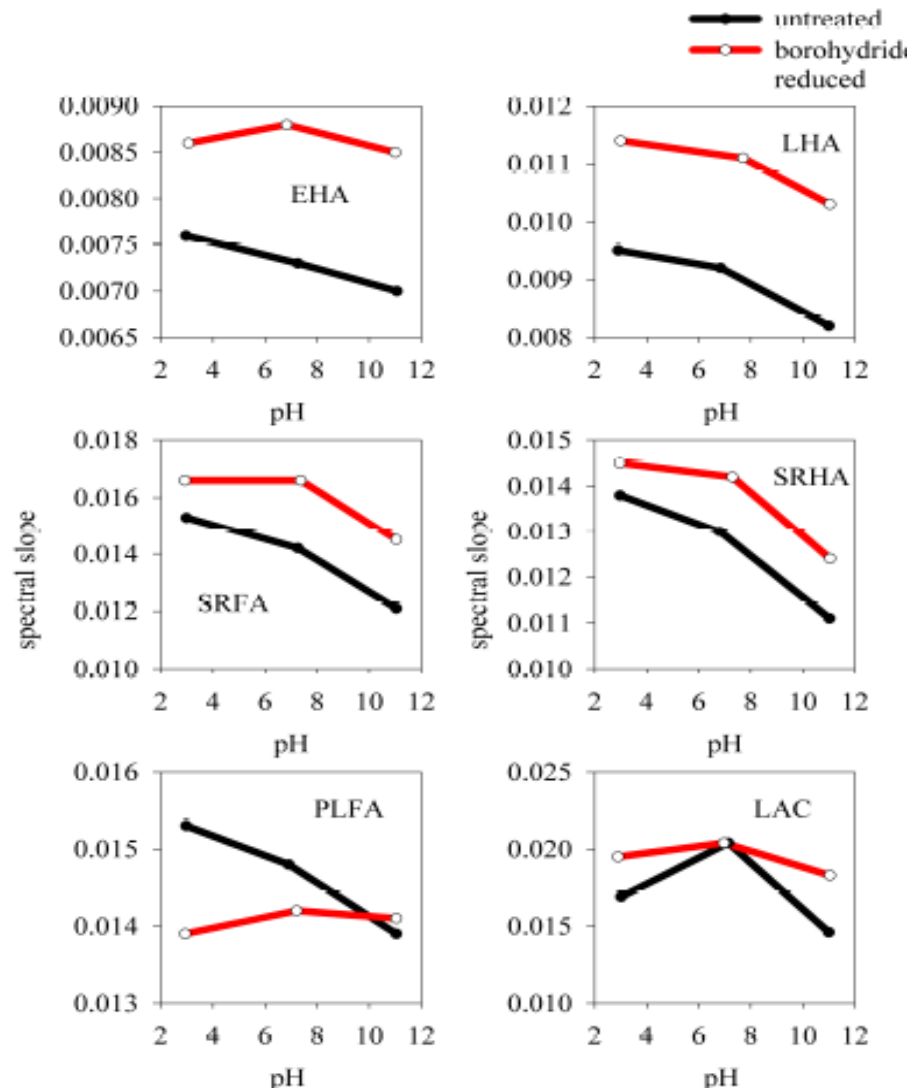


Figure 6.5 Spectral slope (S) as a function of pH. Untreated and borohydride reduced, carbon normalized.

Table 6.3 pH dependence of spectral slope values (0.01 mole L⁻¹ NaCl) associated with UV concentration range optical titrations and borohydride reductions at pH 7.6. Carbon normalized at 350 nm.

sample identification (organic carbon g ⁻¹ material)	untreated [‡]			borohydride reduced [‡]		
	pH	S	r ²	pH	S	r ²
SRHA (0.3974)	2.98	0.0138	0.9982	2.97	0.0145	0.9957
	7.26	0.0130	0.9985	7.29	0.0142	0.9973
	11.03	0.0111	0.9968	11.05	0.0124	0.9585
	7.60	0.0125 ± 0.0002		7.60	0.0146 ± 0.0002	
SRFA (0.5087)	2.98	0.0153	0.9971	2.92	0.0166	0.9956
	7.26	0.0142	0.9977	7.37	0.0166	0.9978
	11.04	0.0121	0.9976	11.04	0.0145	0.9983
	7.60	0.0147 ± 0.0003		7.60	0.0183 ± 0.0004	
PLFA (0.3949)	2.97	0.0153	0.9964	2.93	0.0139	0.9779
	6.91	0.0148	0.9976	7.21	0.0142	0.9808
	11.04	0.0139	0.9985	11.04	0.0141	0.9840
	7.60	0.0151 ± 0.0002		7.60	0.0185 ± 0.0008	
EHA (0.4760)	2.96	0.0085	0.9964	3.06	0.0086	0.9932
	7.26	0.0073	0.9972	6.83	0.0088	0.9932
	11.06	0.0070	0.9971	11.00	0.0085	0.9935
	7.60	0.0076 ± 0.0003		7.60	0.0085 ± 0.0002	
LHA (0.2501)	2.91	0.0095	0.9985	2.97	0.0114	0.9972
	6.84	0.0092	0.9987	7.71	0.0111	0.9971
	11.00	0.0082	0.9995	11.04	0.0103	0.9984
	7.60	0.0095 ± 0.0004		7.60	0.0105 ± 0.0003	

[‡] a* values were calculated at 350 nm (L(mg org. C)⁻¹m⁻¹).

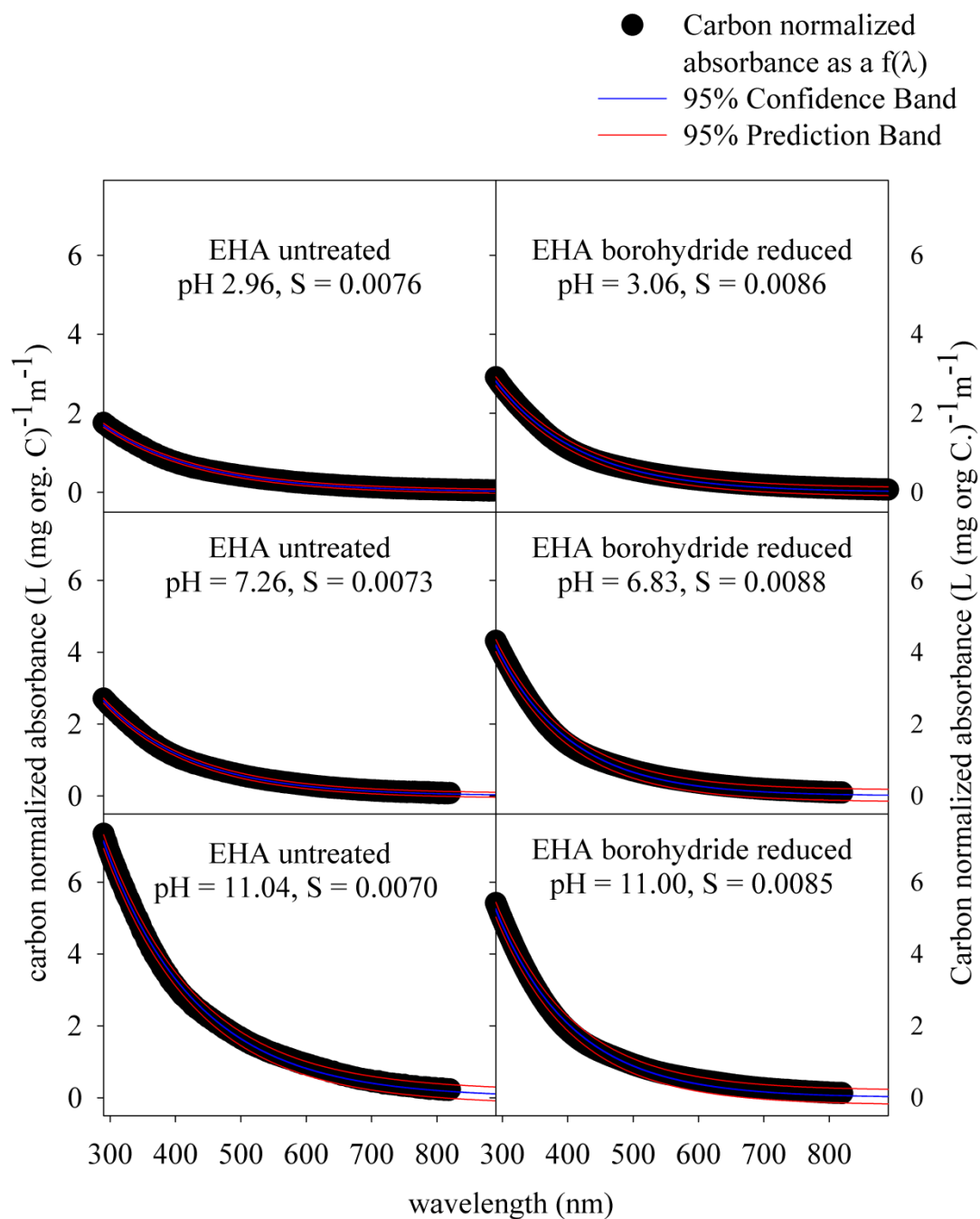


Figure 6.6 Parameterized, carbon normalized Elliott humic acid (EHA) presented as a function of pH. Untreated and borohydride reduced absorbance spectra at low (pH 3.00), neutral (pH 6.00-7.60) and high pH (pH 11.00) pH.

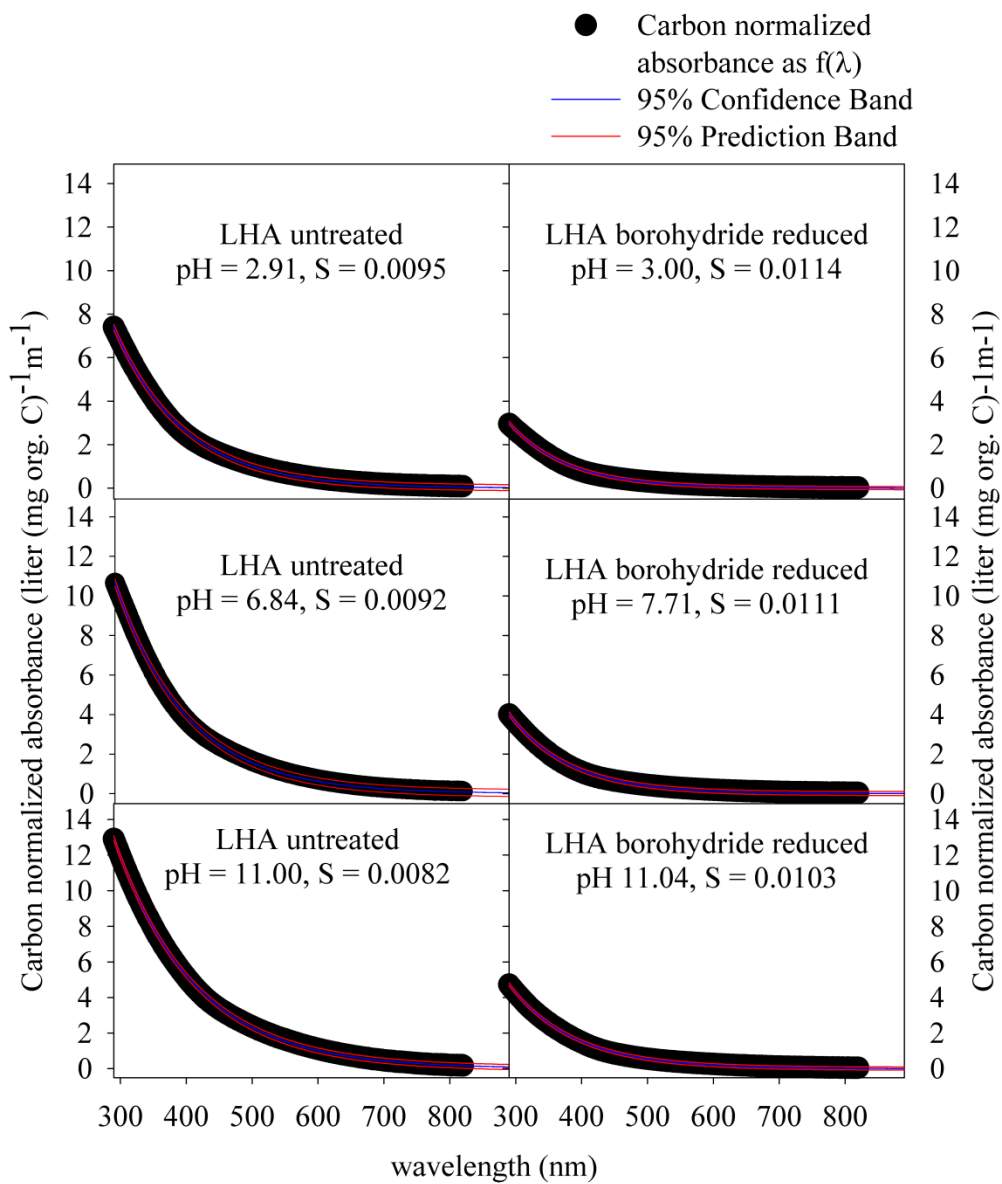


Figure 6.7 Parameterized, carbon normalized Leonardite humic acid (LHA) presented as a function of pH. Untreated and borohydride reduced absorbance spectra at low (pH 3.00), neutral (pH 6.00-7.60) and high pH (pH 11.00) pH.

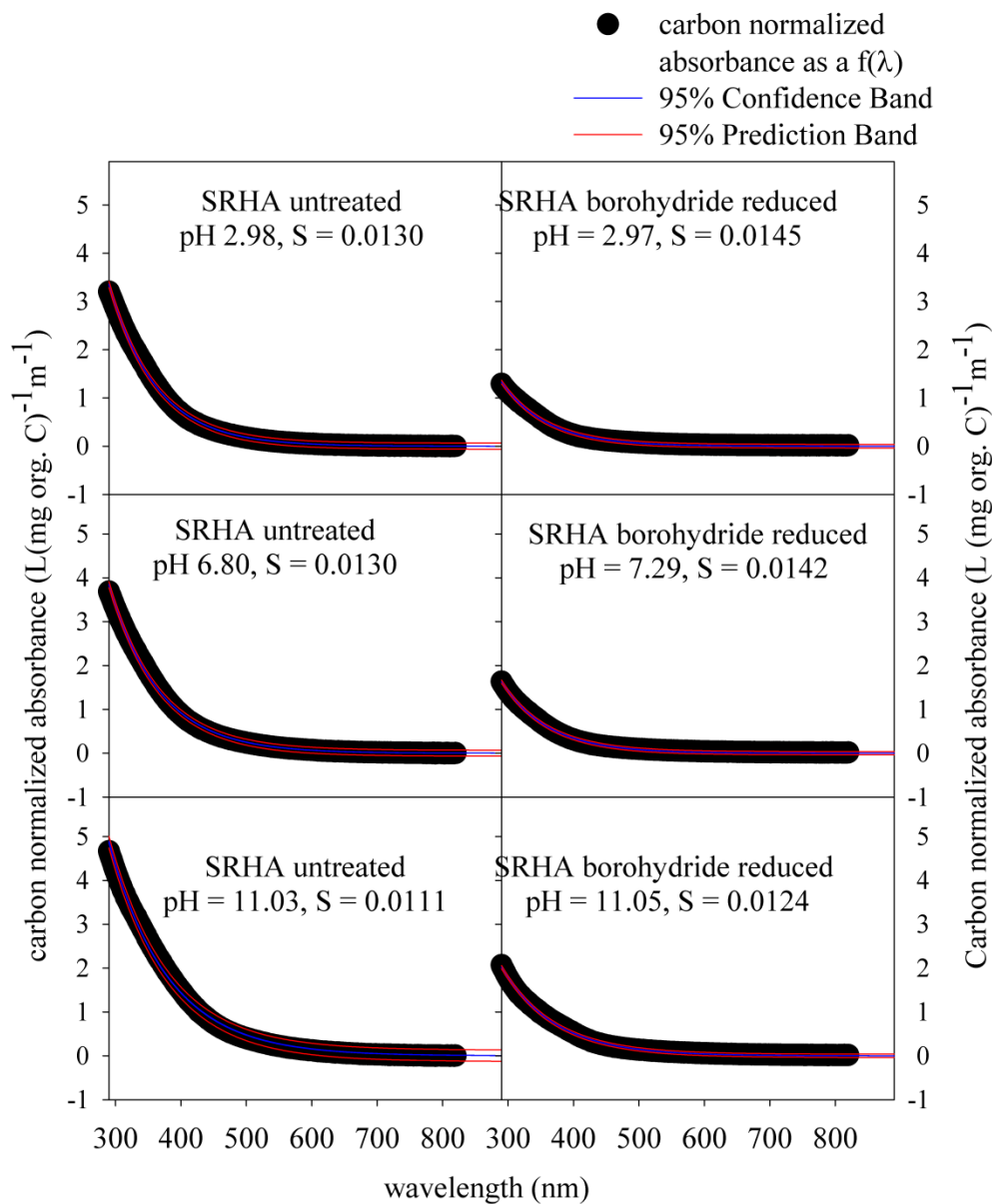


Figure 6.8 Parameterized, carbon normalized Suwannee River humic acid (SRHA) presented as a function of pH. Untreated and borohydride reduced absorbance spectra at low (pH 3.00), neutral (pH 6.00-7.60) and high pH (pH 11.00) pH.

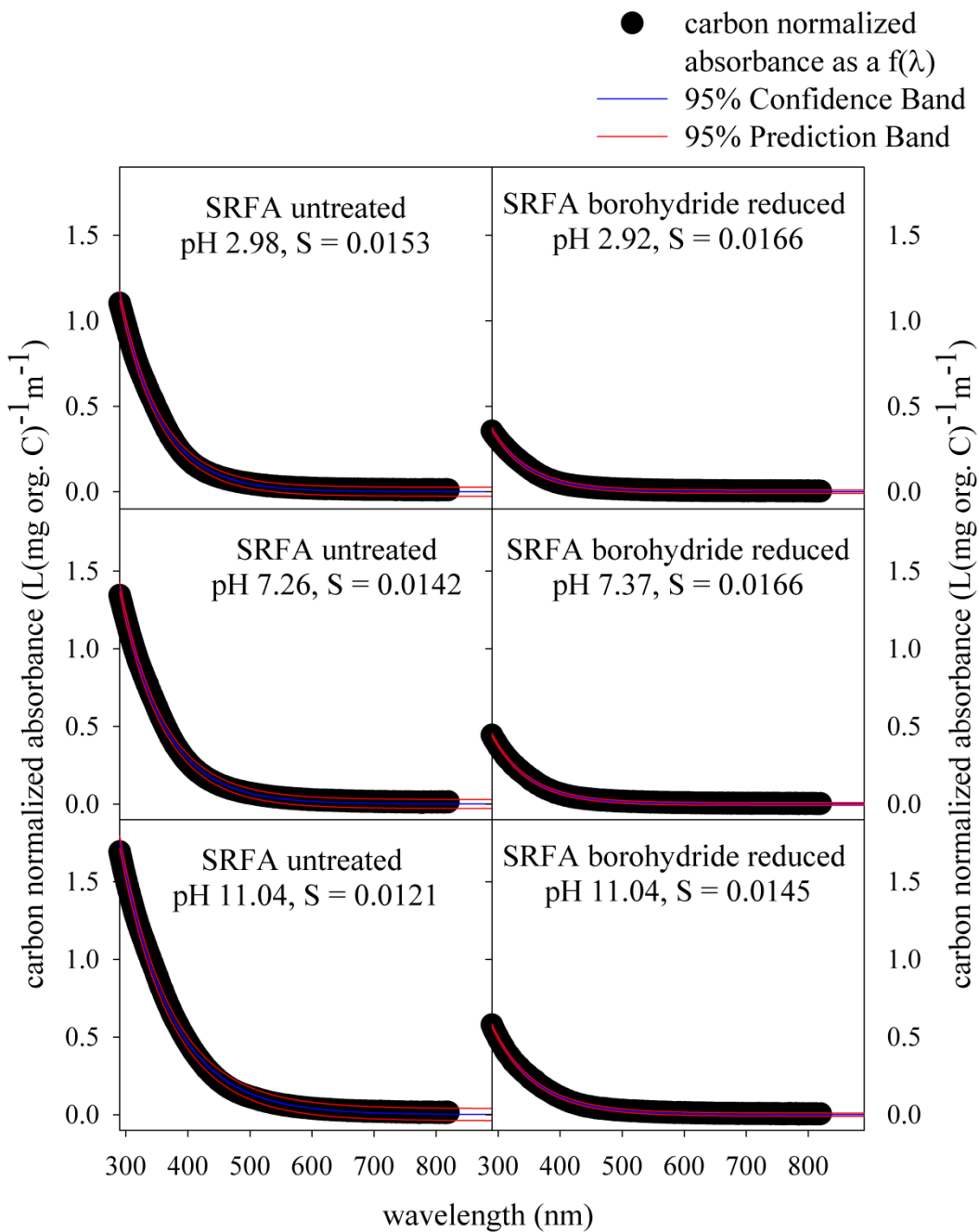


Figure 6.9 Parameterized, carbon normalized Suwannee River fulvic acid (SRFA) presented as a function of pH. Untreated and borohydride reduced absorbance spectra at low (pH 3.00), neutral (pH 6.00-7.60) and high pH (pH 11.00) pH.

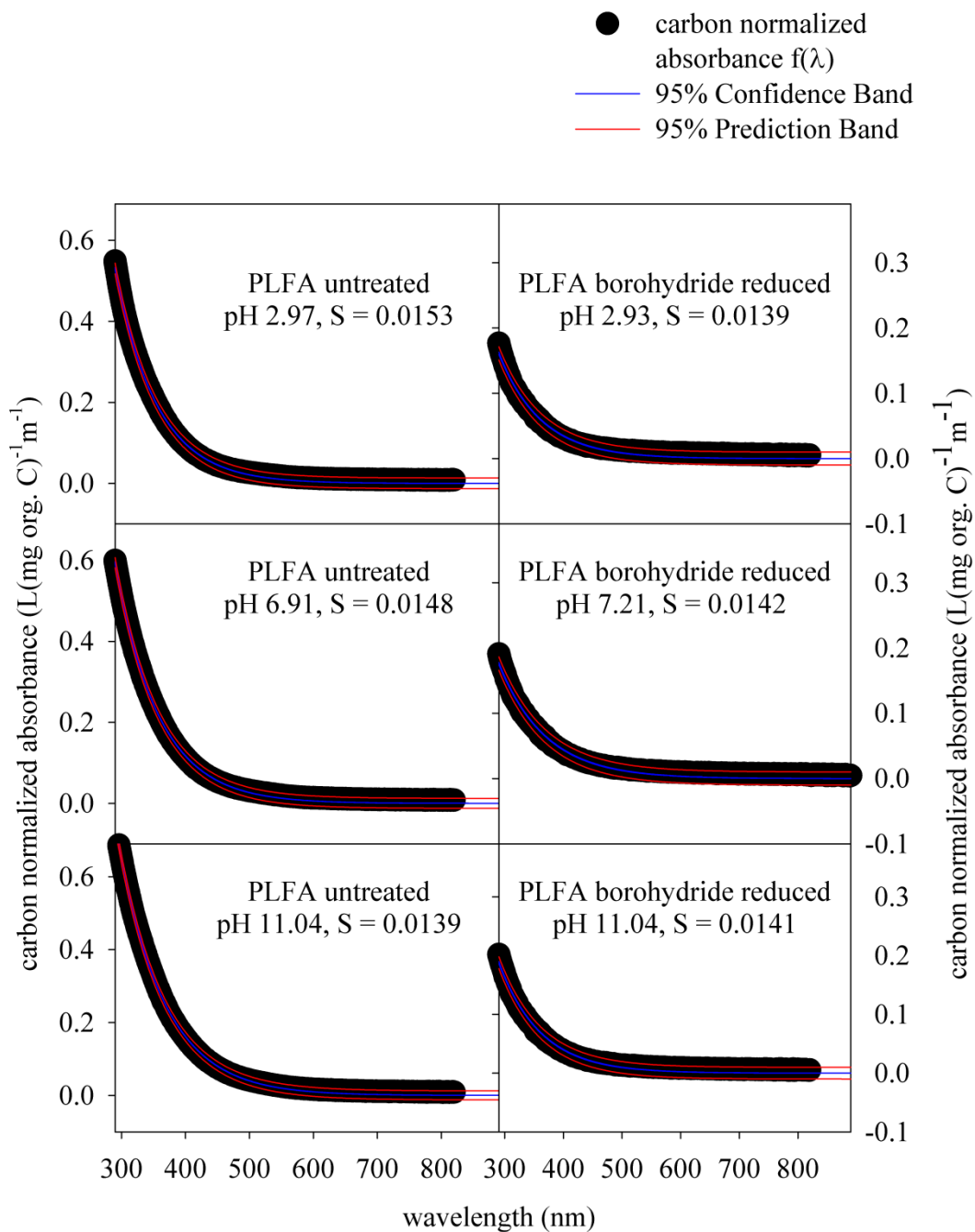


Figure 6.10 Parameterized, carbon normalized Pony Lake fulvic acid (PLFA) presented as a function of pH. Untreated and borohydride reduced absorbance spectra at low (pH 3.00), neutral (pH 6.00-7.60) and high pH (pH 11.00) pH.

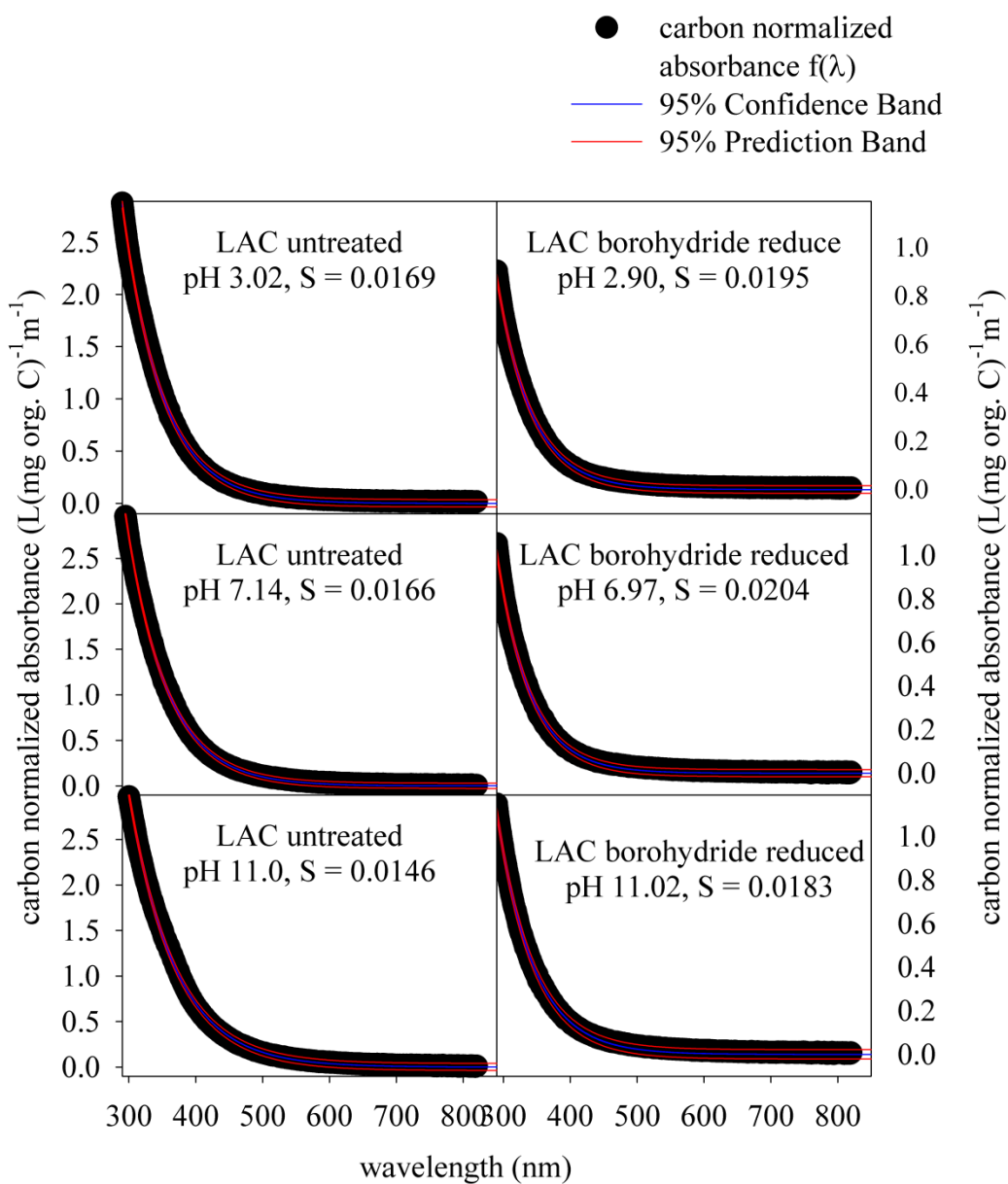


Figure 6.11 Parameterized, carbon normalized Lignin Alkali Carboxylate (LAC) presented as a function of pH. Untreated and borohydride reduced absorbance spectra at low (pH 3.00), neutral (pH 6.00-7.60) and high pH (pH 11.00) pH.

The pH dependent spectral slope (S) values show a consistent pattern of behavior (Fig. 6.5 and Table 6.3). Untreated Leonardite (LHA) and Suwannee River (SRHA) humic acids as well as Suwannee River (SRFA) fulvic acid have lower spectral slope values than do corresponding borohydride reduced spectral slope (S) values at all pHs examined (pH 3.0, pH 6-7 and pH 11.0). The untreated terrestrial soil and aquatic samples exhibit less reduction in slope between pH 3.0 and the neutral pH (pH 6-7) than the degree of change found between the neutral pH (pH 6-7) and pH 11.0.

Untreated Elliott humic acid (EHA) exhibits no difference in the rate of change of the spectral slope (S) value from pH 3.0 to pH 11.0; the spectral slope (S) of untreated EHA decreases as pH increases at a uniform rate as shown in Figs. 6.5 and 6.6. The borohydride reduced spectral slope (S) value of EHA between pH 3.0 and the neutral pH (pH 6-7) increase, but the spectral slope (S) decreases between the neutral pH point and pH 11.0 (Figs. 6.5 and 6.6). The borohydride reduced Leonardite humic acid (LHA) exhibits the same pattern as its untreated counterpart but each point is found at a higher spectral slope (S) value (Figs. 6.5 and 6.7).

Borohydride reduced SRHA and SRFA show a slight or no decrease, respectively, in the spectral slope (S) value between pH 3.0 and pH 6-7, and a more pronounced reduction in spectral slope (S) between the neutral pH point and the high pH point (pH 11.0), as shown in Figs. 6.5, 6.8 and 6.9. The neutral pH spectral slope (S) values are consistent with the spectral slope (S) values reported in Chapter 5, which was completed at pH 7.6, with no supplemental ionic strength, or removal of residual borate.

The Lignin Alkali Carboxylate (LAC) untreated and borohydride reduced samples follow a similar pattern spectral slope (S) value increases from low to neutral pH and decreasing from neutral to high pH. The borohydride reduced LAC sample has an overall higher spectral slope

(S) value except at neutral pH where the untreated and borohydride reduced spectral slope (S) values are of equal magnitude as shown in Figs. 6.5 and 6.11. The neutral pH points of untreated and borohydride reduced LAC samples from Chapter 5 have a 15 % difference when comparing reduced to untreated LAC samples.

Pony Lake fulvic acid (PLFA) differs from the other samples examined. The spectral slope (S) value of the untreated PLFA sample is higher in magnitude than the pH matched borohydride reduced sample. The borohydride reduced sample increases in magnitude slightly at the neutral pH point (pH 6-7), while the untreated sample decreases but remains at a higher value than does the borohydride reduced, pH matched sample. At high pH (pH 11.00) the borohydride reduced spectral slope (S) has a higher value than the pH matched reduced sample presented in Figs. 6.5 and 6.10.

The untreated PLFA is consistent with the spectral slope (S) value reported in Chapter 5. The borohydride reduced spectral slope (S) value of PLFA at the neutral pH point is not consistent with the Chapter 5 spectral slope (S) values. The differences between the spectral slope (S) data generated from the borohydride reduced data (Chapter 5) and the spectral slope (S) data from the optical titrations (Chapter 6) at the neutral pH point are, 1. the concentration of the material used, 2. the removal of residual borate (cleaned with Sephadex G-10 column) and 3. the manipulation of the ionic strength.

The untreated pH dependent spectral slope (S) values (with the exception of LAC) decreases with increasing pH from pH 3-11 supporting the presence of titratable chromophores. Based on the first derivative plots of the titrations, it is likely that the chromophores are grouped in two distributions that become more distinct as materials derived from lignin phenols

(terrestrially based material) are exported from soil systems into waterways and subjected to photobleaching.

The spectral slope (S) of untreated microbial source of fulvic acid (PLFA) also decreases with increasing pH and has a bimodal distribution of titratable groups, but PLFA based on NMR analysis does not contain phenolic type groups (Fang, Mao, Cory, McKnight and Schmidt-Rohr (2011)) with the likely exception of quinone groups ((Hiraishi, Ueda and Ishihara (1998)), (Hiraishi, Masamune and Kitamura (1989)), (Liu, Linning, Nakamura, Mino, Matsuo and Forney (2000)). Quinones are frequently used as a biomarker of microbial activity in wastewater and activated sewage sludge (Hiraishi, Ueda and Ishihara (1998)), (Hiraishi, Masamune and Kitamura (1989)), (Liu, Linning, Nakamura, Mino, Matsuo and Forney (2000)).

The borohydride reduced spectral slope (S) values are always higher in value than their untreated pH matched counterparts with the exception of PLFA at low and neutral pH. Borohydride reduced spectral slope (S) values of PLFA show almost no titratable change over the entire pH range titrated. This is in contrast to the other fulvic acid (SRFA), which decreases in spectral slope (S) value over the neutral (pH 6-7) to high pH (pH 11.0) range. The humic acids are very similar to SRFA showing little to no change in spectral slope (S) between pH 3 to pH 6-7, but an increasingly lower spectral slope (S) as pH increases.

Borohydride reduction in the case of PLFA appears to reduce the impact of the chromophore distribution that was titratable prior to reduction. It is possible that borohydride reduction of unquenched quinones would not positively impact the spectral slope (S) value because spectral slopes (S) are measured from an absorbance of 290 nm and longer wavelengths. Many of the quinones and hydroquinone absorption maxima are located at shorter wavelengths

than those include in the spectral slope (S) calculation, while reduced aromatic ketones would be able to influence the absorbance interval used to calculate the spectral slope (S).

A major difference between the Chapter 5 and Chapter 6 spectral slope (S) data is the concentration of the samples used to generate the spectral slope (S). In Chapter 5, the concentration of the borohydride reduced sample is 266 mg L^{-1} while the concentration used in Chapter 6 was 30 mg L^{-1} , the a^* value is $1.17 \text{ L (mg org. C}^{-1}) \text{ m}^{-1}$. The difference in concentration would allow the red edge of the unquenched acceptor moieties in the high concentration sample to extend past 290 nm increasing the spectral slope (S) in the high concentration sample but possibly not effecting the spectral slope (S) in the low concentration sample because the red edge of the unquenched acceptor species does not extend past 290 nm which is the traditional boundary of spectral slope (S) calculations. The Chapter 5 and Chapter 6 data support quinones as the acceptor moiety in PLFA. A second difference between the visible range, high concentration borohydride reductions and the relatively low concentration optical titrations is the use of the Sephadex G-10 column to remove residual borate that would otherwise interfere with the optical titration. Table 6.3 presents both sets of data. The borohydride reductions carried out at pH 7.6 were completed with at least three replicates and concentrations that were within the optical range of the instrument.

6.3.5 Optical Titration Spectra and Difference Plots

Carbon normalized absorbance spectra as a function of pH, with corresponding difference spectra (ΔA) are presented in a series of figures. Figure 6.12 is Suwannee River humic acid (SRHA). Figure 6.13 is Suwannee River fulvic acid (SRFA). Figure 6.14 is Pony Lake fulvic acid (PLFA). Figure 6.15 is Elliott humic acid (EHA). Figure 6.16 is Leonardite humic acid (LHA). Figure 6.17 is Lignin Alkali Carboxylate (LAC). Each figure exhibits a variable number of absorbance spectra corresponding to titration points from pH 3.00 to pH 11.00 for untreated and borohydride reduced samples. The number of absorbance spectra is intrinsic to each sample. Each absorbance spectra (untreated and borohydride reduced) is identified by a different color that is linked to the pH point where it was collected. Difference spectra (ΔA) are generated by subtracting the absorbance at pH 3 from the other absorbance spectra x where, x is the absorbance spectra at any pH point titrated. The difference spectra are identified by the same color as the absorbance spectra that generated it. Untreated samples are in the upper panels and borohydride reduced samples are in the lower panels of each figure.

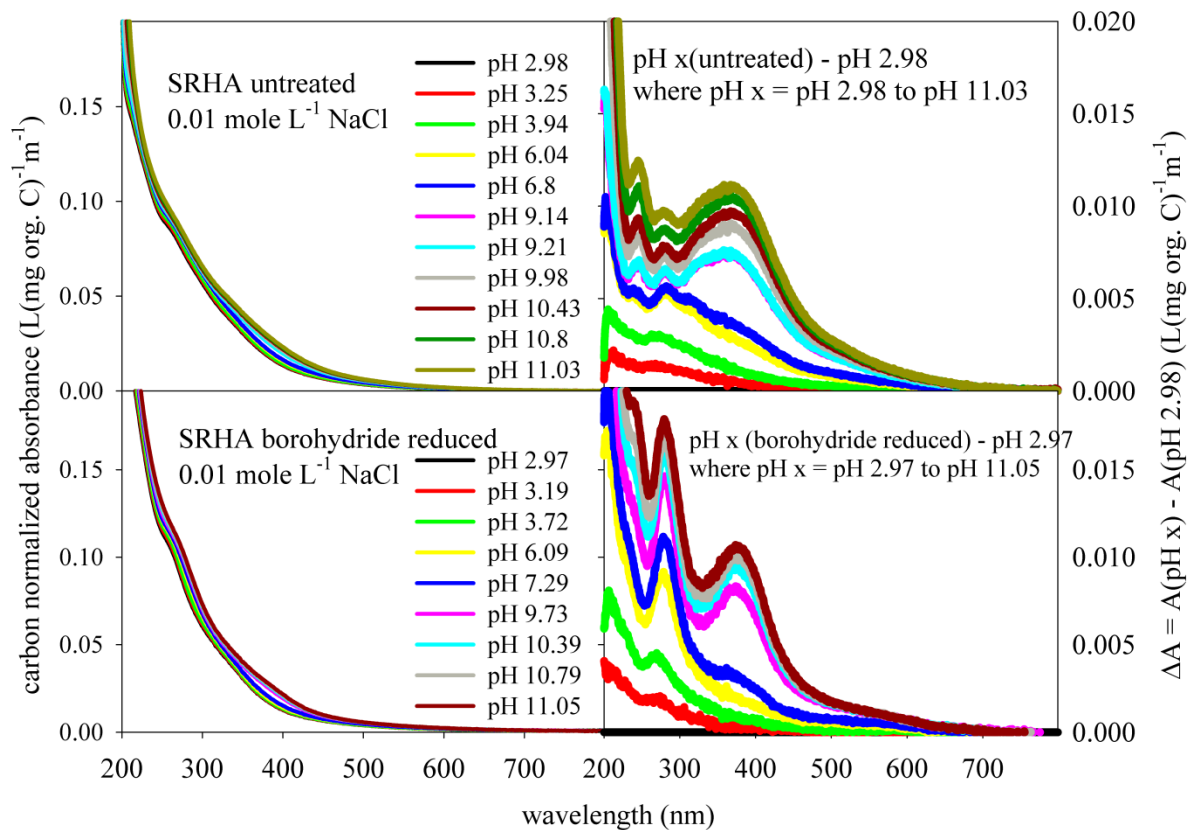


Figure 6.12 Absorbance spectra of the optical titrations (left panels) and difference plots (right panels) of carbon normalized Suwannee River humic acid (SRHA) untreated (upper panels) and borohydride reduced (lower panels).

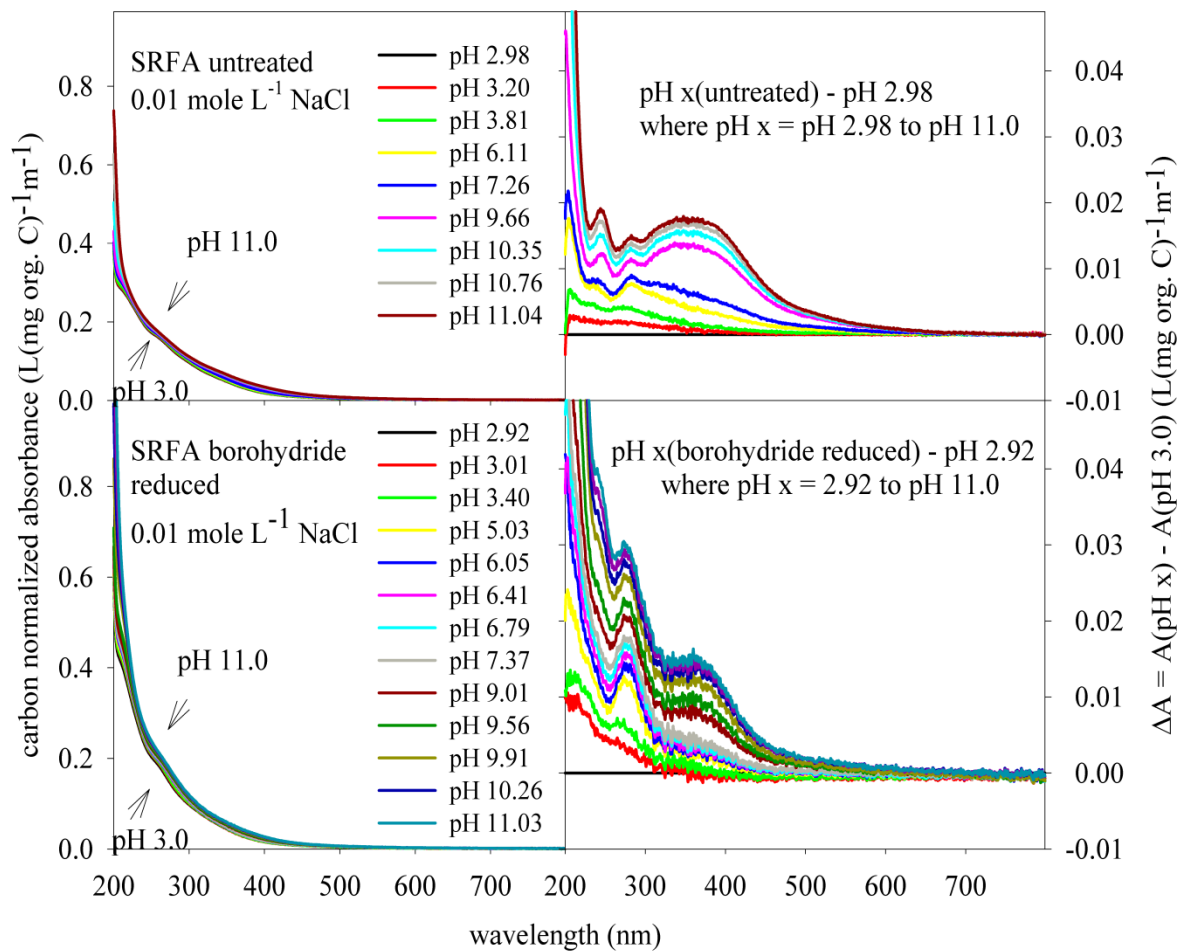


Figure 6.13 Absorbance spectra of the optical titration and difference spectra of carbon normalized Suwannee River fulvic acid (SRFA). Untreated SRFA upper panels. Borohydride reduced SRFA (lower panels).

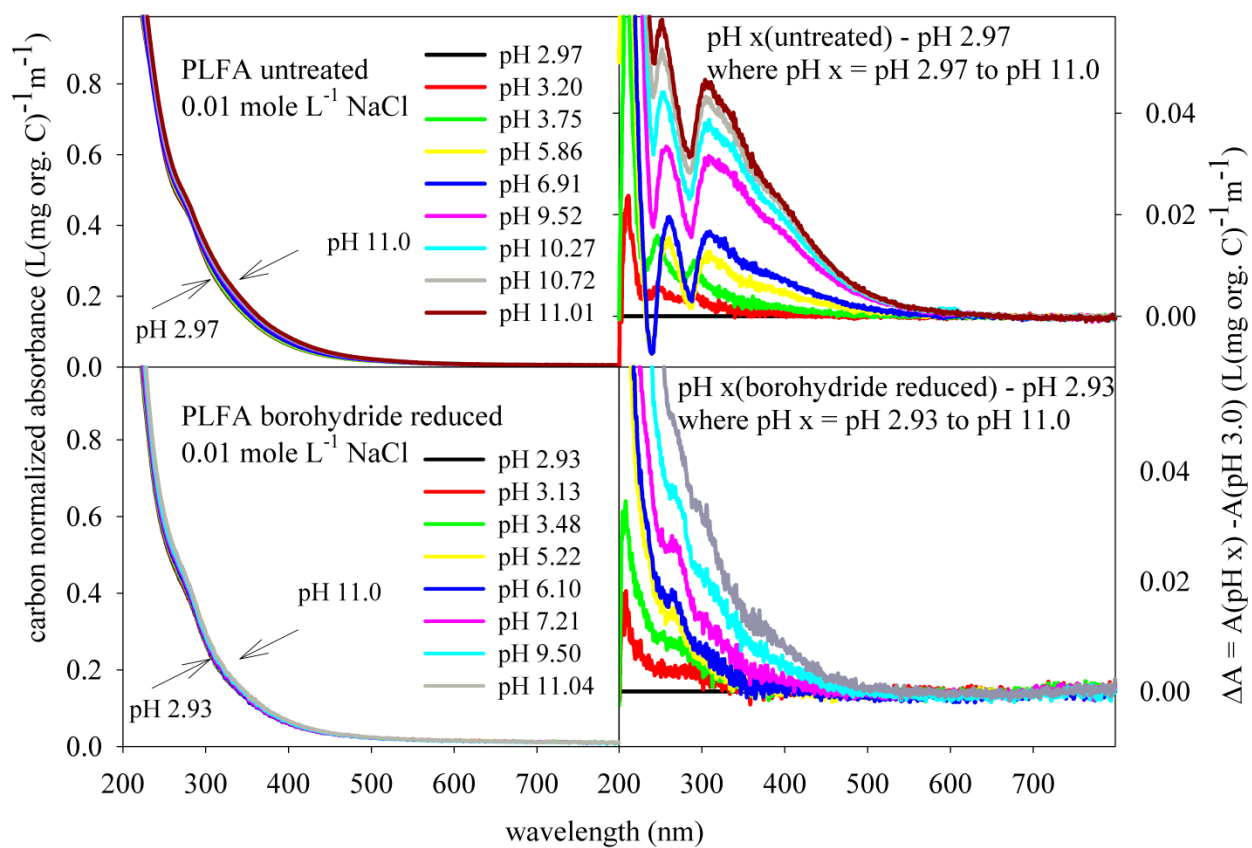


Figure 6.14 Absorbance spectra of the optical titration and difference spectra of carbon normalized Pony Lake fulvic acid (PLFA). Untreated PLFA upper panels. Borohydride reduced PLFA (lower panels).

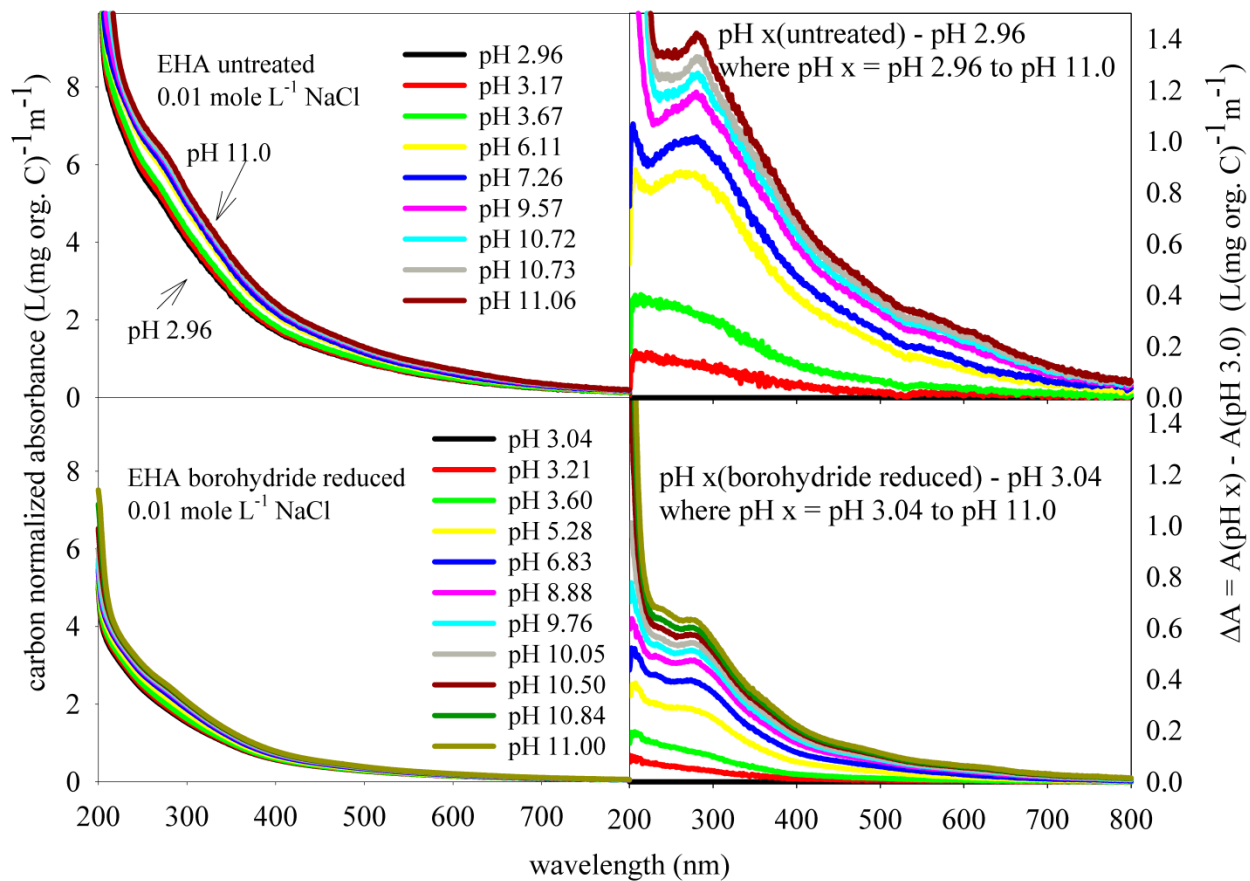


Figure 6.15 Absorbance spectra of optical titrations and difference plots of carbon normalized Elliott humic acid (EHA) untreated (upper panels) and borohydride reduced (lower panels).

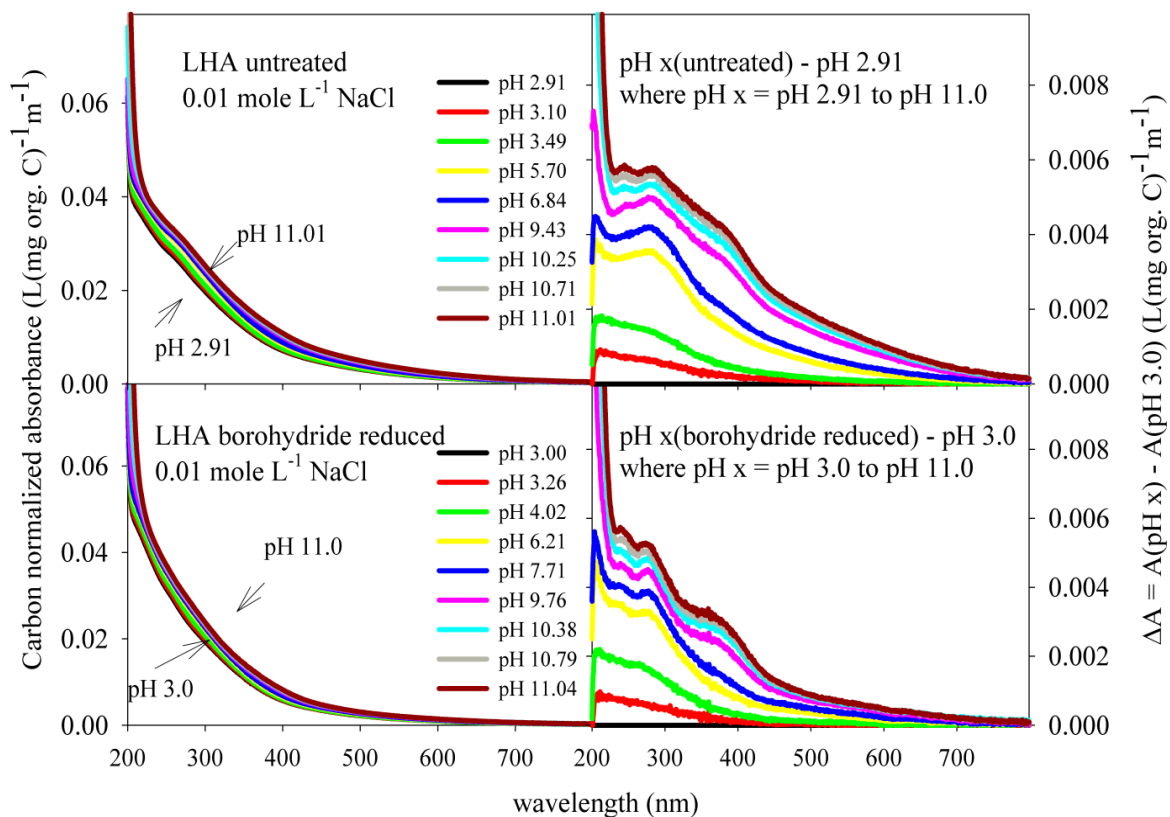


Figure 6.16 Absorbance spectra of the optical titrations (left panels) and difference plots (right panels) of carbon normalized Leonardite humic acid (LHA) untreated (upper panels) and borohydride reduced (lower panels).

Untreated carbon normalized difference spectra (ΔA) of SRHA shown in Fig. 6.12, have a broad pronounced peak centered at 350 nm and extending into the visible region to 650 nm. Two smaller peaks emerge in the difference spectra at 220 and 280 nm above pH 6.8. Borohydride reduces the magnitude and breadth of the peaks centered at 350 nm. The long wavelength absorbance blue shifts but the maximum remains at 350 nm. The two peaks at 220 and 280 nm increase in magnitude but don't shift wavelength. The SRFA difference spectra shown in Fig. 6.13 follow the same pattern as SRHA, but the peak in the visible range of the spectra is red shifted to 370 nm, emergent at the same pH as SRHA. The peaks in the UV range at 220 and 280 nm are both evident, in the untreated and borohydride reduced SRFA samples (Fig. 6.13). Borohydride reduction of SRFA decreases the visible peak and concurrently increases the UV peaks at 220 and 280 nm.

The difference spectra (ΔA) of untreated Pony Lake fulvic acid (PLFA) shown in Fig. 6.14 is unlike any other fulvic or humic acid difference spectra examined in that the degree of pH dependent change is much more extreme than the other samples examined. Positively increasing peaks are evident at 220 nm until pH 5.86. Above pH 6.91, the long wavelength continues to increase fairly uniformly, but extends to a lesser extent converging to no differential absorbance by 550 nm. The molar extinction coefficient (ϵ) data support the linearity of PLFA at pH 7.6.

Two distinct pools of titratable groups are evident one above pH 7.0 and a second group below pH 7.0. The presence of two titratable group distributions in the difference plot is constant with other difference plots within this study and found by (Dryer, Korshin and Fabbicino (2008)). Borohydride reduction of PLFA eliminates all major difference spectra features. A small shoulder peak remains, shifting to the red with increasing pH. The difference spectra of borohydride reduced PLFA supports the presence of quinones possibly acting as

acceptors. Heterocyclic moieties and secondary and tertiary amines would not be impacted by borohydride reduction. Quinones or cyclic ketones are vulnerable to borohydride reduction and have the potential to be present in PLFA acting as acceptors. Elimination of these acceptor moieties by the reduction is consistent with the first derivative plot, spectral slope and difference (ΔA) data.

The untreated carbon normalized difference (ΔA) plots of soil derived humic acid (EHA) exhibits absorbance that extends to 820 nm (Fig 6.15). EHA has a pronounced peak at 280 nm, but no peak corresponding to the SRHA peak located at pH 220 nm as shown in Figs. 6.12 and 6.15. The difference plot of the low concentration UV range spectra show a feature in the long range absorbance at 550 nm (Fig. 6.15). This feature is repeated in the high concentration 0.10 and 0.01 mole L⁻¹ NaCl difference plots, presented in Appendix 2 in Figs. A2.6 and A2.7 and appears to be pH dependent apparent at pH 6 and above. Upon borohydride reduction the entire difference spectra decreases in magnitude uniformly retaining the long wavelength, pH dependent feature evident in the low concentration (UV range difference spectra 200-800 nm) and the high concentration (visible range spectra > 350 nm). The pH dependent features evident in the EHA difference spectra may be related to the underlying chromophore present in the fluorescence spectra in Chapter 5 It is unlikely that this feature is part of the electronic interaction extended wavelength tail produced by donors and acceptors because it appears in both the untreated and borohydride reduced spectra.

Leonardite humic acid (LHA) differs from EHA as seen in Fig. 6.16, an inflection can be observed between pH 6.84 and pH 9.43 centered at 380 nm. In a similar manner as EHA, LHA absorbance extends to 820 nm. Peaks in the UV range of the spectra at 220 and 280 nm are evident in the LHA titration emerging at pH above 3.49 for the 280 nm and at 9.43 for the 220

nm peaks. Borohydride reduction decreases the visible portion of the difference spectra while, retaining the inflection point evident in the untreated titration. The inflection at 380 nm decreased to a lesser degree than the extended tail did. It appears as a peak in the reduction spectra more closely matches the pattern evident in the difference spectra of the Suwannee river materials than the other soil derived humic acid, EHA.

Lignin alkali carboxylate is a commercial form of lignin. The untreated difference plot (ΔA) shows two discernable peaks at absorbance 280 nm and 380 nm (Fig. 6.17). The peak located at 280 nm blue shifts at pH values above 9.39. The peak at 380 nm is also pH dependent disappearing at pH below 6.74. The peak at 380 nm is eliminated upon borohydride reduction. The peak at 280 nm is reduced in magnitude and converges with the continuum of low wave length peaks below 250 nm as shown in Fig. 6.17. The first derivative plot shows one titratable group located in the NICA-Donnan identified phenolic distribution.

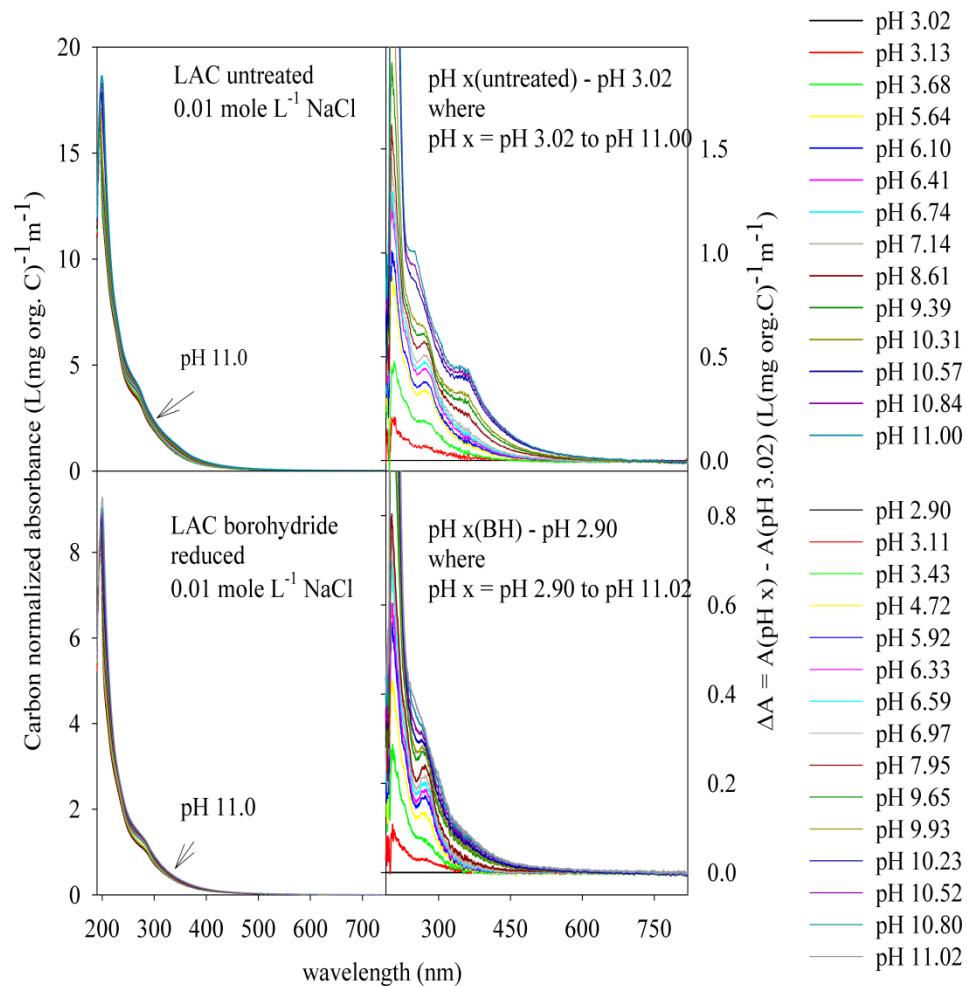


Figure 6.17 Absorbance spectra (left panels) and difference plots (right panels) of the optical titration of carbon normalized Lignin Alkali Carboxylate (LAC). Untreated LAC (upper panels). Borohydride reduced LAC (lower panels).

The untreated and borohydride reduced high concentration (> 350 nm) titrations of SRFA and PLFA are shown in Figs. 6.18 and 6.19, respectively, at ionic strength of 0.01 mole L^{-1} NaCl highlights the optical differences found between the two fulvic acids in the study. The other ionic strengths (0.10 and 1.00 mole L^{-1} NaCl) are included in Appendix 2. The SRFA constantly shows a smoothly declining difference plot that converges into the baseline at long wavelengths. The untreated and borohydride reduced PLFA samples with 0.01 and 0.10 mole L^{-1} NaCl show a reversal in absorbance above pH 4.00 located at 490 nm . This feature is not evident in the low concentration (UV range) difference plots. The low concentration PLFA elucidates the UV range of the absorbance spectra resulting in an undetectable absorbance at long wavelengths. It is possible that, based on the high concentration of nitrogen in PLFA when compared to SRFA that this peak is related to titratable nitrogen containing moieties. This chromophore is not borohydride reducible and appears to be more prominent upon reduction, further implicating nitrogen containing compounds.

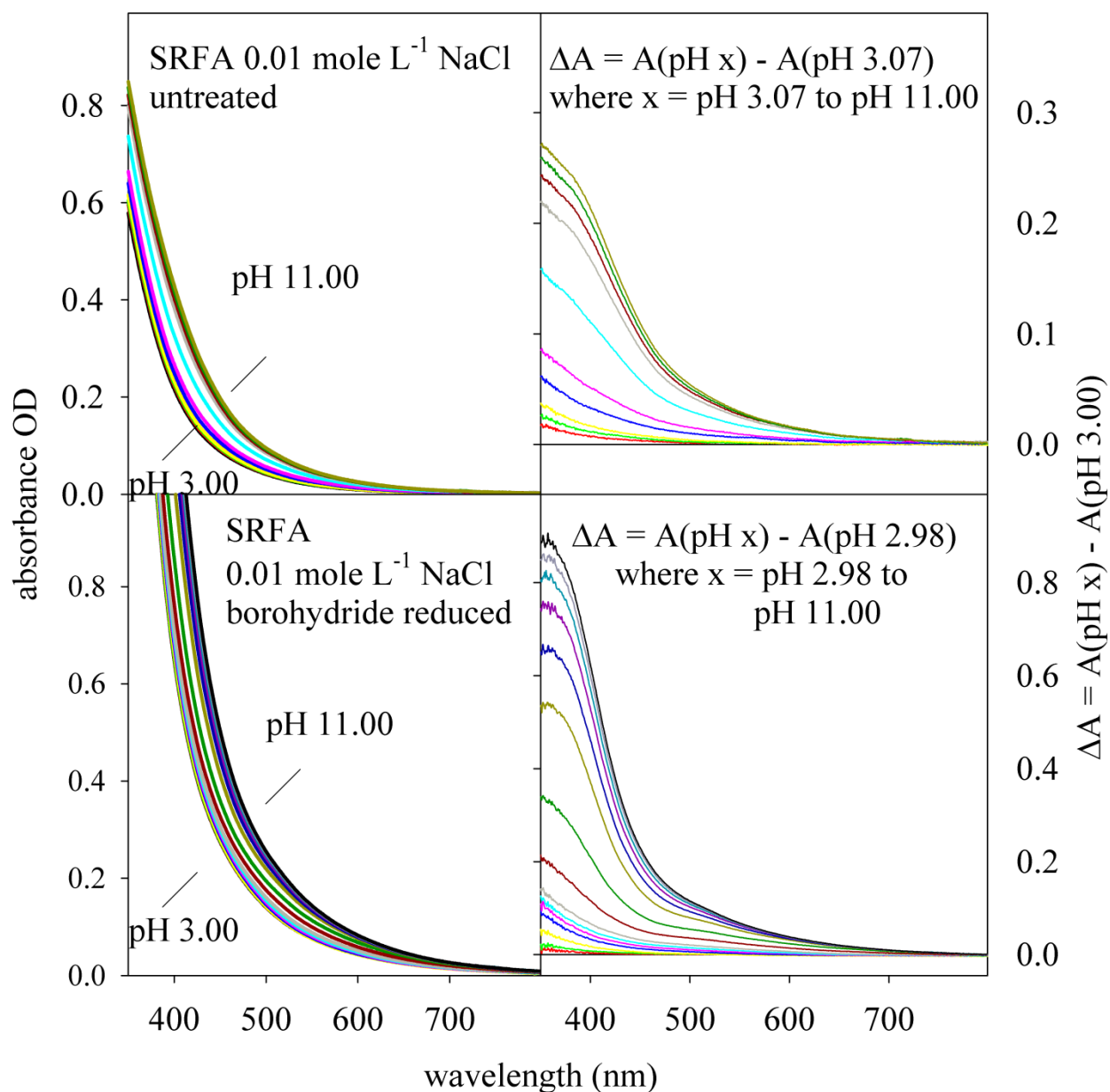


Figure 6.18 Absorbance (left panels) and difference spectra (right panels) of untreated (upper panels) and borohydride reduced (lower panels) of Suwannee River fulvic acid (SRFA) at 0.01 mole L⁻¹ ionic strength. Untreated (100 mg L⁻¹, $a^* = 3.39$). Borohydride reduced (760 mg L⁻¹, $a^* = 1.88$). Borohydride reduced samples were passed through a Sephadex G-10 column.

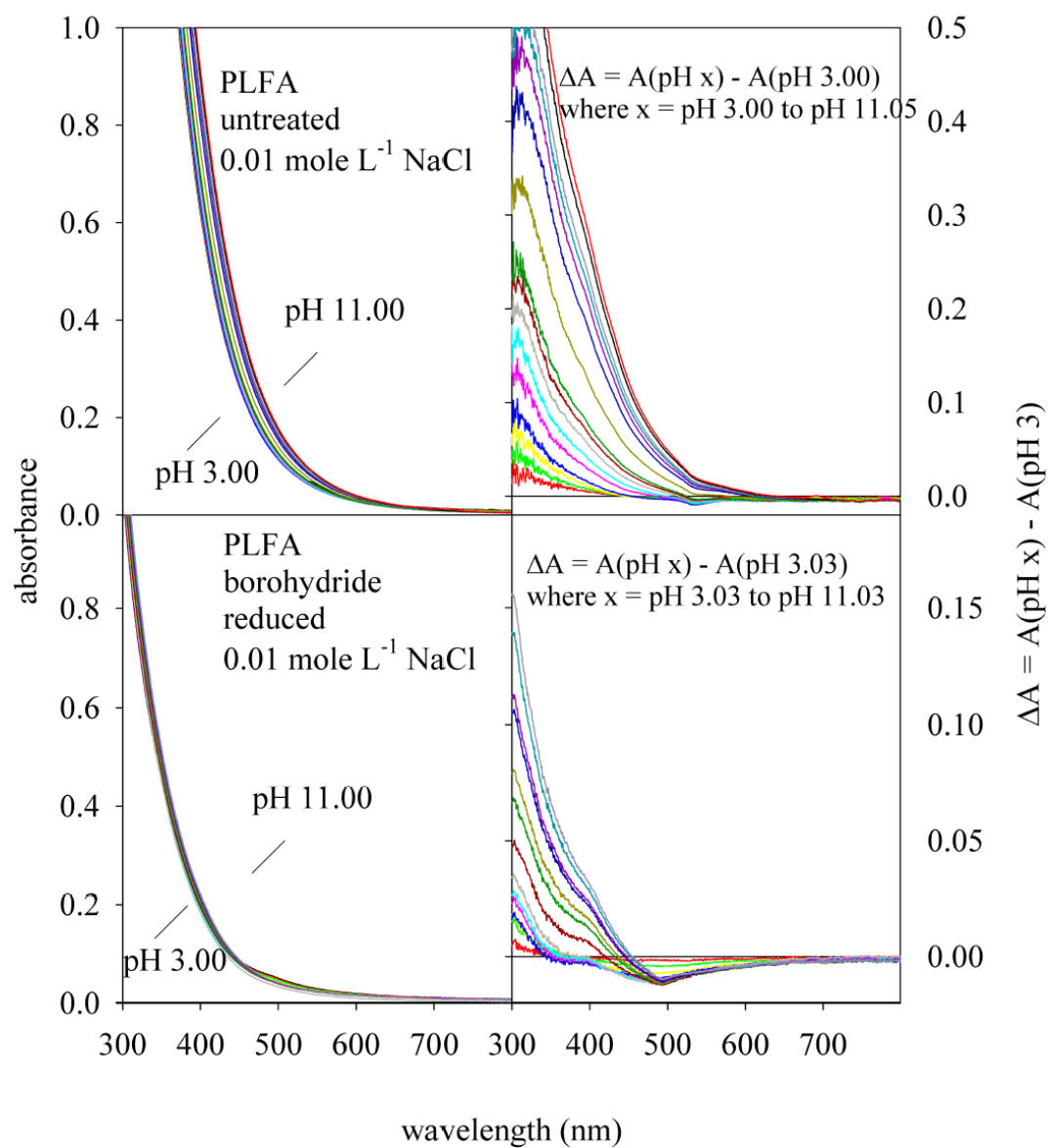


Figure 6.19 Absorbance (left panels) and difference spectra (right panels) of untreated (upper panels) and borohydride reduced (lower panels) of Pony Lake fulvic acid (PLFA) at 0.01 mole L⁻¹ ionic strength. Untreated (500 mg L⁻¹, $a^* = 1.34$). Borohydride reduced (266 mg L⁻¹, $a^* = 1.17$). Borohydride reduced samples were passed through a Sephadex G-10 column.

6.4 Conclusions

Pony Lake fulvic acid generates extended long wavelength absorbance due to electronic interactions in a similar manner as terrestrially derived humic and fulvic acids despite differences in source material. Two distributions of titratable chromophores interact to produce the long wavelength absorbance characteristic of humic and fulvic acids and CDOM. The bimodal distribution of titratable groups is consistent with data generated from the NICA-Donnan model, but optical titrations require less material to generate.

The untreated soil derived humic acids exhibit a broader, less defined distribution of titratable groups possibly reflecting a greater heterogeneity of chemical species than do the other untreated humic and fulvic acids. Upon borohydride reduction of soil derived humic acids a clear bimodal distribution of titratable species is observable. The bimodal distribution of the borohydride reduced soil derived humic acids is consistent with the first derivative plots of aquatic humic acids from terrestrial origins. The first derivative plots of the optical titrations of borohydride reduced terrestrial humic acids may mirror natural processes as terrestrial humic material is exported into waterways and exposed to photochemical processes.

PLFA does not contain phenolic groups with the exception of quinones which can be generated from microbial sources. Spectral slope, optical titration and difference spectra indicate that quinones may act as acceptor moieties in PLFA. Quinones do not appear to be an important component of electronic interactions of terrestrially based aquatic or soil derived humic or fulvic acids. Quinones may act as an electron buffer but do not appear to be an important component of the optical properties of terrestrial humic acids.

Soil derived humic acids as evidenced by the difference plots may have additional chromophores that are present in the material but do not participate in the electronic interactions.

Therefore they are not involved in generation of extended long wavelength absorbance despite evidence of discrete absorbance at long wavelengths, as observed in deference plots of terrestrial humic substances. Differential absorbance at long wavelengths is not observed for the aquatic sources of terrestrial humic acids. This supports the long established premise that export of soil derived humic material is on a continuum that eliminates labile material as the humic and fulvic acids are exported into fresh water and marine environments and acted upon by photochemical and chemical processes.

Chapter 7 Raman Spectroscopy of Lignin Phenols, Quinones and Suwannee River Humic and Fulvic Acids

Chapter 7 Overview

Raman spectroscopy and surface enhanced Raman spectroscopy are described in the context of their ability to overcome the inherent background fluorescence associated with CDOM/HS in Sec. 7.1. Section 7.2 describes the materials and methods used in this series of experiments, including the materials used (Sec. 7.2.1), apparatus (Sec. 7.2.3), surface enhanced Raman (SERS) techniques (Sec. 7.2.4), preparation of the silver electrodes (Sec. 7.2.4.1) and preparation of the silver plate (Sec. 7.2.4.2). The results of the experiments are presented and discussed in Section 7.3. Section 7.3.1 details the production of nano-features generated from cyclic voltammetry. Section 7.3.2 presents data about the calibration of the silver electrodes and plate using pyridine (Sec 7.3.2.1) and crystal violet (Sec. 7.3.2.2). The SERS spectra of terrestrially sourced monomer compounds are presented and discussed in Section 7.3.3. Selected quinones are presented in section 7.3.3.1. Selected lignin phenols are presented in Section 7.3.3.2. The SERS spectra of borohydride reduced Suwannee River humic acid (SRHA) and p-methyl benzoquinone are presented and discussed in Section 7.3.4. Section 7.4 details possible conclusions and highlights the need for future work.

7.1 Introduction

Raman spectroscopy is generally able to provide useful structural information from molecules and polymeric systems. The intensity of Raman active functional groups is based on

the polarizability of the molecular electron cloud subjected to electromagnetic radiation with energy of E . Raman intensity is E^4 (Agarwal and Atalla (2000)). In the case of humic substances and CDOM the strong fluorescence, a characteristic optical property, interferes with acquisition of functional information (Boyle, Guerriero, Thiallet, Del Vecchio and Blough (2009)), (Coble (2004)). In order to overcome the fluorescence interference, it should be possible to generate the surface enhanced Raman spectroscopy (SERS) spectra of related quinone/hydroxyquinone/phenolic analog products by using sodium borohydride reduction reaction to reduce carboxylic functional groups, thus disrupting predicted charge transfer bands. This method of reduction when applied to HS has been used to successfully generate the predicted products as identified by Fourier Transform Infrared resonance (FTIR) and proton nuclear magnetic resonance ($^1\text{H-NMR}$) (Tinnacher and Honeyman (2007)). The ability to correlate predicted terrestrially sourced lignin monomers with reduced and thus partially or completely unquenched source material may provide definitive information about the underlying structure that generates the unique optical properties associated with CDOM.

The intensity of SERS spectra relies in part on proximity of the target molecule to nanostructures of coinage metals. The relationship is described in Eq. 7.1.

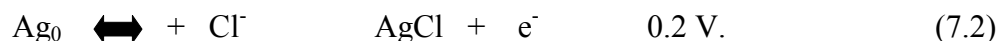
$$I = (1 + r/a)^{-10}, \quad (7.1)$$

where I is intensity of the Raman mode and a is the average size of the field enhancement and r is distance from the surface to the absorbate. Localized field enhancement increases the Raman intensity by a factor of 10 so when combined with Raman intensity the resultant intensity can increase by as much as 10^4 . Additionally, chemical enhancement mechanisms can further increase the intensity of the Raman active modes by 10^2 . Chemical enhancement can result from excitation of absorbate localized electronic resonances and/or metal-to-absorbate charge transfer

resonances, i.e. resonance Raman scattering (RRS). A favorable combination of all possible enhancements can increase the intensity of the Raman mode by as much as 10^9 - 10^{10} . The increase in intensity in conjunction with the borohydride induced breakdown of the CDOM structure can provide structural data not available in untreated humic substance or by normal Raman spectroscopy (Opsahl and Benner (1997)), (Johansson (2005)).

Nano-features can be generated in several ways, including electrochemically, by chemically roughening a surface, generating a thin film on a glass plate or forming colloids. In order to produce nano-features from silver metal an oxidative reductive cycle (ORC) is used producing nano-features ranging in size from 25-500 nm (Opsahl and Benner (1997)), (Aroca (2006)).

The oxidation (anodic) half of the cycle presented in Equation 7.2,



The number of silver ions reduced from the silver chloride (AgCl) layer is the total cathodic charge. Silver plate was also chemically roughened.

7.2 Materials and Methods

7.2.1. Materials

Silver plate (1 x 1 x 0.128 inch) (99.95%) was purchased from Surepure Chemicals, Florham Park, NJ USA. The roughened silver electrodes were prepared from 1.0 mm diameter silver wire 99.9 % (Aldrich Chemicals, Milwaukee, WI USA).

Reagent grade pyridine and anhydrous pyridine were purchased from Fisher Scientific (Waltham, MA USA), crystal violet was purchased from J.T. Baker and company (Phillipsburg NJ USA). A 2.85-mM aqueous solution of crystal violet was prepared. Vanillic acid (4-hydroxy-3-methoxy-benzoic acid) ($C_8H_8O_4$) (98.5 %), vanillin ($C_8H_8O_3$), (99 %), acetovanillone ($C_9H_{10}O_3$) (98 %), syringic acid ($C_9H_{10}O_5$) (97 %), syringaldehyde (3,5-dimethoxy-4-hydroxybenzaldehyde ($C_9H_{10}O_4$) (98 %), acetosyrinone (3',5'-dimethoxy-4'-hydroxyacetophenone ($C_{10}H_{12}O_4$) (97 %), p-hydroxy cinnamic acid, trans ($C_9H_8O_3$) (98 %) and 2, 5-dimethyl-p-benzoquinone ($C_8H_8O_2$) were purchased from Acros Organics, New Jersey, USA. Ferulic acid was purchased from MP Biochemicals Inc (2925 Fountin Pkwy. Solon, OH USA). 4-hydroxybenzoic acid, 2, 6-dimethyl-1-benzoquinone ($C_8H_8O_2$) (99%), 2,5-dihydroxy-1,4-benzoquinone ($C_6O_4H_4$) (98 %), tetra hydroxy-1,4-benzoquinone hydrate ($C_6H_4O_6$), and methyl-1,4-benzoquinone were purchased from Aldrich Chemicals. p-benzoquinone ($C_6H_4O_2$) (99 %) and sodium borohydride were purchased from Sigma. Suwannee River humic and Fulvic acids were purchased from Fluka Chemicals. Reagent quality water was supplied by a reverse osmosis (RO) water system.

7.2.2. Apparatus

SERS Spectra were collected using a Horiba Jobin Yvon Raman Spectrophotometer with a charged coupled detector (CCD), a 532-nm diode laser or a helium neon laser (633 nm) from 100- 2500 Cm^{-1} . The Raman spectrophotometer was equipped with a conofocal microscope turret with (x, y, z) movable stage. The spectra were collected using a 100 μm hole and a 100 μm slit. Spectra were accumulated for 20 cycles, RTD 1 second and exposure was 5

seconds. A Princeton Applied Research potentiostat/galvanostat Model 263 A controlled by Power Suite software in the potentiostat mode was used to execute the oxidation-reduction cycle using a three electrode system consisting of a Standard Calomel Electrode (SCE) reference, a platinum auxiliary electrode and silver wire working electrode. The instruments used in this series of experiments are located at the United States Department of Agriculture, in the Laboratory of Walter F. Schmidt.

7.2.3 Preparation of Silver Electrodes

Surface enhanced Raman spectra (SERS) spectra were collected on roughened silver electrodes or silver plate. The silver wire was flattened by compression between stainless steel plates. The silver wire was roughened using an oxidation-reduction cycle (ORC) carried out in 0.1 mole L⁻¹ potassium chloride (KCl) electrolyte solution. The electrolyte solution was prepared daily and degassed with UHP nitrogen gas for 30 minutes prior to the ORC. The potential was ramped in two steps -0.4 to +0.25 V back to -0.4 V. The scan rate was 50 mVs⁻¹. Samples were dropped onto the roughened silver electrode using a micro-pipette and evaporated under a stream of UHP nitrogen gas.

7.2.4 Preparation of Silver Plate

The silver plate was prepared using a cleaning and chemical roughening procedure involving an initial cleaning with an emory cloth (grit 600b), followed by alternating RO water and 12 mole L⁻¹ hydrochloric acid rinse until the Raman spectra of the plate showed no features. The plate was prepared for the addition of a sample by applying a 6 mmole L⁻¹ solution of sodium borohydride in an electrolyte concentration of 1 mmole L⁻¹ of KCl. The Ag plate was

dried with UHP nitrogen gas. The target sample, in this case SRHA, SRFA or monomer compounds, in 1 mM KCl at pH 10 was applied to the Ag plate and dried with UHP nitrogen gas. The sample was rinsed off the silver plate with 6 mole L⁻¹ hydrochloric acid and re-dried with UHP nitrogen gas in order to ensure a thin film of material was present on the silver plate for subsequent spectra accumulation.

7.3 Results and Discussion

7.3.1 Oxidation-Reduction Cycle

Nano-features facilitate SERS spectra. The nano-features were produced using an oxidation-reduction cycle in the presence of chloride ions. Fig. 7.1 shows the development of the nano-features in the anodic or oxidative half of the cycle. Cyclic voltammetry uses a three electrode system using a reference electrode, a counter electrode and a working electrode. The working electrode is scanned in a triangular wave from -0.4 V to 0.3 V and back. The anodic current is the peak that has positive current with maxima 2.2 e^{-3} .

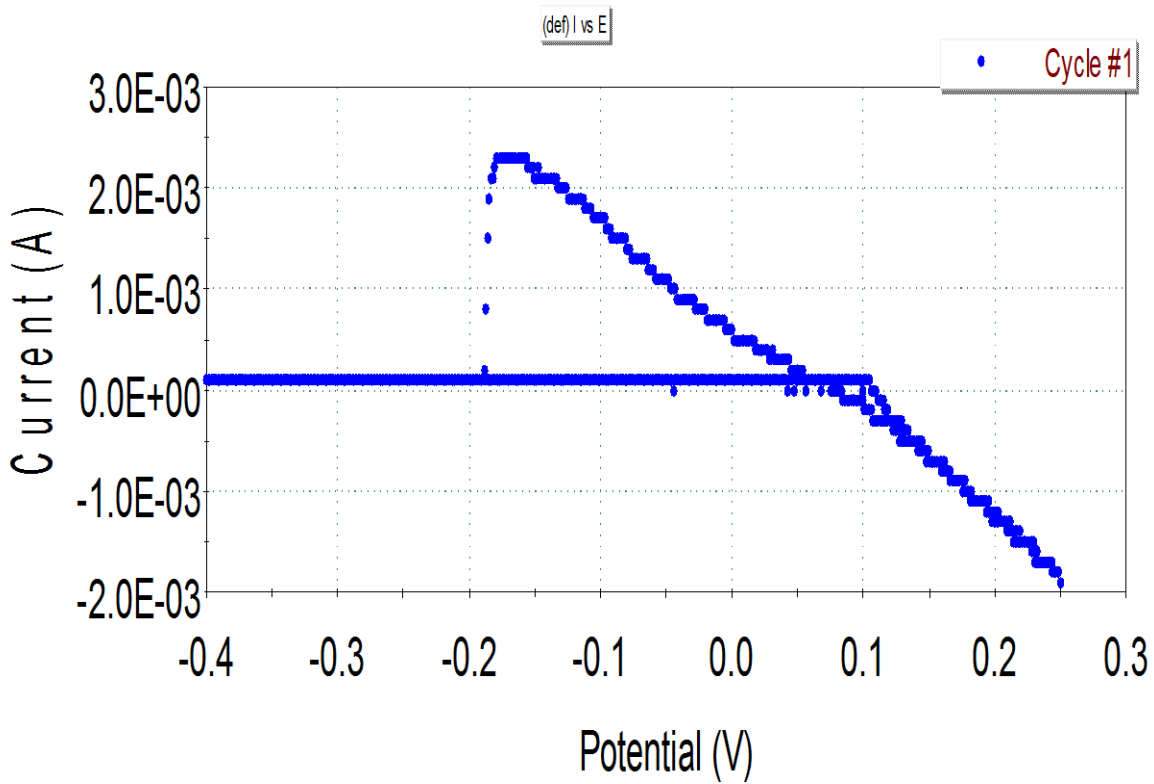


Figure 7.1 Oxidation-Reduction cycle from the potentiostat presented as current (A) as a function of potential (V) shows the development of nanostructures

7.3.2 Calibration of the silver electrodes and plate

Pyridine and crystal violet were used to calibrate the roughed silver electrodes and plate. Experimental results were compared to literature and theoretical results (Jeanmarie and Van Duyne (1977a)), (Willems and Van Duyne (2007)), (Johansson (2005)).

7.3.2.1 SERS Spectra of Pyridine

Pyridine has been observed to produce intense spectra when associated in a thin film with coinage metals including silver for over 40 years (Fleischmann, Hendra and McQuillan (1974)), (Albrecht and Creighton (1977)). Pyridine (C_5H_5N) has C_{2v} symmetry that produces a strong Raman signal that is intensified by surface enhanced Raman phenomena including (1) local electromagnetic field enhanced and (2) chemical enhancement mechanism including excitation of absorbate localized electronic resonances and metal-to-absorbate charge transfer, as shown in Fig. 7.2 and Table 7.1 (Stiles, Dieringer, Shah and Van Duyne (2008)), (Willems and Van Duyne (2007)), (Jeanmarie and Van Duyne (1977b)). Figure 7.2 is the SERS spectra of anhydrous pyridine on silver plate. Table 7.1 includes experimental SERS spectra of pyridine from silver plate and the roughened silver electrodes. A comparison of the experimental results with Jeanmarie and Van Duyne, 1977 data shows consistency in the fundamental symmetry groups. The percent difference between individual fundamental frequency groups ranges from 0.2 to 6 % (Table 7.1). Theoretical pyridine fundamental frequencies are also presented and are consistent with the theoretical results from both silver plate and silver electrodes.

Pyridine anhydrous on Ag Plate (Cleaned with 0.5 M HCl)

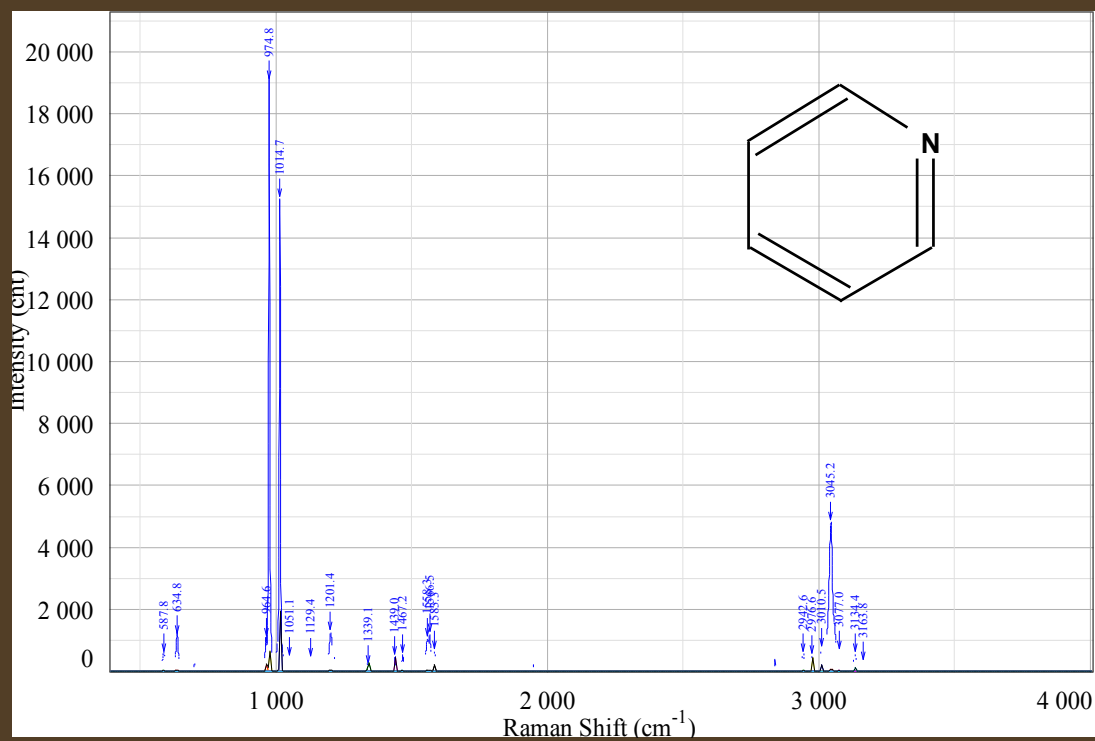


Figure 7.2 SERS spectra of pyridine on silver plate

Table 7.1 Experimental, historical and theoretical symmetry (C_2V) of pyridine from SERS spectra. a1, b1 and B1 are symmetry point groups.

C_2V Symmetry	Heighton Ag plate (-0.4V)	Heighton Ag wire (-0.4V)	Jeanmarie (1977) (-0.2V)	Jeanmarie (1977) (-0.6V)	Johansson J.Phys Chem (2005) calc. <i>ab</i> <i>initio</i> Ag+-Pyr	* Δ %
a1	583	589	623	623	615(589)	6
b1	628	634	651	651	697	4
a1	972	975	1008	1006	985 (973)	4
a1	1011	1014	1036	1035	1014	2
a1	1050		1068	1066	1047	2
b1	1129	1130	1153	1155	1115	2
a1	1197	1191	1214	1215	1198	1
a1	1462	1465	1489	1482	1478	2
B1	1550	1554	1571	1570		1
a1	3043	3041	3067	3056		0.2

* Δ Percent difference between Heighton ACS grade pyridine and Jeanmarie and Van Duyne, 1977, 0.2V pyridine

7.3.2.2 SERS Spectra of Crystal Violet

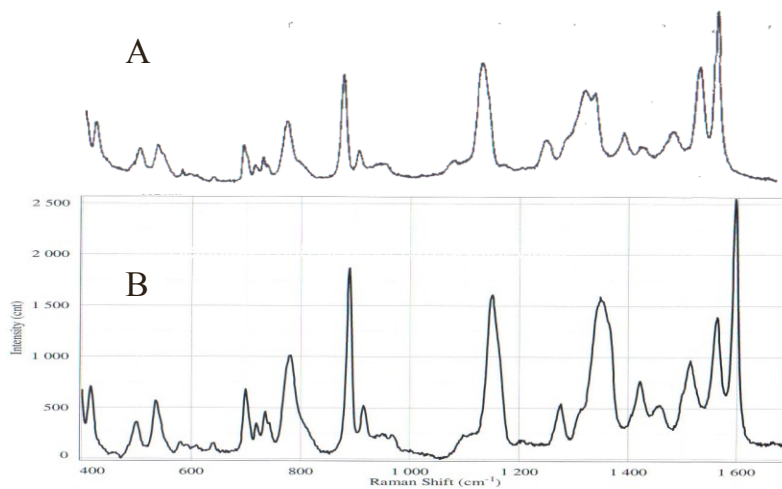
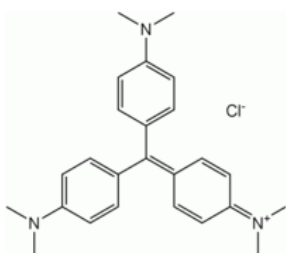
Crystal violet is an organic dye that has multiple Raman active modes making it a valuable SERS standard with an accessible history of spectra. The experimental Raman spectra presented in Fig. 7.3, panel B closely matches the literature spectra (Fig. 7.3, panel A) (Jeanmarie and Van Duyne (1977b)).

SERS spectra of crystal violet standard on roughened Ag electrode

Jeanmarie and Van Dyne, 1977 (trace amount) (A)

Heighton, 2008 (2.85 mM aqueous) (B)

$C_{25}H_{30}ClN_3$



Methanaminium, N-(4-(bis(4-(dimethylamino)phenyl)methylene)-2,5-cyclohexadien-1-ylidene)-N-methyl-, chloride

Figure 7.3 Crystal Violet SERS spectra on silver roughened electrode

7.3.3 SERS Spectra of Terrestrially Sourced Monomer Compounds

7.3.3.1 Quinones

Surface enhanced Raman spectra (SERS) were collected on roughened silver plate. The following quinones and their structures are presented in Fig. 7.4: 2,6-dimethyl-1,4-benzoquinone (light blue line); 2,5-dihydroxy-1,4-benzoquinone (red line); tetra-hydroxy-1,4-benzoquinone (black line); methyl-1,4-benzoquinone (orange line); 3,5-di-tert-butyl-1,2-benzoquinone (brown line); 2,3-dimethoxy-5-methyl-p-benzoquinone (green line); and 1,4-benzodiol (hydroquinone) (dark blue line); and duroquinone (pink line). Spectra were collected using a helium neon laser (633 nm) from 100- 2000 Cm^{-1} .

All of the untreated quinones studied exhibit medium to strong surface enhanced Raman spectral peaks between 1570 - 1670 cm^{-1} (Fig. 7.4). Wavenumbers in this region are characteristic of quinone carbonyl group $\text{C}=\text{O}$ stretching vibrations, as well as $\text{C}=\text{C}$ aromatic stretching vibrations. The spectra of 1, 4-benzodiol (hydroquinone) (blue line) exhibits different absorbance bands than do quinones in Fig. 7.4. The double peak centered at 800 cm^{-1} is consistent with an (OH) deformation combined with a (C-O) stretch. A small peak in the same frequency range is observed for 2,5-dihydroxy-1,4-benzoquinone (red line) and hydroxy-p-quinone (black line). The 1,4-benzodiol (hydroquinone) (dark blue line) exhibits a peak at 1350 that is consistent with in plane OH deformation. Peaks between 400 and 500 cm^{-1} can be attributed to ring C-C-C planar deformations. Methyl-1,4-benzoquinone (orange line) has an Raman shift at 1360 cm^{-1} that can be attributed to the methyl group. Weak peaks centered at 1443 cm^{-1} from the spectra of 3,5 di-tert-butyl-1,2-benzoquinone (brown line), duroquinone (pink line) and 2,6-dimethyl-1,4-benzoquinone (light blue line) are likely related to methyl CH

groups associated with a quinone ring. The quinone containing methoxy groups (-OCH₃) (green line) exhibit weak peaks between 1185 to 1200 cm⁻¹ and between 1435 to 1470 cm⁻¹. The second distribution of methoxy Raman shifts overlaps with the shifts attributed to methyl groups attached to a ring structure (Socrates (2001)).

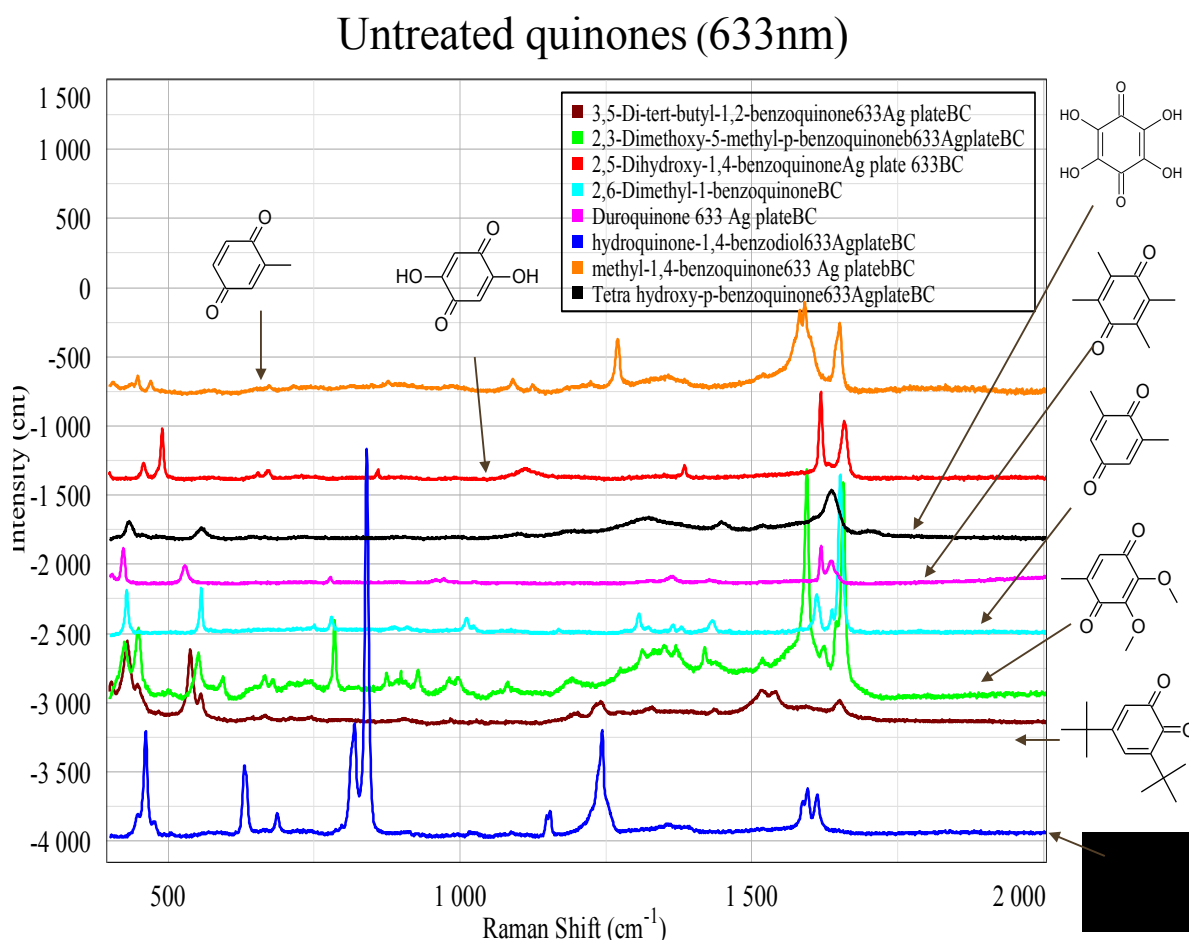


Figure 7.4 SERS spectra of selected untreated quinones

7.3.3.2 Lignin Phenols

Surface enhanced Raman spectra (SERS) were collected on roughened silver plate. The following lignin phenols and their structures are presented in Fig. 7.5: vanillic acid (purple line), acetovanillone (pink line), syringic acid (brown line), syringaldehyde (light blue line), acetosyrinone (red line), p-hydroxy cinnamic acid (green line) and, ferulic acid (dark blue line). Spectra were collected using a helium neon laser (633 nm) from 100- 2000 Cm^{-1} .

The SERS spectra of untreated lignin phenols (Fig.7.5) exhibit peaks between 1550 to 1650 cm^{-1} consistent, with the presence of C=C and C=O stretching vibrations. The highest energy C=O peak from the spectra of syringic acid (brown line) has a carboxylic group associated with a ring. This is consistent with the energy of the Raman shifts expected from the structures associated with each compound. It would be expected that ferulic acid (dark blue line) would also exhibit similar peaks but this compound produces a relatively weaker spectra possibly due symmetry considerations. The selected lignin phenol spectra also show numerous peaks in the regions 1185 to 1200 cm^{-1} and between 1435 to 1470 cm^{-1} consistent, with methyl groups on a aromatic ring and methoxy group Raman shifts (Socrates (2001)).

Untreated lignin phenols

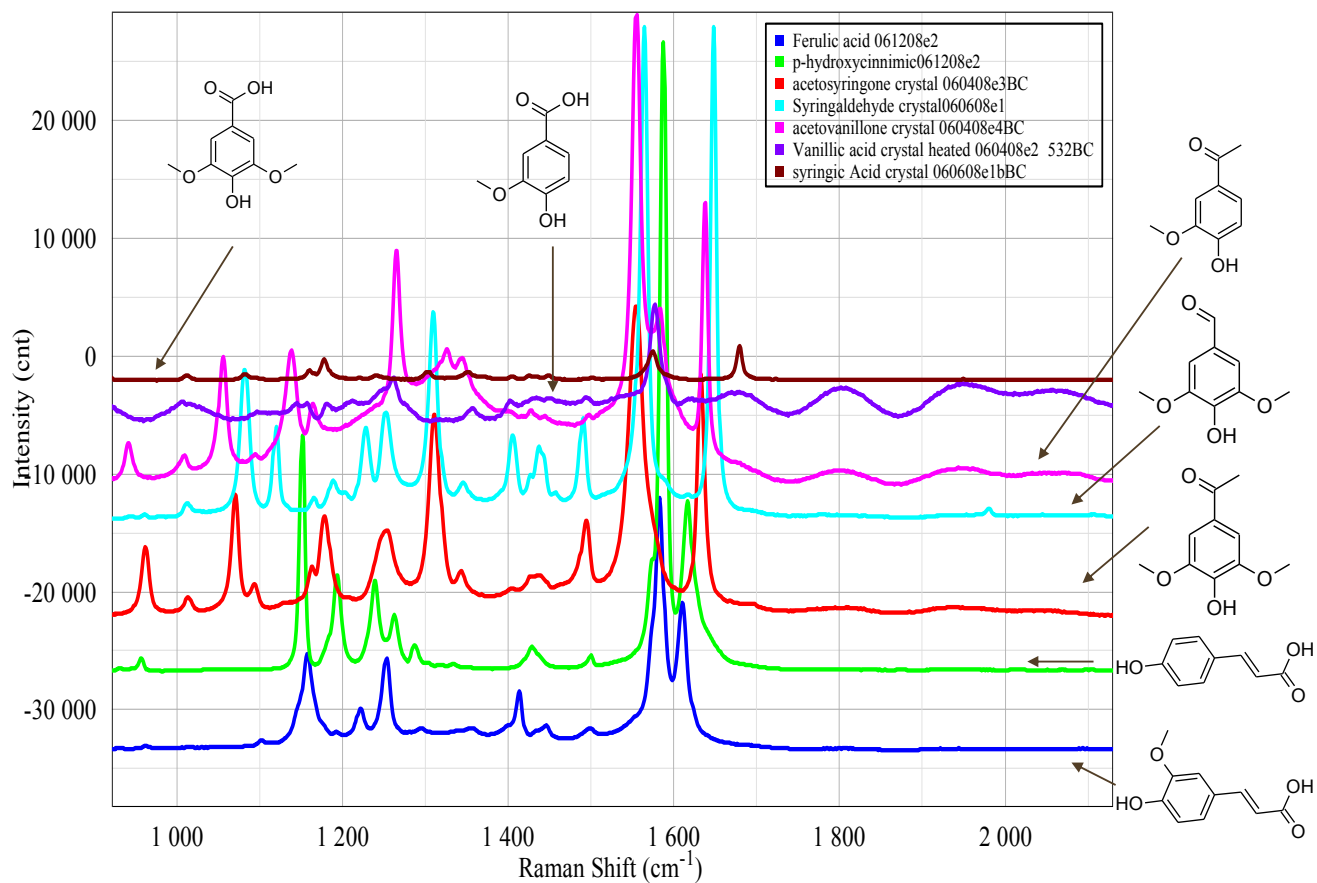


Figure 7.5 SERS spectra of selected untreated lignin phenols

7.3.4 SERS spectra of Suwannee River humic acids

A comparison between borohydride reduced methyl benzoquinone and borohydride reduced Suwannee River humic acid is shown in Fig. 7.6. There are clear similarities in the carbonyl region between 1500 and 1650 cm^{-1} . The borohydride induced reduction and broadening of the Raman peak associated with the C=O stretch at 1630 cm^{-1} corresponds to the emergence of a phenolic –OH deformation vibration and C-O stretch combination at 1430 cm^{-1} . The C=C stretch remains but is weaker and red shifted by 30 cm^{-1} in the borohydride reduced methyl benzoquinone spectra. The borohydride reduced SRHA spectra is complicated and cannot be definitively interpreted. Future work should involve borohydride reduction and collection of Raman spectra of the model compounds presented in this paper, as well as nitrogen containing model compounds identified in Chapters 2 and 3.

The SERS spectra of borohydride reduced SRHA are shown in Figs. 7.7 and 7.8. The spectra have been enlarged and divided into two figures for clarity. Carboxylic acids and esters have Raman spectral peaks that occur between 1700 and 1900 cm^{-1} . Raman peaks in this region don't occur in borohydride reduced humic acid and are not presented. There is a significant difference between the model compounds and the borohydride reduced Raman peaks in that the borohydride reduced SRHA, is more complicated than the unreduced model compounds. To proceed further in the interpretation of SERS Raman spectra of CDOM and humic substances, reductions of both model compounds and additional humic substances would have to be undertaken.

Surface enhanced Raman spectra of borohydride reduced SRFA and p-methyl benzoquinone

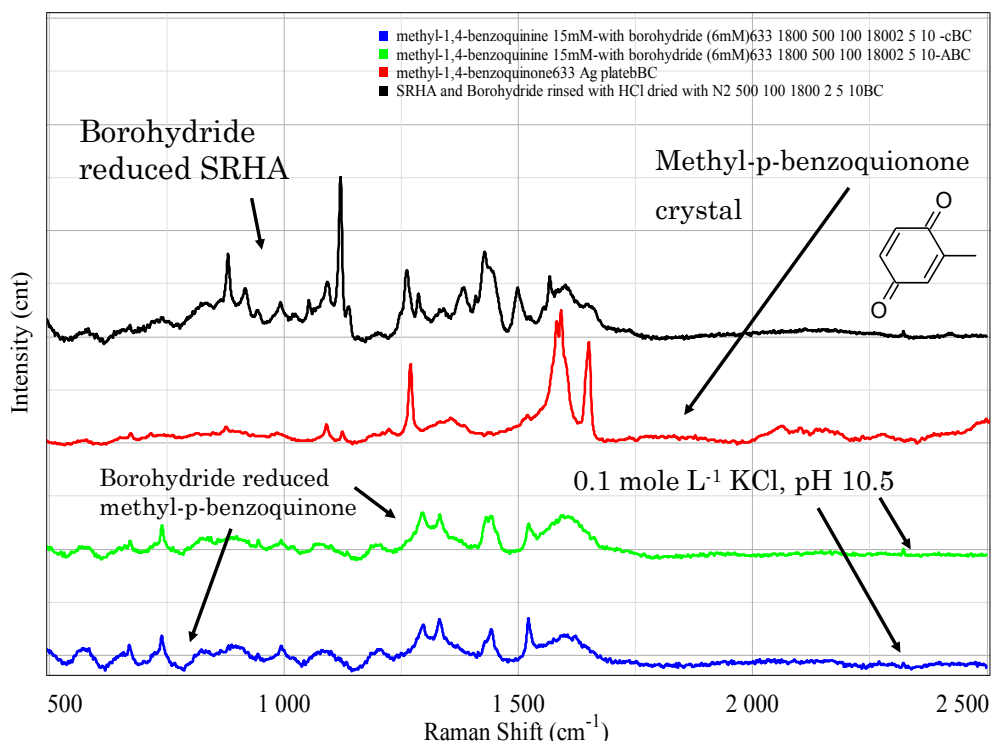


Figure 7.6 SERS spectra of borohydride reduced SRFA and p-methyl benzoquinone

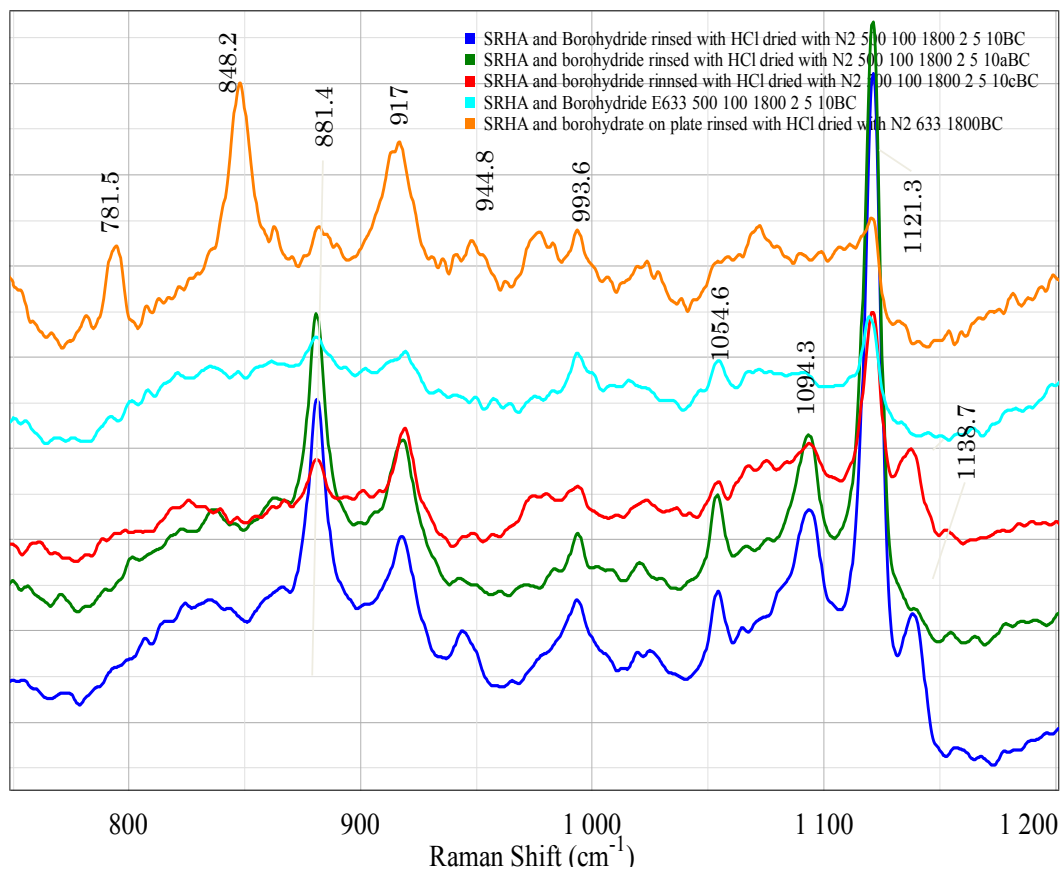


Figure 7.7 SERS spectra of borohydride reduced SRHA from 750 – 1200 cm^{-1}

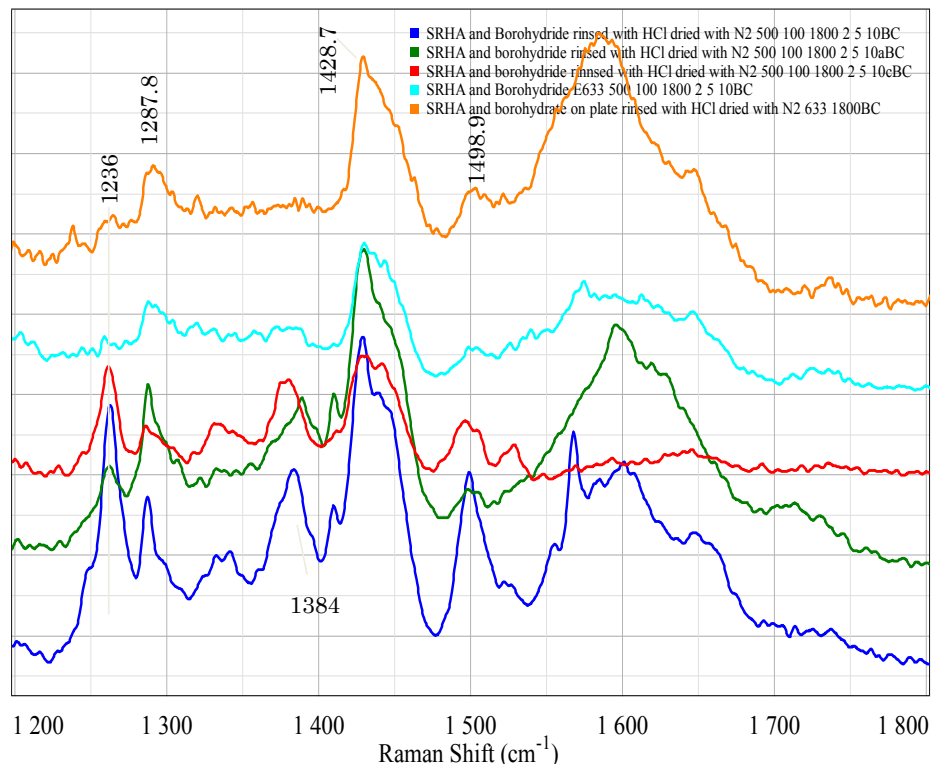


Figure 7.8 SERS spectra of borohydride reduced SRHA from 1200 – 1800 cm⁻¹

7.4 Conclusions and Future Work

Borohydride reduction of the humic acid SRHA yield surface enhanced Raman spectra while unreduced SRHA is swamped by fluorescence background (not shown). Despite the progress made in generating background free spectra of HS, significant questions remain in the context of generating and interpreting SERS spectra of CDOM and HS. The generation of spectra has several procedural issues, namely, are the large humic molecules oriented consistently to the surface of the coinage metal? Is the molecule in close enough proximity to the coinage metal and in a thin enough film so that the proximity rule is not violated (Equation 7.1). These questions may be addressed by carefully and sequentially reducing humic material while simultaneously assuring that an absorbance spectrum at long wavelengths is eliminated. This would ensure that all electronic interactions are eliminated and produce Raman spectra wholly dependent on CDOM/HS precursor material. Examination of the consistency between fully reduced materials with partially reduced material may help address this problem and provide some assurance that spectra can be generated in a reproducible fashion. This step once achieved will allow for confident comparison of different HS samples.

Interpretation of Raman spectra from Figs. 7.6, 7.7 and 7.8 is consistent with the presence of lignin phenols and quinones, but these are not the only possible interpretation of the spectra. Heterogenic aromatic compounds containing nitrogen or sulfur may also be present and have Raman spectral peaks in the similar ranges as lignin phenols and quinones. Additional compounds should be examined and should include nitrogen containing species. Further the lignin phenols and quinones with the exception of methyl-p-quinone, were not borohydride reduced. The SERS spectra of reduced lignin phenols and quinones may aide in the interpretation of SERS spectra of humic materials.

The Raman shifts between 1500-1650 cm^{-1} reflecting C=C and C=O stretching vibrations of borohydride reduced SRHA more closely resemble borohydride reduced methyl-p-benzoquinone than they do the untreated methyl-p-benzoquinone. Borohydride reduction of other potential model compounds may aid in the spectral interpretation of what is assuredly a complicated structure. In light of the complexity of SRHA it might provide insight into the progression of humic material from terrestrial to aquatic systems to borohydride reduce soil derived humic material or lignin samples.

8 Conclusions and Future Work

Borohydride reduction increases the spectra slope (S) of the terrestrial, aquatic and microbial humic and fulvic acids, examined regardless of the concentration of the reduced sample with the exception of Pony Lake fulvic acid (PLFA). Borohydride reduction of the target groups; phenols, quinones and aromatic ketones disrupts electronic interactions, increasing the spectral slope due to the components of the electronic interactions no longer being quenched. Pony Lake fulvic acid may contain a higher relative amount of quinones than other sources of fulvic acid as indicated by oxygen derived recovery at short (< 320 nm) wavelengths. Long wavelength absorbance recovery is not observed for any of the humic or fulvic acids in the study including PLFA possibly implicating non-recoverable disruption of the macro structure upon borohydride reduction. Non-recoverable disruption of the macro structure is also evident at high ionic strength (1.00 mole L⁻¹ as NaCl). The baseline of the extended wavelength tail increases generating negative valued difference spectral values (S) at high ionic strength. The samples with the exception of untreated Leonardite humic acid (LHA) do not physically precipitate out of solution but the absorption base line at low pH begins to gain in absorbance. This does not happen at the lower level ionic strengths (0.01 and 0.10 mole L⁻¹).

The spectral slope (S) is also affected by changes in pH. Deprotonation of the NICA-Donnan identified phenolic group disrupts the electronic interactions proposed to explain the long wavelength characteristics of chromophoric dissolved organic matter (CDOM) and the humic/fulvic acids used to model optical behavior of CDOM. Donor/acceptor functional groups in electronic interactions extend optical absorbance into the visible range of the absorbance spectra. Titration of model humic and fulvic acid changes the spectral slope (S) values of

untreated and borohydride reduced humic and fulvic materials, with the exception of borohydride reduced PLFA. PLFA may be using secondary amines, heterocyclic compounds or some as yet unidentified species as electronic interaction donors and very likely quinones as the acceptor moiety. PLFA may be alone in its dependence of quinones in generating electronic interaction long wavelength extended absorbance. Quinones do not appear to be an important contributor to long wavelength absorbance compared to other participating moieties such as aromatic ketones in terrestrially derived aquatic humic and fulvic acids, as well as in soil derived humic acids.

Evidence such as spectral slope data, difference plots, optical titrations, first derivative plots and fluorescence emission data support a hierarchy of digenesis for terrestrially sourced materials. Leonardite (LHA) and Elliot (EHA) humic acids likely have a greater diversity of functional groups some of which overlay the long wavelength absorption tail generated by electronic interactions. These extra chromophores may be related to stacked black carbon or some as yet unidentified moieties. The spectral slope values are more gradual (lower spectral slope value (S)) than the aquatic spectral slope values (higher spectral slope value (S)). This may correspond to photobleaching or other physical or chemical process as soil derived HS are exported to water ways and concurrently loose associated or labile chromophores that overlay the absorption spectra but do not participate in the electronic interactions or participate in a limited way as they are eliminated between points of generation (soil HA vs. aquatic HA). Aquatic, terrestrially derived moieties represent the recalcitrant back bone of the soil derived humic acids.

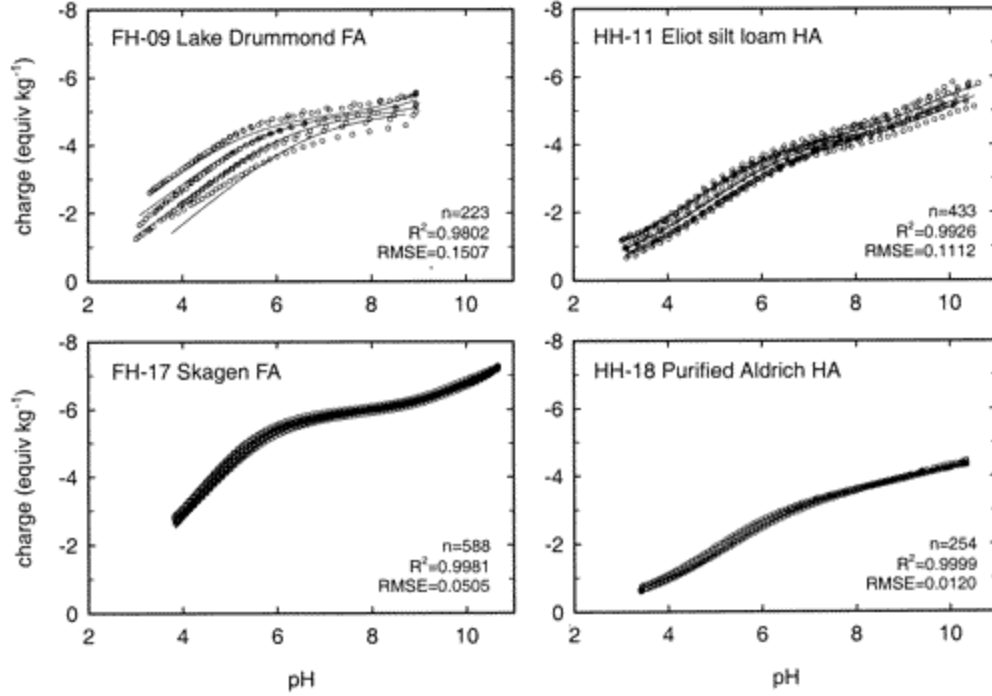
Absorbance and fluorescence spectra can generate tangential information about the structural underpinnings generating the unique optical properties associated with CDOM/HS, but

upon complete borohydride reduction terrestrially generated CDOM/HS should produce monomer compounds providing primary information about the chemical species able to produce extended long wavelength absorbance and the characteristic fluorescence excitation emission matrix spectra (EEMS) (Chapters 1 and 5). Further pursuit of standard methodologies for the generation of SERS spectra, including expanding the monomer species to nitrogen containing compounds and finding a chemical probe that works on nitrogen containing compounds would positively impact this work.

The Raman experiments detailed in Chapter 7, although preliminary hold the potential to identify monomer compounds explicitly. Identification of monomer compounds could proceed, if borohydride reduction is able to eliminate the charge transfer bands responsible for the long wavelength absorbance associated with HS/CDOM. Experimental variables, such as getting consistently thin films on the coinage metal, must be explored before SERS can be confidently applied to the analysis of HS/CDOM in the environment.

Appendix 1 NICA-Donnan Model

The NICA-Donnan Model uses a mono-protic acid to titrated HS, DOM or CDOM from pH 3 to pH 11 at multiple ionic strengths in order to fit the ionic strength replicates onto a master curve. The master curve provides generic NICA-Donnan terms b and Q . The b term is an adjustable parameter that depends on the identity of the HS and the ionic strength (mole L^{-1}) and Q is the maximum pH value of a distribution of chemical species. The master curve and the titrations that generate it are plotted as negative acid equivalence per mass of substance titrated as a function of pH. Figure A1 is an example from of two fulvic acids and two humic acids that that have been modeled using the NICA-Donnan model (Milne, Kinniburgh and Tipping (2001))



A1.1 NICA-Donnan model fits to representative datasets, showing the worst (top) and one of the best (bottom) model fits to the data for each of fulvic (left) and humic (right) acids. Symbols show observed data; continuous lines show the model fits. (Milne, Kinniburgh and Tipping (2001)).

The non-ideal competitive absorption model (NICA) has its basis in the Hill equation

A1.1 which describes cooperative affinity binding of species i on a homogeneous substrate:

$$\Theta_{i,L} = \frac{(K_i c_i)^{n_i}}{1 + (K_i c_i)^{n_i}}, \tag{A1.1}$$

where $\Theta_{i,L}$ is the fraction of reference sites occupied by species i , L is local binding sites with equal affinity, K_i is the intrinsic affinity or chemical affinity of species i for the reference sites, c_i is the concentration or activity of i in solution and n_i is the stoichiometry of the binding sites.

The Hill equation was originally developed in the early 1900's to describe oxygen binding to hemoglobin. It is most often used to describe the number of ligands needed to bind to receptor to produce a physical effect. It is only physically accurate under the condition of one ligand and one receptor or in a case of extreme cooperation. In other words the first ligand must bind to a much lesser degree than subsequent ligands for the generated Hill coefficient to reflect physical accuracy. A physical example of the Hill coefficient is the case of oxygen binding with hemoglobin. In order for the Hill equation to generate the correct number of ligands (oxygen molecules) binding to hemoglobin each of the four oxygen molecules must simultaneously bind, which is physically unlikely (Weiss (1997)). Although the Hill equation is too simplistic to accurately describe all but the most extreme cases, it can be modified and serves as a good starting point for derivation of the NICA model (Koopal, Saito, Pinheiro and Riemsdijk (2005)), (Koopal, van Riemsdijk and Kinniburgh (2001)).

The Hill equation can be easily modified to describe competitive binding of species i by allowing $i = 1 \dots j$). The local site or the environment is the solution immediately adjacent to the binding site as opposed to the bulk properties of the solution. The local binding site is designated (L) and as it is participating in the competitive binding must have equal energy for each species i (1- j). The modified Hill equation for competitive binding is Equation A1.2.

$$\Theta_{i,L} = \frac{(K_i c_i)^{n_i}}{1 + \sum (K_i c_i)^{n_i}} \quad (A1.2)$$

Equation A1.2 can be rewritten as Equation A1.3.

$$\Theta_{i,L} = \frac{(K_i c_i)^{n_i}}{\sum_i (K_i c_i)^{n_i}} \cdot \frac{\sum_i (K_i c_i)^{n_i}}{1 + \sum_i (K_i c_i)^{n_i}}, \quad (\text{A1.3})$$

where the first term on the right hand side of the equation is the fraction of sights bound with species i and the second term describes the total number of reference sites, occupied by any ionic species. If you consider that Q_i is the participating number of reference sites it is related to the total number or density of reference sites (Q_{\max}) by the relationship in equation A1.4

$$Q_i = n_i \Theta_{i,L} Q_{\max}, \quad (\text{A1.4})$$

where n_i is the molecules of i , L indicates a localized solution near the binding site as opposed to the bulk solution and Θ is the fraction of reference sites occupied by i .

Equation A1.2 gives the competitive binding of the binding species i to a homogeneous substrate. Each component i has two parameters associated with the modified Hill equation A1.2, namely the intrinsic affinity K_i and a stoichiometric factor n_i . In order to extend the Hill equation to heterogeneous substrates, Equation A1.3 representing the local isotherm in an integral binding equation is combined with a generic affinity distribution. The generic affinity distribution confers to both metals and protons the same distribution shape, but moves different species on the intrinsic or chemical affinity axis. The following integral binding equation is the NICA Equation A1.5

$$\Theta_{i,t} = \frac{(K_i c_i)^{n_i}}{\sum_i (K_i c_i)^{n_i}} \cdot \frac{\{\sum_i (K_i c_i)^{n_i}\}^p}{1 + \{\sum_i (K_i c_i)^{n_i}\}^p}, \quad (\text{A1.5})$$

where $\theta_{i,t}$ is the fraction of all sites occupied by species i , K_i is the median value of the affinity distribution of species i , specific to each individual species, and p is the generic or one size fits all width of the affinity distribution.

Now the total amount of bound component i is $Q_{i,t}$ is represented in equation A1.6.

$$Q_{i,t} = n_i \Theta_{i,t} Q_{\max,t}, \quad (\text{A1.6})$$

where $Q_{i,t}$ is the total amount of a species i bound to the heterogeneous substrate, $Q_{\max,t}$ is the density of the reference sites, n_i is the number of molecules of i bound to each reference site or the stoichiometric term. The term $Q_{\max,t}$ must be determined independently for each species of i (1- j). The binding of protons is used to determine the density of the binding sites $Q_{\max,t}$, which can be designated as $Q_{\max,H}$. Equation A1.7 can now be normalized to the concentration of protons (H):

$$Q_{i,t} = (n_i/n_H) \Theta_{i,t} Q_{\max,H}, \quad (\text{A1.7})$$

The NICA model addresses two areas of complexity inherent in HS. The first is site heterogeneity and the second is stoichiometry of the binding sites (Kinniburgh, Milne, Benedetti, Pinheiro, Filius, Koopal and Van Riemsdijk (1996)), (Koopal, van Riemsdijk and Kinniburgh (2001)), (Milne, Kinniburgh, Van Riemsdijk and Tipping (2003)). Based on proton binding curves, it has been observed that humic substances represented as humic and fulvic acid exhibit two binding sites or a bimodal distribution with peaks centered at pKa of about 3 and the second broader distribution centered between pH 8-10. The peaks have been associated with carboxylic sites and phenolic sites, respectively (Christensen, Tipping, Kinniburgh, and Christensen (1998)), (Koopal, van Riemsdijk and Kinniburgh (2001)), (Milne, Kinniburgh and Tipping (2001)). Using a bimodal treatment the NICA model for proton binding can be expressed as a summation of two binding sites in Equation A1.8.

$$Q_H = Q_{\max1,H} \cdot \frac{(K_{H1}[H_s])^{p1}}{1 + (K_{H1}[H_s])^{p1}} + Q_{\max2,H} \cdot \frac{(K_{H2}[H_s])^{p2}}{1 + (K_{H2}[H_s])^{p2}}, \quad (\text{A1.8})$$

where the p_1 and p_2 and the widths of the respective distributions, Q_{\max} is the total amount of binding sites within each distribution, p is the width of the distribution, K is median value of the affinity distribution for in this case only protons, $[H_s]$ is the concentration of protons at the HS surface of each binding site. If the NICA model was extended to include competing ions, for each additional ion four terms would have to be considered K_{i1} , K_{i2} , n_{i1} and n_{i2} . These four terms are in addition to the four terms generated from the proton binding $Q_{\max1}$, $Q_{\max2}$ (mol kg^{-1}) and p_1 and p_2 that are characteristic of each HS (Milne, Kinniburgh, Van Riemsdijk and Tipping (2003)).

A third point of complexity in the system is electrostatic interactions. If the HS is viewed or modeled as colloid with a distribution of functional groups that can be deprotonated, then as the pH goes up so does the charge on the colloidal particle. The negatively charged particles are neutralized by positively charged counter ions at the binding sites so that the bulk solution has a neutral charge but local binding sites have variable negative charge. The size, shape, charge and interactivity of functional groups as they are titrated (protonated/deprotonated) governs the electrostatic interactions. Clearly, the electrostatics of HS is as complex as the heterogeneity found in and between the HS and not easily described. These electrostatic interactions are addressed by combining the NICA model with a sub-model the Donnan model. Separating the electrostatic affinity from the intrinsic or chemical affinity that a species i (proton or cation) experiences near the binding site allows for modeling of only the chemical affinity near the binding site. This concentration of the binding species differs from the combined electrostatic and chemical affinity in the bulk solution by a Boltzmann factor, presented in Equation A1.9 (Koopal, Saito, Pinheiro and Riemsdijk (2005)), (Koopal, van Riemsdijk and Kinniburgh (2001)), (De Wit, van Riemsdijk and Koopal (1993)).

$$a_{i, LOC} = a_{i, bulk} \exp(-z_i F \Psi_{loc} / RT), \quad (A1.9)$$

where $a_{i, LOC}$ is the concentration or ion activity at the local binding site, $a_{i, bulk}$ is the concentration or ion activity in the bulk solution, z_i is the valence of the particle i , Ψ_{loc} is the characteristic electrostatic potential at the location of the binding sites, F is the Faraday constant, R is the ideal gas constant, T is the absolute temperature.

Several simplifying assumptions must be made in regard to the size, shape conformation of the HS in the Donnan sub model in order include it in the calculation. If a humic substance is considered to be colloidal than the generalization can be made that it has a uniform electrical double layer, allowing for the calculation of the electrostatic potential (Ψ_s) as a single term by use of the Boltzmann distribution (De Wit, van Riemsdijk and Koopal (1993a)). Inherent in the double layer model are two differing physical representations HS, ion penetrable sphere or ion impenetrable sphere. The penetrable sphere is the Donnan gel family of models and the impenetrable sphere describes a family of models called the surface charge model (Koopal, van Riemsdijk and Kinniburgh (2001)), (Koopal, Saito, Pinheiro and Riemsdijk (2005)). The surface charge models assume all charge is at the surface of the particle in a uniform distribution. The Donnan gel family of models accounts for the charge over the entire volume of the sphere. Both physical representations require consideration of pH and ionic strength to arrive at particle size. Experimentally, pH and/or ionic strength have not always been considered in arriving at a volume. Nonetheless both physical representations have been used successfully to model HS (Avena, Koopal and van Riemsdijk (1999)), (Benedetti, Milne, Kinniburgh, Van Riemsdijk and Koopal (1995)), (de Wit, van Riemsdijk and Koopal (1993a)), (de Wit, van Riemsdijk and Koopal (1993b)), (Nederlof, De Wit, Van Riemsdijk and Kopal (1993)), (De Wit, Van Riemsdijk, Nederlof, Kinniburgh and Koopal (1990)). Because the electrostatic potential (Ψ_{loc}) is

dependent on the size, shape and charge on the particle and the counter ions contained in the electrostatic double layer and those values are unknown, an iterative parameter called the Donnan volume (V_D) that accounts for the size and shape are used to solve for in the electrostatic potential (Ψ_{loc}). This value can then be used to solve Equation A1.9 for the local activity of i at the binding site. An equation for charge neutrality is as follows in Equation A1.10.

$$\frac{q}{V_D} + \sum_i z_i(a_{iD} - a_i) = 0 \quad , \quad (A1.10)$$

where $a_{iD} = a_i \exp(-z_i F \Psi_D / RT)$ is the activity of i in the Donnan Volume (V_D) in moles Liter⁻¹, and $\Psi_D = \Psi_{LOC}$ is the Donnan potential and q is the charge in moles kg⁻¹ or equivalents kg⁻¹ humic material. The equation is solvable for Ψ_D if the charge on the counter ion and bulk solution activities are known. An empirical relationship (equation A1.11) has been developed by (Benedetti, Milne, Kinniburgh, Van Riemsdijk and Koopal (1995)) and (Milne, Kinniburgh and Tipping (2001)) to describe V_D which is adjustable and accounts for the dependence of the relationship between ionic strength and the size of the double layer.

$$\log V_D = -1 + b(1 - \log I) \quad , \quad (A1.11)$$

where b is an adjustable parameter that depends on the HS and I is the ionic strength (mole L⁻¹). Milne, 2001 studied proton binding of 25 fulvic acids and 24 humic acids and found an empirical relationship given by Equation A1.11. The best b parameter for FA was 0.6 and the best b parameter for HA 0.5 (Milne, Kinniburgh and Tipping (2001)). The concentration of the ionic strength governs the degree to which the double layer extends into the bulk solution. A large ionic strength has a small double layer, while a small ionic strength has a double layer that extends well out into the bulk solution. Milne, 2001 gives an example of a large Donnan volume of 80 L kg⁻¹ at an ionic strength of 0.001 mole L⁻¹ corresponding to a b value of 0.7, while a

Donnan volume of 1 L kg^{-1} at an ionic strength of $0.001 \text{ mole L}^{-1}$ has a b value of 0.25. The b value like the Q value (number of binding sites at an identified pH distribution) is a function of the HS titrated (Milne, Kinniburgh and Tipping (2001)). These data were fitted to the NICA-Donnan model using a non-linear least squares optimization code (Milne, Kinniburgh and Tipping (2001)).

In practice a master curve is generated by using the electrostatic model described in Equation A.1.9. If the model is a valid description of the electrostatics of the HS in question then a graph of the charge in moles kg^{-1} or equivalents kg^{-1} humic material ($-q$) versus pH near the functional site (pH_{loc}) will yield a single merged master curve from a sequential series of solutions of increasing ionic strength (de Wit, van Riemsdijk and Koopal (1993a)), (Koopal, Saito, Pinheiro and Riemsdijk (2005)). The value for q (charge in moles kg^{-1} or equivalents kg^{-1} humic material) is obtained from the pH titration, of a known amount of HS. In order to generate enough points for the titration a large amount of material is needed which precludes some natural marine sample that are difficult to obtain. A first derivative plot of the binding curve provides a semi-analytical distribution of the differential distribution of the binding populations (Koopal, Saito, Pinheiro and Riemsdijk (2005)). In humic and fulvic acids the distribution is well known to be bimodal and attributable to a suite of carboxylic acid groups and phenolic groups. Milne, 2001 summarized the optimal parameter values for the proton binding data for the NICA-Donnan model Q_{max1H} , Q_{max2H} , $\log K_{\text{H1}}$, $\log K_{\text{H2}}$, b , Q_{total} , $Q_1\%$ and $Q_2\%$ for 25 fulvic acids and 23 humic acids generating generic terms for humic and fulvic acids (see their table 4) (Milne, Kinniburgh and Tipping (2001)). From this data it can be concluded that humic and fulvic acids have different site densities and binding affinities but that they overall were very similar to each other and consistent with the other widely used model the Model VI or the Windermere Humic

Acid Model (WHAM). The generic proton terms, because they are based on physical principles, have been used with success to model other systems in soil and water matrixes (Koopal, Saito, Pinheiro and Riemsdijk (2005)).

Appendix 2 Supplementary Information for Chapter 6: Optical Titrations of Aquatic, Terrestrial and Microbial Humic Substances

Optical titrations and difference spectra for the high concentration (visual range absorbance, 350 to 820 nm) trials presented in Chapter 6 as potentiometric titrations are presented here as supplemental information. Figures A2.1 through A2.16 encompass the humic and fulvic acids titrated in the study, both untreated and borohydride reduced and ionic strength of 0.01, 0.10 and 1.00 mole L⁻¹ as sodium chloride. The 0.01 mole L⁻¹ ionic strength treatments of SRFA and PLFA are presented in Chapter 6 as Figs. 6.18 and 6.19. Table A2.1 summarizes sample identification, treatment status (untreated or borohydride reduced), Appendix 1 Figure number, ionic strength, concentration (mg L⁻¹), and absorbance coefficient (a^* , pH 7.6, 350 nm).

Humic Acids SRHA and EHA at high ionic strength (1.00 mole L⁻¹) did not fall out of solution visually and were titrated to completion but their absorbance and difference spectra indicate structural changes occurred at low pH impacting the baseline. The humic acid LHA visibly formed precipitate and the titration was not completed over the entire pH range.

The fulvic acid PLFA, borohydride reduced, 1.00 mole L⁻¹ ionic strength treatment was titrated to completion but the matching absorbance and difference spectra indicate structural changes that were not apparent by visual inspection. The lower level ionic strength treatments of borohydride reduced PLFA both reflect a titratable isobestic point that decreases in absorbance at 480 nm at pH above 4.18. This is addressed in Chapter 6 using the lowest level ionic strength treatment of PLFA and compared to the SRFA 0.01 mole L⁻¹ ionic strength treatment.

Figures A2.17 through A2.22 exhibit the absorbance spectral points at each measured titration point as a function of pH for Suwannee River Humic Acid (SRHA), Suwannee River Fulvic Acid (SRFA), Elliott Humic Acid (EHA), Leonardite Humic Acid (LHA), Pony Lake

Fulvic Acid (PLFA) and Lignin Alkali Carboxylate (LAC). Each titration point represents 1.25 μmoles of titrant. The titration pH range is 3.00 to 11.00. The concentrations are in mole L^{-1} otherwise designated as N.

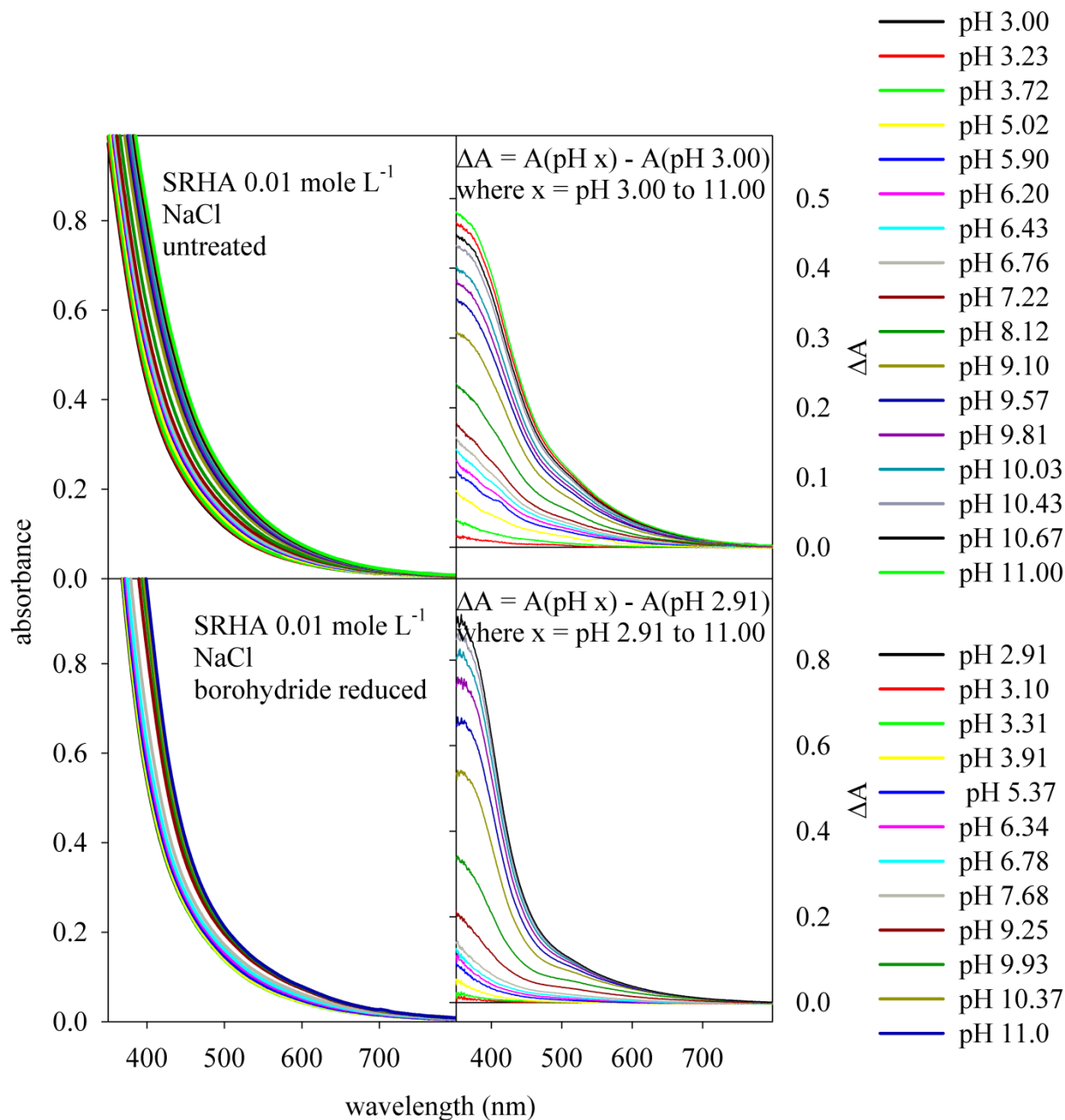
Table A2.1 Summary of High Concentration Visible Absorbance Range (350-800 nm) Figures Presented in Appendix 2

Sample Identification	Untreated or borohydride reduced	Figure Number	Ionic strength (N) as (NaCl)	Concentration mg L ⁻¹	<i>a</i> * (350nm, pH 7.6) untreated (conc.mg L ⁻¹) reduced (conc. mg L ⁻¹)
SRHA*	untreated	A2.1	0.01	100	7.94 (20 mg L ⁻¹) 4.55 (23mg L ⁻¹)
	reduced	A2.1	0.01	200	
	untreated	A2.2	0.10	100	
	reduced	A2.2	0.10	200	
	untreated	A2.3	1.00	100	
	reduced ^{&}	A2.3	1.00	200	
SRFA*	untreated	A2.4	0.10	100	3.38 (26mg L ⁻¹) 1.88 (23 mg L ⁻¹)
	reduced	A2.4	0.10	760	
	untreated	A2.5	1.00	100	
	reduced	A2.5	1.00	760	
EHA*	untreated	A2.6	0.01	50	8.87 (50 mg L ⁻¹) 5.50 (48 mg L ⁻¹)
	reduced	A2.6	0.01	48	
	untreated	A2.7	0.10	50	
	reduced	A2.7	0.10	48	
	untreated ^{&}	A2.8	1.00	50	
	reduced ^{&}	A2.8	1.00	48	
LHA*	untreated	A2.9	0.01	50	12.68 (13 mg L ⁻¹) 20.23 (12 mg L ⁻¹)
	reduced	A2.9	0.01	75	
	untreated	A2.10	0.10	50	
	reduced	A2.10	0.10	75	
	untreated [#]	A2.11	1.00	50	
	reduced [#]	A2.11	1.00	75	
PLFA*	untreated	A2.12	0.10	500	1.34 (75 mg L ⁻¹) 1.17 (30 mg L ⁻¹)
	reduced	A2.12	0.10	226	
	untreated	A2.13	1.00	500	
	reduced ^{&}	A2.13	1.00	226	
LAC*	untreated	A2.14	0.01	LAC was normalized to SRFA	
	reduced	A2.14	0.01		
	untreated	A2.15	0.10		
	reduced	A2.15	0.10		
	untreated	A2.16	1.00		
	reduce ^{&}	A2.16	1.00		

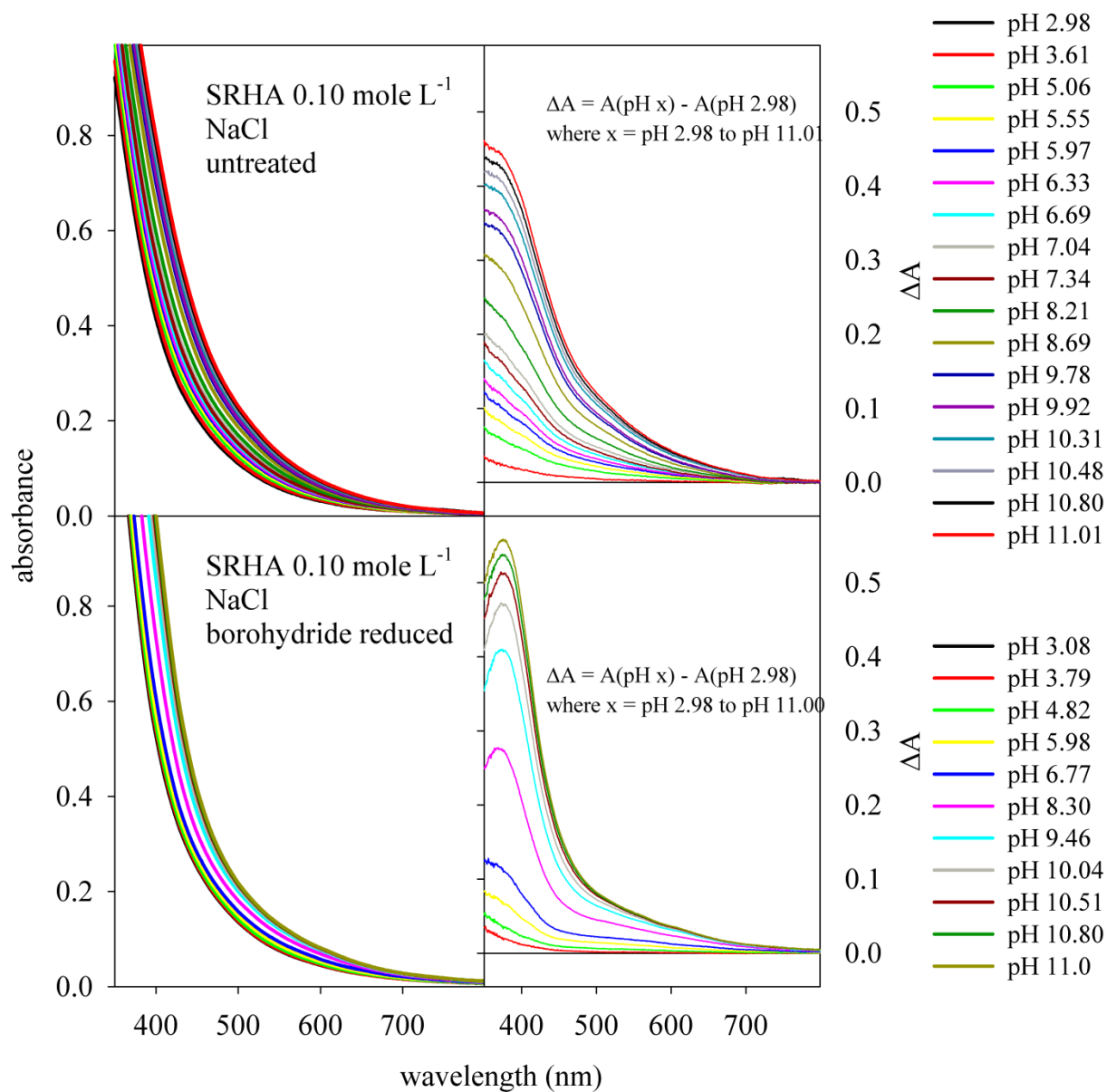
*SRHA= Suwannee River Humic Acid, SRFA= Suwannee River Fulvic Acid, EHA= Elliott Humic Acid, LHA= Leonardite Humic Acid, PLFA=Pony Lake Fulvic Acid, LAC= Lignin Alkali Carboxylate.

[&] absorbance and difference spectra of the optical titrations indicate macro-level structural changes that were not apparent by visual inspection.

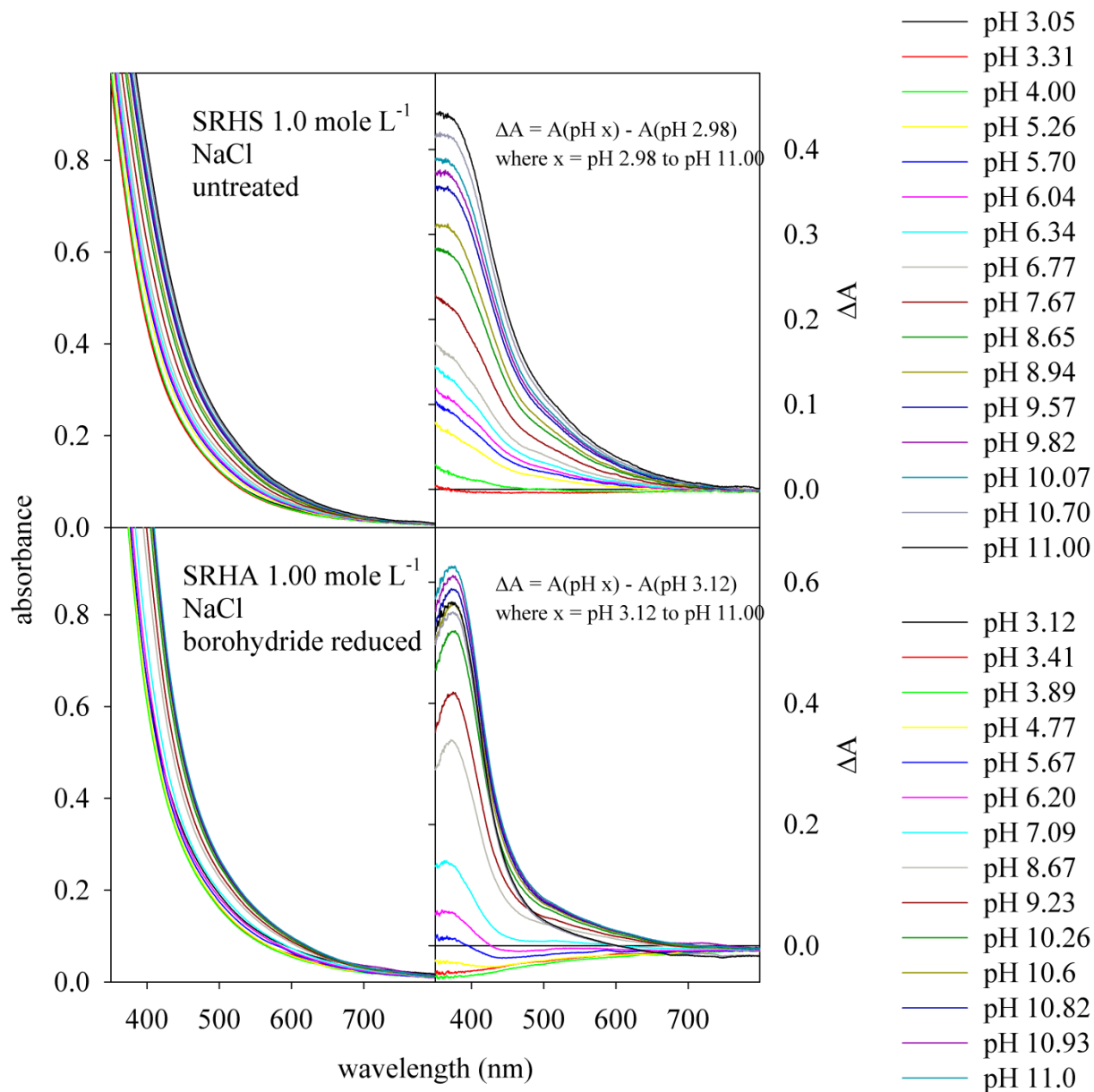
[#] precipitated out of solution at low pH.



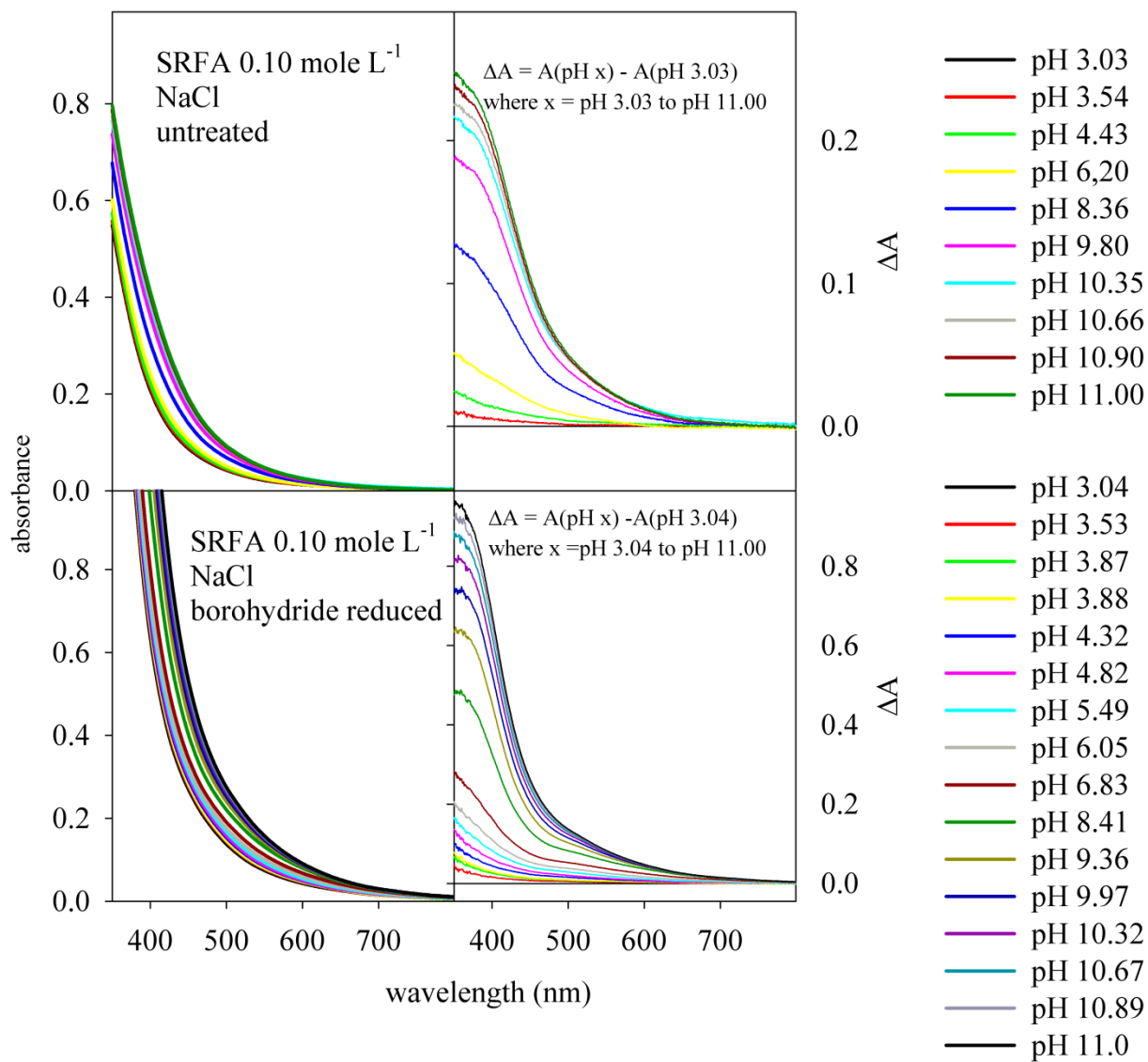
A2.1 Absorbance (left panels) and difference (ΔA) (right panels) spectra of the optical titration of 0.01 mole L⁻¹ ionic strength (as NaCl) Suwannee River humic acid (SRHA).



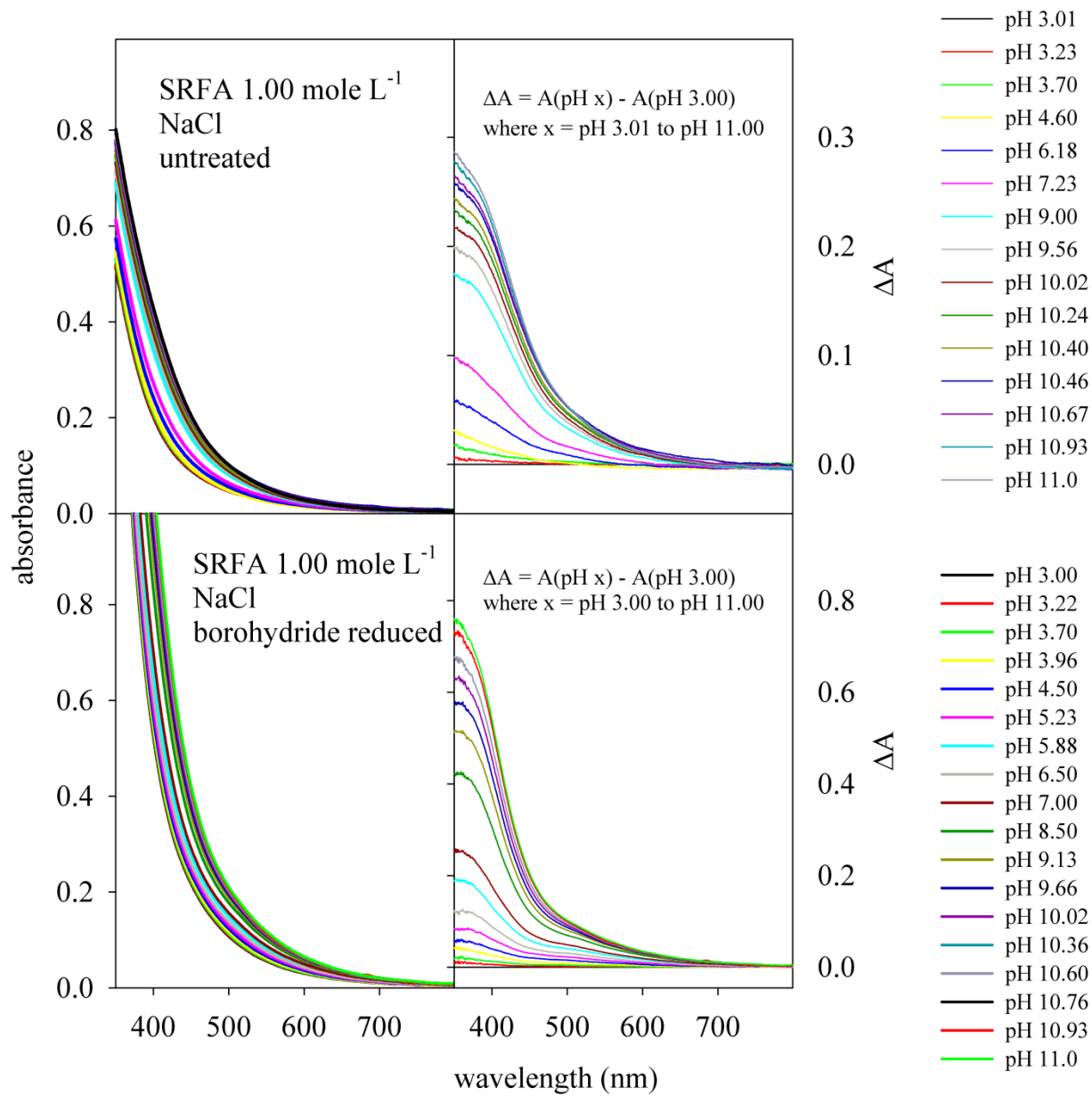
A2.2 Absorbance (left panels) and difference (ΔA) (right panels) spectra of the optical titration of 0.10 mole L⁻¹ ionic strength (as NaCl) Suwannee River humic acid (SRHA).



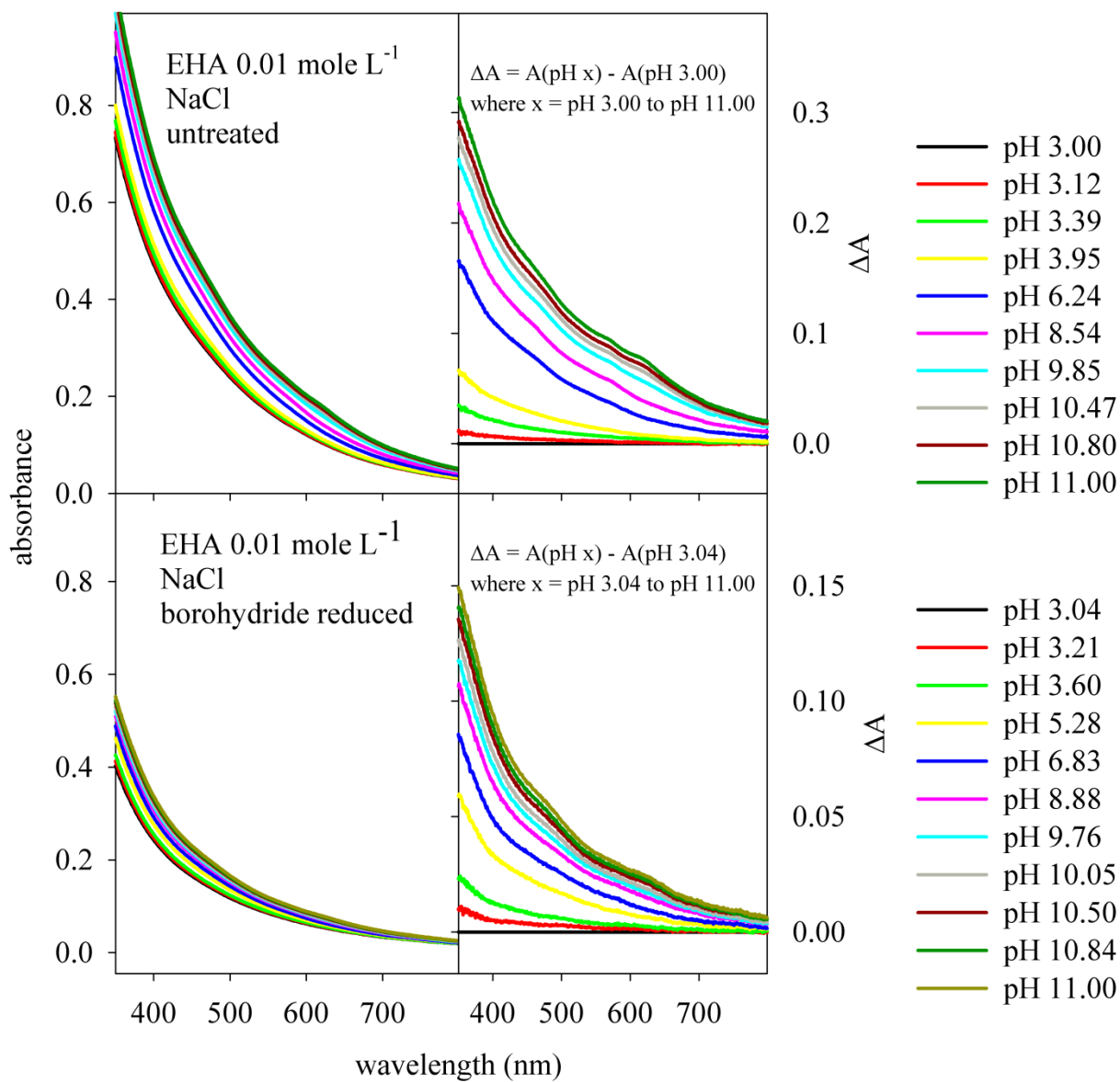
A2.3 Absorbance (left panels) and difference (ΔA) (right panels) spectra of the optical titration of 1.00 mole L⁻¹ ionic strength (as NaCl) Suwannee River humic acid (SRHA).



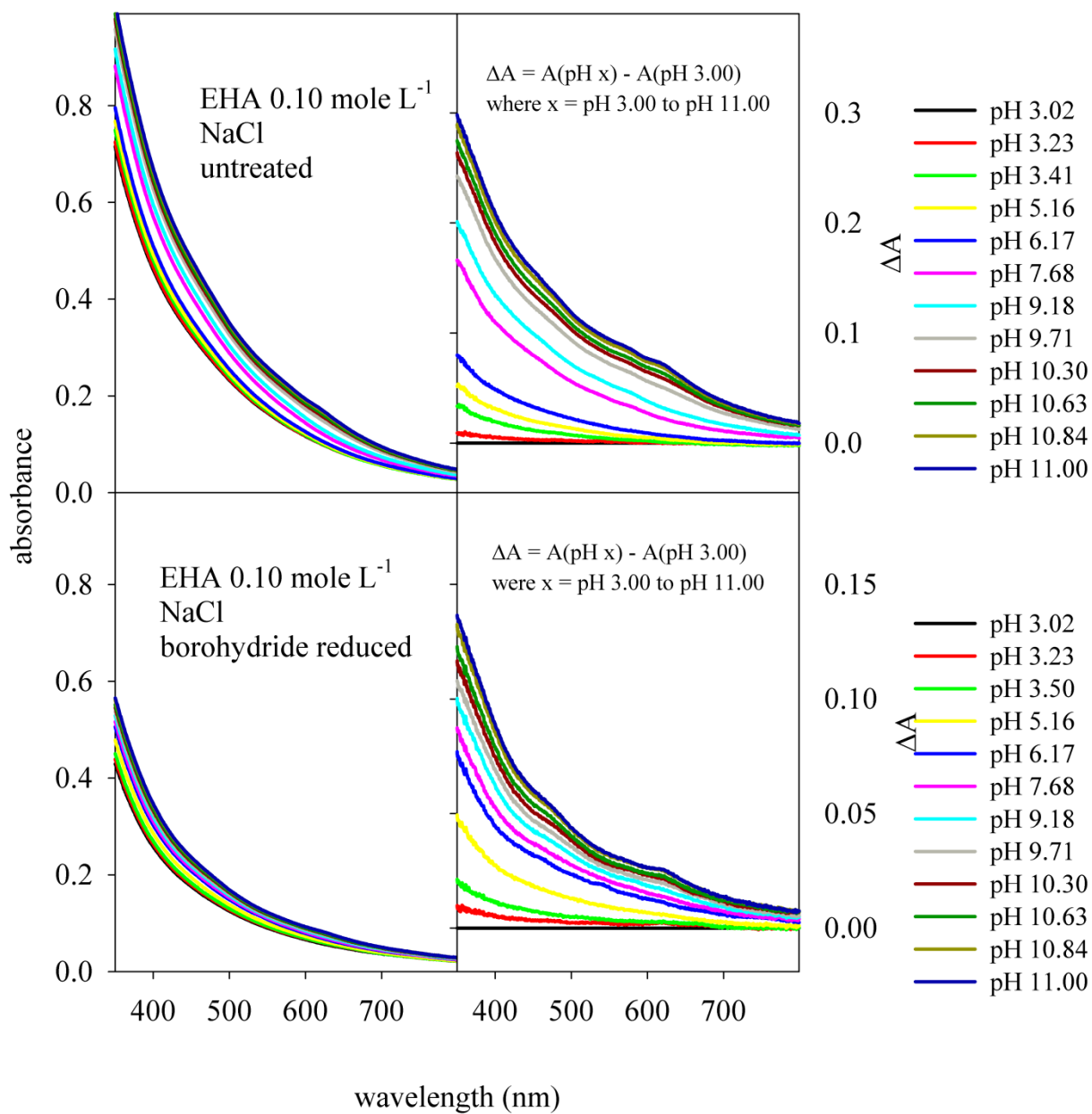
A2.4 Absorbance (left panels) and difference (ΔA) (right panels) spectra of the optical titration of 0.10 mole L⁻¹ ionic strength (as NaCl) Suwannee River fuming acid (SRFA).



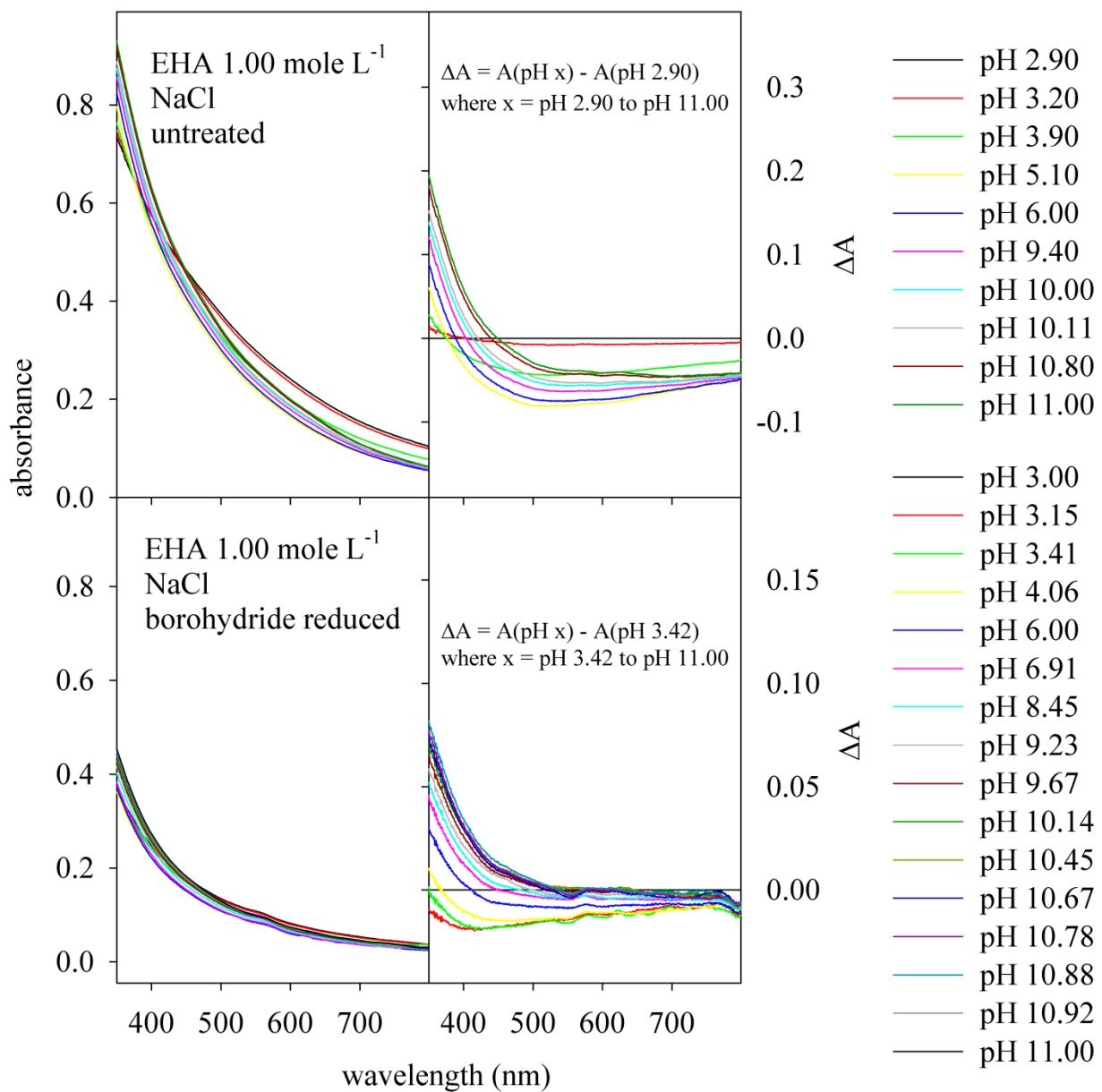
A2.5 Absorbance (left panels) and difference (ΔA) (right panels) spectra of the optical titration of 1.00 mole L⁻¹ ionic strength (as NaCl) Suwannee River fuming acid (SRFA).



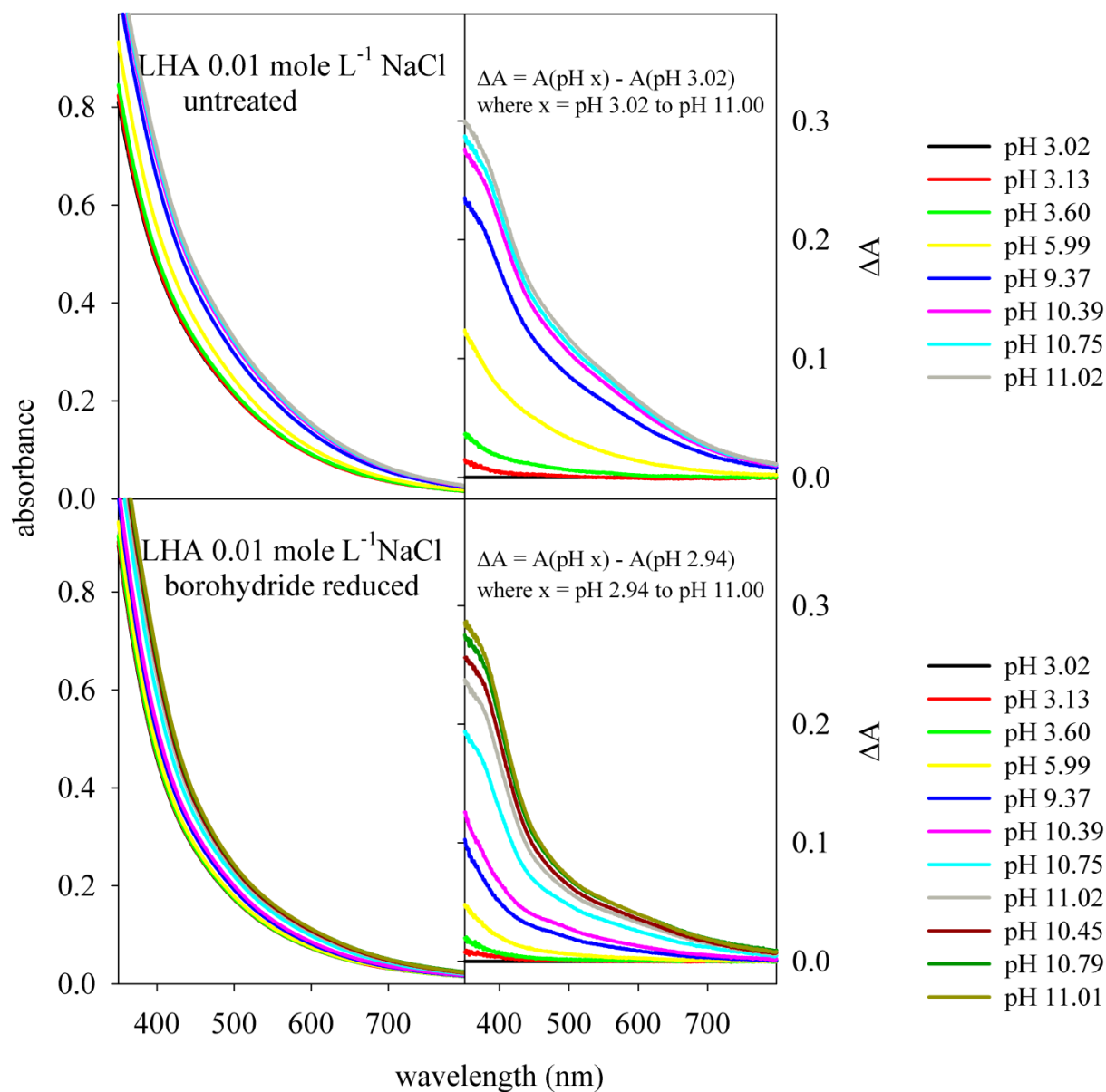
A2.6 Absorbance (left panels) and difference (ΔA) (right panels) spectra of the optical titration of 0.01 mole L⁻¹ ionic strength (as NaCl) Elliott humic acid (EHA).



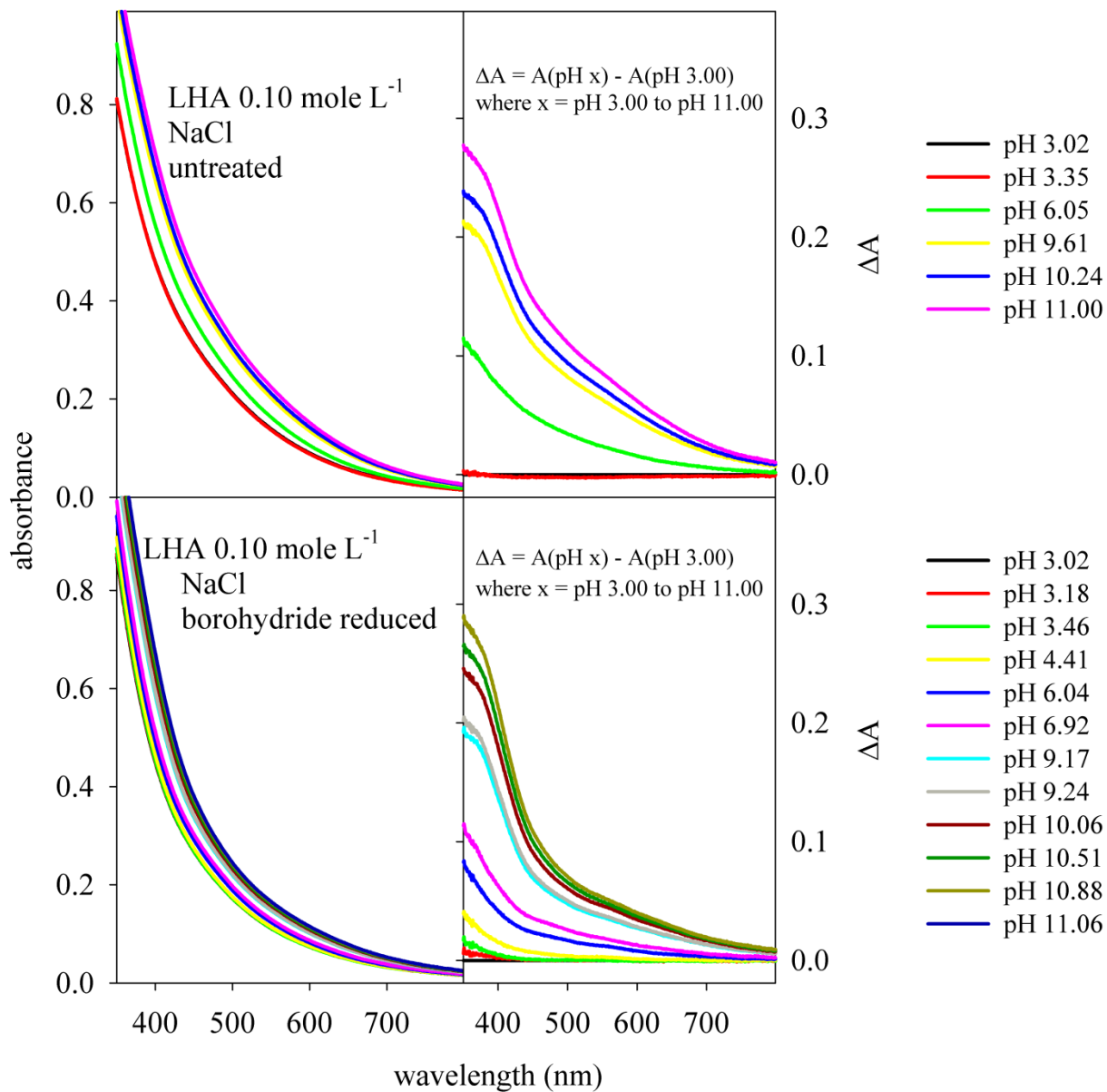
A2.7 Absorbance (left panels) and difference (ΔA) (right panels) spectra of the optical titration of 0.10 mole L⁻¹ ionic strength (as NaCl) Elliott humic acid (EHA).



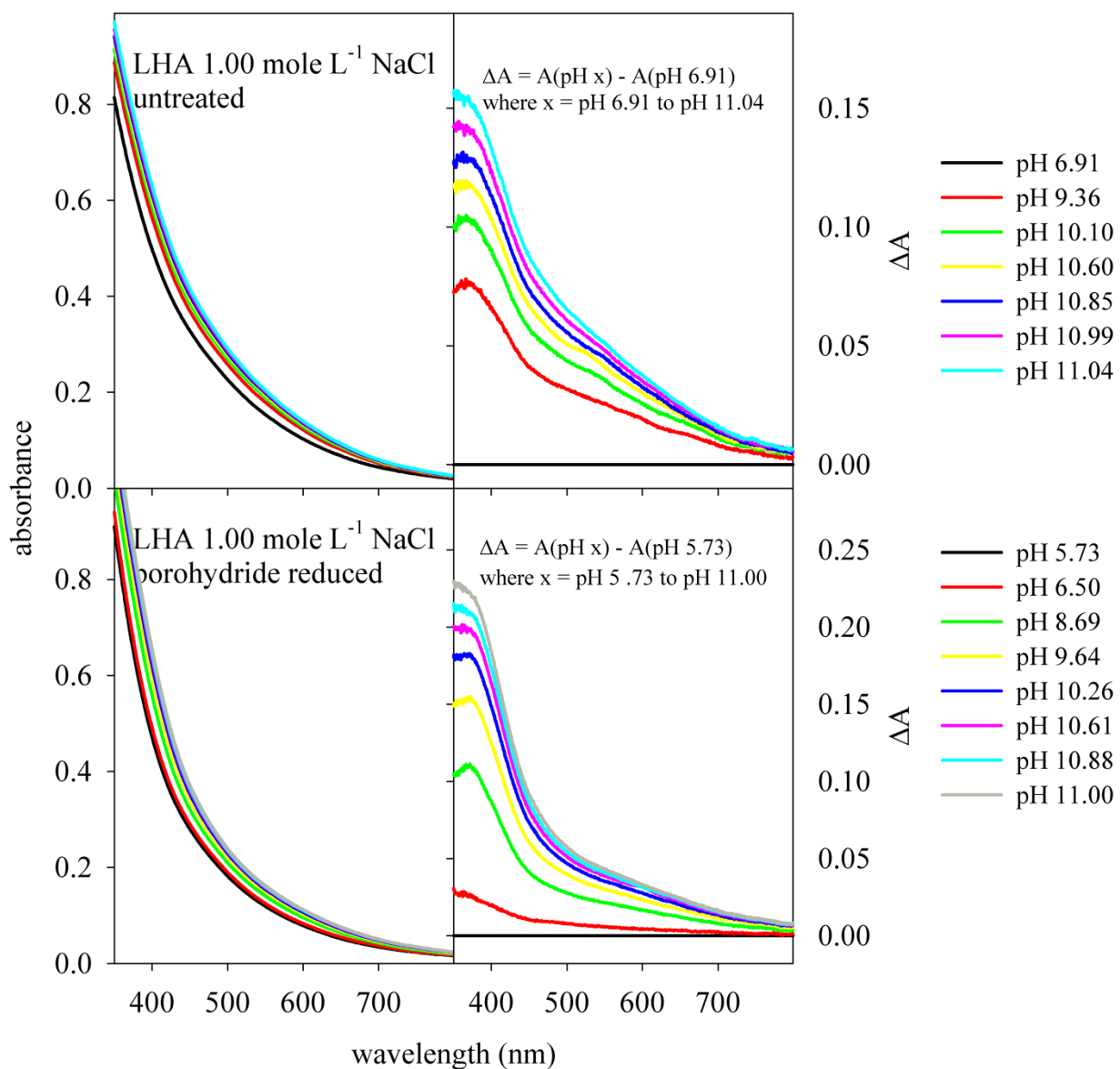
A2.8 Absorbance (left panels) and difference (ΔA) (right panels) spectra of the optical titration of 1.00 mole L⁻¹ ionic strength (as NaCl) Elliott humic acid (EHA).



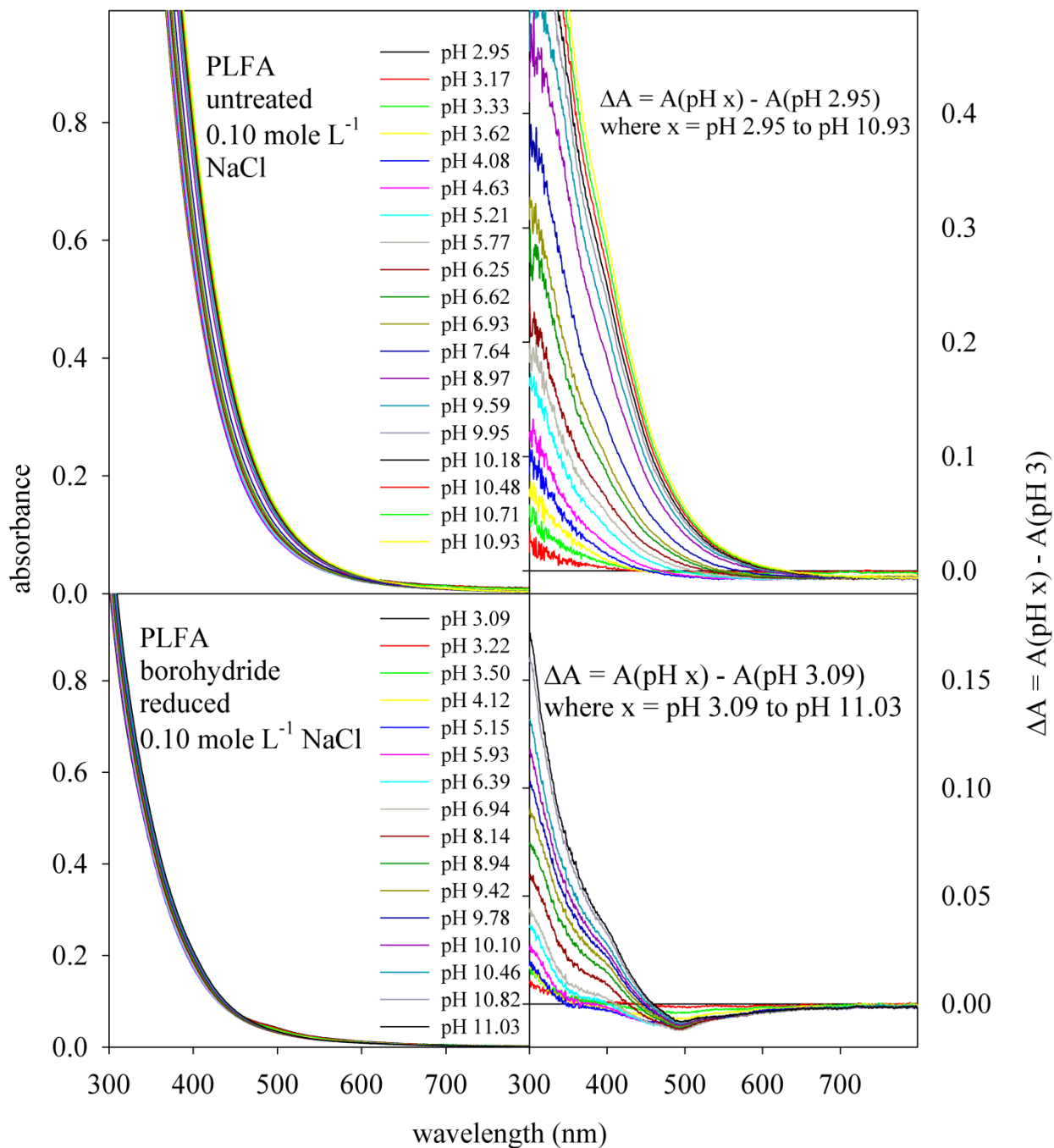
A2.9 Absorbance (left panels) and difference (ΔA) (right panels) spectra of the optical titration of 0.01 mole L⁻¹ ionic strength (as NaCl) Leonardite humic acid (LHA).



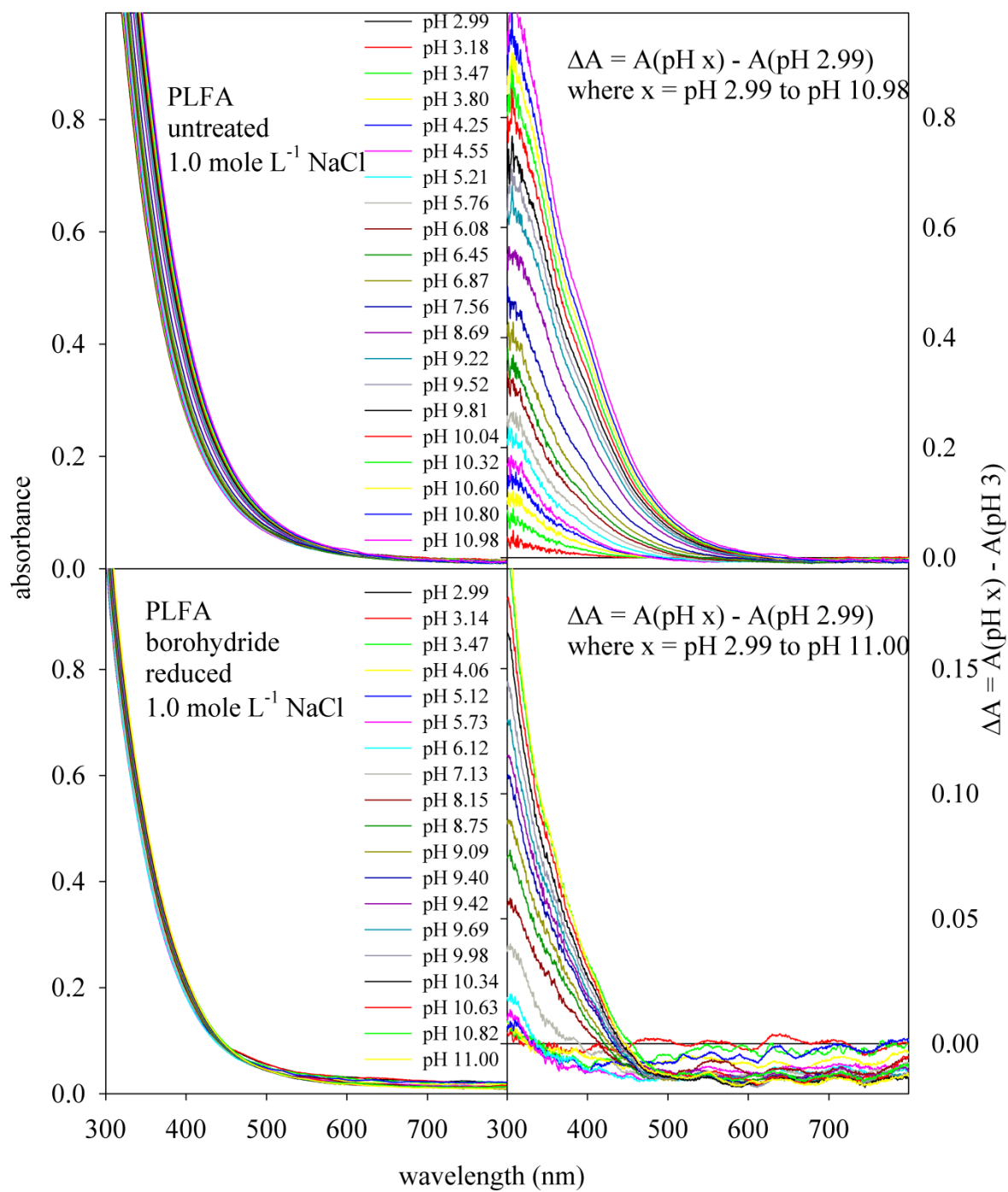
A2.10 Absorbance (left panels) and difference (ΔA) (right panels) spectra of the optical titration of 0.10 mole L⁻¹ ionic strength (as NaCl) Leonardite humic acid (LHA).



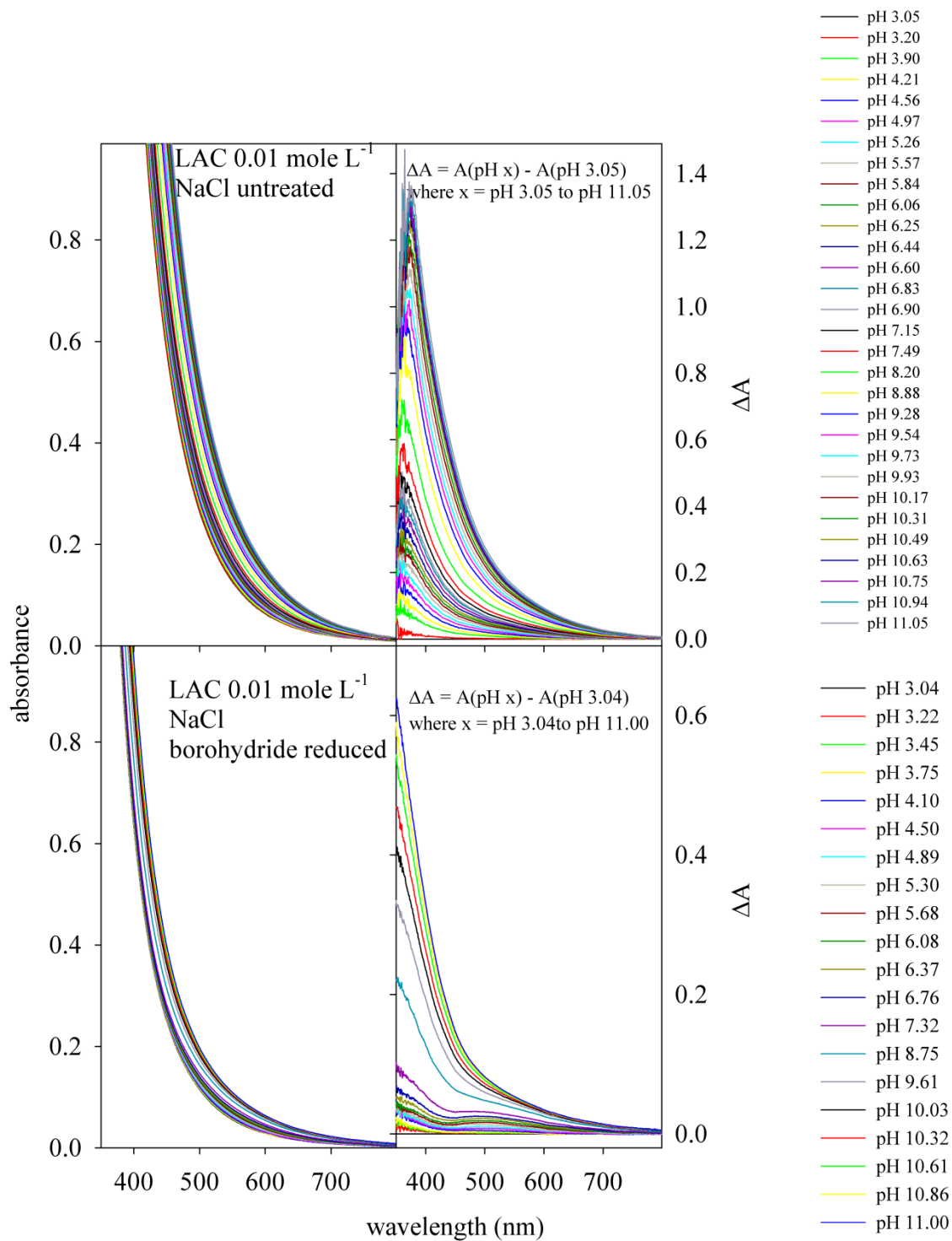
A2.11 Absorbance (left panels) and difference (ΔA) (right panels) spectra of the optical titration of 1.00 mole L⁻¹ ionic strength (as NaCl) Leonardite humic acid (LHA).



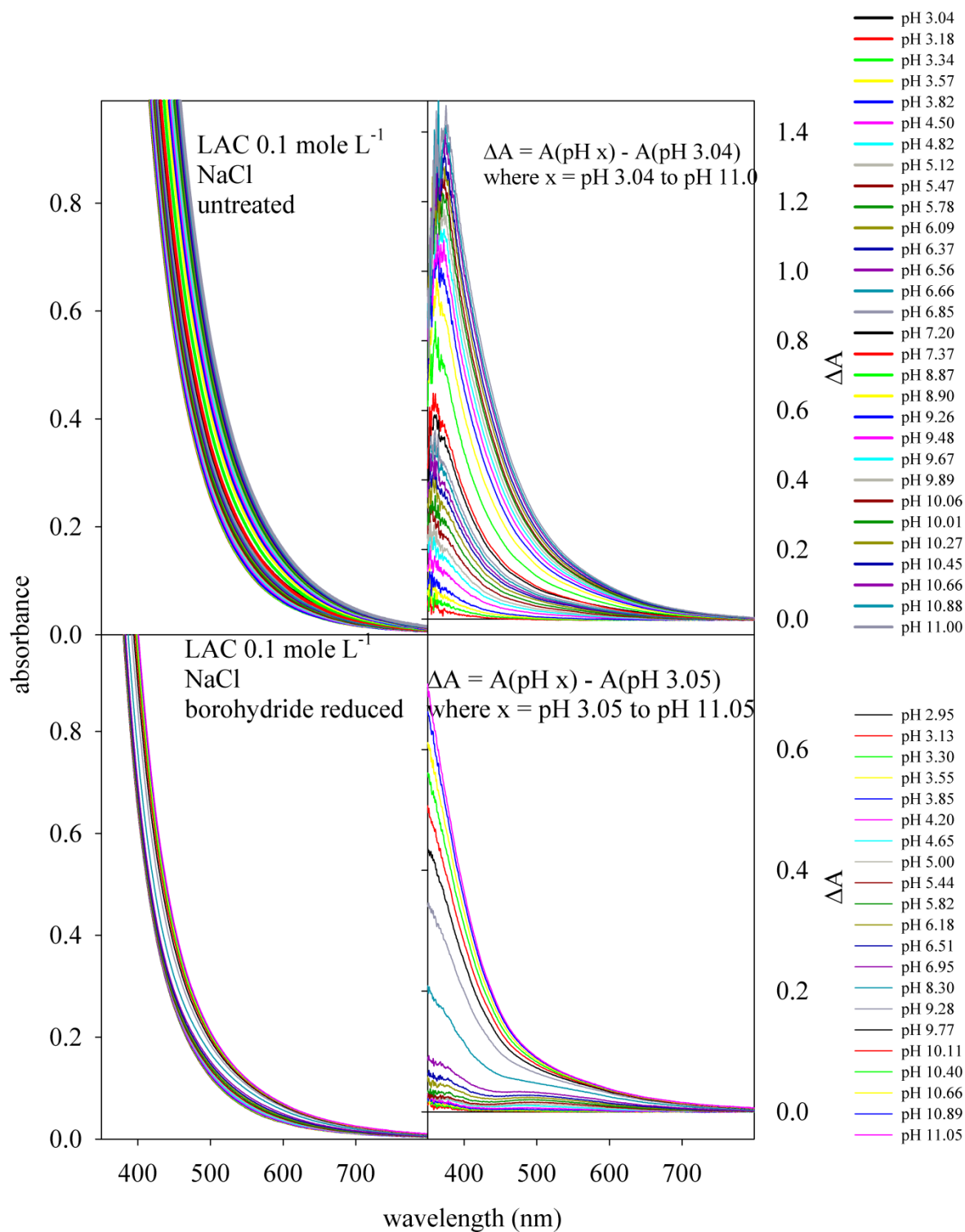
A2.12 Absorbance (left panels) and difference (ΔA) (right panels) spectra of the optical titration of 0.10 mole L⁻¹ ionic strength (as NaCl) Pony Lake fulvic acid (PLFA).



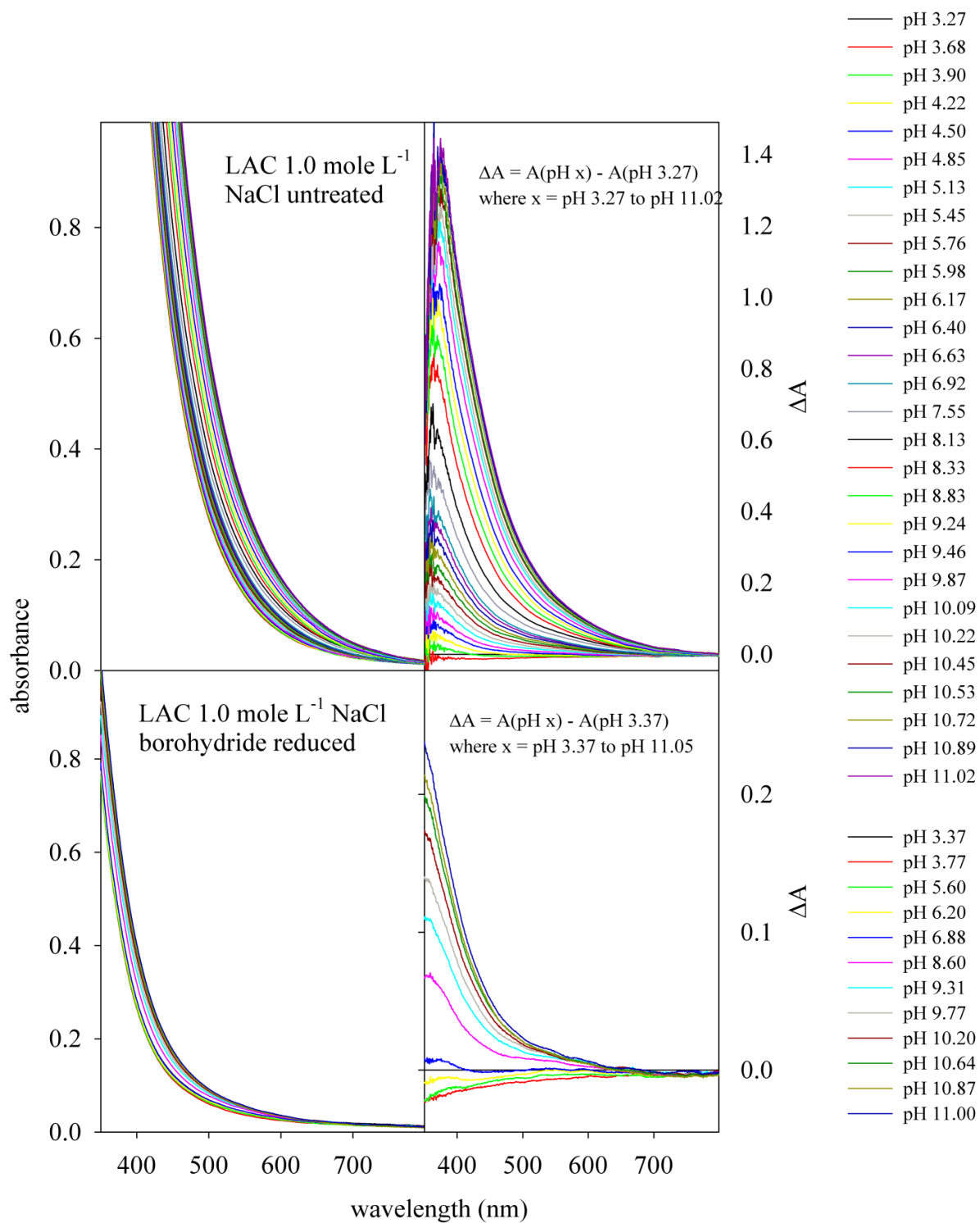
A2.13 Absorbance (left panels) and difference (ΔA) (right panels) spectra of the optical titration of 1.00 mole L⁻¹ ionic strength (as NaCl) Pony Lake fulvic acid (PLFA).



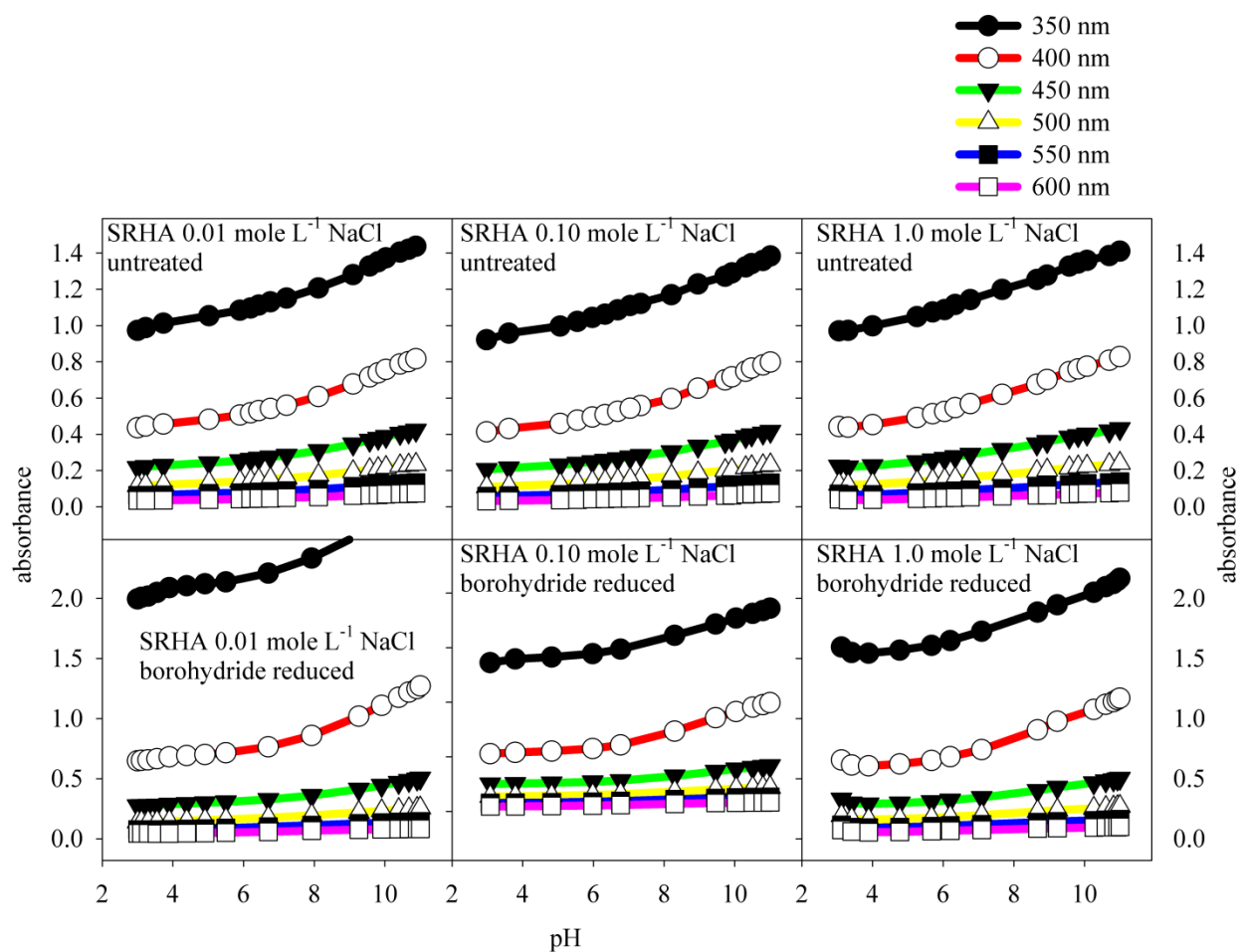
A2.14 Absorbance (left panels) and difference (ΔA) (right panels) spectra of the optical titration of 0.01 mole L⁻¹ ionic strength (as NaCl) Lignin Alkali Carboxylate (LAC).



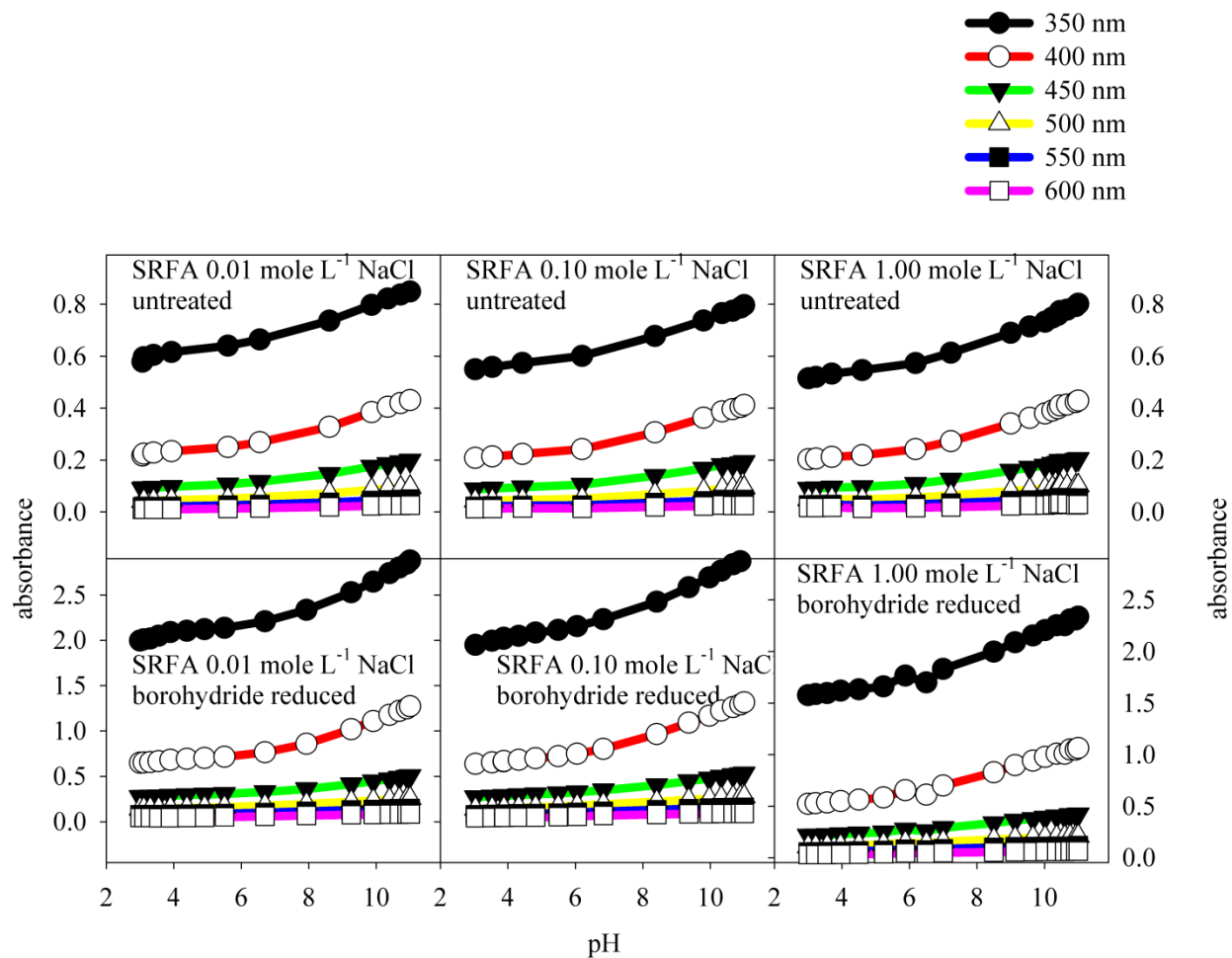
A2.15 Absorbance (left panels) and difference (ΔA) (right panels) spectra of the optical titration of 0.10 mole L⁻¹ ionic strength (as NaCl) Lignin Alkali Carboxylate (LAC).



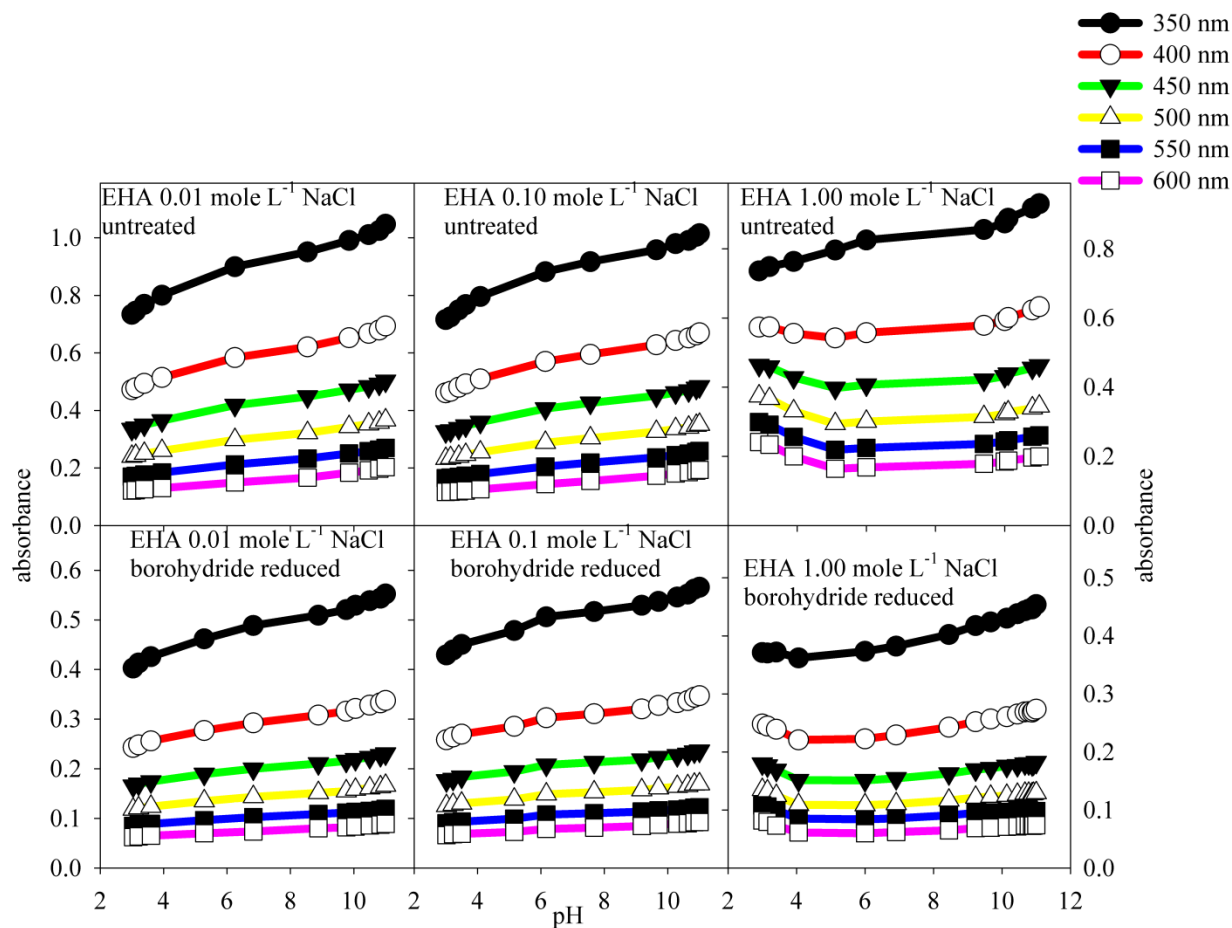
A2.16 Absorbance (left panels) and difference (ΔA) (right panels) spectra of the optical titration of 1.00 mole L⁻¹ ionic strength (as NaCl) Lignin Alkali Carboxylate (LAC).



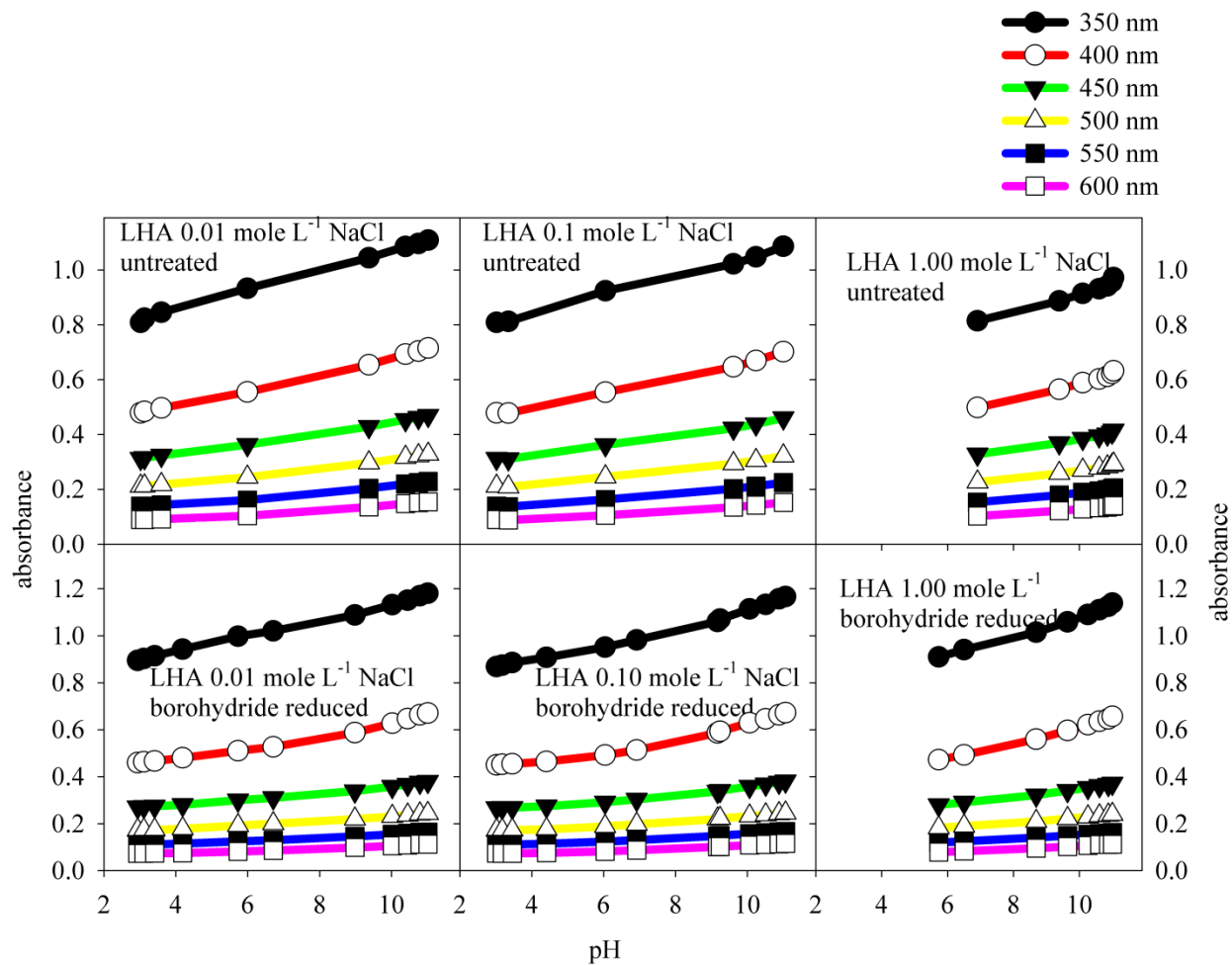
A2.17 Absorbance as a function of pH for Suwannee River humic acid (SRHA) at ionic strengths 0.01 mole L⁻¹ (left panels), 0.10 mole L⁻¹ (middle panels) and 1.0 mole L⁻¹ (right panels). Untreated SRHA (upper panels). Borohydride reduced SRHA (lower panels).



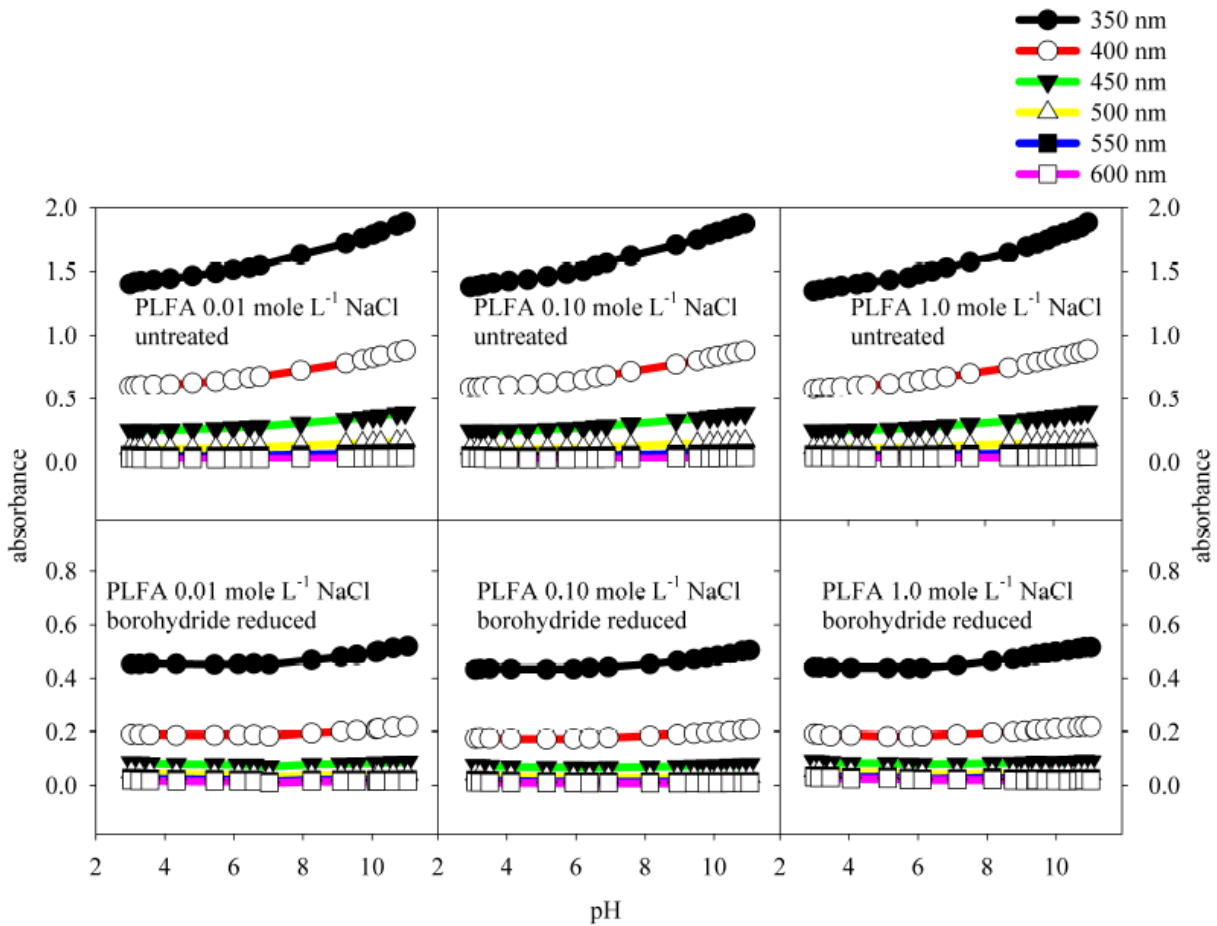
A2.18 Absorbance as a function of pH for Suwannee River fulvic acid (SRFA) at ionic strengths 0.01 mole L⁻¹ (left panels), 0.10 mole L⁻¹ (middle panels) and 1.0 mole L⁻¹ (right panels). Untreated SRFA (upper panels). Borohydride reduced SRFA (lower panels).



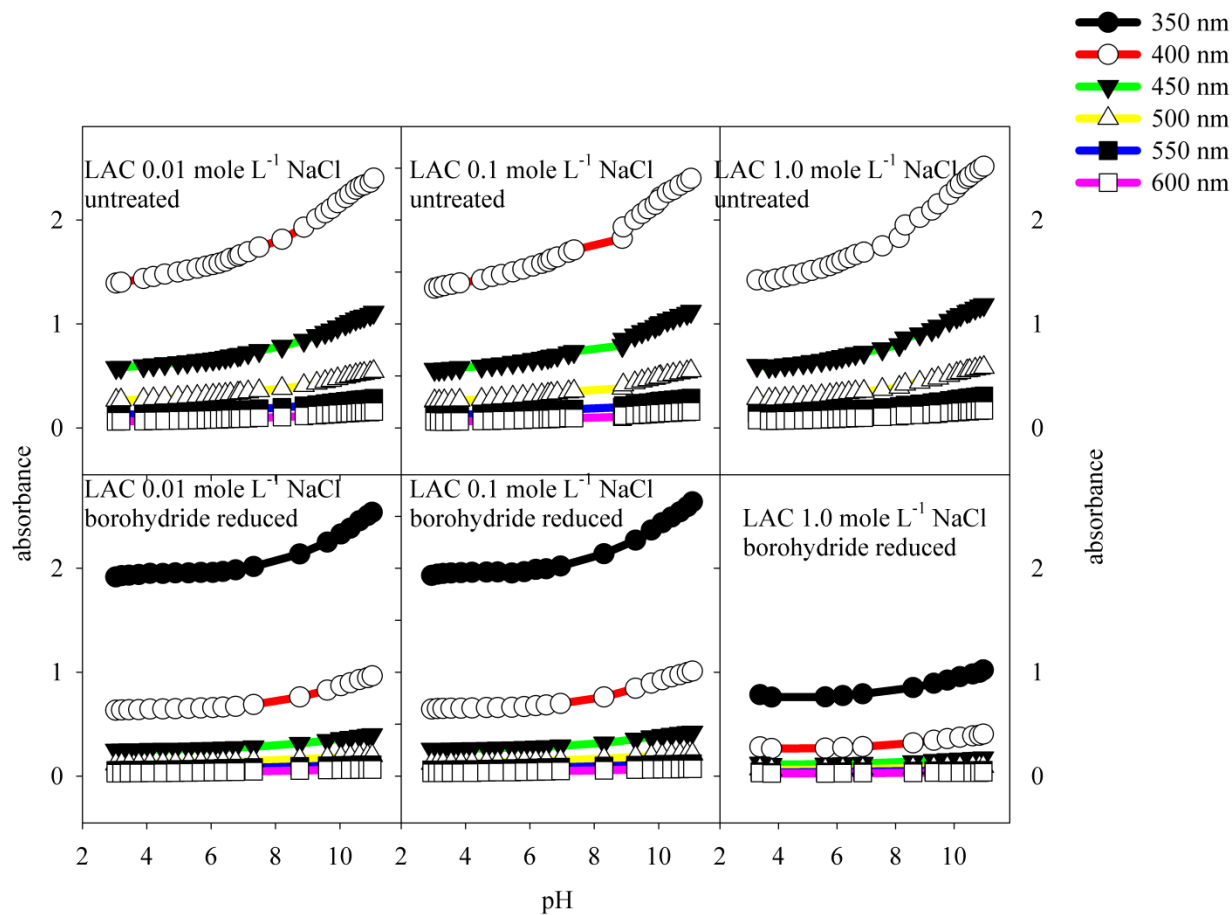
A2.19 Absorbance as a function of pH for Elliott humic acid (EHA) at ionic strengths 0.01 mole L^{-1} (left panels), 0.10 mole L^{-1} (middle panels) and 1.0 mole L^{-1} (right panels). Untreated EHA (upper panels). Borohydride reduced EHA (lower panels).



A2.20 Absorbance as a function of pH for Leonardite humic acid (LHA) at ionic strengths 0.01 mole L⁻¹ (left panels), 0.10 mole L⁻¹ (middle panels) and 1.0 mole L⁻¹ (right panels). Untreated LHA (upper panels). Borohydride reduced LHA (lower panels).



A2.21 Absorbance as a function of pH for Pony Lake fulvic acid (PLFA) at ionic strengths 0.01 mole L⁻¹ (left panels), 0.10 mole L⁻¹ (middle panels) and 1.0 mole L⁻¹ (right panels). Untreated PLFA (upper panels). Borohydride reduced PLFA (lower panels).



A2.22 Absorbance as a function of pH for Lignin Alkali Carboxylate (LAC) at ionic strengths 0.01 mole L⁻¹ (left panels), 0.10 mole L⁻¹ (middle panels) and 1.0 mole L⁻¹ (right panels). Untreated LAC (upper panels). Borohydride reduced LAC (lower panels).

Appendix 3 Raman Theory

A.3.1 Raman Spectral Theory

The phenomena of Raman scattering is the result of inelastic scattering of a photon with a molecule of interest. Energy is transferred either from the photon to the molecule of interest or from the molecule to the photon resulting in Stokes Raman and anti-Stokes Raman frequency shifts, respectively. These process are diagramed in Fig. A3.1.

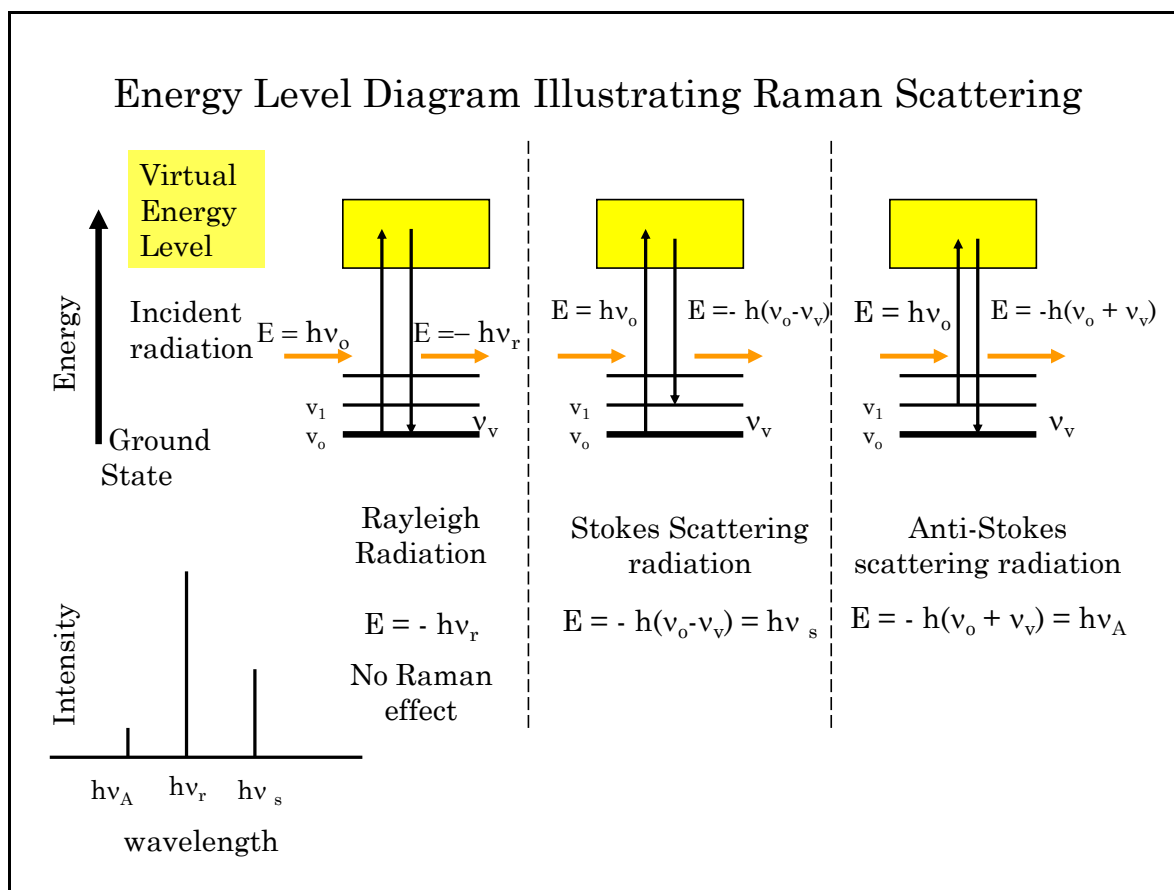


Figure A3.1 Raman Scattering Energy Levels, including Rayleigh radiation and Stokes/Anti-Stokes scattering radiation that produce Raman scattering.

The degree of polarizability (α) of the molecular electron cloud as it is subject to the electric field (E) of electromagnetic radiation resulting in an induced dipole (p) is the measure of Raman activity and is described by Equation (A3.1) (Aroca (2006)), (Dieringer, Shah, Stuart, Whitney, Yonzon, Young, Zhang and Van Duyne (2006)), (Agarwal and Atalla (2000)), (Jeanmarie and Van Duyne (1977a)).

$$p = \alpha E, \quad (\text{A3.1})$$

Raman spectra can provide detailed information about the functional groups in a molecule.

A.3.2 Surface Enhanced Raman Scattering (SERS)

Surface Enhanced Raman Scattering (SERS) is the enhancement of the electromagnetic field surrounding small metal structures. A metal structure is considered small when compared to incoming radiation wavelengths. Incident photons interacting with nano-structures can create surface plasmons that in turn create strong local electric fields. The enhanced electric field can be made to coincide geometrically with an absorbate molecule of interest. The optical properties of the absorbed species can be greatly enhanced by the enhanced electric field. The basic mechanism of SERS is unresolved but the choice of materials that produce plasmons in the visible range is supported theoretically (Aroca (2006)), (Dieringer, Shah, Stuart, Whitney, Yonzon, Young, Zhang and Van Duyne (2006)), (Agarwal and Atalla (2000)), (Jeanmarie and Van Duyne (1977a)). The coinage metals, silver (Ag), gold (Au) and copper (Cu) have been used successfully to produce SERS spectra.

The nano-structure and the absorbed molecule of interest can be considered as two oscillating dipoles shifted by the inelastic scatter or Raman scatter frequency. The enhanced Raman Effect is the coherent addition of the frequency of the chemical species of interest and the plasmonic field normalized to plasmonic field if the species of interest is absent. This interpretation assumes only Van der Waals forces between the molecule of interest and the plasmon producing substrate. The inclusion of chemical effects between the molecule of interest and metal nanostructure producing the plasmons is operationally defined as interactions at levels of bonding energies (Aroca (2006)). Chemical effects have been cited in many SERS publications and require careful analyses as chemical effects produce altered spectra (Aroca (2006)), (Johansson (2005)).

Agarwal and Atalla, 2000 used Raman spectroscopy to identify lignin-model compounds including; stilbenes and quinones, as well as chromophores that are present in small quantities in lignocellulosic material. They then compared borohydride bleached pulp wood with non-bleached pulp wood, noting spectral differences. In the subsequently identified hydroquinone/p-quinone redox system, photo yellowing of pulpwood could be correlated with borohydride reduction. Their data indicated that model compounds could be used to model changes in lignin and lignocellulosic material.

Bibliography

- Aeschbacher M., Sander M. and Schwarzenbach R. P. (2010) Novel Electrochemical Approach to Assess the Redox Properties of Humic Substances. *Environ. Sci. Technol.* **44**, 87–93.
- Aeschbacher M., Vergari D., Schwarzenbach R. P. and Sander M. (2011) Electrochemical Analysis of Proton and Electron Transfer Equilibria of the Reducible Moieties in Humic Acids. *Environ. Sci. Technol.* **45**, 8385–8394.
- Agarwal and Atalla (2000) *Using Raman spectroscopy to identify chromophores in lignin-lignocellulosics. In Lignin: Historical, Biological, and Materials Perspectives.*, ACS Publications, Washington D.C.
- Albrecht M. G. and Creighton J. A. (1977) Anomalously intense Raman spectra of pyridine at a silver electrode. *J. Am. Chem. Soc.* **99**, 5215–5217.
- Allard B. (2006) A comparative study on the chemical composition of humic acids from forest soil, agricultural soil and lignite deposit: Bound lipid, carbohydrate and amino acid distributions. *Geoderma* **130**, 77–96.
- Allard B. and Derenne S. (2007) Oxidation of humic acids from an agricultural soil and a lignite deposit: Analysis of lipophilic and hydrophilic products. *Organic Geochemistry* **38**, 2036–2057.
- Aluwihare L. I., Repeta D. J. and Chen R. F. (1997) A major biopolymeric component to dissolved organic carbon in surface sea water. **387**, 166–169.
- Amon R. M. W., Rinehart A. J., Duan S., Louchouart P., Prokushkin A., Guggenberger G., Bauch D., Stedmon C., Raymond P. A., Holmes R. M., McClelland J. W., Peterson B. J., Walker S. A. and Zhulidov A. V. (2012) Dissolved organic matter sources in large Arctic rivers. *Geochimica et Cosmochimica Acta* **94**, 217–237.
- Aroca R. (2006) *Surface enhanced vibrational spectroscopy.*, John Wiley and Sons.
- Avena M. J., Koopal L. K. and van Riemsdijk W. H. (1999) Proton Binding to Humic Acids: Electrostatic and Intrinsic Interactions. *Journal of Colloid and Interface Science* **217**, 37–48.
- Baker A. and Spencer R. G. M. (2004) Characterization of dissolved organic matter from source to sea using fluorescence and absorbance spectroscopy. *Science of The Total Environment* **333**, 217–232.
- Baldock J. and Skjemstad J. (2000) Role of the soil matrix and minerals in protecting natural organic materials against biological attack. *Organic Geochemistry* **31**, 697–710.
- Barbeau K., Rue E. L., Bruland K. W. and Butler A. (2001) Photochemical cycling of iron in the surface ocean mediated by microbial iron(III)-binding ligands. *Nature* **413**, 409–413.

- Benedetti M. F., Milne C. J., Kinniburgh D. G., Van Riemsdijk W. H. and Koopal L. K. (1995) Metal Ion Binding to Humic Substances: Application of the Non-Ideal Competitive Adsorption Model. *Environ. Sci. Technol.* **29**, 446–457.
- Benedetti M. F., Van Riemsdijk W. H. and Koopal L. K. (1996) Humic Substances Considered as a Heterogeneous Donnan Gel Phase. *Environmental Science & Technology* **30**, 1805–1813.
- Benner R. and Kaiser K. (2010) Biological and photochemical transformations of amino acids and lignin phenols in riverine dissolved organic matter. *Biogeochemistry* **102**, 209–222.
- Benner R., Louchouart P. and Amon R. M. W. (2005) Terrigenous dissolved organic matter in the Arctic Ocean and its transport to surface and deep waters of the North Atlantic. *Global Biogeochem. Cycles* **19**, GB2025.
- Blough N. V. and Green S. A. (1995) Spectroscopic characterization and remote sensing of non-living organic matter. In *The role of non-living organic matter in the Earth's carbon cycle* Proc. Dahlem Conf. Wiley. pp. 23–45.
- Blough N. V. and Del Vecchio R. (2002) Chapter 10 - Chromophoric DOM in the Coastal Environment. In *Biogeochemistry of Marine Dissolved Organic Matter* (eds. Dennis A. Hansell and Craig A. Carlson). Academic Press, San Diego. pp. 509–546.
- Blough N. V. and Zepp R. (1995) Reactive Oxygen Species in Natural Waters. In *Active Oxygen: Reactive Oxygen Species in Chemistry* Chapman and Hall. pp. 280–321.
- Boyle E. S., Guerriero N., Thiallet A., Vecchio R. D. and Blough N. V. (2009) Optical properties of humic substances and CDOM: Relation to structure. *Environmental science & technology* **43**, 2262–2268.
- Brady and Weil (2002) *The Nature and Properties of Soils*. 13th ed., Prentice Hall.
- Bricaud A., Morel A. and Prieur L. (1981) Absorption by Dissolved Organic Matter of the Sea (Yellow Substance) in the UV and Visible Domains. *Limnology and Oceanography* **26**, 43–53.
- Brown A., McKnight D. M., Chin Y. P., Roberts E. C. and Uhle M. (2004) Chemical characterization of dissolved organic material in Pony Lake, a saline coastal pond in Antarctica. *Marine Chemistry* **89**, 327–337.
- Chen R. F., Bissett P., Coble P., Conmy R., Gardner G. B., Mary Ann Moran, Wang X., Wells M. L., Whelan P. and Zepp R. G. (2004) Chromophoric dissolved organic matter (CDOM) source characterization in the Louisiana Bight. *Marine Chemistry* **89**, 257–272.
- Chin Yu-Ping, Aiken G. and O'Loughlin E. (1994) Molecular Weight, Polydispersity, and Spectroscopic Properties of Aquatic Humic Substances. *Environ. Sci. Technol.* **28**, 1853–1858.

- Christensen J. B., Tipping E., Kinniburgh D. G., Grun C. and Christensen T. H. (1998) Proton binding by groundwater fulvic acids of different age, origins, and structure modeled with the Model V and NICA-Donnan model. *Environmental science & technology* **32**, 3346–3355.
- Cleyden J., Greeves N., Warren S. and Wothers P. (2001) *Organic Chemistry.*, Oxford, Oxford.
- Coble P. (2004) *Colored Dissolved Organic Matter in the Coastal Ocean: An Optical Tool for Coastal Zone Environmental Assessment & Management.*, DTIC Document.
- Coble P. G. (2007) Marine optical biogeochemistry: The chemistry of ocean color. *Chemical reviews* **107**, 402–418.
- Dahl E. E., Saltzman E. S. and Bruyn W. J. de (2003) The aqueous phase yield of alkyl nitrates from ROO + NO: Implications for photochemical production in seawater. *Geophys. Res. Lett.* **30**, 1271.
- Dalal R. and Mayer R. (1986) Long term trends in fertility of soils under continuous cultivation and cereal cropping in southern Queensland. II. Total organic carbon and its rate of loss from the soil profile. *Soil Res.* **24**, 281–292.
- Del Vecchio Rossana and Blough N. V. (2004) On the Origin of the Optical Properties of Humic Substances. *Environmental Science & Technology* **38**, 3885–3891.
- Del Vecchio R. and Blough N. V. (2002) Photobleaching of chromophoric dissolved organic matter in natural waters: kinetics and modeling. *Marine Chemistry* **78**, 231–253.
- Del Vecchio R. and Blough N. V. (2004) Spatial and seasonal distribution of chromophoric dissolved organic matter and dissolved organic carbon in the Middle Atlantic Bight. *Marine chemistry* **89**, 169–187.
- De Wit J. C. M., van Riemsdijk W. H. and Koopal L. K. (1993a) Proton binding to humic substances. 1. Electrostatic effects. *Environ. Sci. Technol.* **27**, 2005–2014.
- De Wit J. C. M., van Riemsdijk W. H. and Koopal L. K. (1993b) Proton binding to humic substances. 2. Chemical heterogeneity and adsorption models. *Environmental Science & Technology* **27**, 2015–2022.
- De Wit J. C. M., Van Riemsdijk W. H., Nederlof M. M., Kinniburgh D. G. and Koopal L. K. (1990) Analysis of ion binding on humic substances and the determination of intrinsic affinity distributions. *Analytica Chimica Acta* **232**, 189–207.
- Dittmar T. (2008) The molecular level determination of black carbon in marine dissolved organic matter. *Organic Geochemistry* **39**, 396–407.

- Dryer D. J., Korshin G. V. and Fabbicino M. (2008) In Situ Examination of the Protonation Behavior of Fulvic Acids Using Differential Absorbance Spectroscopy. *Environ. Sci. Technol.* **42**, 6644–6649.
- Fang X., Chua T., Schmidt-Rohr K. and Thompson M. L. (2010) Quantitative ¹³C NMR of whole and fractionated Iowa Mollisols for assessment of organic matter composition. *Geochimica et Cosmochimica Acta* **74**, 584–598.
- Fang X., Mao J., Cory R. M., McKnight D. M. and Schmidt-Rohr K. (2011) ¹⁵N and ¹³C/¹⁴N NMR investigation of the major nitrogen-containing segment in an aquatic fulvic acid: Evidence for a hydantoin derivative. *Magnetic Resonance in Chemistry* **49**, 775–780.
- Fimmen R. L., Cory R. M., Chin Y.-P., Trouts T. D. and McKnight D. M. (2007) Probing the oxidation–reduction properties of terrestrially and microbially derived dissolved organic matter. *Geochimica et Cosmochimica Acta* **71**, 3003–3015.
- Fleischmann M., Hendra P. J. and McQuillan A. J. (1974) Raman spectra of pyridine adsorbed at a silver electrode. *Chemical Physics Letters* **26**, 163–166.
- Galí M. and Simó R. (2010) Occurrence and cycling of dimethylated sulfur compounds in the Arctic during summer receding of the ice edge. *Marine Chemistry* **122**, 105–117.
- Gardiner J. A. and Collat J. W. (1965) Kinetics of the Stepwise Hydrolysis of Tetrahydroborate Ion. *J. Am. Chem. Soc.* **87**, 1692–1700.
- Glasser, Northey and Schultz eds. (2000) *Lignin: Historical, Biological and Materials Perspectives*.
- Golanoski K. S., Fang S., Del Vecchio R. and Blough N. V. (2012) Investigating the Mechanism of Phenol Photooxidation by Humic Substances. *Environ. Sci. Technol.* **46**, 3912–3920.
- Goldstone J. V., Pullin M. J., Bertilsson S. and Voelker B. M. (2002) Reactions of Hydroxyl Radical with Humic Substances: Bleaching, Mineralization, and Production of Bioavailable Carbon Substrates. *Environ. Sci. Technol.* **36**, 364–372.
- Goldstone J. V., Del Vecchio R., Blough N. V. and Voelker B. M. (2004) A Multicomponent Model of Chromophoric Dissolved Organic Matter Photobleaching. *Photochemistry and Photobiology* **80**, 52–60.
- Green S. A. and Blough N. V. (1994) Optical absorption and fluorescence properties of chromophoric dissolved organic matter in natural waters. *Limnology and Oceanography*, 1903–1916.
- Gross K. C. and Seybold P. G. (2001) Substituent effects on the physical properties and pK_a of phenol. *International Journal of Quantum Chemistry* **85**, 569–579.
- Guin P. S., Das S. and Mandal P. C. (2011) Electrochemical Reduction of Quinones in Different Media: A Review. *International Journal of Electrochemistry*, 1–22.

- Hansell D. A., Carlson C. A., Repeta D. J. and Schlitzer R. (2009) Dissolved organic matter in the ocean: a controversy stimulates new insights. *Oceanography* 22 no. 4 (2009: 202-211).
- Haumaier L. and Zech W. (1995) Black carbon—possible source of highly aromatic components of soil humic acids. *Organic Geochemistry* **23**, 191–196.
- Hayes M. H. . ed. (1989) *Humic Substances II. In Search of Structure.*, Wiley.
- Hedges J. I., Keil R. G. and Benner R. (1997) What happens to terrestrial organic matter in the ocean? *Organic Geochemistry* **27**, 195–212.
- Hedges J. I., Mayorga E., Tsamakis E., McClain M. E., Aufdenkampe A., Quay P., Richey J. E., Benner R., Opsahl S. and Black B. (2000) Organic matter in Bolivian tributaries of the Amazon River: A comparison to the lower mainstream. *Limnology and Oceanography* **45**, 1449–1466.
- Heighton L., Schmidt W. F. and Siefert R. L. (2008) Kinetic and Equilibrium Constants of Phytic Acid and Ferric and Ferrous Phytate Derived from Nuclear Magnetic Resonance Spectroscopy. *Journal of Agricultural and Food Chemistry* **56**, 9543–9547.
- Hernes P. J. and Benner R. (2003) Photochemical and microbial degradation of dissolved lignin phenols: Implications for the fate of terrigenous dissolved organic matter in marine environments. *J. Geophys. Res.* **108**, 3291.
- Hernes P. J. and Benner R. (2002) Transport and diagenesis of dissolved and particulate terrigenous organic matter in the North Pacific Ocean. *Deep Sea Research Part I: Oceanographic Research Papers* **49**, 2119–2132.
- Hiraishi A., Masamune K. and Kitamura H. (1989) Characterization of the bacterial population structure in an anaerobic-aerobic activated sludge system on the basis of respiratory quinone profiles. *Applied and Environmental Microbiology* **55**, 897.
- Hiraishi A., Ueda Y. and Ishihara J. (1998) Quinone Profiling of Bacterial Communities in Natural and Synthetic Sewage Activated Sludge for Enhanced Phosphate Removal. *Applied and Environmental Microbiology* **64**, 992.
- Hwang J. and Druffel E. R. M. (2003) Lipid-Like Material as the Source of the Uncharacterized Organic Carbon in the Ocean? *Science* **299**, 881–884.
- Inaba K., Takahashi Y., Ito K. and Hayashi S. (2006) Critical role of a thiolate-quinone charge transfer complex and its adduct form in de novo disulfide bond generation by DsbB. *PNAS* **103**, 287–292.
- Jeanmarie and Van Duyne (1977a) Surface Raman spectroelectrochemistry, part 1: heterocyclic, aromatic, and aliphatic amine adsorbed on the anodized silver electrode. *J Electroanal Chem* **84**, 1–20.

- JJenekhe S. A., Lu L. and Alam M. M. (2001) New Conjugated Polymers with Donor–Acceptor Architectures: Synthesis and Photophysics of Carbazole–Quinoline and Phenothiazine–Quinoline Copolymers and Oligomers Exhibiting Large Intramolecular Charge Transfer. *Macromolecules* **34**, 7315–7324.
- Johannessen S. C. and Miller W. L. (2001) Quantum yield for the photochemical production of dissolved inorganic carbon in seawater. *Marine Chemistry* **76**, 271–283.
- Johansson P. (2005) Illustrative direct ab initio calculations of surface Raman spectra. *Physical Chemistry Chemical Physics* **7**, 475.
- Jones R. D. and Amador J. A. (1993) Methane and carbon monoxide production, oxidation, and turnover times in the Caribbean Sea as influenced by the Orinoco River. *J. Geophys. Res.* **98**, 2353–2359.
- Jørgensen L., Stedmon C. A., Kragh T., Markager S., Middelboe M. and Søndergaard M. (2011a) Global trends in the fluorescence characteristics and distribution of marine dissolved organic matter. *Marine Chemistry* **126**, 139–148.
- Kieber D. J. and Blough N. V. (1990) Determination of carbon-centered radicals in aqueous solution by liquid chromatography with fluorescence detection. *Anal. Chem.* **62**, 2275–2283.
- Kinniburgh D. G., Milne C. J., Benedetti M. F., Pinheiro J. P., Filius J., Koopal L. K. and Van Riemsdijk W. H. (1996) Metal Ion Binding by Humic Acid: Application of the NICA-Donnan Model. *Environmental Science & Technology* **30**, 1687–1698.
- Kögel-Knabner I. (2002) The macromolecular organic composition of plant and microbial residues as inputs to soil organic matter. *Soil Biology and Biochemistry* **34**, 139–162.
- Koopal L. K., Saito T., Pinheiro J. P. and Riemsdijk W. H. (2005) Ion binding to natural organic matter: General considerations and the NICA-Donnan model. *Colloids and Surfaces A: Physicochemical and Engineering Aspects* **265**, 40–54.
- Koopal, van Riemsdijk and Kinniburgh (2001) Humic matter and contaminants. General aspects and modeling metal ion binding. *Pure Appl. Chem* **73**, 2005–2016.
- Krull E. S., Baldock J. A. and Skjemstad J. O. (2003) Importance of mechanisms and processes of the stabilisation of soil organic matter for modelling carbon turnover. *Functional Plant Biol.* **30**, 207–222.
- Lane C. F. (1974) Sodium Cyanoborohydride-A highly Selective Reducing Agent for Organic Functional Groups. *Synthesis*, 135–146.
- Lanne R. W. P. M. and Koole L. (1982) The relation between fluorescence and dissolved organic carbon in the Ems-Dollart Estuary and the western Wadden Sea. *Netherlands Journal of Sea Research* **15**, 217–227.

- Lau C. K., Dufresne C., Belanger P. C., Pietre S. and Scheiget J. (1986) Reductive deoxygenation of aryl aldehydes and ketones and benzylic, allylic, and tertiary alcohols by zinc iodide-sodium cyanoborohydride. *J. Org. Chem.* **51**, 3038–3043.
- Leenheer J. A., Wershaw R. L. and Reddy M. M. (1995) Strong-Acid, Carboxyl-Group Structures in Fulvic Acid from the Suwannee River, Georgia. 2. Major Structures. *Environmental Science & Technology* **29**, 399–405.
- Letscher R. T., Hansell D. A. and Kadko D. (2011) Rapid removal of terrigenous dissolved organic carbon over the Eurasian shelves of the Arctic Ocean. *Marine Chemistry* **123**, 78–87.
- Lind J., Shen X., Eriksen T. E. and Merenyi G. (1990) The one-electron reduction potential of 4-substituted phenoxyl radicals in water. *J. Am. Chem. Soc.* **112**, 479–482.
- Liu W. T., Linning K. D., Nakamura K., Mino T., Matsuo T. and Forney L. J. (2000) Microbial community changes in biological phosphate-removal systems on altering sludge phosphorus content. *Microbiology (Reading, Engl.)* **146 (Pt 5)**, 1099–1107.
- Lou T. and Xie H. (2006) Photochemical alteration of the molecular weight of dissolved organic matter. *Chemosphere* **65**, 2333–2342.
- Lützow M., Kögel-Knabner I., Ekschmitt K., Matzner E., Guggenberger G., Marschner B. and Flessa H. (2006) Stabilization of organic matter in temperate soils: mechanisms and their relevance under different soil conditions – a review. *European Journal of Soil Science* **57**, 426–445.
- Ma J., Del Vecchio R., Golanoski K. S., Boyle E. S. and Blough N. V. (2010) Optical properties of humic substances and CDOM: effects of borohydride reduction. *Environmental science technology* **44**, 5395–5402.
- Mahieu N., Randall E. W. and Powlson D. S. (1999) Statistical Analysis of Published Carbon-13 CPMAS NMR Spectra of Soil Organic Matter. *Soil Science Society of America Journal* **63**, 307–319.
- Mao J., Cory R. M., McKnight D. M. and Schmidt-Rohr K. (2007) Characterization of a nitrogen-rich fulvic acid and its precursor algae from solid state NMR. *Organic Geochemistry* **38**, 1277–1292.
- Mao J., Fang X., Schmidt-Rohr K., Carmo A. M., Hundal L. S. and Thompson M. L. (2007) Molecular-scale heterogeneity of humic acid in particle-size fractions of two Iowa soils. *Geoderma* **140**, 17–29.
- Mao J.-D. and Schmidt-Rohr K. (2006) Absence of Mobile Carbohydrate Domains in Dry Humic Substances Proven by NMR, and Implications for Organic-Contaminant Sorption Models. *Environ. Sci. Technol.* **40**, 1751–1756.

- Mao J.-D. and Schmidt-Rohr K. (2004) Accurate Quantification of Aromaticity and Nonprotonated Aromatic Carbon Fraction in Natural Organic Matter by ^{13}C Solid-State Nuclear Magnetic Resonance. *Environ. Sci. Technol.* **38**, 2680–2684.
- Matsumura Y. and Takahashi H. (1979) Potentiometric redox titration of quinone in carbon black with NaBH_4 and I_2 . *Carbon* **17**, 109–114.
- Maurer F., Christl I. and Kretzschmar R. (2010) Reduction and Reoxidation of Humic Acid: Influence on Spectroscopic Properties and Proton Binding. *Environmental Science & Technology* **44**, 5787–5792.
- McKnight D., Boyer E., Westerhoff P., Doran P., Kulbe T. and Andersen D. (2001) Spectrofluorometric characterization of dissolved organic matter for indication of precursor organic material and aromaticity. *Limnol. Oceanogr.* **46**, 38–48.
- McKnight D. M., Andrews E. D., Spaulding S. A. and Aiken G. R. (1994) Aquatic fulvic acids in algal-rich antarctic ponds. *Limnology and Oceanography* **39**, 1972–1979.
- Milne C. J., Kinniburgh D. G., Van Riemsdijk W. H. and Tipping E. (2003) Generic NICA-Donnan model parameters for metal-ion binding by humic substances. *Environmental science & technology* **37**, 958–971.
- Milne C. J., Kinniburgh D. G. and Tipping E. (2001) Generic NICA-Donnan Model Parameters for Proton Binding by Humic Substances. *Environmental Science & Technology* **35**, 2049–2059.
- Moore R. M. and Blough N. V. (2002) A marine source of methyl nitrate. *Geophys. Res. Lett.* **29**, 1737.
- Moran M. A., Sheldon W. M. and Zepp R. G. (2000) Carbon Loss and Optical Property Changes during Long-Term Photochemical and Biological Degradation of Estuarine Dissolved Organic Matter. *Limnology and Oceanography* **45**, 1254–1264.
- Moran M. A. and Zepp R. G. (1997) Role of Photoreactions in the Formation of Biologically Labile Compounds from Dissolved Organic Matter. *Limnology and Oceanography* **42**, 1307–1316.
- Nakanoa H. (1993) Quasidegenerate perturbation theory with multiconfigurational self-consistent-field reference functions. *J. Chem. Phys.* **99**, 7983–7992.
- Nederlof M. M., De Wit J. C. M., Van Riemsdijk W. H. and Koopal L. K. (1993) Determination of proton affinity distributions for humic substances. *Environ. Sci. Technol.* **27**, 846–856.
- Nelson J. R. and Guarda S. (1995) Particulate and dissolved spectral absorption on the continental shelf of the southeastern United States. *J. Geophys. Res.* **100**, 8715–8732.

- Nocentini C., Certini G., Knicker H., Francioso O. and Rumpel C. (2010) Nature and reactivity of charcoal produced and added to soil during wildfire are particle-size dependent. *Organic Geochemistry* **41**, 682–689.
- Obernosterer and Benner (2004) Competition between biological and photochemical processes in the mineralization of dissolved organic carbon. *Limnology and Oceanography* **49**, 117–124.
- Opsahl S. and Benner R. (1997) Distribution and cycling of terrigenous dissolved organic matter in the ocean. **386**, 480–482.
- Opsahl S. and Benner R. (1998) Photochemical Reactivity of Dissolved Lignin in River and Ocean Waters. *Limnology and Oceanography* **43**, 1297–1304.
- Rose A. L. and Waite T. D. (2003) Kinetics of Hydrolysis and Precipitation of Ferric Iron in Seawater. *Environ. Sci. Technol.* **37**, 3897–3903.
- Rose A. L. and Waite T. D. (2006) Role of superoxide in the photochemical reduction of iron in seawater. *Geochimica et Cosmochimica Acta* **70**, 3869–3882.
- Shkrob I. A., Depew M. C. and Wan J. K. S. (1992) Free Radical Induced Oxidation of Alkoxyphenols: Some Insights Into the Processes of Photoyellowing of Papers. *Research on Chemical Intermediates* **17**, 271–285.
- Skjemstad J. O., Reicosky D. C., Wilts A. R. and McGowan J. A. (2002) Charcoal Carbon in U.S. Agricultural Soils. *Soil Science Society of America Journal* **66**, 1249.
- Socrates G. (2001) *Infrared and Raman Characteristic Group Frequencies*. 3rd ed., John Wiley and Sons, New York.
- Southworth B. A. and Voelker B. M. (2003) Hydroxyl Radical Production via the Photo-Fenton Reaction in the Presence of Fulvic Acid. *Environ. Sci. Technol.* **37**, 1130–1136.
- Stedmon C. A., Amon R. M. W., Rinehart A. J. and Walker S. A. (2011) The supply and characteristics of colored dissolved organic matter (CDOM) in the Arctic Ocean: Pan Arctic trends and differences. *Marine Chemistry* **124**, 108–118.
- Stedmon C. A., Markager S. and Kaas H. (2000) Optical Properties and Signatures of Chromophoric Dissolved Organic Matter (CDOM) in Danish Coastal Waters. *Estuarine, Coastal and Shelf Science* **51**, 267–278.
- Stiles P. L., Dieringer J. A., Shah N. C. and Van Duyne R. P. (2008) Surface-Enhanced Raman Spectroscopy. *Annual Review of Analytical Chemistry* **1**, 601–626.
- Sutton R. and Sposito G. (2005) Molecular Structure in Soil Humic Substances: The New View. *Environmental Science & Technology* **39**, 9009–9015.

- Thorn K. A., Younger S. J. and Cox L. G. (2010) Order of Functionality Loss during Photodegradation of Aquatic Humic Substances. *J. Environ. Qual.* **39**, 1416–1428.
- Thurman E. M. (1985) *Organic Geochemistry of Natural Waters.*, Springer.
- Tinnacher R. M. and Honeyman B. D. (2007) A New Method to Radiolabel Natural Organic Matter by Chemical Reduction with Tritiated Sodium Borohydride. *Environ. Sci. Technol.* **41**, 6776–6782.
- Toole D. A., Slezak D., Kiene R. P., Kieber D. J. and Siegel D. A. (2006) Effects of solar radiation on dimethylsulfide cycling in the western Atlantic Ocean. *Deep Sea Research Part I: Oceanographic Research Papers* **53**, 136–153.
- Tossell J. A. (2009) Quinone–hydroquinone complexes as model components of humic acids: Theoretical studies of their structure, stability and Visible–UV spectra. *Geochimica et Cosmochimica Acta* **73**, 2023–2033.
- Twardowski M. S., Boss E., Sullivan J. M. and Donaghay P. L. (2004) Modeling the spectral shape of absorption by chromophoric dissolved organic matter. *Marine Chemistry* **89**, 69–88.
- Vaughan P. P. and Blough N. V. (1998) Photochemical Formation of Hydroxyl Radical by Constituents of Natural Waters. *Environ. Sci. Technol.* **32**, 2947–2953.
- Vermerris and Nicholson (2006) In *Phenolic compound biochemistry* Springer, Netherlands.
- Vodacek A., Blough N. V., DeGrandpre M. D., Peltzer E. T. and Nelson R. K. (1997) Seasonal Variation of CDOM and DOC in the Middle Atlantic Bight: Terrestrial Inputs and Photooxidation. *Limnology and Oceanography* **42**, 674–686.
- Vodacek A., Hoge F. E., Swift R. N., Yungel J. K., Peltzer E. T. and Blough N. V. (1995) The Use of in Situ and Airborne Fluorescence Measurements to Determine UV Absorption Coefficients and DOC Concentrations in Surface Waters. *Limnology and Oceanography* **40**, 411–415.
- Voelker B. M., Morel F. M. M. and Sulzberger B. (1997) Iron Redox Cycling in Surface Waters: Effects of Humic Substances and Light. *Environ. Sci. Technol.* **31**, 1004–1011.
- Voelker B. M. and Sedlak D. L. (1995) Iron reduction by photoproduct superoxide in seawater. *Marine Chemistry* **50**, 93–102.
- Voelker B. M., Sedlak D. L. and Zafiriou O. C. (2000) Chemistry of Superoxide Radical in Seawater: Reactions with Organic Cu Complexes. *Environ. Sci. Technol.* **34**, 1036–1042.
- Weiss J. N. (1997) The Hill equation revisited: uses and misuses. *FASEB J* **11**, 835–841.
- Wetzel R. G. (2001) *Limnology, Lake and River Ecosystems.*, Academic Press, USA.

- Whitehead R. F., de Mora S., Demers S., Gosselin M., Monfort P. and Mostajir B. (2000) Interactions of ultraviolet-B radiation, mixing, and biological activity on photobleaching of natural chromophoric dissolved organic matter: A mesocosm study. *Limnology and Oceanography* **45**, 278–291.
- Willets K. A. and Van Duyne R. P. (2007) Localized Surface Plasmon Resonance Spectroscopy and Sensing. *Annual Review of Physical Chemistry* **58**, 267–297.
- Xie P., Liu W., Fu Q., Wang R., Liu J. and Wei Q. (2004) Intercomparison of NO_x, SO₂, O₃, and aromatic hydrocarbons measured by a commercial DOAS system and traditional point monitoring techniques. *Adv. Atmos. Sci.* **21**, 211–219.
- Xing B., McGill W. B., Dudas M. J., Maham Y. and Hepler L. (1994) Sorption of phenol by selected biopolymers: isotherms, energetics, and polarity. *Environ. Sci. Technol.* **28**, 466–473.
- Yacobi Y. Z., Alberts J. J., Takacs M. and McElvaine M. (2003) Absorption spectroscopy of colored dissolved organic carbon in Georgia (USA) rivers: the impact of molecular size distribution. *J Limnol* **62**, 41–46.
- Yamauchi O. and Odani A. (1985) Structure-stability relationship in ternary copper(II) complexes involving aromatic amines and tyrosine or related amino acids. Intramolecular aromatic ring stacking and its regulation through tyrosine phosphorylation. *J. Am. Chem. Soc.* **107**, 5938–5945.
- Zafiriou O. C., Voelker B. M. and Sedlak D. L. (1998) Chemistry of the Superoxide Radical (O₂⁻) in Seawater: Reactions with Inorganic Copper Complexes. *J. Phys. Chem. A* **102**, 5693–5700.
- Zepp R. G., Erickson III, Paul and Sulzberger (2007) Interactive effects of solar UV radiation and climate change on biogeochemical cycling. *Photochemical & Photobiological Sciences* **6**, 286–300.
- Zhu Z. and Gunner M. R. (2005) Energetics of Quinone-Dependent Electron and Proton Transfers in Rhodobacter sphaeroides Photosynthetic Reaction Centers. *Biochemistry* **44**, 82–96.